



**A center of excellence in earth sciences and engineering®**

Geosciences and Engineering Division  
6220 Culebra Road • San Antonio, Texas, U.S.A. 78238-5166  
(210) 522-5160 • Fax (210) 522-5155

April 17, 2015  
Contract No. NRC-41-09-011  
Account No. 20.15265.28.003  
Job Code F1251

U.S. Nuclear Regulatory Commission  
ATTN: Ms. Zahira Cruz  
FSME/DWMEP/DURLD/SP  
Mail Stop 8F-5  
Rockville, MD 20555

Subject: Intermediate Milestone 20.15265.28.003.030, Modeling of Net Infiltration through Soil Covers At Selected Title II Uranium Mill Tailings Sites (Final Report)

Dear Ms. Cruz:

This letter documents completion of deliverable 20.15265.28.003.030 by the Center for Nuclear Waste Regulatory Analyses (CNWRA®) for Subtask 3 of Task Order 28, Engineered Cover Support for Decommissioning and Uranium Recovery, of Contract NRC-41-09-011. The file also is being placed on the U.S. Nuclear Regulatory Commission (NRC)/CNWRA shared computer drive in the Task Order 28 folder as Microsoft® Word and Portable Document Format files.

This report focuses on simulations of net infiltration and deep percolation through soil covers at three Title-II-In-Closure uranium mill tailing impoundments: Gas Hills West (American Nuclear), Wyoming; Highland (Exxon), Wyoming, and Church Rock (UNC), New Mexico. The scope of work for this activity is based on CNWRA recommendations in the Subtask 3, Activity 2 report of Task Order 28 under the same NRC contract and includes (i) evaluation of the numerical methods used by GEO-SLOPE's GeoStudio 2012 Vadose/W simulation module, and their effect on the reliability of the infiltration calculations; and (ii) analysis of the effect uncertainty in soil cover hydraulic properties on the net infiltration estimates. The final report addresses NRC comments on the previously transmitted draft final report.

If you have any questions concerning this deliverable, please do not hesitate to contact Robert Lenhard at (210) 522-6418 or me at (210) 522-3266.

Sincerely,

Miriam Juckett  
Program Manager  
Environmental Protection and  
External Hazards Assessment

MJ/mh  
cc:  
H. Arlt  
D. Persinko  
D. Mandeville

GED Directors  
GED Managers

Record Copy B-IQS  
CNWRA QA



Washington Office  
1801 Rockville Pike, Suite 105 • Rockville, Maryland 20852-1633

**FINAL REPORT**

**MODELING OF NET INFILTRATION THROUGH  
SOIL COVERS AT SELECTED TITLE II  
URANIUM MILL TAILINGS SITES**

*Prepared for*

**U.S. Nuclear Regulatory Commission  
Contract NRC-41-09-011**

**Task 28, Subtask 3**

*Prepared by*

**Gary Walter  
Cynthia Dinwiddie**

**Center for Nuclear Waste Regulatory Analyses  
San Antonio, Texas**

**April 2015**

## PREVIOUS REPORTS IN SERIES

| <b>Intermediate Milestone/<br/>ADAMS Accession Nos.</b> | <b>Report Title</b>  | <b>Date Issued</b> |
|---|--|--------------------|
| 06004.01.007.265/<br>ML072950120                        | Evaluation of Approaches to Simulate Engineered Cover Performance and Degradation  | October 2007       |
| 14003.01.007.320/<br>ML082980094                        | Software Validation Test Plan and Report for Geostudio™ Vadose/W® 2007 Version 7.11  | October 2008       |
| 15265.21.021.160/<br>ML12256A992                        | Analysis of Mill Tailings Cover Performance (Analysis of Eleven Title-II-in-Closure Uranium Mill Tailing Sites)  | August 2012        |
| 15265.28.001.100/<br>ML12363A176                        | Feasibility Study for Development of a Long-Term, Densely Monitored, Engineered Soil Cover Testbed Facility at Southwest Research Institute® in San Antonio, Texas (Final Report)  | December 2012      |
| 15265.28.002.010, -.020/<br>ML14015A328                 | Methods for Monitoring Net Inflow Through Soil Covers of Uranium Mill Tailings Impoundments (Final Report)   | November 2013      |
| 15265.28.003.010/<br>ML14058A381                        | Activity 1: Evaluation of Unsaturated Flow Codes and Selected Approach Methods for Monitoring Net Inflow Through Soil Covers of Uranium Mill Tailings Impoundments (Letter Report) | February 2014      |
| 15265.28.003.020/<br>ML14260A090                        | Activity 2: Proposed Plan of Action to Characterize Final Soil Cover Properties and Obtain Input Parameter Values for Near-Field Modeling with the Vadose/W 2012 Code              | September 2014     |
| 15265.28.004.050  | Uranium Tailings Impoundments: Bottom Liners and Their Performance (Final Report)  | February 2015      |

# CONTENTS

| Section  | Page |
|--|------|
| FIGURES.....   | v    |
| TABLES.....  | x    |
| 1 INTRODUCTION.....  | 1-1  |
| 2 BASIS FOR SITE SELECTION .....                                   | 2-1  |
| 3 NUMERICAL MODEL AND LIMITATIONS .....                            | 3-1  |
| 3.1 Climate-Driven Calculations .....                              | 3-1  |
| 3.1.1 Surface Flux Algorithm .....                                 | 3-1  |
| 3.1.2 Transpiration .....  | 3-4  |
| 3.1.3 Soil Freezing and Thawing .....                              | 3-5  |
| 3.2 Numerical Flow Model .....                                     | 3-7  |
| 3.3 Model Limitations.....   | 3-8  |
| 4 GAS HILLS WEST MODEL AND SIMULATION RESULTS.....                 | 4-1  |
| 4.1 Description of the Gas Hills West Model .....                  | 4-1  |
| 4.1.1 Model Domain and Grid.....                                   | 4-4  |
| 4.1.2 Material Properties .....                                    | 4-9  |
| 4.1.3 Boundary Conditions .....                                    | 4-14 |
| 4.1.4 Initial Conditions.....                                      | 4-16 |
| 4.2 Simulation Results .....                                       | 4-17 |
| 4.3 Results of Semi-Refined Gas Hills West Pond 2 Simulations..... | 4-18 |
| 4.4 Summary of Gas Hills West Pond 2 Simulations.....              | 4-30 |
| 5 HIGHLAND MODEL AND SIMULATION RESULTS .....                      | 5-1  |
| 5.1 Description of the Highland (Exxon), Wyoming, Model.....       | 5-1  |
| 5.1.1 Model Domain and Mesh.....                                   | 5-4  |
| 5.1.2 Material Properties .....                                    | 5-7  |
| 5.1.3 Boundary Conditions (Including Vegetation).....              | 5-27 |
| 5.1.4 Initial Conditions.....                                      | 5-36 |
| 5.2 Simulation Results .....                                       | 5-41 |
| 6 CHURCH ROCK NORTH CELL MODEL AND SIMULATION RESULTS .....        | 6-1  |
| 6.1 Description of the Church Rock (UNC), New Mexico, Model.....   | 6-1  |
| 6.1.1 Model Domain and Mesh.....                                   | 6-3  |
| 6.1.2 Material Properties .....                                    | 6-4  |
| 6.1.3 Boundary Conditions (Vegetation was not Modeled) .....       | 6-9  |
| 6.1.4 Initial Conditions.....                                      | 6-11 |
| 6.2 Simulation Results .....                                       | 6-17 |
| 7 EVALUATION OF MODEL RESULTS AND RECOMMENDATIONS.....             | 7-1  |
| 7.1 Site Selection.....  | 7-1  |
| 7.2 Numerical Model and Limitations .....                          | 7-1  |
| 7.3 Results of Gas Hills West Simulations .....                    | 7-2  |
| 7.4 Results of Highland Site Simulations.....                      | 7-3  |
| 7.5 Results for Church Rock Simulations.....                       | 7-5  |

|       |  |     |
|-------|--|-----|
| 7.6   | Summary and Recommendations .....                              | 7-5 |
| 7.6.1 | Summary of Numerical Simulations and Water Balance Issues..... | 7-5 |
| 7.6.2 | Recommendations for Future Simulations .....                   | 7-6 |
| 8     | REFERENCES.....  | 8-1 |

## FIGURES

| Figure | Page   |
|--------|--|
| 2-1    | Locations of Wyoming Title-II-In-Closure Soil Covers and Remote Automated Weather Stations that Archive Required Climate Data.....2-1  |
| 2-2    | Locations of New Mexican Title-II-In-Closure Soil Covers and Remote Automated Weather Stations that Archive Required Climate Data.....2-2  |
| 3-1    | Flow Chart of the Vadose/W Algorithm Used to Compute Surface Flux.....3-2  |
| 3-2    | The Becker, et al. (1992) Thermal Conductivity vs. Saturation Functions .....3-6   |
| 4-1    | Schematic Showing Planned Cover Construction for Pond #2 at the Gas Hills West Site.....4-1  |
| 4-2    | Locations of Soil Borings through Interim Cover with Soil Classifications .....4-2   |
| 4-3    | Approximate Soil Boring Locations and Interim Cover Thickness in Meters.....4-3  |
| 4-4    | Function Describing Interim Cover Thickness Based on Soil Boring Logs .....4-4   |
| 4-5    | Transect Used to Construct Two-Dimensional Model .....4-5  |
| 4-6    | Profiles of Cover Layers at Gas Hills West Pond 2 Along Model Transect.....4-6   |
| 4-7    | Top of Tailings Pond 2 Looking Northwest .....4-7  |
| 4-8    | Satellite Image of Gas Hills West Pond 2 from October 7, 2004 .....4-7   |
| 4-9    | Estimated Original Ground Surface in Relation to Impound Topography .....4-8   |
| 4-10   | Configuration of Impoundment Embankment Used to Construct Two-Dimensional Model .....4-9   |
| 4-11   | Variation of Pore Water Pressure with Volumetric Water Content in the Gas Hills West Pond 2 Model .....4-11  |
| 4-12   | Variation of Hydraulic Conductivity with Volumetric Water Content in the Gas Hills West Pond 2 Model .....4-12   |
| 4-13   | Material in the Two-Dimensional Gas Hills West Pond 2 Model.....4-13   |
| 4-14   | Materials Used in the One-Dimensional Gas Hills West Pond 2 Model.....4-13   |
| 4-15   | Location of the Fales Rock RAWs with Respect to Gas Hills West Site .....4-15  |
| 4-16   | Daily Liquid Precipitation at Fales Rock, Wyoming .....4-15  |
| 4-17   | Comparison of Precipitation Frequencies Based on the Fales Rock Weather Data with Precipitation Event Frequencies for Western Wyoming.....4-16   |
| 4-18   | Finite Element Mesh and Materials in the Semi-Refined Model .....4-18  |
| 4-19   | Daily Precipitation, Cumulative Lower Boundary Flow, Water Balance Error, Cumulative Change in Storage, and Cumulative Water Added Based on the Semi-Refined Gas Hills West Pond 2 Model with Precipitation Distributed Sinusoidally Over 1 Hour .....4-19 |
| 4-20   | Cumulative Precipitation Reported by Vadose/W Compared To Cumulative Precipitation Computed from the Fales Rock Input Data for the 1-Hour, Sinusoidal Summer Precipitation Simulation.....4-20   |
| 4-21   | Simulated Change in Volumetric Water Content at Selected Nodes in the Gas Hills West Semi-Refined Model Simulation 1-Hour Sinusoidal Simulation .....4-21  |
| 4-22   | Daily Precipitation, Cumulative Lower Boundary Flow, Water Balance Error, Cumulative Change in Storage, and Cumulative Water Added Based on the Semi-Refined Gas Hills West Pond 2 Model with Precipitation Distributed Uniformly Over 1 Hour .....4-22    |
| 4-23   | Cumulative Precipitation Reported By Vadose/W Compared to Cumulative Precipitation Computed from the Fales Rock Input Data for the 1-Hour, Constant Average Summer Precipitation Simulation.....4-23   |

## FIGURES

| Figure  | Page |
|---|------|
| 4-24 Simulated Change in Volumetric Water Content at Selected Nodes in the Gas Hills West Semi-Refined Model Simulation 1-Hour Constant Average Simulation .....  | 4-24 |
| 4-25 Daily Precipitation, Cumulative Lower Boundary Flow, Water Balance Error, Cumulative Change in Storage, and Cumulative Water Added Based on the Semi-Refined Gas Hills West Pond 2 Model with Precipitation Distributed Uniformly Over 24 Hours .....  | 4-25 |
| 4-26 Cumulative Precipitation Reported By Vadose/W Compared to Cumulative Precipitation Computed from the Fales Rock Input Data for Precipitation Distributed over 24 Hours .....   | 4-26 |
| 4-27 Simulated Change in Volumetric Water Content at Selected Nodes in the Gas Hills West Semi-Refined Model Simulation with Precipitation Distributed Over 24 Hours.....   | 4-27 |
| 4-28 Daily Precipitation, Cumulative Lower Boundary Flow, Water Balance Error, Cumulative Change in Storage, and Cumulative Water Added Based on the Semi-Refined Gas Hills West Pond 2 Model with Precipitation Distributed Uniformly Over 24 Hours and High Sandy Silty Clay Hydraulic Conductivity ..... | 4-28 |
| 4-29 Cumulative Precipitation Reported by Vadose/W Compared to Cumulative Precipitation Computed from the Fales Rock Input Data for Precipitation Distributed Over 24 Hours with High Sandy Silty Clay Hydraulic Conductivity .....   | 4-29 |
| 4-30 Simulated Change in Volumetric Water Content at Selected Nodes in the Gas Hills West Semi-Refined Model Simulation with Precipitation Distributed Over 24 Hours with High Sandy Silty Clay Hydraulic Conductivity.....   | 4-30 |
| 4-31 Comparison of Results of Simulations Using Different Summer Precipitation Distributions and Elevated Saturated Hydraulic Conductivity of Sandy Silty Clay Materials.....   | 4-31 |
| 5-1 (a) Selected Transect for a Two-Dimensional Net Infiltration Model across the Highland Uranium Mill Tailings Impoundment Cover at the Swale Divide; (b) Swale Subwatershed Divide.....  | 5-3  |
| 5-2 Cross-Section through the Highland Uranium Mill Tailings Impoundment and Soil Cover along the Swale Divide .....  | 5-4  |
| 5-3 Highland Model Domain .....   | 5-5  |
| 5-4 Highland Model Discretization .....   | 5-6  |
| 5-5 Map View of Highland Mill Tailings Impoundment Soil Units Superimposed by Swales and Approximation of Swale Divide .....  | 5-8  |
| 5-6 Transformed Topsoil 145 Particle Size Data and van Genuchten Model Fits.....  | 5-10 |
| 5-7 Comparison of Topsoil 145 2-Parameter van Genuchten and Hybrid Data Point Functions.....  | 5-11 |
| 5-8 Topsoil 145 Hydraulic Conductivity Functions of Pore Water Pressure for Deep and Shallow Topsoil Units .....  | 5-12 |
| 5-9 Soil Moisture Characteristic Functions that Represent the Three Approved Radon Barrier Materials Used in the Highland Uranium Milling Tailings Impoundment Soil Cover .....   | 5-14 |
| 5-10 Silty Clay Hydraulic Conductivity Model for the Highland Radon Barrier .....   | 5-15 |
| 5-11 Horizontal Air and Water Relative Permeabilities and Intrinsic Permeabilities of Tailings Dam Sand Core XII, Selected for use by Exxon Production Research Company in Their Modeling of Highland Sandstone Units .....   | 5-16 |

## FIGURES

| Figure | Page  |
|--------|---|
| 5-12   | Horizontal Soil Water Characteristic Curves of Tailings Dam Sand Cores; That for Core XII was Selected by Exxon Production Research Company to Model Highland Sandstone Units and in this Modeling to Represent Sandy Tailings.....5-17 |
| 5-13   | Sandy Tailings Moisture Characteristic Based Upon the Horizontal Soil Water Characteristic Curves of Tailings Dam Sand Core XII.....5-18  |
| 5-14   | Highland Sandy Tailings Hydraulic Conductivity Function.....5-19  |
| 5-15   | Summary Comparison of Highland Soil Column Moisture Characteristic Functions....5-20  |
| 5-16   | Summary Comparison of Highland Soil Column Horizontal Hydraulic Conductivity Functions of Negative Pore Water Pressure .....5-21  |
| 5-17   | Summary Comparison of Highland Thermal Conductivity Functions.....5-26  |
| 5-18   | Summary Comparison of Highland Volumetric Specific Heat Capacity Functions.....5-27   |
| 5-19   | Hourly Precipitation Frequency by Month (1949–2001) Based on Station Data in Casper, Cheyenne, Lander and Sheridan, Wyoming .....5-28   |
| 5-20   | Estimated Leaf Area Index Function for the Highland Site .....5-30  |
| 5-21   | Estimated Rooting Depth Function for the Highland Site .....5-31  |
| 5-22   | Typical Plant Moisture Limiting Factor Function of Pore Water Pressure (i.e., Matric Suction) Used in the Highland Model .....5-32  |
| 5-23   | Highland Seasonal Soil Temperature Estimate at 10-Centimeter Depth Based Upon Hu and Feng and Rochelle Hills Air Temperatures.....5-33  |
| 5-24   | Mean Multilevel Subsurface Ground Temperatures Measured at Torrington, Wyoming .....5-34  |
| 5-25   | 10-Centimeter Ground Temperatures Measured at Torrington, Wyoming, Compared to Staff’s Equivalent Ground Temperature Estimate from Figure 5-23.....5-34   |
| 5-26   | Mean Annual Ground Temperatures Computed from Multilevel Data Measured at Torrington, Wyoming .....5-35   |
| 5-27   | Approximation of Hydrostatic Initial Condition Estimated for Use in Starting a Year-Long Rochelle Hills Climate Spinup Simulation of the Highland Soil Cover .....5-36  |
| 5-28   | Volumetric Water Content Markedly Decreased in Deep Layers during Year-Long Rochelle Hills Climate Spinup Simulation of the Highland Soil Cover .....5-37   |
| 5-29   | Initial Conditions for Starting the Long-term Rochelle Hills Climate-Driven Model of the Highland Soil Cover .....5-38  |
| 5-30   | Unexplained Water Balance Error Occurred During Day 3,697 of Preliminary Long-Term Rochelle Hills Climate Simulation .....5-39  |
| 5-31   | Initial Conditions (i.e., Pore Water Pressure Profile) for the Final Long-Term, Climate-Driven Simulation of the Highland Soil Cover .....5-39  |
| 5-32   | Thermal Initial Conditions (Day 365) for Starting the Long-Term Rochelle Hills Climate Driven Simulation of the Highland Soil Cover .....5-40   |
| 5-33   | Cumulative Water Balance Components .....5-41   |
| 5-34   | Apparent Monotonic Decrease in Magnitude of Volumetric Water Content within and below the Radon Barrier .....5-42   |
| 5-35   | Temporal Evolution of Vertical Hydraulic Conductivity in the Highland Sandy Tailings Suggests Pulses of Deep Percolation May Extend below Radon Barrier from Day 0 through 3,287 .....5-42  |
| 5-36   | Temporal Evolution of Vertical Hydraulic Conductivity in the Highland Sandy Tailings Suggests Continuous Drying below Radon Barrier during This Interval .....5-43  |
| 5-37   | Temporal Evolution of Vertical Hydraulic Conductivity in the Highland Sandy Tailings Suggests Pulses of Deep Percolation May Extend Below Radon Barrier from Day 5,113 to 6,940 and from Day 7,305 to 7,830 .....5-43                   |

## FIGURES

| Figure   | Page |
|--|------|
| 6-1 Church Rock Model Domain.....  | 6-2  |
| 6-2 Church Rock Central Cell Model Discretization .....  | 6-3  |
| 6-3 Development of Moisture Characteristic Function for the Church Rock Radon<br>Barrier and Topsoil .....   | 6-5  |
| 6-4 Summary Comparison of Church Rock Soil Column Moisture<br>Characteristic Functions .....   | 6-6  |
| 6-5 Summary Comparison of Church Rock Hydraulic Conductivity Functions .....   | 6-7  |
| 6-6 Summary Comparison of Church Rock Central Cell Thermal Conductivity Functions...   | 6-8  |
| 6-7 Summary Comparison of Church Rock Central Cell Volumetric Specific Heat<br>Capacity Functions .....  | 6-9  |
| 6-8 Approximation of Hydrostatic Initial Condition Estimated for Use in Starting a<br>Year-Long Zuni Buttes Climate Spinup Simulation of the Church Rock Central<br>Cell Soil Cover.....                           | 6-11 |
| 6-9 Volumetric Water Content Markedly Decreased in Deep Layers during Year-Long<br>Zuni Buttes Climate Spinup Simulation of the Church Rock Soil Cover .....   | 6-12 |
| 6-10 Initial Conditions for Starting the Long-term Zuni Buttes Climate-Driven<br>Simulation of the Church Rock Soil Cover .....  | 6-12 |
| 6-11 Hydraulic Initial Conditions (Day 7,680) for Starting the Final 3,210-Day-Long<br>Zuni Buttes Climate-Driven Simulation of the Church Rock Soil Cover .....   | 6-13 |
| 6-12 Annually Decreasing Volumetric Water Contents Observed as Moisture in the<br>Soil Column Equilibrates with Local Climate Forcing (Years 1–8).....   | 6-14 |
| 6-13 Soil Column Responds to Local Climate Forcing after Equilibration has Occurred<br>(Years 8–21).....   | 6-15 |
| 6-14 Thermal Initial Conditions (Day 365/April 4) for Starting the Zuni Buttes<br>Expanded-Length Climate Driven Simulation of the Church Rock Soil Cover .....  | 6-16 |
| 6-15 Thermal Initial Conditions (Day 7,680/April 14) for Starting the Final Zuni Buttes<br>Climate Driven Simulation of the Church Rock Soil Cover .....   | 6-17 |
| 6-16 Mesh Cumulative Mass Balance Components and Resulting Error in the Zuni<br>Buttes Climate-Driven Church Rock Central Cell Soil Cover Simulation .....   | 6-18 |
| 6-17 April 14 Anniversary Volumetric Water Contents in the Church Rock Central Cell<br>Soil Column .....   | 6-19 |
| 6-18 April 14 Anniversary Volumetric Water Content Distributions in the Church Rock<br>Coarse, Sandy Loam Tailings.....  | 6-19 |
| 6-19 Illustration of Drying (Days 0 to 632)/Wetting (Days 632 to 1860)/Drying<br>(Days 1,860 to 3,210) Periods in the Church Rock Tailings .....   | 6-20 |
| 6-20 Volumetric Water Content within the Upper Sandy Tailings Recovered to<br>Approximate Day 631 Conditions (on Day 2,760) 900 Days after Attaining their<br>Maximum Volumetric Water Content (on Day 1860) ..... | 6-20 |
| 6-21 Infiltration Pulses Enter the Radon Barrier during the Period Spanning<br>December 8, 2007 through January 3, 2008 (Days 604–632).....  | 6-21 |
| 6-22 Infiltration Pulses Enter the Radon Barrier during the Period Spanning<br>January 3–26, 2008 (Days 633–653).....  | 6-22 |
| 6-23 Infiltration Pulses Enter the Radon Barrier during the Period Spanning<br>January 27 through February 11, 2008 (Days 654–669).....  | 6-22 |
| 6-24 Infiltration Pulses Enter the Radon Barrier during the Period Spanning<br>December 12–30, 2008 (Days 974–992) .....   | 6-23 |

## FIGURES

| Figure |  | Page |
|--------|--|------|
| 6-25   | Hydraulic Conductivity Monotonically Increased in the Upper Section of the Church Rock Coarse, Sandy Loam Tailings Over a Period of 1,228 Days.....  | 6-24 |
| 6-26   | After Deep Percolation Into the Church Rock Coarse, Sandy Loam Tailings Ceased, 900 Days of Drying Occurred Before the Permeability Profile Recovered to Conditions Approximately the Same as When Deep Percolation Began..... | 6-24 |
| 6-27   | Upper Section of the Coarse, Sandy Loam Tailings Exhibit Further Reduction in Permeability until the End of the Climate Record .....   | 6-25 |
| 7-1    | Comparison of Results of Gas Hills West, WY, Simulations Using Different Summer Precipitation Distributions and Elevated Saturated Hydraulic Conductivity of Sandy Silty Clay Materials.....                                   | 7-3  |
| 7-2    | Mesh Cumulative Water Balance Components for the Highland, WY, Simulation.....   | 7-4  |
| 7-3    | Mesh Cumulative Water Balance Components and Resulting Error in the Zuni Buttes Climate-Driven Church Rock Central Cell Soil Cover Simulation .....  | 7-6  |

## TABLES

| Table   | Page |
|---|------|
| 2-1 Summary of Remote Automated Weather Station Metadata Relevant to Highland and Gas Hills West Title-II-In-Closure Soil Covers Sites in Wyoming ..... | 2-2  |
| 4-1 Average Material Properties Assigned in the Gas Hills West Pond 2 Model .....   | 4-10 |
| 5-1 Highland Model Discretization with 2-mm Element Size in Critical Zones .....  | 5-6  |
| 5-2 Topsoil Units Mapped by NRCS at the Highland Mill Tailings Impoundment.....   | 5-7  |
| 5-3 Characteristics of Soil Units 131 and 145 at the Highland Uranium Mill Tailings Impoundment .....   | 5-9  |
| 5-4 Highland Site Material Properties and Textures of Surficial Soil Units to a Depth of 15 cm .....  | 5-10 |
| 5-5 Topsoil Grain Size Data.....  | 5-10 |
| 5-6 Classification/Quantification of Radon Barrier Material and its Heterogeneity .....   | 5-13 |
| 5-7 Plausible Saturated Hydraulic Conductivity Values for Highland Radon Barrier.....   | 5-13 |
| 5-8 Rosetta Clay-Class-Average Hydraulic Properties.....  | 5-14 |
| 5-9 Relative Permeability, Fluid Saturations, Pore Water Pressures, and Hydraulic Conductivity Data Points for Highland Tailings Sand .....             | 5-15 |
| 5-10 Water Saturation, Pore Water Pressure, and Volumetric Water Content (Including van Genuchten Model) .....  | 5-18 |
| 5-11 Best Estimates/Sensitivity-Analysis Ranges for Highland Site Hydraulic Properties ...  | 5-22 |
| 5-12 Becker, et al. (1992) Mean Gravel Thermal Conductivity Data Point Function for Highland's Gravelly Sand Topsoil .....                              | 5-23 |
| 5-13 Becker, et al. (1992) Mean Clay Thermal Conductivity Data Point Function for Highland's Silty Clay Radon Barrier.....                              | 5-23 |
| 5-14 Becker, et al. (1992) Mean Sandy Thermal Conductivity Data Point Function for Highland's Sandy Tailings .....                                      | 5-24 |
| 5-15 Becker, et al. (1992) Mean Silt Thermal Conductivity Data Point Function for Highland's Silty Clay Slimes .....                                    | 5-25 |
| 5-16 Assigned Precipitation Schedule for Highland .....   | 5-29 |
| 5-17 Permanent Reclamation Seeded Cover at Highland.....  | 5-29 |
| 5-18 Plant Moisture Limiting Factor Function.....   | 5-30 |
| 5-19 Preliminary Highland Thermal Initial Conditions.....   | 5-40 |
| 6-1 Church Rock Model Discretization with 2-mm Element Size in Critical Zones.....  | 6-4  |
| 6-2 Church Rock Central Cell Constant Hydraulic Parameters Based Upon Canonie Environmental and MWH Americas, Inc .....                                 | 6-6  |
| 6-3 Assigned Precipitation Schedule for Church Rock.....  | 6-10 |

# 1 INTRODUCTION

This report addresses the requirements of Activity 3 in Subtask 3 of Task Order 28 under the contract titled “Technical Assistance for the Development of Safety and/or Environmental Documents for Uranium Recovery, Fuel Cycle Facilities, Decommissioning, and Other NRC Licensing Support Activities” (NRC–41–09-011, Rev. 0, Chg. 44). This report focuses on simulations of net infiltration and deep percolation through soil covers at three Title-II-In-Closure uranium mill tailing impoundments:

- Gas Hills West (American Nuclear), Wyoming: Pond 2 tailings impoundment cell
- Highland (Exxon), Wyoming: Tailings impoundment cell
- Church Rock (UNC), New Mexico: Central tailings impoundment cell

Net infiltration refers to the water infiltrating through the soil cover that reaches the underlying tailings deposit because it is not removed by evapotranspiration. The scope of work for this activity is based on the Center for Nuclear Waste Regulatory Analyses (CNWRA<sup>®</sup>) recommendations in the Subtask 3, Activity 2 report of Task Order 28 under the same U.S. Nuclear Regulatory Commission (NRC) contract and includes:

- Evaluation of the numerical methods used by GEO-SLOPE’s GeoStudio 2012 Vadose/W simulation module (GEO-SLOPE International Ltd., 2012), hereafter referred to simply as Vadose/W, and their effect on the reliability of the infiltration calculations
- Analysis of the effect uncertainty in soil cover hydraulic properties on the net infiltration estimates.

The simulations documented in this report were performed to lay groundwork for estimating whether or not earthen soil covers installed over Title-II-In-Closure uranium mill tailings impoundments will prevent net infiltration of meteoric water from entering the tailings. The simulations are not intended to determine if original pore water within the tailings is continuing to drain into underlying soil. Due to numerical issues associated with the simulations, an in-depth analysis of the parameters and their uncertainty affecting the simulation of net infiltration was not possible within the funding and timeframe of the contract.

Section 2 of this report describes the rationale for selecting the specific sites for the parameter simulations. Section 3 describes the numerical methods implemented in Vadose/W that are important to simulating net infiltration and evaluating the reliability of resulting net infiltration calculations. Sections 4 through 6 present the results of simulations at the three sites selected for investigation. Section 7 summarizes the results of these analyses and provides recommendations for future efforts to evaluate net infiltration at these and other Title-II-In-Closure sites.

## 2 BASIS FOR SITE SELECTION

The Gas Hills West (American Nuclear), Wyoming, Pond 2 tailings impoundment cell, Highland (Exxon), Wyoming, tailings impoundment cell, and the Church Rock (UNC), New Mexico, Central tailings impoundment cell were selected for modeling because for Title-II-In-Closure soil covers, these three sites represent the full range of

- Climate conditions
- Erosion barrier types (vegetated topsoil; rock mulch sparsely vegetated with botanical volunteers, and riprap)
- Surface drainage feature types

Sufficient information is available on the soil types used to construct the earthen covers to develop plausible parameter sets for their material properties.

The Gas Hills West site (Figure 2-1) is centrally located in Wyoming. Based on information summarized in Walter and Dinwiddie (2014), the Gas Hills West cover has a rock mulch erosion barrier similar to that of the Gas Hills North site, which is located only 3 km [2 mi] to the northeast. While the Gas Hills East site is located only approximately 12 km [7.5 mi] east-northeast of the Gas Hills West site, its disposal cells have a much thicker and coarser riprap erosion barrier.

The Highland site is located in east-central Wyoming, 177 km [110 mi] east-northeast of Gas Hills West, but at a lower elevation (Figure 2-1). It is similar to the Bear Creek,

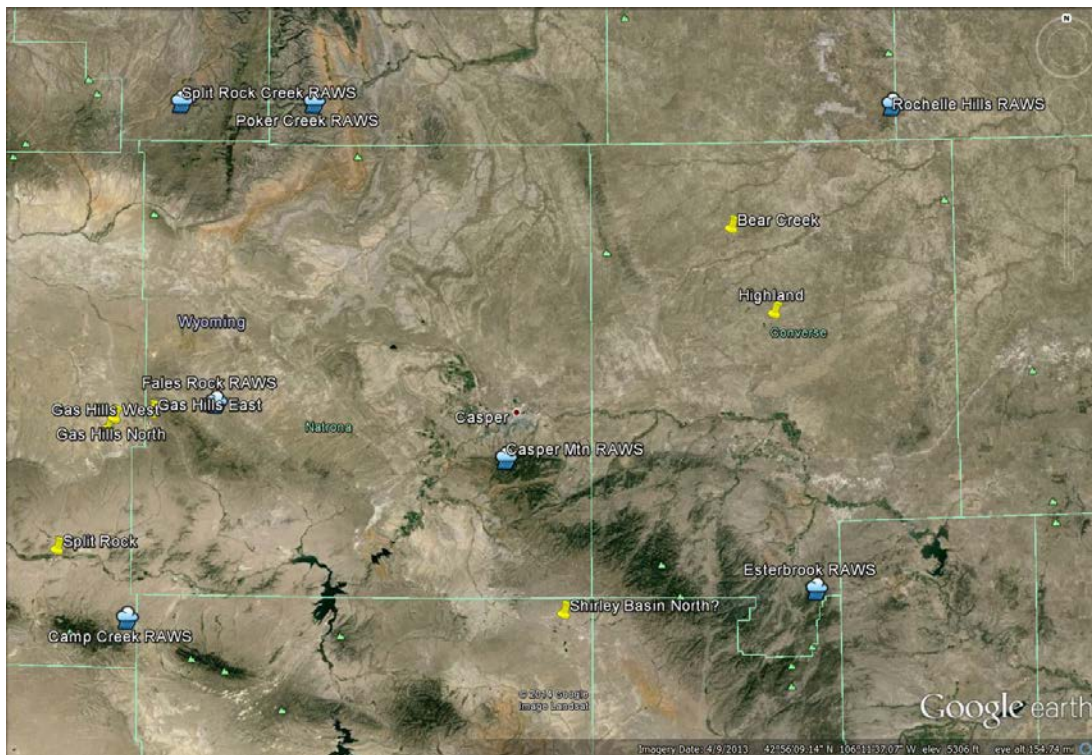


**Figure 2-1. Locations of Wyoming Title-II-In-Closure Soil Covers and Remote Automated Weather Stations that Archive Required Climate Data**

Shirley Basin, and Split Rock sites in terms of climate and vegetated soil cover. Wyoming weather stations with potentially relevant data include those tabulated in Table 2-1.

| <b>Table 2-1. Summary of Remote Automated Weather Station Metadata Relevant to Highland and Gas Hills West Title-II-In-Closure Soil Covers Sites in Wyoming (Lateral Distances are Relative to the Highland Site)</b> |                           |                           |                  |                   |                    |
|---|---------------------------|---------------------------|------------------|-------------------|--------------------|
| <b>RAWS Station</b>   | <b>Distance [km (mi)]</b> | <b>Elevation [m (ft)]</b> | <b>Latitude</b>  | <b>Longitude</b>  | <b>Timeframe</b>   |
| <b>Highland</b>   | <b>0 (0)</b>              | <b>1593 (5226)</b>        | <b>43°04'00"</b> | <b>105°30'00"</b> |                    |
| Rochelle Hills  | 63 (39)                   | 1585 (5200)               | 43°33'02"        | 105°05'32"        | 6/8/1992–Present   |
| Esterbrook*   | 66 (41)                   | 1990 (6529)               | 42°24'55"        | 105°21'40"        | 9/1988–Present     |
| Casper Mtn  | 79 (49)                   | 2359 (7740)               | 42°42'47"        | 106°20'46"        | 8/1992–Present     |
| Poker Creek†  | 132 (82)                  | 1963 (6440)               | 43°33'41"        | 106°58'01"        | 8/1992–Present     |
| Fales Rock  | 147 (91)                  | 1945 (6381)               | 42°51'23"        | 107°16'20"        | 6/1997–Present     |
| Split Rock Creek  | 164 (102)                 | 1829 (6001)               | 43°33'38"        | 107°23'51"        | 9/1988–Present     |
| Camp Creek‡   | 186 (116)                 | 2249 (7379)               | 42°20'45"        | 107°33'10"        | 8/1988–Present     |
| Torrington§   | 164 (102)                 | 1252 (4108)               | 42°03'44"        | 104°11'04"        | Ground Temperature |
| <b>Gas Hills West</b>   | <b>177 (110)</b>          | <b>2134 (7001)</b>        | <b>42°50'00"</b> | <b>107°29'30"</b> |                    |

\*March 1989 data are missing  
†Entire months of data are missing from 2010–2011 timeframe  
‡Entire months of data are missing from 2002–2003 timeframe  
§Torrington is a multilevel ground temperature station rather than a remote automated weather station

The Church Rock site is located in north-central New Mexico, with a climate similar to that of the other Title-II-In-Closure sites in New Mexico (i.e., Ambrosia Lake West and Bluewater). Church Rock has a rock mulch erosion barrier with sparse vegetation, whereas Bluewater has a riprap erosion barrier. No information is available about the Ambrosia Lake cover.

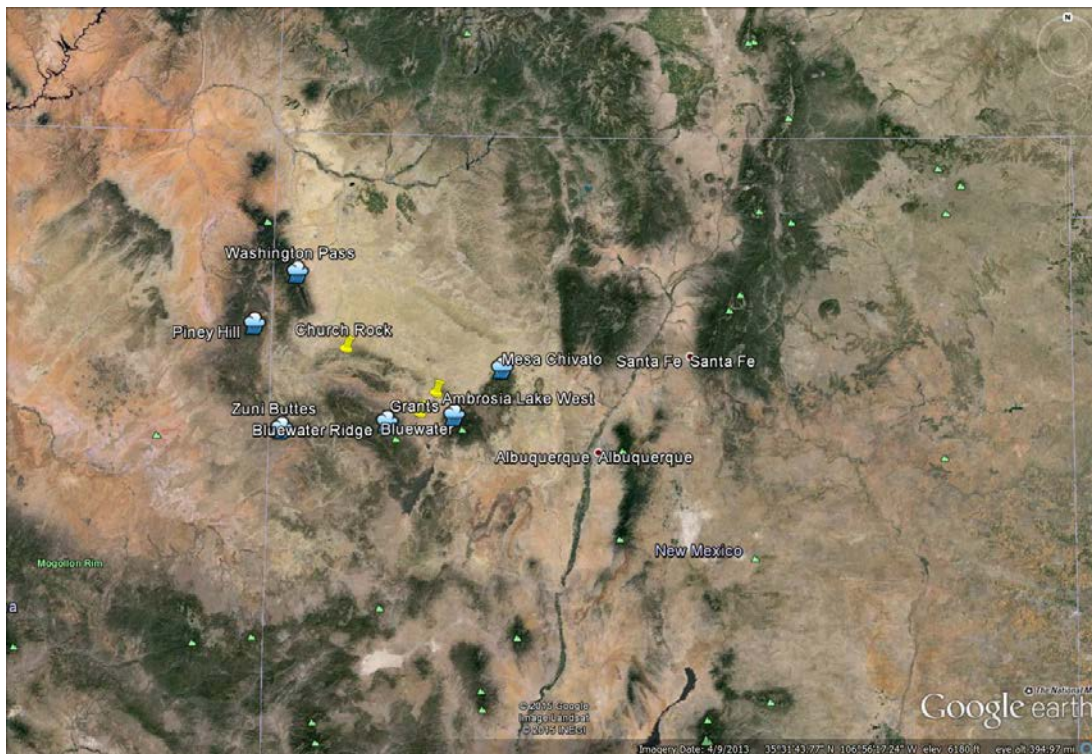


**Figure 2-2. Locations of New Mexican Title-II-In-Closure Soil Covers and Remote Automated Weather Stations that Archive Required Climate Data**

### 3 NUMERICAL MODEL AND LIMITATIONS

GEO-SLOPE's Geostudio 2012 Vadose/W module (hereafter Vadose/W) is a commercial software application for simulating unsaturated flow in porous media. The application is specifically designed for simulating water infiltration and water and vapor flow in landfills and embankments. As such, it includes algorithms for computing evaporative and transpirative water loss under variable meteorological conditions, diversion of precipitation as surface runoff and ponding. Vadose/W also includes algorithms for simulating soil freezing and thawing, and the effects of these processes on infiltration. Additional information from GEO-SLOPE about the capabilities of Vadose/W is at [www.geo-slope.com/products/vadosew.aspx?s=details](http://www.geo-slope.com/products/vadosew.aspx?s=details). Specific features of Vadose/W relevant to simulating infiltration processes at the Title-II-In-Closure soil cover sites are described in this section of the report.

#### 3.1 Climate-Driven Calculations

Vadose/W was selected for use, in part, because of its relatively sophisticated methods for simulating evapotranspiration and runoff, which are needed to establish the climate-driven boundary condition for the upper surface of the model mesh. During each time step of a simulation, the code must calculate a liquid flux to be assigned to the uppermost element in the model mesh based on the precipitation, direct surface evaporation, runoff, and any snow melt during the time steps. Precipitation, air temperature, relative humidity, and wind speed needed to compute these values are supplied by the user on a daily basis, which establishes the maximum time step used by the code. Solar radiation may be input explicitly by the user; alternatively, the user inputs site latitude and an algorithm computes daily solar radiation, sunrise and sunset times. The code may subdivide the daily time step into sub-time steps, referred to in the Vadose/W manual as adaptive time steps, based on such factors as the maximum change in pore water pressure and convergence of the numerical solving. The reader is referred to GEO-SLOPE International, Ltd (2012) for further description of the algorithms. For the purposes of this report, however, it is important to understand how the code computes the surface water flux.

##### 3.1.1 Surface Flux Algorithm

The surface flux algorithm, based on our understanding of the Vadose/W documentation, is illustrated in Figure 3-1. At the beginning of each time step, which may be much smaller than the maximum time step of 1 day (depending on the change in pore water pressure during the previous time step, convergence behavior, and the tolerances set by the user), Vadose/W estimates the potential infiltration rate [ $I$ ] from the precipitation rate [ $P$ ] and actual evaporation rate [ $AE$ ] that would occur during the time step {all in units of [ $L/t$ ]}. If potential infiltration rate is negative, then a negative flux is applied to the surface node and the code proceeds to solve for the pore water pressure distribution. If the estimated infiltration is positive, then the code performs a calculation to determine if the potential infiltration would result in a pore water pressure greater than atmospheric in the surface node. Because a pore water pressure greater than atmospheric would imply that the surface is saturated, resulting in runoff [ $R$ ], the code performs a calculation of the maximum surface flux [infiltration] if the surface node is saturated and re-estimates the potential infiltration rate accounting for runoff by

$$I = P - AE - R \quad (3-1)$$

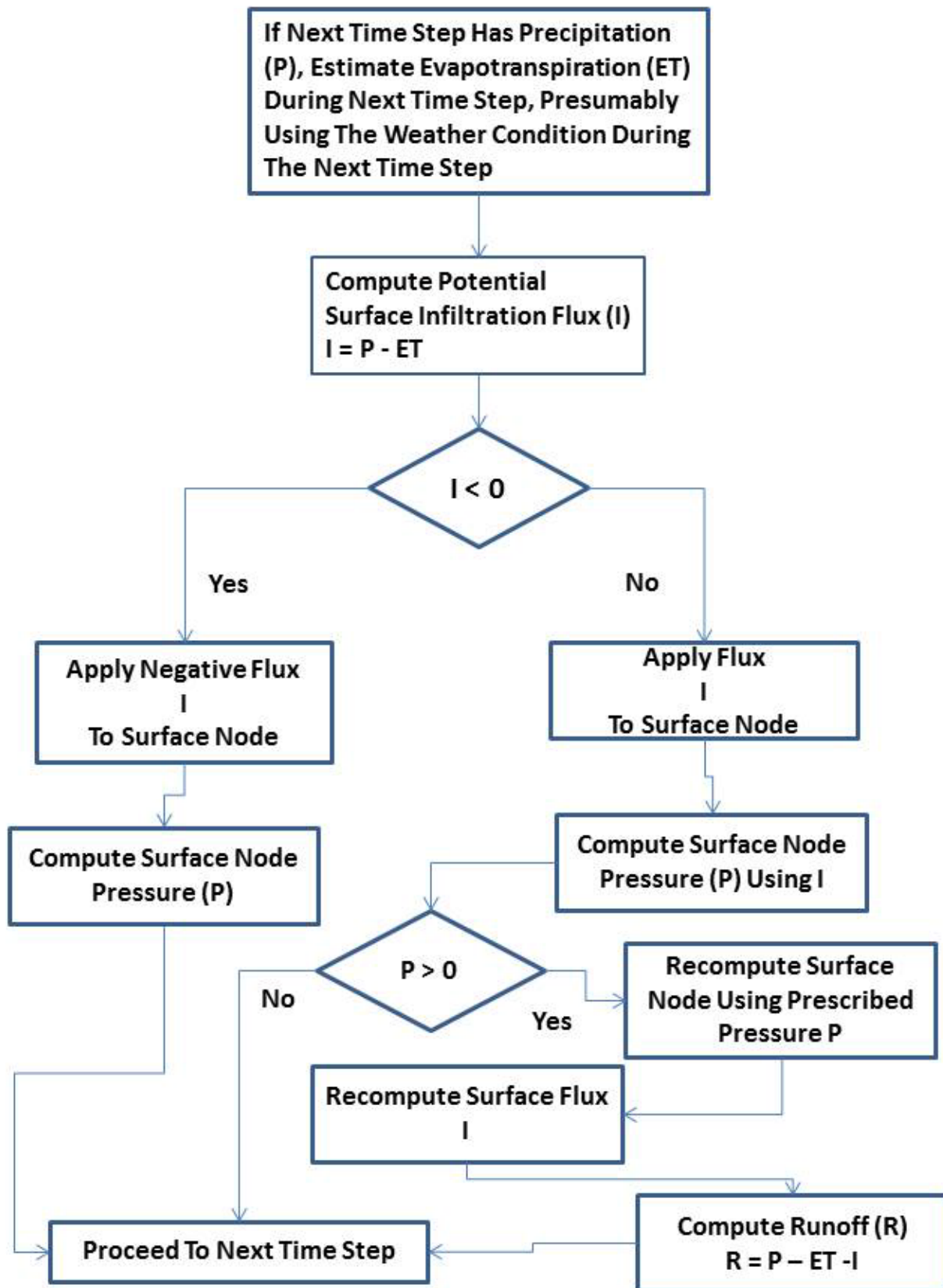


Figure 3-1. Flow Chart of the Vadose/W Algorithm Used to Compute Surface Flux

Because each day of the simulation may be adaptively subdivided into many time steps, particularly during intense precipitation events, this algorithm can, according to GEO-SLOPE International, Ltd. support personnel, result in bookkeeping errors in the water balance (Kelln, 2014). These bookkeeping errors affect the calculated total precipitation and runoff during the simulation, as well as the estimates of evapotranspiration and infiltration.

Runoff,  $R$ , as calculated above, either leaves the model domain or ponds in depressions in the surface mesh to re-infiltrate later. There is an explicit switch that allows water to either pond or runoff.

The actual evaporation [ $AE$ ] rate can be either independently specified, or computed from user-supplied potential evaporation [ $PE$ ], or else computed by the Vadose/W code using the following equation

$$AE = \frac{\Gamma Q_n + \eta E_a}{\Gamma + \eta A} \quad (3-2)$$

where

- $AE$  – Actual evaporation rate [L/t]
- $\Gamma$  – Slope of the saturated vapor pressure versus temperature curve [-]
- $Q_n$  – Net solar radiation flux at the surface [ $M \cdot L^2/t^2$ ]
- $\eta$  – Psychrometric constant [-]
- $E_a$  – Function of wind and relative humidity difference between soil and atmosphere [L/t]
- $A$  – Inverse of the relative humidity at the soil surface [-]

The relative humidity in the soil,  $R_h$  [-], is computed from

$$R_h = \frac{P_r}{P_{sat}} \exp \left[ \frac{\Psi_r M_w}{\rho_w R T} \right] \quad (3-3)$$

where

- $P_r$  – Water vapor pressure in the soil [ $M/L \cdot t^2$ ]
- $P_{sat}$  – Saturated water vapor pressure [ $M/L \cdot t^2$ ]
- $\psi_r$  – Pore water pressure [ $M/L \cdot t^2$ ]
- $M_w$  – Molecular weight of water [-]
- $\rho_w$  – Density of water [ $M/L^3$ ]
- $R$  – Gas constant [ $L^2/T \cdot t^2$ ]
- $T$  – Absolute temperature [T]

Given these relationships, the data needed for Vadose/W to simulate evaporation losses are the relative humidity, minimum and maximum temperature, and wind speed. Vadose/W uses functions of geographical location to compute net solar radiation, although the user can modify these functions based on the orientation of different parts on the numerical mesh.

Any precipitation that falls when the air temperature supplied by the user is less than 0 °C [32 °F] is assumed to be snow and can accumulate until the temperature rises above freezing, at which time the snowmelt can either infiltrate or runoff according the surface boundary flux algorithm. Water can also be lost through sublimation when snow cover exists; however,

Vadose/W documentation does not include a description of the sublimation algorithm. Sublimation rates are highest at temperatures of  $-1\text{ }^{\circ}\text{C}$  [ $30.2\text{ }^{\circ}\text{F}$ ] (Huang and Aughenbaugh, 1987) and are significantly dampened at both colder and warmer temperatures. Vadose/W does not report cumulative water lost as sublimation as a separate component of the cumulative water balance, but states that it can be computed by subtracting the cumulative water balance error from the sum of all other cumulative water balance components as the difference between the reported water balance and the water balance error [GEO-SLOPE International, Ltd, 2012, page 198]. For reference, over the 17-yr timeframe represented by the Fales Rock, Wyoming, climate record, which was used to drive simulations of the Gas Hills West site, approximately 8 percent of the simulated precipitation would have been in the form of snow and only a small fraction of that was likely lost through sublimation, thus the effect of uncounted sublimation of the water balance error may be small. Based on the Zuni Buttes climate record used for the Church Rock simulations, snow may represent approximately 12 percent of the total precipitation.

### 3.1.2 Transpiration

Environmental factors that affect the transpiration rate include air temperature, relative humidity, insolation, wind speed, and soil moisture; however, the calculation of transpiration does not directly depend on the surface flux algorithm. Vadose zone modeling of transpiration requires information such as Leaf Area Index [*LAI*] as a function of growing season, root growth relationship [i.e., seasonally varying root depth], and plant moisture limiting [*PML*] factor relationship [e.g., permanent wilting and limiting points]. Simulating transpiration requires either independent calculation of the transpiration flux or allowing Vadose/W to compute the flux based on soil moisture and climate conditions. Vadose/W combines a nodal root uptake source term with a surface energy term based on canopy cover to account for transpiration in the evapotranspiration process [Tratch, 1996]. Root uptake of soil water depends on root depth and pore water pressure. Under high evaporative demands or conditions of limited plant-available water, leaves close their stoma and reduce transpiration until the plant(s) reach their wilting point, whereupon leaves drop and tissues die.

#### *Leaf Area Index*

*LAI* describes vegetation–atmosphere interactions and essentially represents photosynthetic primary production or biomass production. *LAI* is geometrically defined as half of the total photosynthetic tissue [i.e., leaf] area per unit ground surface area [in units of  $\text{L}^2/\text{L}^2$ ], and it varies seasonally (e.g., see Figure 5-20).

In Vadose/W, the actual evaporation rate [*AE*] is computed as described in Eq. [3-1], but for a vegetated cover, *AE* is then reduced according to site-specific *LAI* using the equation

$$AE = AE[1 - [-0.21 + 0.7\sqrt{LAI}]] \quad (3-4)$$

such that a portion of the received net radiation is partitioned to the vegetation. Vadose/W sets *AE* to zero if *LAI* > 2.7 or to its maximum value if *LAI* is < 0.1 [Tratch, 1996].

The potential transpiration rate [*PT*], which is the energy available to the vegetation [*L/t*], is the following *LAI*-based modification of the potential evaporation rate [*PE*]:

$$PT = PE[-0.21 + 0.7\sqrt{LAI}]; \text{ however, } PT = PE \text{ if } LAI \text{ is greater than } 2.7 \quad (3-5)$$

*Root Depth vs. Growing Season Function*

When vegetation is modeled in Vadose/W, the seasonally variable root depth,  $R_T$  {in units of [L]}, over which the vegetative cover will extract water from the soil profile during the growing season must be specified as model input (e.g., see Figure 5-21).

### *Plant Moisture Limiting Factor*

The plant moisture limiting [*PML*] factor function (e.g., see Table 5-18; dimensionless) specifies the percentage decrease in a plant community's ability to uptake water as the pore water pressure increases. The *PML* function for water distress is typically S-shaped; the factor is always unity at a pore water pressure of 0 kPa [i.e., at complete saturation] and zero at the permanent wilting point [e.g., pore water pressure = -1,500 kPa]. The permanent wilting point is the pore water pressure at which some plants irreversibly wilt and stop transpiring; another important point on the curve includes the limiting point, which is the pore water pressure at which transpiration begins to decrease due to water distress.

### *Actual Transpiration*

At complete soil saturation, the full amount of solar radiation is applied to the roots according to the root depth vs. growing season function,  $R_T$ . If the soil is variably saturated, the actual transpiration rate [*AT*] [L/t] is the potential root water uptake rate (*PRU*) [L/t] reduced by the *PML*, i.e.:

$$AT = PML \cdot PRU \quad (3-6)$$

where

$$PRU = \frac{2PT}{R_T} \left(1 - \frac{R_n}{R_T}\right) A_n \quad (3-7)$$

*PT* – potential transpiration rate [L/t]

$R_T$  – total thickness of root zone [L]

$R_n$  – depth to the node in question [L]

$A_n$  – nodal contributing area of the node in question [L]

*PML*– user-specified plant moisture limiting factor at the current nodal soil pore water pressure.

### **3.1.3 Soil Freezing and Thawing**

Vadose/W also includes algorithms for simulating soil freezing and thawing, which is relevant in Wyoming and New Mexico, and the effects of these processes on the timing of infiltration pulses that may flow into the soil covers. Vadose/W provides two algorithms for computing soil freezing/thawing on its effect on the movement of water through the soil: a simplified thermal model and a full thermal model. Vadose/W offers two thermal material models: a simplified thermal soil model and a full thermal soil model. The simplified thermal soil model may be used when one is not concerned with the influence of soil temperature on evaporation and water flow. The simplified thermal soil model does not require thermal property functions of unfrozen volumetric water content; rather, it assumes that all water in the soil instantaneously changes phase at a single temperature. In reality, water in the soil column gradually changes phase over a finite temperature range, and water in a fine-grained material freezes more slowly and at colder subfreezing temperatures than does water in a coarse-grained material. Thus, it is understood that the simplified thermal material model better approximates the thermal behavior of coarse-grained materials than it does fine-grained materials. For the purposes of

understanding net infiltration into an earthen soil cover, the full thermal soil model may be preferable if cold weather hydrologic processes are important to the site water balance.

### Thermal Conductivity

Thermal conductivity ( $K_{th}$ ) characterizes the ability of a material to transmit heat by conduction. At soil temperatures greater than 0 °C [32 °F], thermal conductivity tends to increase with volumetric water content. At soil temperatures less than 0 °C [32 °F], thermal conductivity is generally greater than that at soil temperatures greater than 0 °C [32 °F] because the thermal conductivity of ice is much greater than that of water. Thus, the thermal conductivity of “frozen” soil is highly dependent on its unfrozen volumetric water content. Soil minerals also play a role; the clayey minerals of fine-grained material that might be used in a radon barrier tend to have lower thermal conductivities than those of quartz-dominated coarse, sandy tailings (Figure 3-2).

The simplified thermal material model assumes that the frozen and unfrozen thermal conductivities do not vary with unfrozen water content. In contrast, the full thermal material model defines thermal conductivity as a function of unfrozen volumetric water content.

For the full thermal model simulations documented in this report, staff used the method of Becker, et al. (1992) to create thermal conductivity vs. volumetric water content data point functions for soil cover and tailings materials consisting of gravel (or rock), sand, silt, and clay. This algorithm is based upon a set of soil particle-size-based coefficients of the following model for saturation ( $S$ ) as a function of soil thermal conductivity ( $K_{th}$ ):

$$S = \lambda_1 [\sinh(\lambda_2 K_{th} + \lambda_3) - \sinh(\lambda_4)] \quad (3-8)$$

where the  $\lambda$  coefficients for the various material types are published in Table 1 of Becker, et al. (1992). The mid-range  $\lambda$  values are for the mean of published soil thermal conductivity data, whereas the low and high values are for the extremes of published data (see also Figure 3-2).

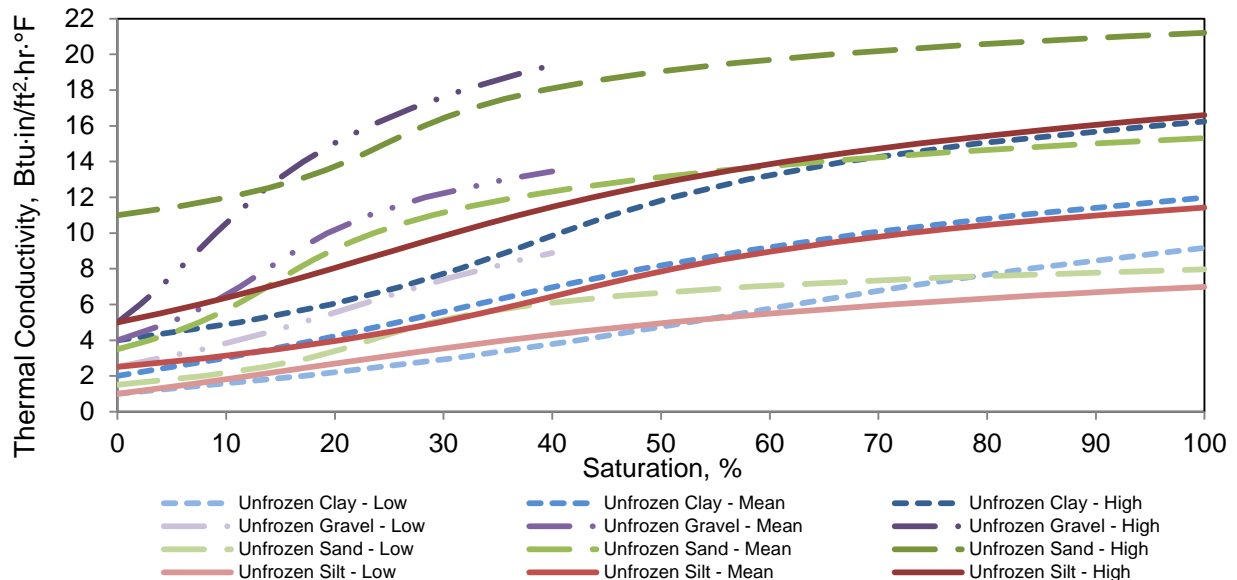


**Figure 3-2. The Becker, et al. (1992) Thermal Conductivity vs. Saturation Functions.**  
**1 kJ/d·m·°C = 12.456 BTU·in/ft²·hr·°F**

Given knowledge of the porosities of the various earthen soil cover and tailings materials, staff converted the saturations in Figure 3-2 into site- and layer-specific volumetric water contents for input into Vadose/W. The y-intercepts of the resulting functions are the dry soil thermal conductivity values. Use of the Becker, et al. (1992) correlations and resulting data point functions are preferred for estimating the unfrozen thermal conductivities rather than calling on Vadose/W to estimate the unfrozen functions with Johansen's (1975) correlation, because the latter is limited to soil saturations greater than 20 percent, which cannot be guaranteed in the arid western U.S. climates of Wyoming and New Mexico.

When solving a full thermal model in VADOSE/W, only the function for the unfrozen zone needs to be specified; the thermal conductivity in the frozen zone ( $K_{thf}$ ) will be back-calculated internally as a function of ice, water, air and soil mineral content. First, the frozen soil thermal conductivity at given volumetric water content (VWC) is calculated assuming all water is frozen (Johansen, 1975)

$$K_{thf} = (K_{thice})^{VWC} (K_{thsoil})^{1-VWC} \quad (3-9)$$

Then, the partially frozen soil thermal conductivity is assumed to be linearly partitioned between the fully unfrozen and fully frozen states by the ice content to water content ratio (GEO-SLOPE International, Ltd, 2012).

#### *Volumetric Heat Capacity*

Volumetric heat capacity characterizes the capacity of a volume of a material to store internal energy as heat while undergoing a temperature change that is not associated with a phase transition. In Vadose/W, the volumetric heat capacity function for the unfrozen zone is estimated based on the dry density of the soil and the sum of the specific heat capacities of its different constituents (namely soil and water, neglecting air). Staff used the de Vries (1963) estimation routine in Vadose/W to construct the unfrozen volumetric heat capacity function. This involves identifying the soil moisture characteristic function for the specific material to delimit the range of water contents over which the volumetric heat capacity must be defined, and the mass specific heat of the soil minerals {generally 0.71 kJ/kg·°C (0.17 Btu/lb·°F)}<sup>1</sup>. The y-intercepts of the resulting functions are the dry soil volumetric specific heat capacities. The volumetric heat capacity of the frozen zone is internally computed as a function of ice, water, and soil mineral contents using relationships described in GEO-SLOPE International, Ltd. (2012).

### **3.2 Numerical Flow Model**

Vadose/W solves for pore water pressure and soil temperatures using the finite-element method. Details of the numerical solution algorithms are presented in GEO-SLOPE International, Ltd (2012) and are discussed here only as they affect the accuracy of the simulations. Vadose/W finite-element meshes are created in one or two dimensions, allowing the construction of model domains in vertical cross-sections through tailings impoundments. Meshes are created by defining the boundaries and geometry of the model domain using points and boundary lines and defining node spacing along boundary lines. The finite-element meshes within the model domain are created by the code, with user control over the types of elements to

<sup>1</sup> The Vadose/W module of GeoStudio 2012 had a typographical error in the de Vries estimation routine user interface, wherein it asked for mass specific heat of the soil minerals in units of kJ/g·°C, yet the value had to be entered in units of kJ/kg·°C. CNWRA staff alerted GEO-SLOPE International, Ltd personnel to this problem, and it was fixed in a subsequent version release of the code.

be created: i.e., triangular or quadrilateral. Quasi-one-dimensional models are constructed by defining nodes only along the lateral boundaries of the model domain.

Pore water pressures and temperatures are computed at the nodes based on water and heat fluxes across the element faces. Vadose/W water fluxes and pore water pressures are computed considering both liquid and vapor flow. The liquid flux is based on Richards Equation and the vapor flux based on Fickian diffusion and the water vapor pressure, which is temperature dependent.

Soil water characteristics, which determine the change in water content and effective hydraulic conductivity as functions of pore water pressure, can be defined using analytical expressions, such as the van Genuechten model, or tabulated data point functions. Material properties affecting heat transport, thermal conductivity and heat capacity can also be defined using analytical or tabular data point functions.

In addition to the upper climate boundary condition, for which the surface flux is computed by the algorithm described in Section 3.1, specified pressure and flux hydraulic boundary conditions can also be defined. A third type of boundary condition, described as free drainage or unit gradient also may be defined. The free drainage boundary condition or equivalent was used at the lower boundary condition for the simulations presented here. This boundary condition assumes that liquid water drains by gravity so that the rate of drainage depends only on the pore water pressure at the boundary and the resulting hydraulic conductivity.

The choice of thermal boundary conditions is similar to those for the hydraulic boundaries: climate, specified temperature, specified heat flux, or unit heat flux.

### 3.3 Model Limitations

In evaluating the performance of Vadose/W for the purposes of estimating net infiltration through uranium mill tailings impoundment earthen covers, it is important to note that the water balance estimates from the simulations are more important than accurate estimates of the pore water pressures within the cover and underlying tailings. This is because net annual infiltration, if any, is likely to be a small percentage of the annual precipitation and annual water balance at these semi-arid and arid site locations. Thus, small errors in computing the precipitation and runoff, possibly due to bookkeeping errors, can result in large relative errors when comparing the net infiltration computed from boundary fluxes or the change in storage to the net infiltration based on the surface water balance. The net infiltration [ $I$ ] into the subsurface model mesh can be computed from the components of the water balance reported by Vadose/W as

$$I = P - R - ET + Q_B \quad (3-10)$$

where  $ET$  is the evapotranspiration and  $Q_B$  are the boundary flows at prescribed pressure or flow boundaries. The net infiltration can also be estimated from the change in storage reported by the code, or as the simulation approaches steady-state from the flux across the lower boundary of the model domain. For the simulations of the Title-II-In-Closure sites studied here, experience indicates that simulations would only approach steady-state after hundreds or thousands of years due to the relatively low permeability of the tailings, so the change in storage [ $\Delta S$ ] must be relied on in computing the water balance error which is

$$\Delta S + \epsilon_S - I + \epsilon_{NI} = \text{absolute error} \quad (3-11)$$

where  $\epsilon_S$  is the error in the change in storage and  $\epsilon_{NI}$  is the error in net infiltration.

Because Vadose/W hydrologic solutions are in terms of pore water pressure, the change in storage is computed from the change in pore water pressure based on the soil water characteristic functions relating volumetric water content to pore water pressure. The error in computing  $\Delta S$  can result from errors in interpolating tabulated soil water characteristic functions or from non-convergence of the pore water pressure solution at particular nodes during the simulation, whereas the error in  $NI$  appears to be due to the bookkeeping problems of the code. When both  $\Delta S$  and  $NI$  are small, error can be significant and, as will be discussed in later sections of this report,  $\Delta S$  can be negative, implying a net drying of the model domain, whereas  $NI$  can be positive, implying net infiltration during the course of the simulation, or vice versa. Such discrepancies make it difficult to evaluate the accuracy of simulation results with respect to whether or not net infiltration is occurring through the earthen cover.

With respect to the errors in computing the change in storage, extreme temporal or spatial changes in pore water pressures can cause errors in the computed change in storage due to either small numerical errors in computing the pore water pressures or non-convergence of the pore water pressure solution at particular nodes<sup>2</sup>. In the case of the following Title-II-In-Closure simulations, these extreme conditions most commonly occur at the surface of the cover, which becomes extremely dry (large negative pore water pressures) between precipitation events or at boundaries between coarse- and fine-grained material layers. Based on the experience of others who have used Vadose/W for similar purposes [Benson, et al. 2004, 2005; Bohnhoff, 2005; Khire and Mijares, 2008; Bohnhoff, et al., 2009; Mijares, et al., 2010], very fine node spacings, on the order of millimeters, may be required to obtain water balance errors of less than 1 mm/yr, based on Equation 3-11. Simulation results obtained from the Title-II-In-Closure site models reported in the following sections indicates that even use of very finely discretized elements does not always result in acceptable water balance errors.

---

<sup>2</sup> Note that Vadose/W simulations continue to run even when pressure and temperature solutions do not converge at some nodes.

## 4 GAS HILLS WEST MODEL AND SIMULATION RESULTS

### 4.1 Description of the Gas Hills West Model

The model for the Gas Hills West site was developed for Pond 2. Figure 4-1 is an illustration of the general construction of the cover planned for Pond 2. Drawings of the as-built cover are not available.

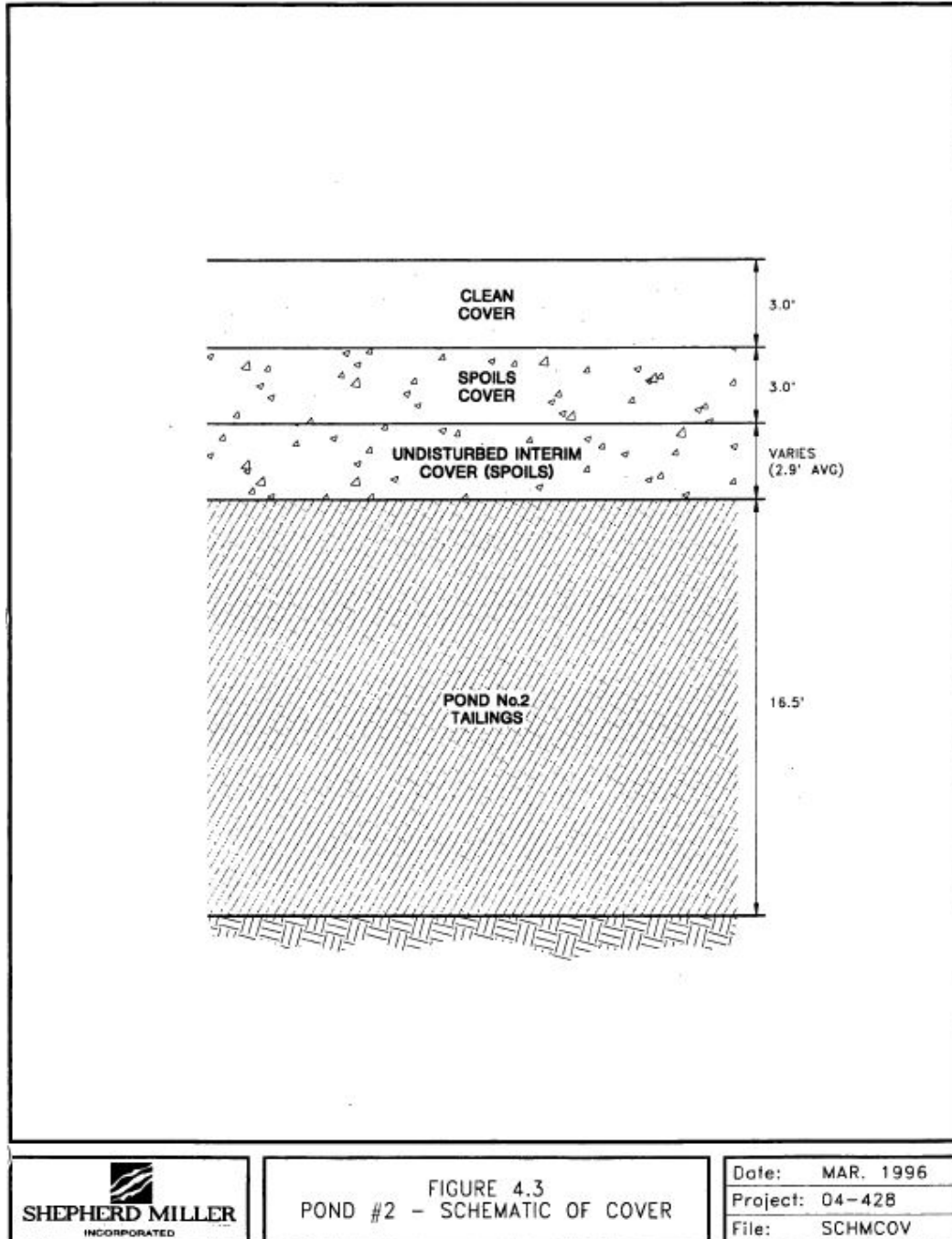


Figure 4-1. Schematic Showing Planned Cover Construction for Pond #2 at the Gas Hills West Site (Shepherd Miller, 1996)

According to soil boring logs in the reclamation plan, the interim cover is characterized as sandy, silty clay with gravel (logs for T-21 through T-25) [Figure 4-2]. The underlying tailings vary from sandy silt [SM] near the top of the impoundment to lean clay [CL] near the edge of the tailings as illustrated in Figure 4-2. The tailings were described as moist to wet at the time of the investigation.

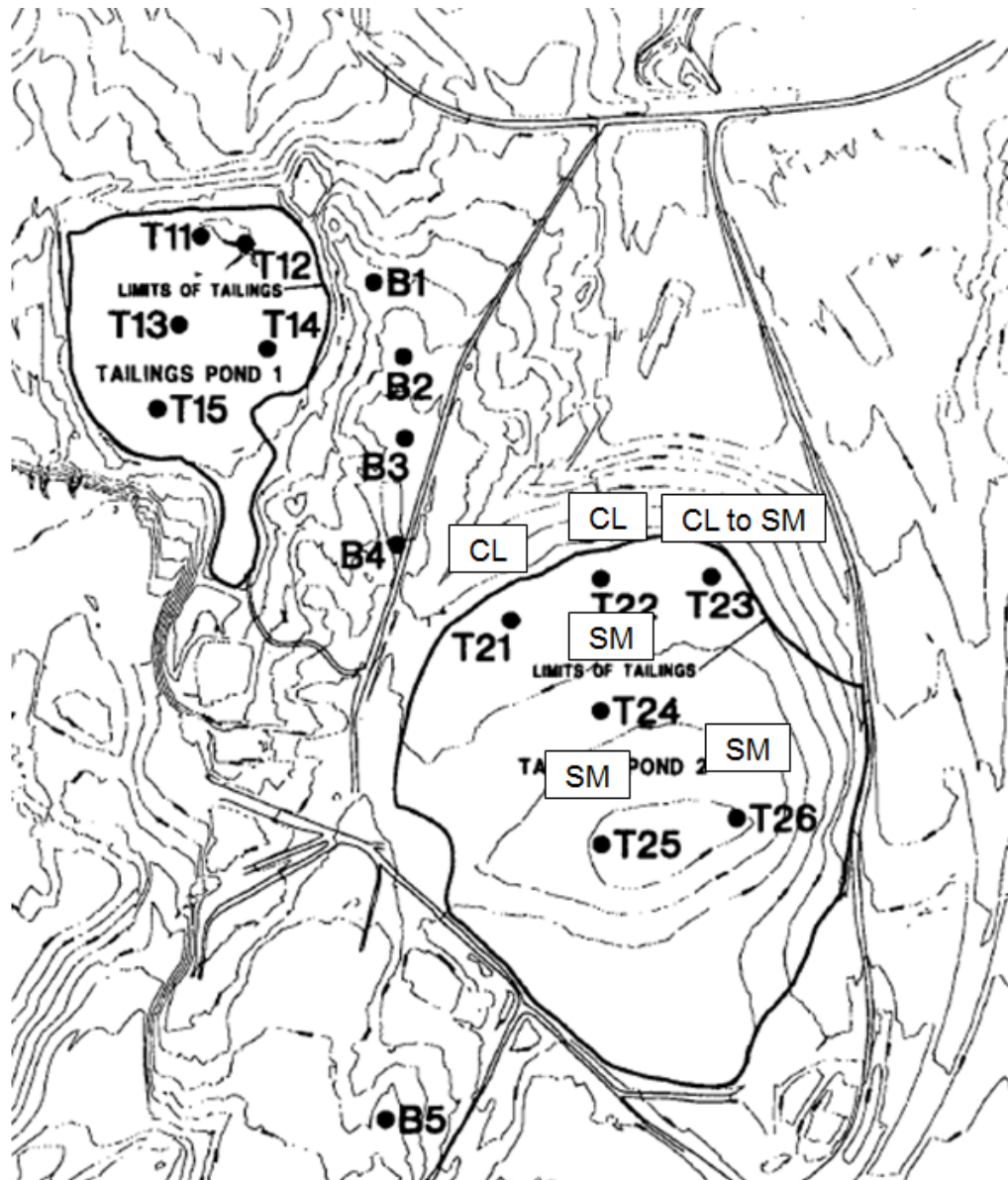
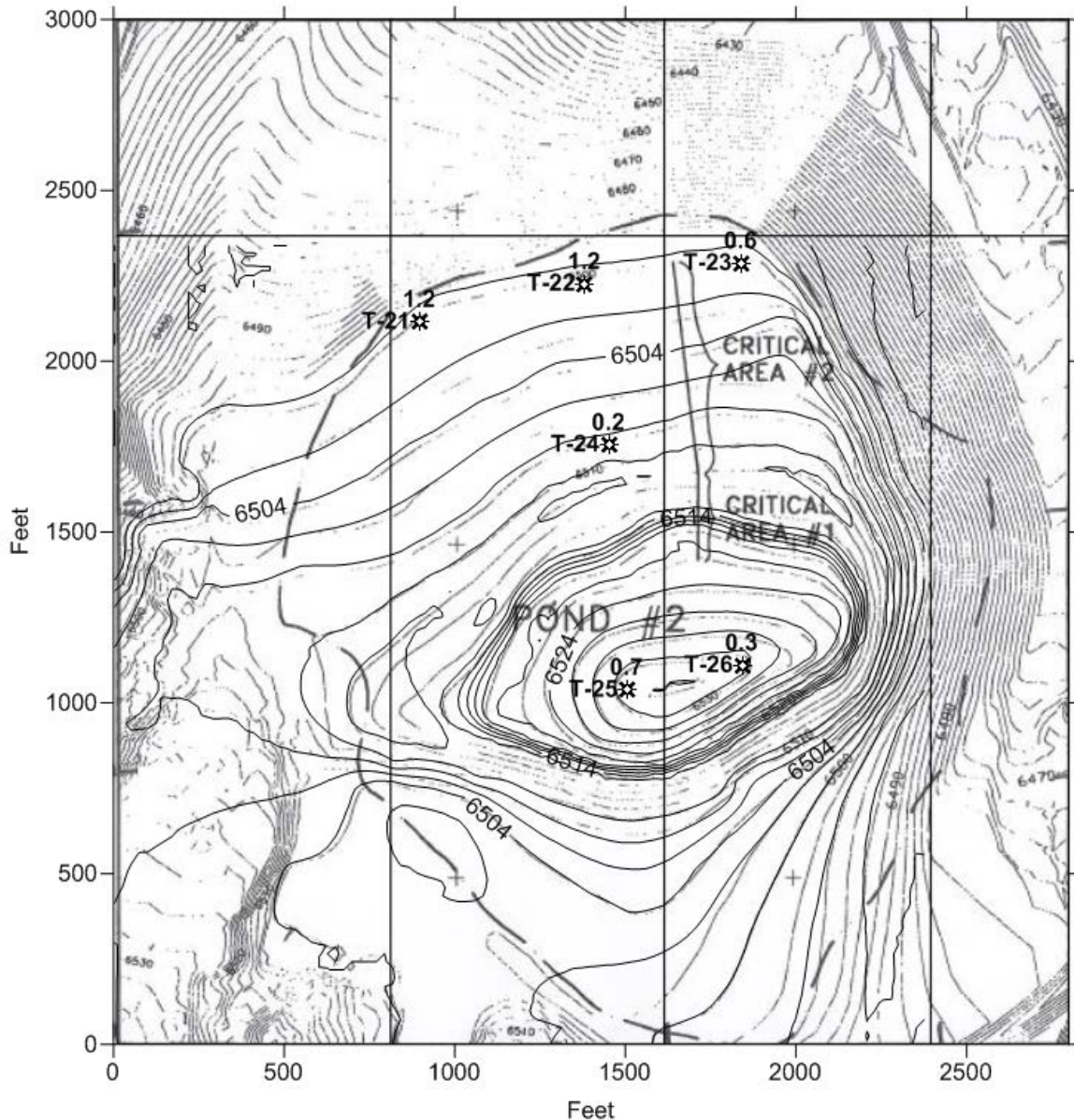


Figure 4-2. Locations of Soil Borings through Interim Cover with Soil Classifications. Boxes Show Soil Classification of Tailings (modified from Figure A-1, Shepherd Miller, 1996)

Although the reclamation plan states that the interim cover averages 2.9 ft [0.9 m] in thickness, the soil boring logs indicate that the interim cover is as thin as 8 inches [0.2 m] near crest of Pond 2 and increases to approximately 48 inches [1.2 m] near the edge of the tailings [Figure 4-3].



**Figure 4-3. Approximate Soil Boring Locations and Interim Cover Thickness in Meters (1 meter = 3.28 ft)**

For modeling purposes, the interim cover thickness was assumed to vary with elevation according to the quadratic function shown in Figure 4-4. A constraint point was added to prevent the function from being less than zero. The correlation was done by subtracting 6400 ft [1951 m] from the actual cover elevations.

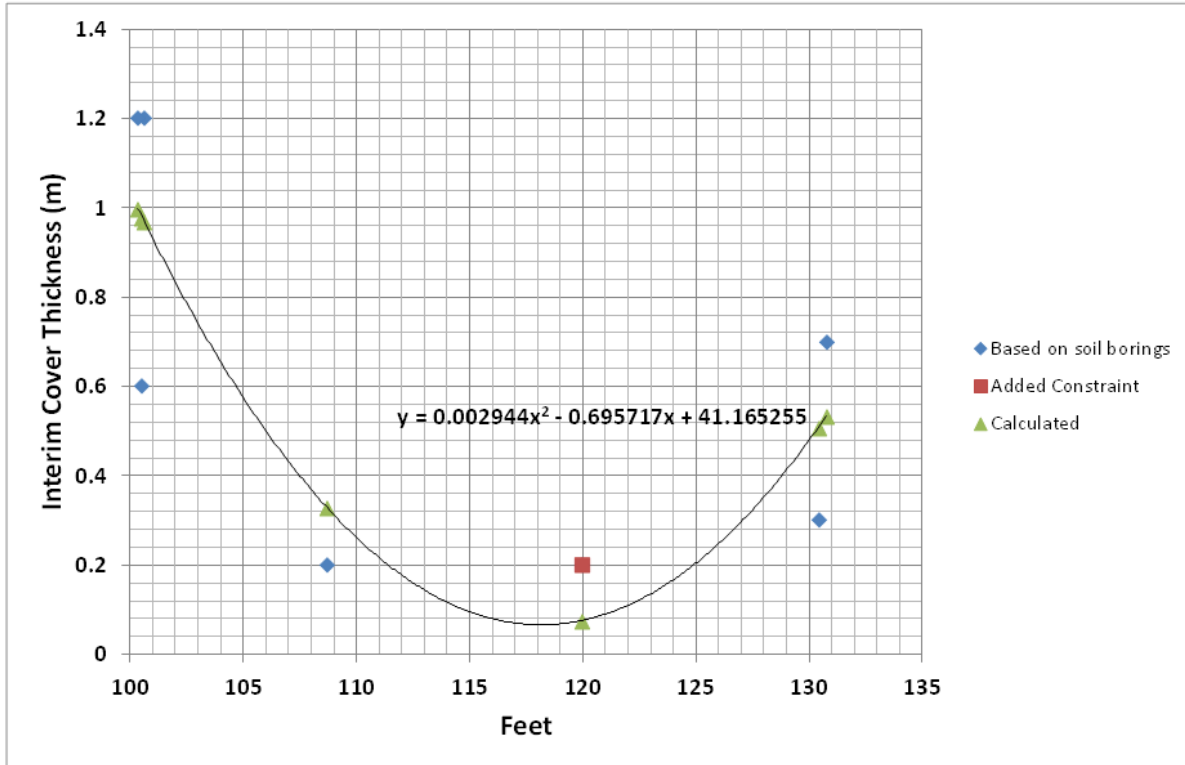


**Figure 4-4. Function Describing Interim Cover Thickness Based on Soil Boring Logs**

The reclamation plan states that the radon barrier will consist of 3 ft [0.9 m] of “mine spoils” and 3 ft [0.9 m] of “clean borrow”. Because the interim cover is described as “mine spoils,” the first 3 ft [0.9 m] of the radon barrier were assumed to consist of the same material as the interim cover, that is, sandy silty clay. The properties assumed for the mine spoils and clean borrow in the radon modeling (Shepherd Miller, 1996) were similar; the only difference being the mine spoils was assigned a porosity of 0.4 and the clean borrow a porosity of 0.39. Thus, the clean borrow is assumed to be a sandy silty clay similar to the mine spoils. The overlying erosion barrier was specified as 3 in [0.08 m] of 1.5 in [3.8 cm] median diameter gravel.

#### 4.1.1 Model Domain and Grid

The model for Pond 2 was initially planned to be constructed as a two-dimensional cross-section along the slope of Pond 2. As will be explained later, the model domain was reduced to one-dimension due to convergence and water balance problems with the simulations. The two-dimensional cross-section model is described here for completeness and because the one-dimension model was extracted from it.

As-built drawings of the final soil cover are not available. The proposed final cover elevations were digitized from Figure 5.5 in Shepherd Miller [1996] and then contoured using Surfer 10™. The proposed final contours are assumed to represent the elevation after adding 3 ft [0.8 m] of mine spoils and 3 ft of clean borrow. Thus, the original tailings surface would be at an elevation of  $z_{tailings} z_{final} - 6 ft - b_{interim}$  where  $z_{final}$  is the final cover elevation and  $b_{interim}$  is the interim cover thickness.

The two-dimensional model was constructed along the transect shown in Figure 4-5. The transect generally follows the slope of the final soil cover and extends to the edge of the tailings deposit.

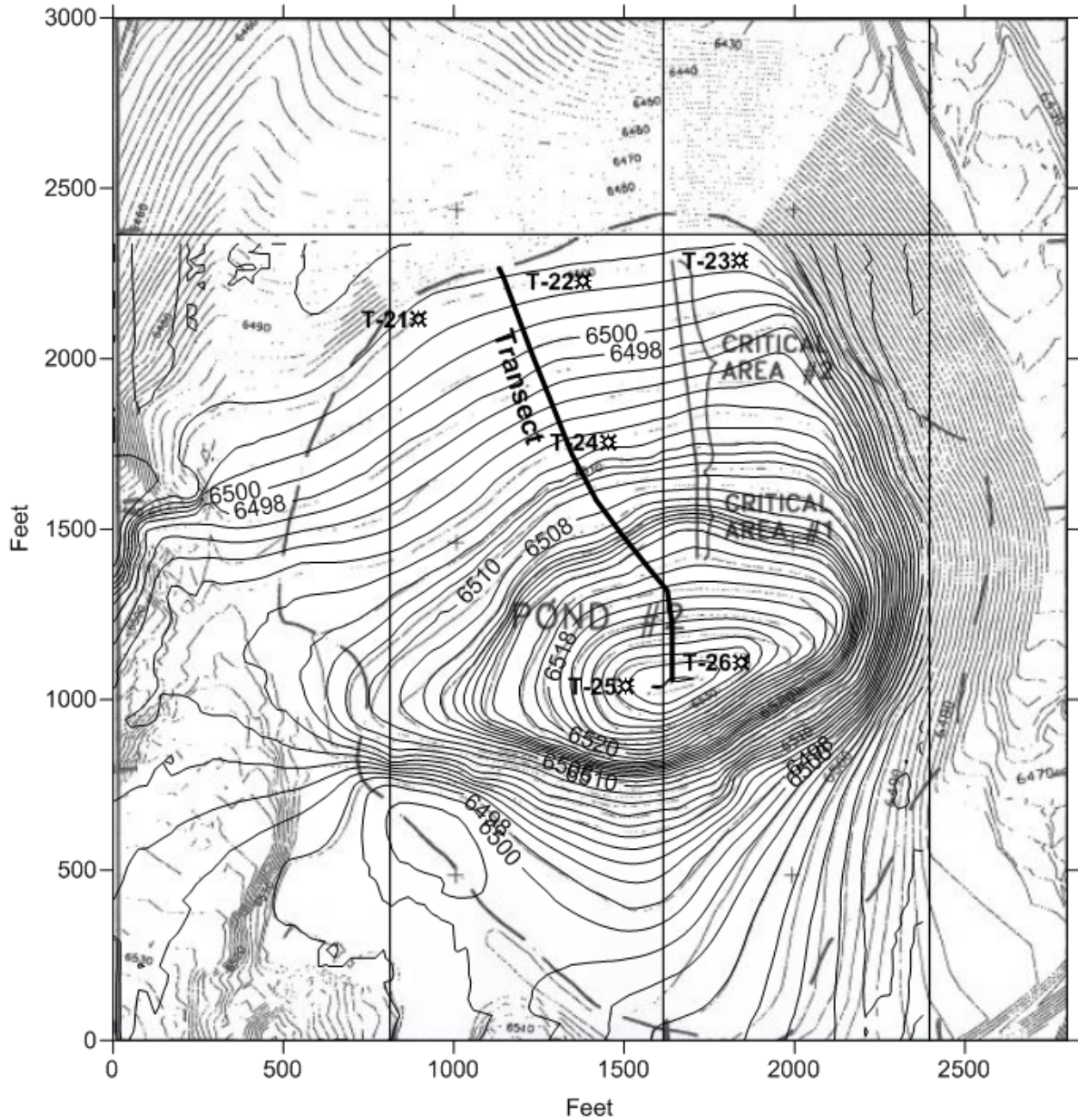
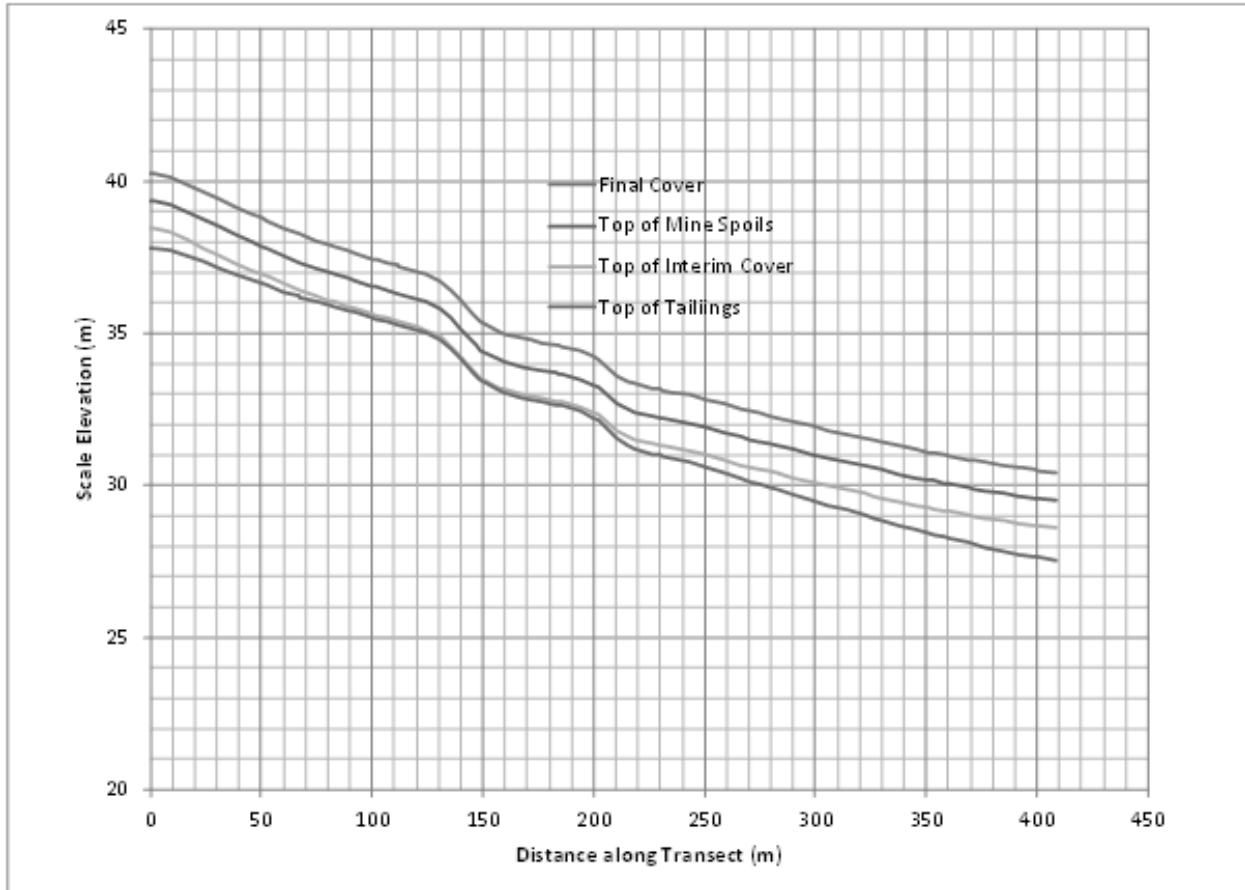


Figure 4-5. Transect Used to Construct Two-Dimensional Model (Contours are Proposed Final Cover Elevations from Shepherd Miller, 1996)



**Figure 4-6. Profiles of Cover Layers at Gas Hills West Pond 2 Along Model Transect**

Figure 4-6 shows the scaled elevation of the layers included in the model. The elevations were scaled to an absolute elevation of 6400 ft [1950 m] above mean sea level and distances and scaled elevations converted to meters.

Based on a photo from the September 10, 2001 inspection report [ML012570148] of the top of Tailings Pond 2 looking northwest (Figure 4-7), the surface appears to be covered with rock mulch with some sparse grass as opposed to the gravel rip rap referenced in the reclamation plan. Due to limited information on the state of vegetation at the site, the site was modeled without vegetation, which would lead to possible over-estimation of net infiltration.

No information is available on the original ground surface or the surface on which the tailings were placed. In addition, the tailings were re-graded, making it difficult to set a lower physical boundary for the tailings.



**Figure 4-7. Top of Tailings Pond 2 Looking Northwest  
[from the September 10, 2001 inspection report (ML012570148)]**

Pond 2 appears to have been constructed in a drainage channel based on this Google Earth image shown in Figure 4-8.



**Figure 4-8. Satellite Image of Gas Hills West Pond 2 from October 7, 2004  
(from Google Earth™)**

The tailings may or may not have been impounded behind an initial embankment in the drainage channel. An embankment was assumed to have been constructed to retain the tailings as they were deposited. The original ground surface beneath Pond 2 was estimated from the 1957 topography shown on United States Geological Survey 7.5 minute topographic map for the Puddle Springs Quadrangle. The original surface elevation was then computed starting from an elevation of 6460 ft MSL [1970 m] at the approximate location of the transect through Pond 2 used to determine impoundment surface elevation. The relationship between the estimated original land surface and the proposed reclaimed tailings is shown in Figure 4-9.

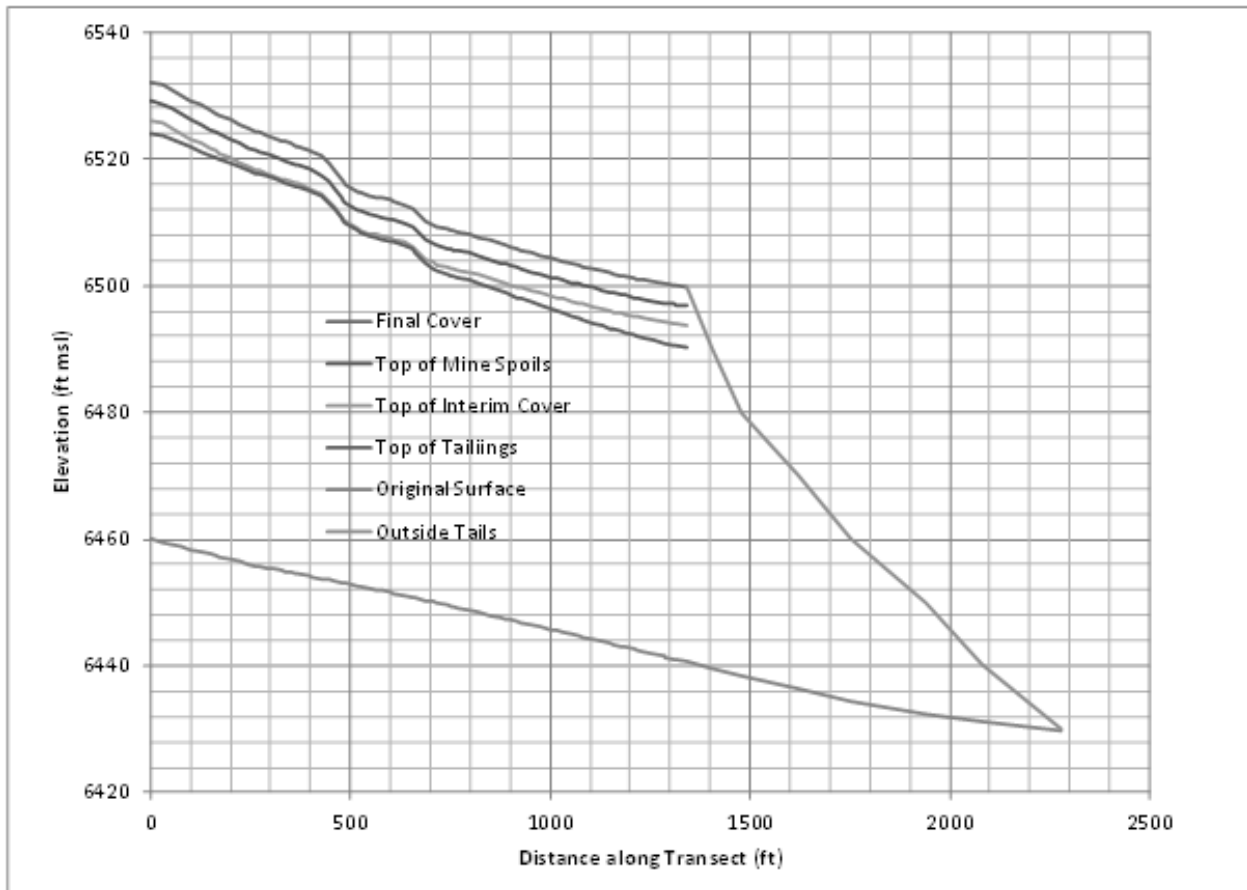


**Figure 4-9. Estimated Original Ground Surface in Relation to Impound Topography**

No information is available on the geometry of the original tailings embankment, but because the tailings pond was constructed in Willow Springs Draw, there is an assumed embankment. Based on the slope of the topography north of Pond 2 shown in Drawing 4 from the reclamation plan (Shepherd Miller, 1996), the slope outside the area identified as containing tailings was approximately 7 horizontal to 1 vertical. This was assumed to have been the slope of both upstream and downstream sides of the original embankment, although the embankment may have been constructed over time and built over some of the tailings deposits. The resulting configuration along the transect is shown in Figure 4-10. The actual distribution of tailings and the embankment material is likely to be more complex.

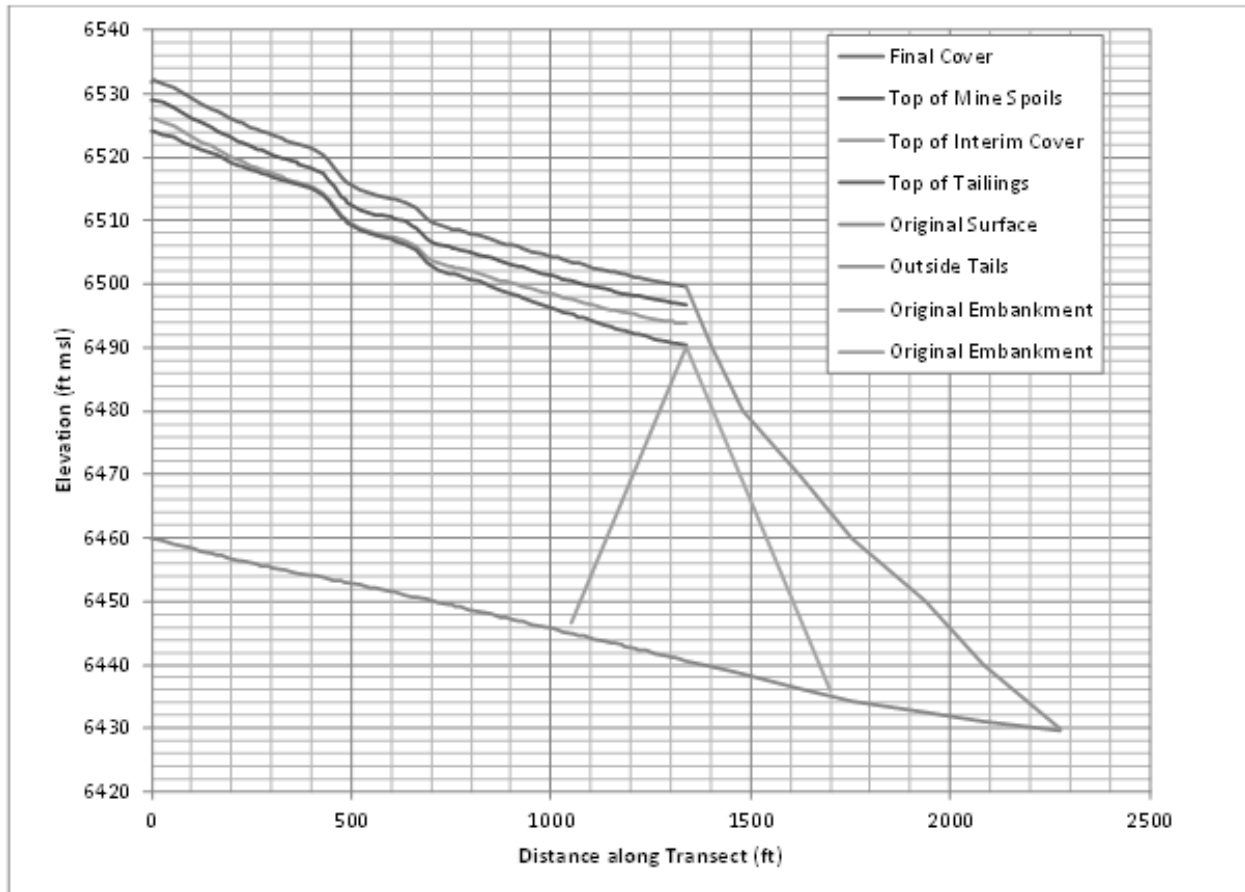


**Figure 4-10. Configuration of Impoundment Embankment Used to Construct Two-Dimensional Model**

#### 4.1.2 Material Properties

The following soil types were assigned to the model layers based on descriptions of the soil types in reclamation plan and soil boring logs (Shepherd Miller, 1996):

- Original Alluvium: silty sand
- Original Embankment: clean borrow consisting of sandy, silty clay
- Tailings: sandy silt (sandy loam) to lean clay
- Interim Cover: sandy, silty clay
- Mine Spoils: sandy, silty clay
- Clean Borrow: sandy, silty clay
- Erosion Barrier over Tailing: silty sand (loamy sand) with porosity and hydraulic conductivity reduced for gravel
- Erosion Barrier over Embankment: 3-inch median diameter rock.

Because no direct measurements of soil water characteristics were available for the materials comprising Pond 2, the following average properties were assigned based on Table 4 in Rawls, et al. (1989):

| Material                            | Model Layers   | VWC (m <sup>3</sup> /m <sup>3</sup> ) |       | Bubbling Pressure [kPa (ft H <sub>2</sub> O)] | van Genuchten λ | K <sub>sat</sub> (m/day) ft/day |
|-------------------------------------|--|---------------------------------------|-------|---|-----------------|---------------------------------|
|                                     |  | sat                                   | res   |   |                 |                                 |
| Sandy, silty clay (sandy clay loam) | Parts of tailings, interim cover, mine spoils, clean borrow, original embankment | 0.39                                  | 0.068 | 5.79 (1.93)                                   | 0.319           | 0.103 (0.337)                   |
| Lean clay (clay)                    | Parts of tailings  | 0.47                                  | 0.09  | 8.35 (2.78)                                   | 0.135           | 0.014 (0.047)                   |
| Sandy silt (sandy loam)             | Original alluvium, parts of tailings   | 0.45                                  | 0.041 | 2.95 (0.98)                                   | 0.378           | 0.622 (2.04)                    |
| Silty sand (loamy sand)             | Tailings Erosion barrier   | 0.13                                  | 0.006 | 1.57 (0.52)                                   | 0.394           | 0.186 (0.61)                    |

The properties for the rock mulch were based on those for silty sand assuming that the rock occupied 70 percent of the bulk volume, leaving 30 percent for the silty sandy. Thus, the bulk porosity was 0.3 times the saturated porosity of the silty sand and the bulk saturated hydraulic conductivity was 0.3 times the saturated hydraulic conductivity for silty sand. The bubbling pressure and van Genuchten are those for silty sand. The variations of pore water pressure and hydraulic conductivity with water content were modeled using the van Genuchten model (van Genuchten, 1980) given by

$$\frac{VWC - VWC_{res}}{VWC_{sat} - VWC_{res}} = [1 + (\alpha\Psi)^n]^{-m} \quad (4-1)$$

VWC – volumetric water content [L<sup>3</sup>/L<sup>3</sup>]

VWC<sub>res</sub> – residual volumetric water content [L<sup>3</sup>/L<sup>3</sup>]

VWC<sub>sat</sub> – saturated volumetric water content (porosity) [L<sup>3</sup>/L<sup>3</sup>]

α – air entry parameter [1/P], equivalent to 1/h<sub>B</sub> where h<sub>B</sub> is the air entry or bubbling pressure

n and m are related to the pore size distribution parameter λ by

$$n = \lambda + 1 \text{ and} \\ m = \lambda / (\lambda + 1) = \lambda / n$$

Ψ – pore water pressure [P]

and

$$K(VWC) = K_{sat} \left\{ \frac{VWC - VWC_{res}}{VWC_{sat} - VWC_{res}} \right\}^n \left\{ 1 - \left( 1 - \left[ \frac{VWC - VWC_{res}}{VWC_{sat} - VWC_{res}} \right]^{1/m} \right)^m \right\}^2 \quad (4-2)$$

K<sub>sat</sub> – saturated hydraulic conductivity [L/t].

Negative pore water pressure (i.e., suction) as a function of volumetric water content for the modeled materials are shown in Figure 4-11 (based on the van Genuchten model); Figure 4-12 shows the corresponding variation in hydraulic conductivity.

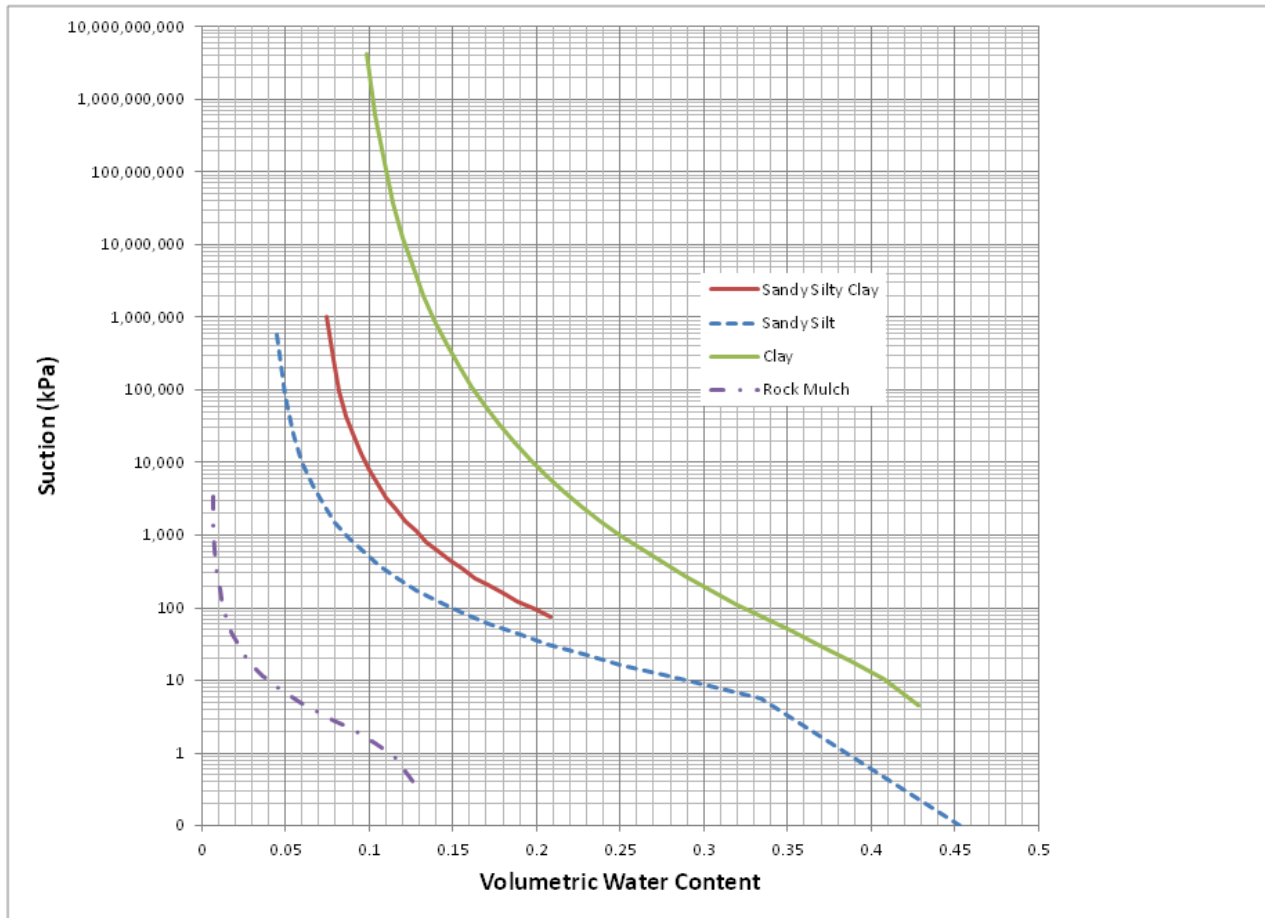


**Figure 4-11. Variation of Pore Water Pressure with Volumetric Water Content in the Gas Hills West Pond 2 Model (1 kPa = 0.33 ft H<sub>2</sub>O)**

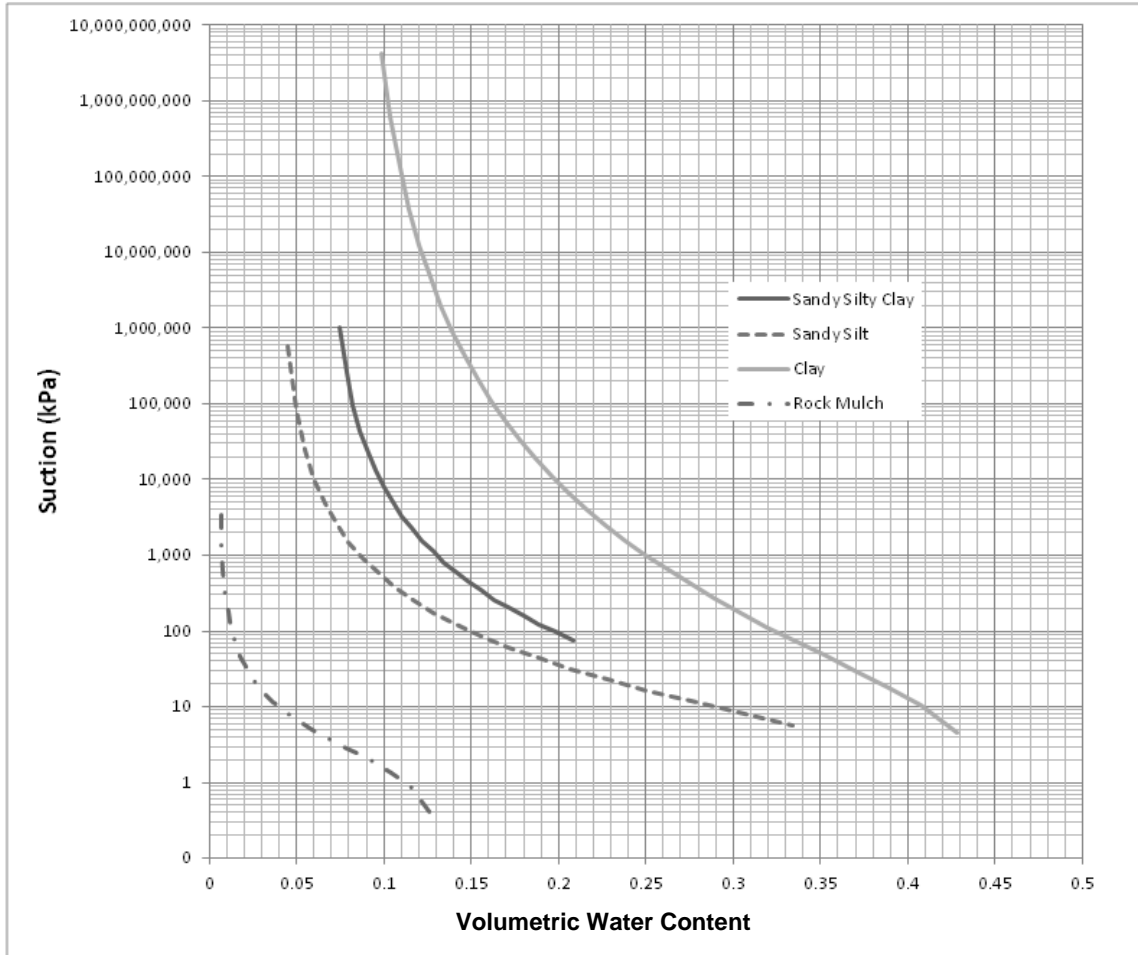


**Figure 4-12. Variation of Hydraulic Conductivity with Volumetric Water Content in the Gas Hills West Pond 2 Model**

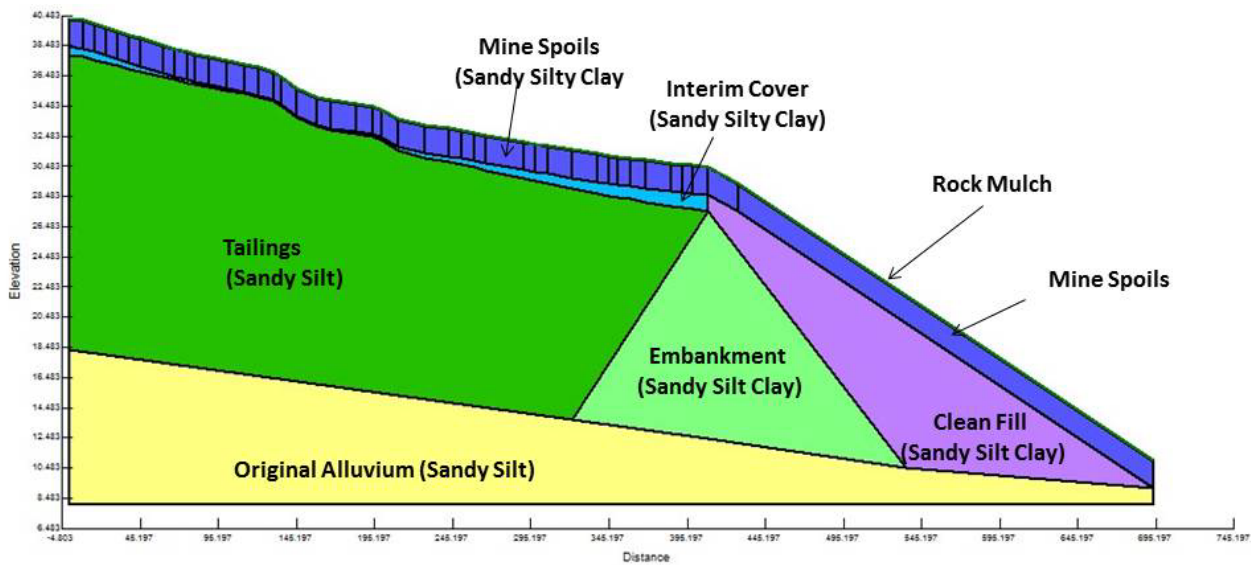


**Figure 4-13. Material in the Two-Dimensional Gas Hills West Pond 2 Model**

The two-dimensional model proved to be impractical for use based on long simulation times and the fact that Vadose/W does not route runoff across the surface of the model, although runoff can accumulate in any low spots on the model grid surface. For these reasons, a one-dimensional column was extracted from the two-dimensional model to further investigate potential net infiltration at the site.

The 1-dimension model, shown in Figure 4-14, was extracted from the middle portion of the two-dimensional model. The 1-dimension model was truncated in the tailings based on preliminary simulations that indicated that the underlying alluvium did not influence the simulation results. The erosion barrier (rock mulch) was assigned a thickness of 3 in [0.076 m]; the mine spoils a thickness of 6 ft [1.8 m], and the interim cover a thickness of 2 ft [0.63 m].

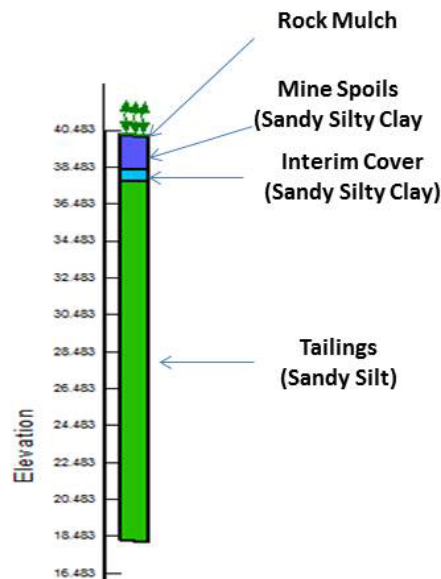


**Figure 4-14. Materials Used in the One-Dimensional Gas Hills West Pond 2 Model. Vertical Elevation in Meters (1 m = 3.28 ft).**

Due to the similarity of soil types at this site and the lack of detailed information on soil properties, uniform values of thermal conductivity (20 kJ/day·m·°C [3.2 BTU/day·ft·°F] unfrozen, 2 kJ/day·m·°C [0.32 BTU/day·ft·°F] frozen) and volumetric specific heat (2,500 kJ/m<sup>3</sup>·°C [37 BTU/ft<sup>3</sup>·°F] both unfrozen and frozen) were assigned to the materials in the model. The simulations were performed with the simplified thermal model in Vadose/W.

### 4.1.3 Boundary Conditions

Two types of boundary conditions were applied to the surface of the model: specified flux and climate. The specified flux boundary condition was used to create a quasi-steady state pore water pressure distribution as described in Section 4.1.4.

Climate-driven boundary conditions in Vadose/W are applied in two ways. Weather records (precipitation, air temperature, wind speed, and relative humidity) are used to calculate the water flux applied to the surface of the model grid. These parameters, along with calculated pore water pressures, are used to calculate the evaporative and transpirative fluxes from elements below the surface that are defined as having climate-driven boundary conditions, which were assigned to the rock mulch and mine spoils zones of the model. However, due to the lack of specific information on vegetation at the site, the simulations were performed without vegetation.

The climate record was based on the meteorological record from the Remote Automated Weather Station (RAWS) at Fales Rock, Wyoming (latitude 42.8568 °N, longitude -107.2722 °E, elevation 6380 ft msl [1945 m]), obtained from Western Regional Climate Center (2015a). This station is the closest RAWS station to Gas Hills West [approximately 29 km (18 mi)] east, Figure 4-15) and has a 17-yr record (i.e., 6/25/1997 through 6/12/2014). The station record includes

- Minimum and Maximum Daily Temperature
- Minimum and Maximum Daily Relative Humidity
- Total Daily Liquid Precipitation
- Daily Average Wind Speed

that are required as input to Vadose/W.

Some daily climate data were missing from the Fales Rock RAWS record. Missing records were replaced by the average values over the period of record. The Fales Rock RAWS precipitation data were checked to see if they were representative of long-term precipitation records for Central Wyoming by comparing the return interval for daily precipitation for the Fales Rock RAWS data with the 2, 5, 10, 25, 50 and 100-yr 24-hr precipitation events from the Western U.S. Precipitation Frequency Maps (<http://www.wrcc.dri.edu/pcpnfreq.html>, Western U.S. Precipitation Frequency Maps, NOAA Atlas 2 published in 1973, accessed June 16, 2014). The liquid precipitation records for Fales Rock are shown in Figure 4-16. In the future, modeling should also account for solid precipitation by creating a representative hybrid precipitation record that appropriately weights relevant SNOTEL<sup>3</sup> solid precipitation data for the Fales Rock region.

---

<sup>3</sup> SNOTEL is an automated system of more than 600 snow telemetry stations operated by the Natural Resources Conservation Service in the Western United States.

Figure 4-17 compares the daily precipitation event frequencies from the Fales Rock data with a best fit regression through the precipitation events from the Western Wyoming frequency maps, and the recurrence interval of precipitation events inferred from the regression. Although the Fales Rock record underestimates the intensity of precipitation events with return intervals less than 5 yrs compared to the extrapolated Western Wyoming frequency maps, it contains two relatively large precipitation events with return intervals of approximately 5 and 30 yrs. Based on this comparison, the Fales Rock data were considered adequately representative of current climate at the site.

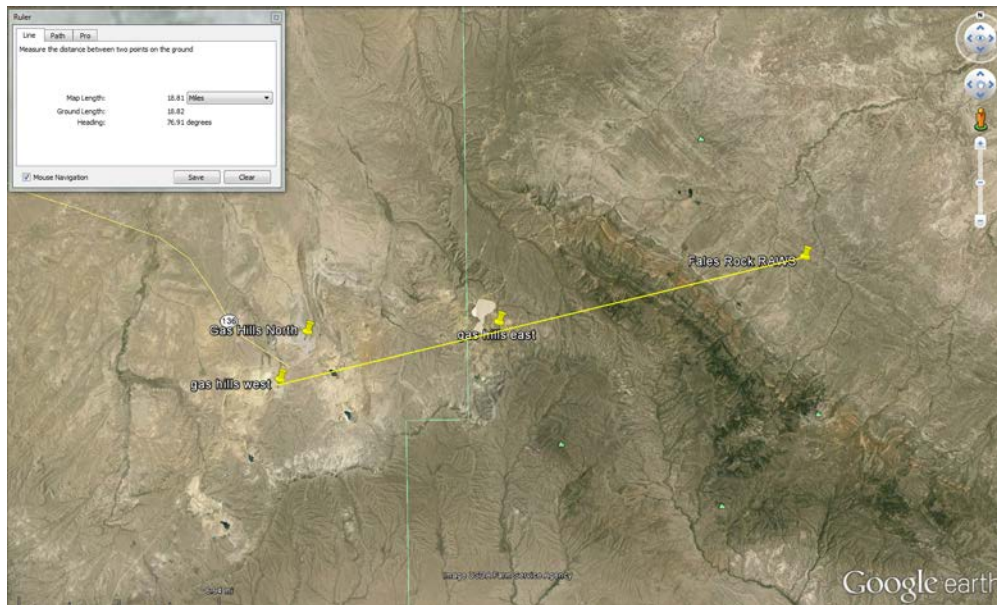


Figure 4-15. Location of the Fales Rock RAWS with Respect to Gas Hills West Site

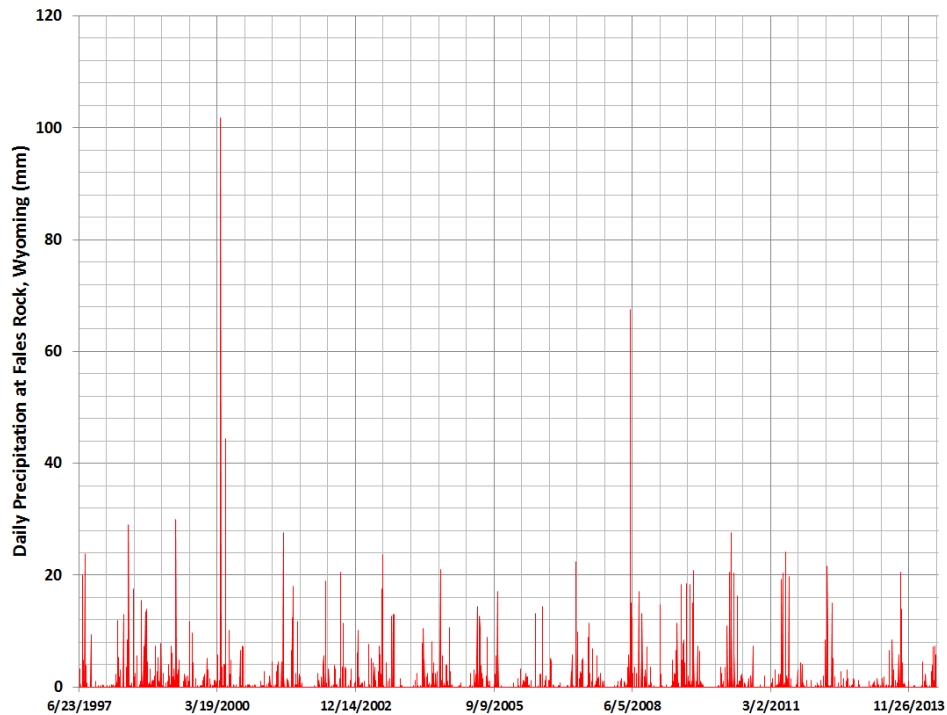
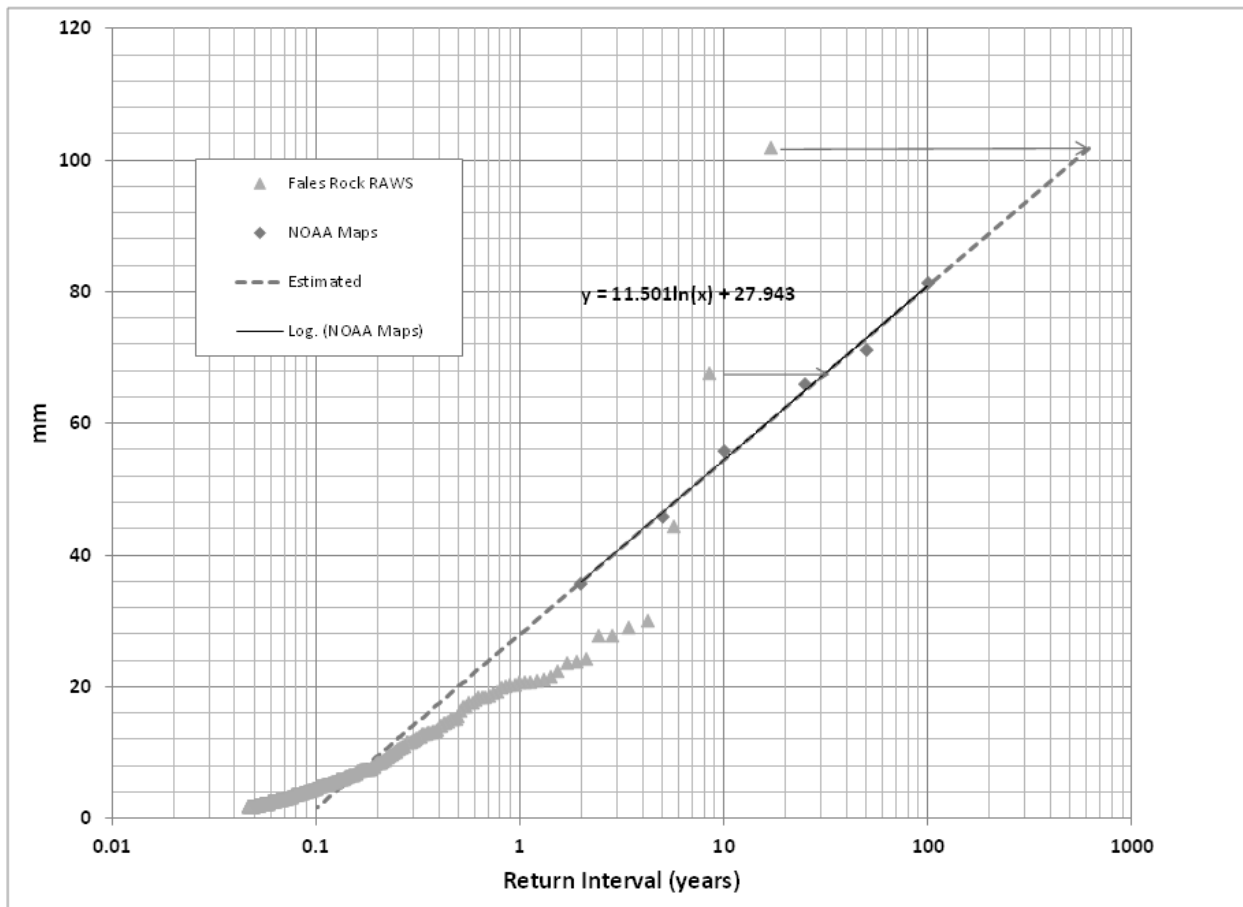


Figure 4-16. Daily Liquid Precipitation at Fales Rock, Wyoming (1 mm = 0.039 in)



**Figure 4-17. Comparison of Precipitation Frequencies Based on the Fales Rock Weather Data with Precipitation Event Frequencies for Western Wyoming (1 mm = 0.039 in)**

Vadose/W uses daily precipitation data but also requires that the timing and duration of the precipitation event be specified. Because the Fales Rock data contain only total daily precipitation, durations for precipitation events need to be assigned. Convective precipitation events occurring between Julian days 140 and 275 (June 24 and October 2) were assigned a nominal duration of 1 hour, although the duration of these events was varied to investigate the effect of precipitation intensity on the water balance performance of the model. Precipitation events outside this date range were assumed to be due to frontal weather systems and were assigned a 24-hr duration.

#### 4.1.4 Initial Conditions

Prior to simulating actual climate records, all of the simulations were initialized by running a simulation with a constant surface flux to create a quasi-steady state pore water pressure distribution. The upper boundary was assigned a flux of 0.00394 in/yr [0.1 mm/yr] and the lower boundary condition is unit gradient. The value of the upper boundary flux was selected to establish a minimal initial water content and negligible rate of change in storage so that the simulations of actual climate conditions would be sensitive to small changes in the water content. That is, if the actual climate resulted in net infiltration through the cover, it would be revealed by an increase in the water content in the model even if the net infiltration was a very small fraction of the total water balance. Likewise, a decrease in water content would indicate a

negative overall water balance or net drying of the site. The quasi-steady state simulations were run in a transient model for a period of 450,000 days (1,232 yrs) until the flux out of the lower boundary had approximately stabilized. The resulting pore water pressures were used as the initial condition for the actual climate simulations.

Note that the constant flux initial condition does not represent the actual pore water pressure distribution that currently exists in the tailings impoundment because (1) the tailings were deposited wet and may still be draining, and (2) the site has been subject to the actual climate since the cover was installed.

A constant temperature lower boundary condition of 46 °F [8 °C] equal to the average annual temperature at Fales Rock was used in all of the simulations.

## **4.2 Simulation Results**

Numerous simulations were performed using both the 2-dimensions and one-dimensional models to improve the numerical convergence of the simulations and reduce the mass balance errors. Because of the need to continually refine the spatial structure of the finite element mesh to reduce the mass balance error, the simulations ultimately focused on the one-dimensional model. The initial simulations with the one-dimensional model used a relatively coarse mesh. These simulations suffered from numerical convergence problems at nodes in the rock mulch erosion barrier and underlying cover materials where extreme changes in the water content and pore water pressures occurred due to drying between rare precipitation events and the wetting during the events. Numerical experiments were also performed to investigate the effect of changing soil water characteristics in the upper two layers and the duration of precipitation events to see if the model convergence and water balance could be improved. These changes failed to produce water balance errors that were viewed to be acceptable and, in some cases, the simulated precipitation record reported by Vadose/W did not match in the input climate record. Simulations with the precipitation spread uniformly over 24 hours did, however, improve the agreement between the cumulative precipitation reported by Vadose/W and that specified in the Fales Rock input file. As mentioned in Section 3.1.1, the support section of Geo-Slope International stated that Vadose/W has “bookkeeping” problems when the adaptive time stepping algorithm resulted in very small time steps during each day of the simulation.

Because these initial attempts to simulate infiltration at Pond 2 did not appear to improve the water balances, a model containing a much refined grid was constructed based on the experience of others reported in Section 3.3. The refined grid model had node spacings as close as 0.08 in [2 mm]. The fine grid model ran extremely slowly on a desktop computer with Intel Core™ i7 CPU (2.94 GHz, 2927 MHz, 4 Core, 8 Logical) processor taking up to 24 hrs to simulate only a few hundred days of the Fales Rock climate record. The short term simulations still had convergence problems and mass balance errors. Given the slowness of the fine grid model simulations and lack of improvement in the water balance, using the fine grid model to simulate the full Fales Rock climate was determined to be impractical, and use of the fine grid model was terminated. The results of a less refined model to simulate 7 yrs of the Fales Rock climate and illustrate the questions regarding net infiltration through the cover based on the ambiguous water balance results are presented in Section 4.3.

### 4.3 Results of Semi-Refined Gas Hills West Pond 2 Simulations

The semi-refined grid simulations were performed with Vadose/W 2012, Version 8.13.1.9253. The finite element mesh and material distribution in the semi-refined model are shown in Figure 4-18. The rock mulch (erosion barrier) representing the upper 3 in (7.6 cm) of the model had a vertical node spacing of 0.6 in [1.5 cm], the mine spoils layer a node spacing of 3.6 in [9.1 cm], and the interim cover layer a node spacing of 2.4 in [6.1 cm]. Boundary and initial conditions for the climate simulates were as previously described.

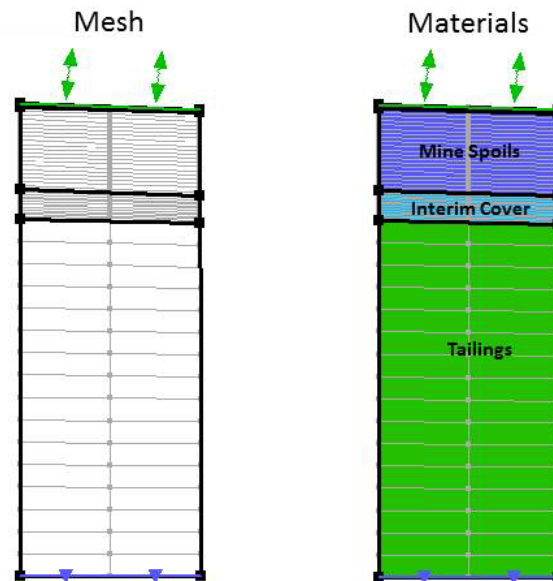


**Figure 4-18. Finite Element Mesh and Materials in the Semi-Refined Model**

Three separate simulations were performed in which the temporal distribution of summer precipitation was varied. The first simulation assumed a nominal 1-hr summer storm with the precipitation varying in a sinusoidal manner during the event<sup>4</sup>. A second simulation was performed in which the summer precipitation intensity was the total daily precipitation averaged over 1 hour. This is referred to as the “constant average” precipitation distribution. A third simulation was performed in which both the summer and winter daily precipitation were assumed to occur at a constant rate over 24 hrs. The results of these simulations are described in the following paragraphs to illustrate the effect of precipitation intensity of the simulation results, particularly on the water balance information reported by Vadose/W.

The results of the 1-hr, sinusoidal summer precipitation simulation using the first 7 yrs of the Fales Rock weather data are summarized in Figures 4-19 and 4-20. Figure 4-19 shows the daily precipitation based on the Fales Rock weather data (vertical lines above the horizontal zero axis), the cumulative lower boundary flux (dashed line immediately below the zero horizontal axis), the cumulative change in storage reported by Vadose/W, the water balance error reported by Vadose/W, and the net water added ( $I = P - R - ET + Q_B$ , net infiltration from Equation 2-7) calculated from the components of the water balance reported by Vadose/W. The cumulative precipitation reported by Vadose/W was 5.3 in [135 mm] less than the input precipitation, a difference of -10 percent.

<sup>4</sup> Vadose/W sets the maximum allowed adaptive time step to 2 hours when the sinusoidal distribution is chosen.

Both the cumulative change in storage and cumulative water added are positive, indicating that water was being added to the model domain. The annual rate of water gain based on the change in storage was 1.5 in/yr [39 mm/yr] and 1.3 in/yr [33 mm/yr] based on the net water added calculation. The cumulative water balance error reported by Vadose/W was 0.23 in/yr [6 mm/yr] which agrees reasonably well with the difference between the change in storage and the net water added. However, the simulated changes in volumetric water content shown in Figure 4-21 indicate a net water loss in the center of the radon cover (mine spoils in Figure 4-21) that conflicts with the water balance data reported by Vadose/W.

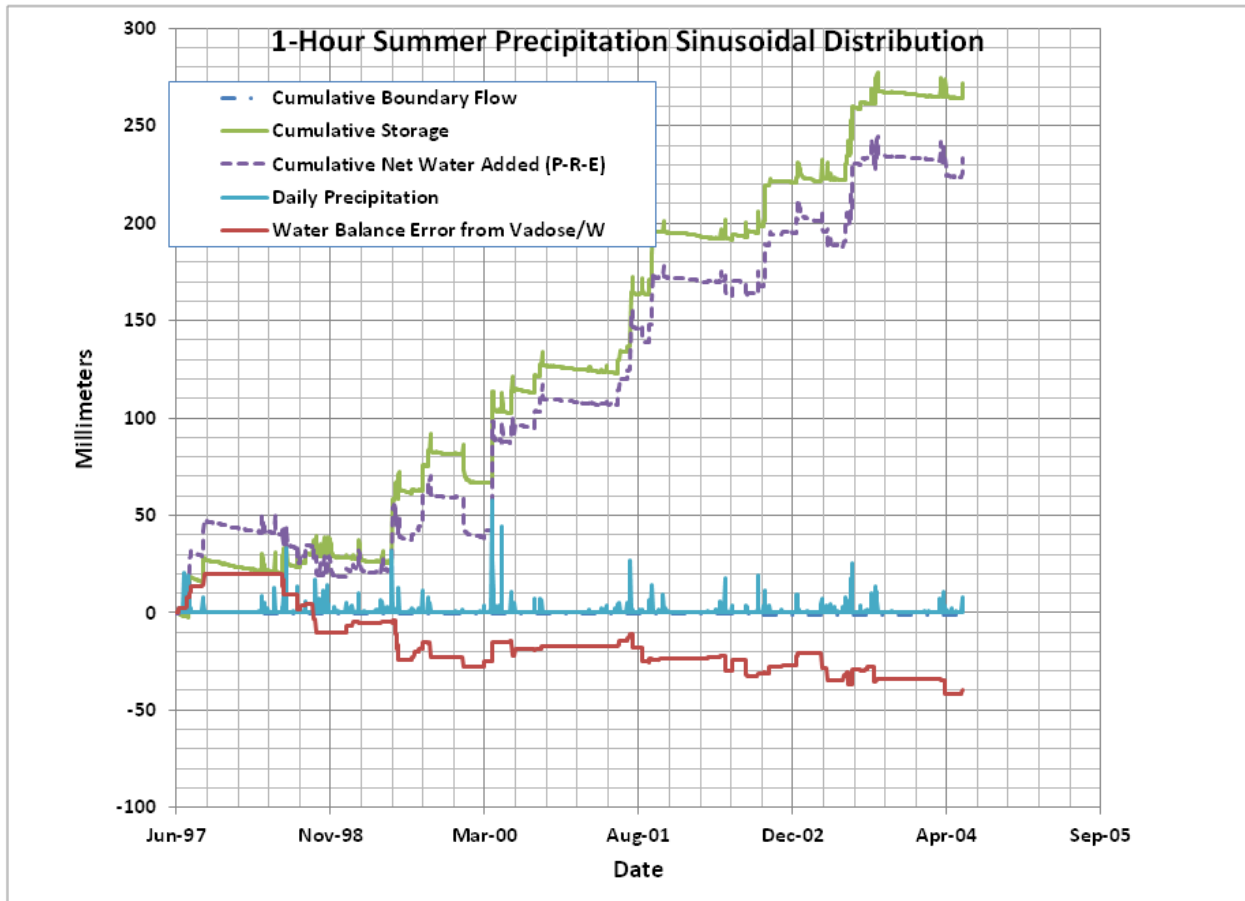


**Figure 4-19. Daily Precipitation, Cumulative Lower Boundary Flow, Water Balance Error, Cumulative Change in Storage, and Cumulative Water Added Based on the Semi-Refined Gas Hills West Pond 2 Model with Precipitation Distributed Sinusoidally Over 1 Hour (1 mm = 0.039 in)**

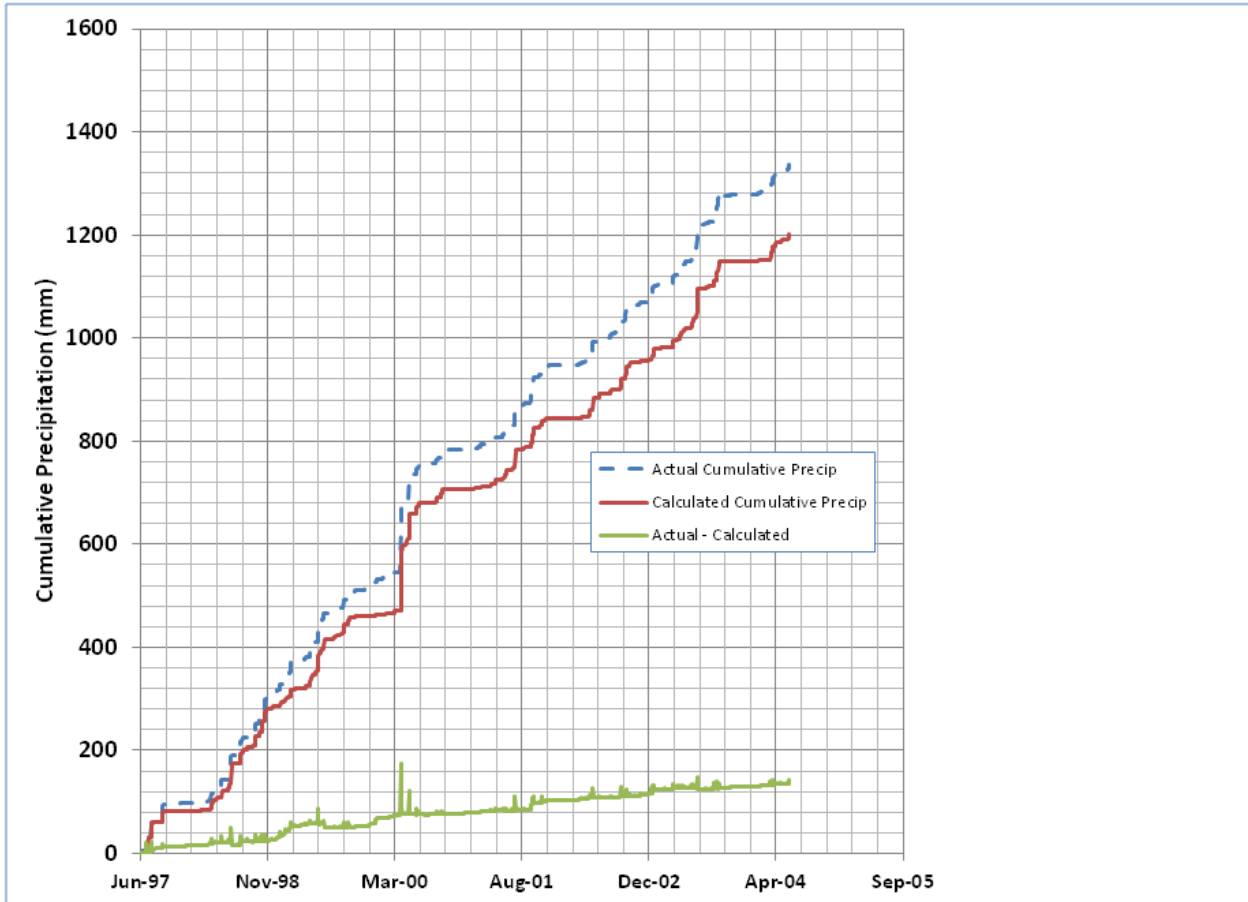


**Figure 4-20. Cumulative Precipitation Reported by Vadose/W Compared to Cumulative Precipitation Computed from the Fales Rock Input Data for the 1-Hour, Sinusoidal Summer Precipitation Simulation (1 mm = 0.039 in)**

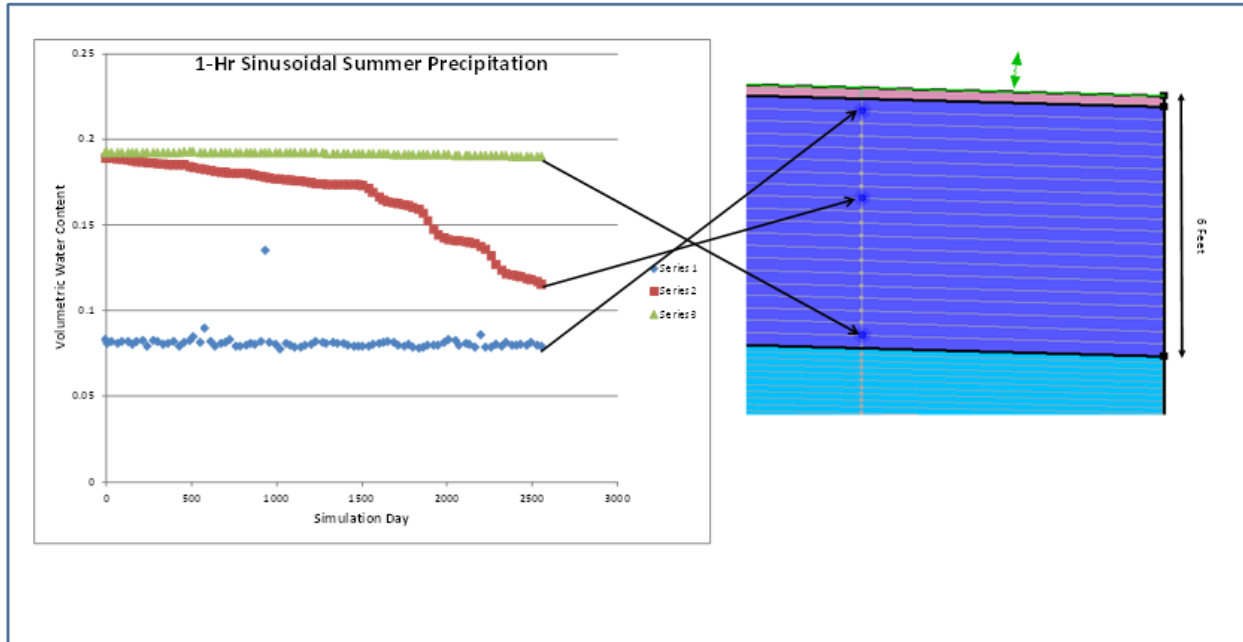


**Figure 4-21. Simulated Change in Volumetric Water Content at Selected Nodes in the Gas Hills West Semi-Refined Model Simulation 1-Hour Sinusoidal Simulation**

The results of the simulation using the 1-hr, constant average summer precipitation are shown in Figures 4-22, 4-23, and 4-24 in terms of the cumulative water balance components, simulated versus input cumulative precipitation, and changes in volumetric water content, respectively. The change in storage reported by Vadose/W for this simulation indicates a net increase in water in the model domain at a rate of 0.16 in/hr [4 mm/yr] and virtually no increase of the net water added. The cumulative water balance error reported by Vadose/W was -1 in [-26 mm] over the period of the simulation or -0.1 in/yr [-3 mm/yr]. Despite the apparent increase in storage, the simulation results indicate that the volumetric water content in the radon barrier decreased over the course of the simulation (Figure 4.24). The difference between the precipitation reported by Vadose/W and that specified in the input was -21 in [-552 mm], much larger than the difference for the simulation using the sinusoidal summer precipitation.

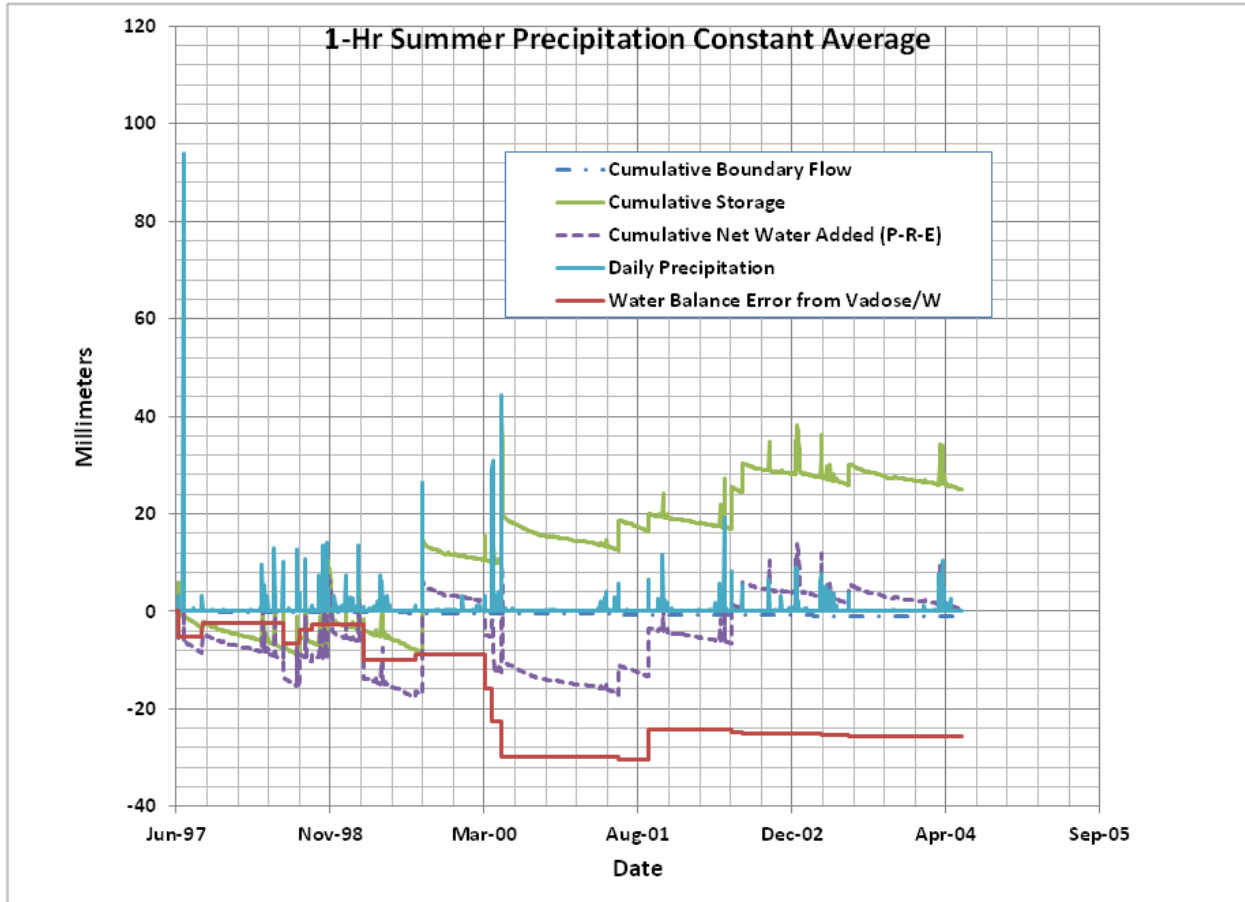


**Figure 4-22. Daily Precipitation, Cumulative Lower Boundary Flow, Water Balance Error, Cumulative Change in Storage, and Cumulative Water Added Based on the Semi-Refined Gas Hills West Pond 2 Model with Precipitation Distributed Uniformly Over 1 Hour (1 mm = 0.039 in)**

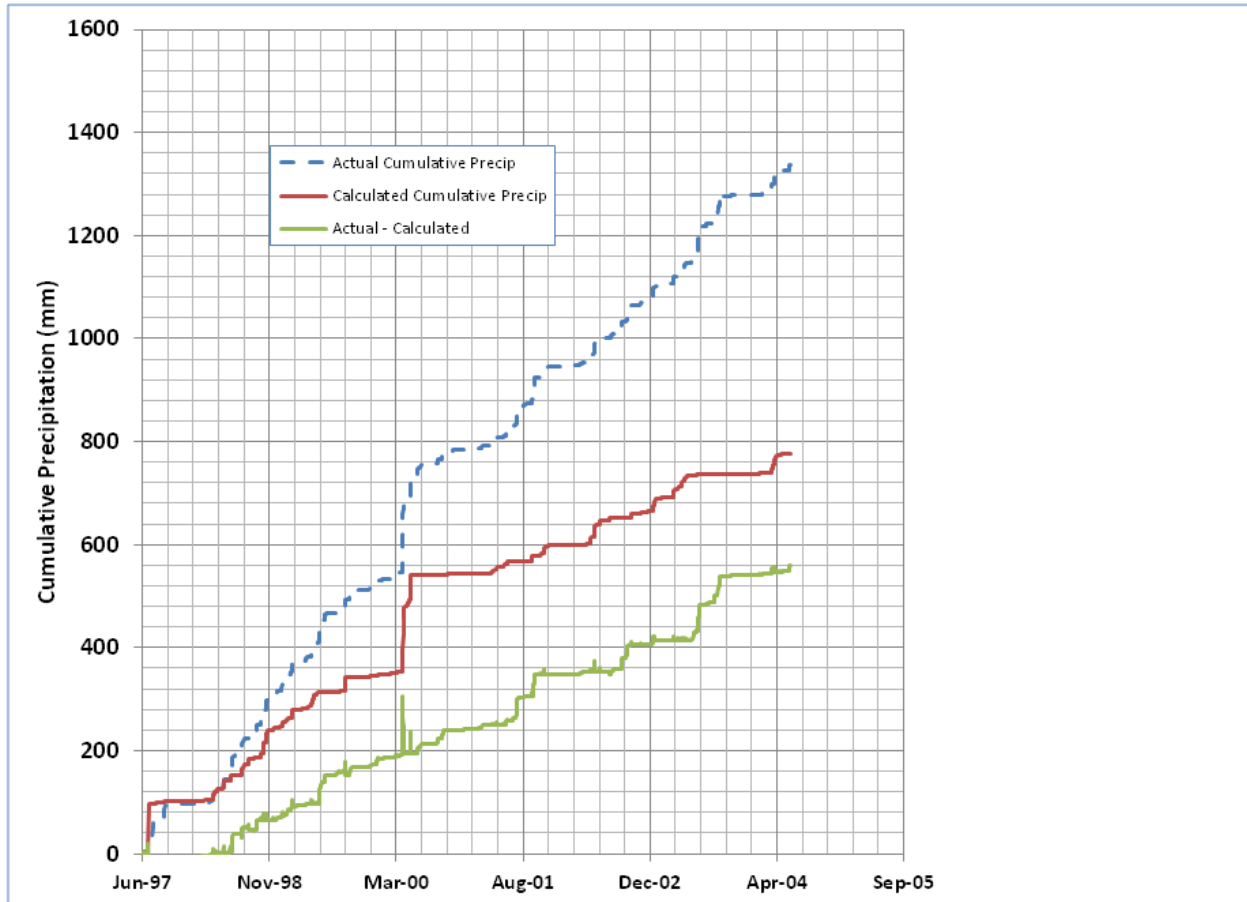


**Figure 4-23. Cumulative Precipitation Reported By Vadose/W Compared to Cumulative Precipitation Computed from the Fales Rock Input Data for the 1-Hour, Constant Average Summer Precipitation Simulation (1 mm = 0.039 in)**

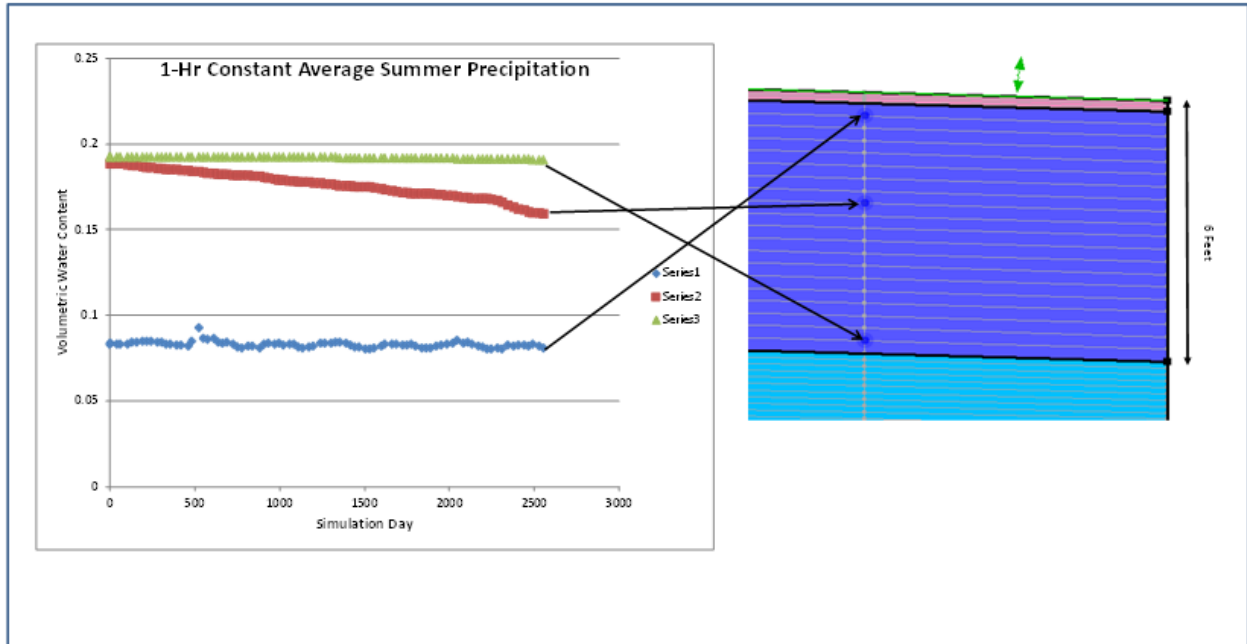


**Figure 4-24. Simulated Change in Volumetric Water Content at Selected Nodes in the Gas Hills West Semi-Refined Model Simulation 1-Hour Constant Average Simulation**

Finally, the results of the simulation in which both summer and winter precipitation were distributed over 24 hours are shown in Figures 4-25 through 4-27. For the simulation, both the cumulative storage and cumulative net water added were negative (Figure 4-25) indicating water loss from the model domain and no net infiltration. The rate of loss based on the change in storage was 0.3 in/yr [-8 mm/yr] and 0.39 in/yr [-10 mm/yr] based on the net water added, which agree reasonably well. The cumulative water balance error reported by Vadose/W was -0.7 in [-18 mm] over the 7-yr simulation. The cumulative precipitation reported by Vadose/W was 4.2 in [106 mm] less than the cumulative precipitation in the input report, a difference of -8 percent. As with the other two simulations, the volumetric water content decreased in the radon barrier (Figure 4-27) which, in this case, is consistent with the water balance.

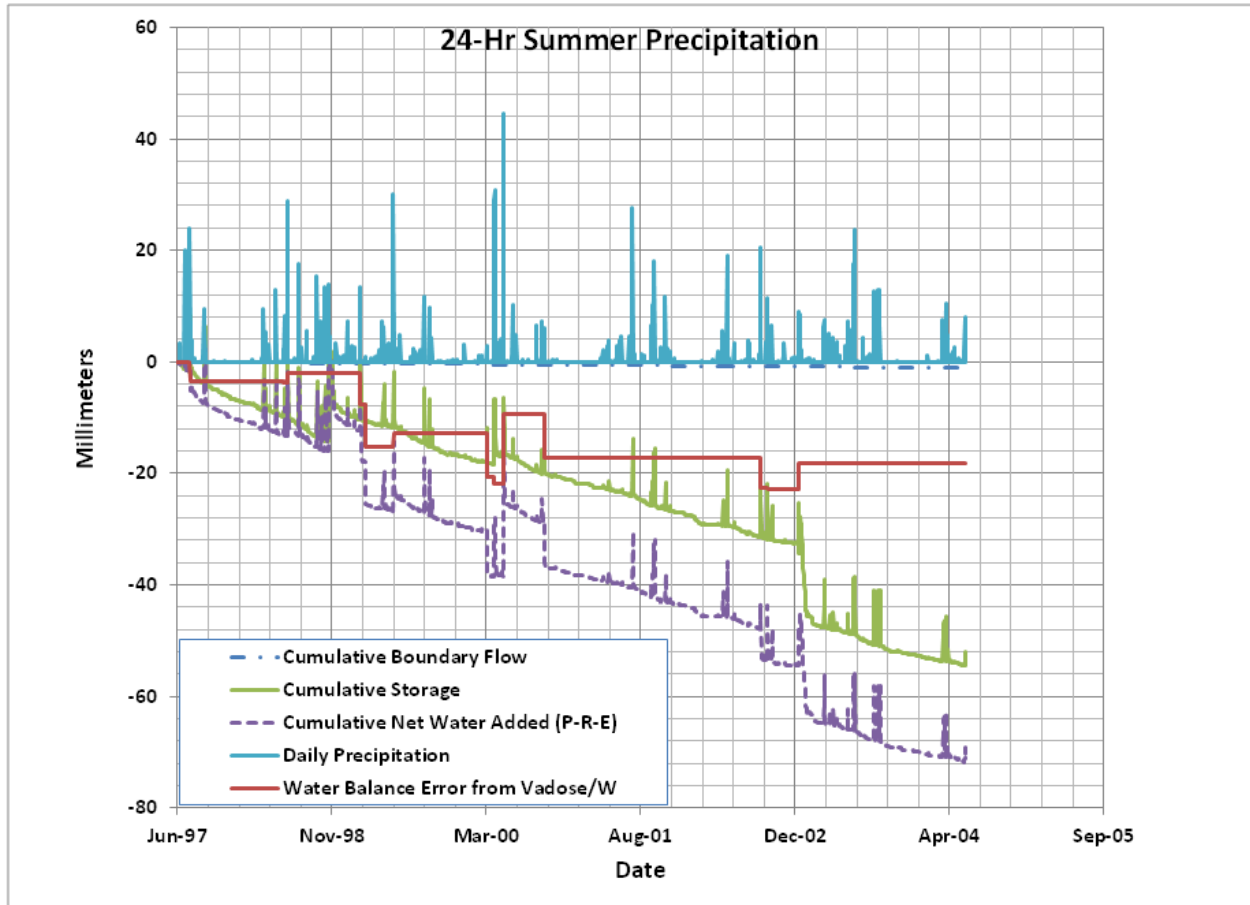


**Figure 4-25. Daily precipitation, Cumulative Lower Boundary Flow, Water Balance Error, Cumulative Change in Storage, and Cumulative Water Added Based on the Semi-Refined Gas Hills West Pond 2 Model with Precipitation Distributed Uniformly Over 24 Hours (1 mm = 0.039 in)**

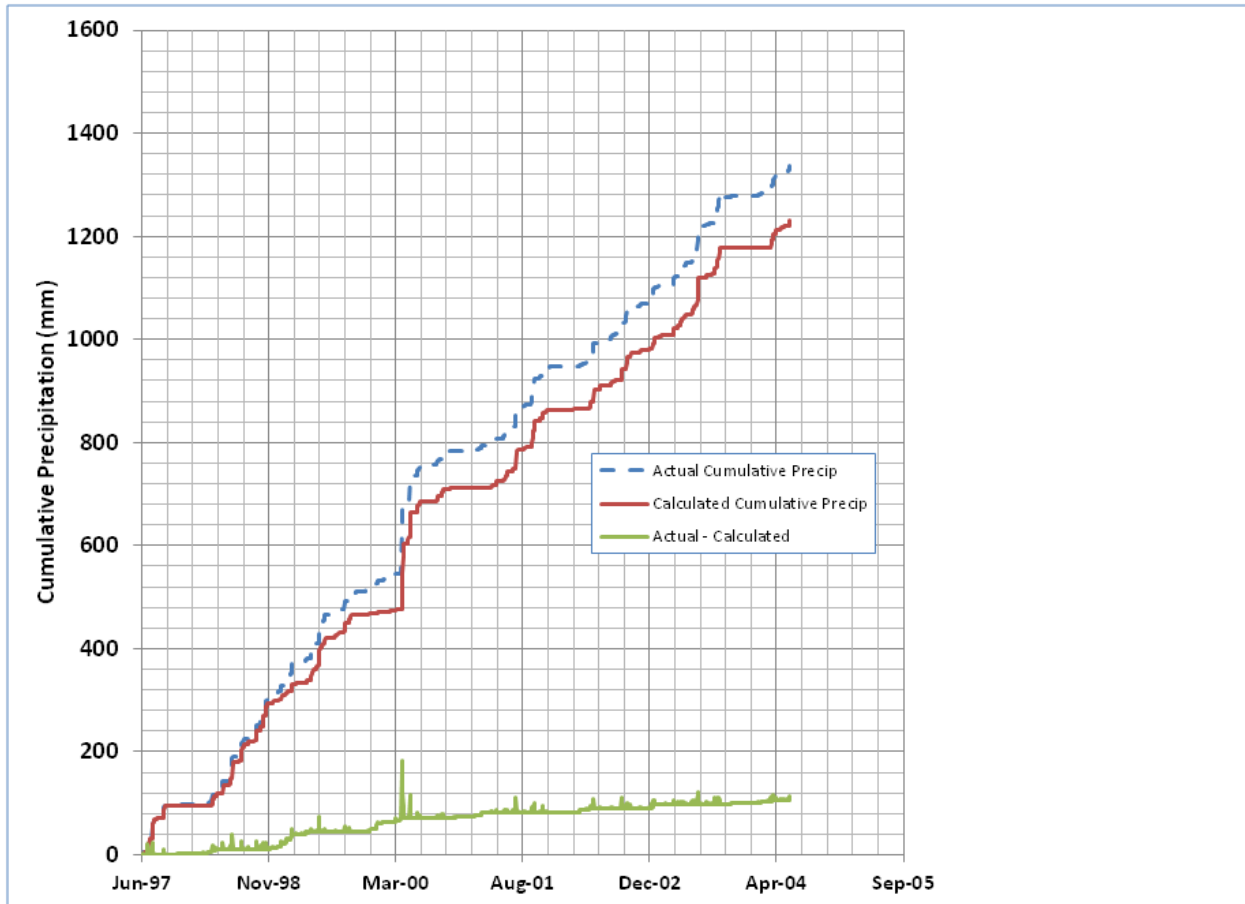


**Figure 4-26. Cumulative Precipitation Reported By Vadose/W Compared to Cumulative Precipitation Computed from the Fales Rock Input Data for Precipitation Distributed Over 24 Hours (1 mm = 0.039 in)**

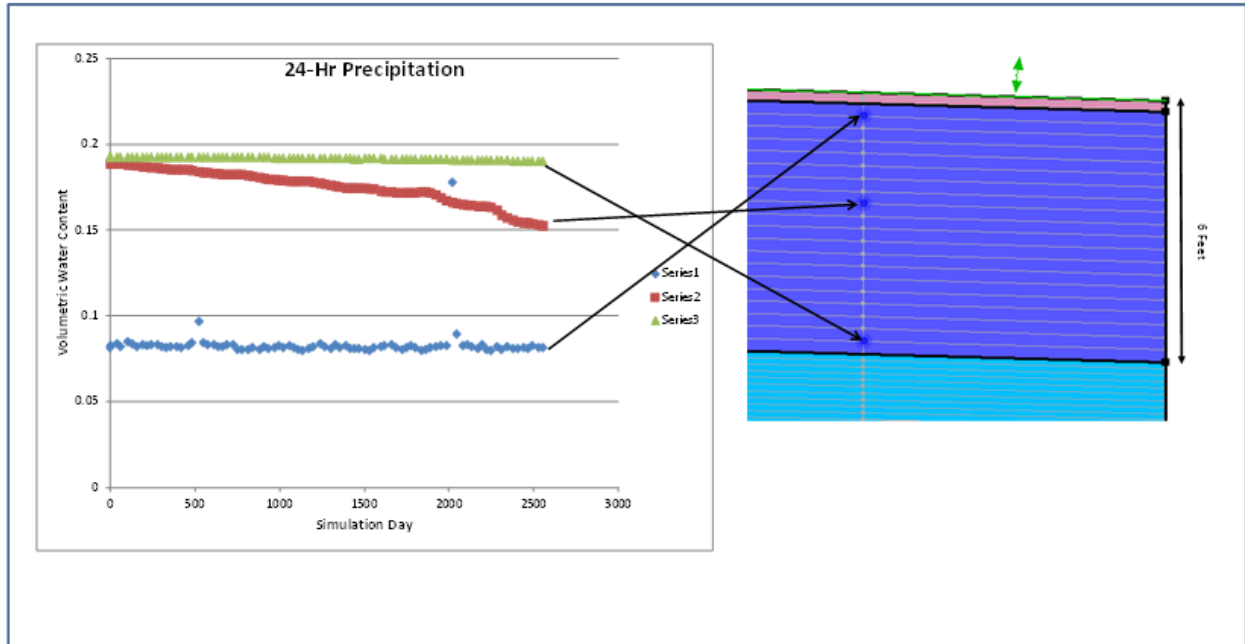


**Figure 4-27. Simulated Change in Volumetric Water Content at Selected Nodes in the Gas Hills West Semi-Refined Model Simulation with Precipitation Distributed Over 24 Hours**

A simulation using the 24-hr summer/winter precipitation record was also run with the saturated hydraulic conductivity of the sandy silty clay materials comprising the cover increased by an order of magnitude from the average value (3.4 ft/day versus 0.34 ft/day [ $1.2 \times 10^{-5}$  m/s versus  $1.2 \times 10^{-6}$  m/s]) to evaluate the effect of hydraulic parameters on the simulation results. The 24-hr precipitation distribution was chosen because it was the only simulation for which the water balance was consistent with the simulated changes in volumetric water content. The results of this simulation are shown in Figures 4-28 through 4-30. This simulation resulted in more negative water balance (less net water added) and had an annualized water balance error of only 0.007 in/yr [0.18 mm/yr]. Cumulative precipitation reported by Vadose/W was 4.1 in [105 mm] less than the input precipitation (8 percent less).

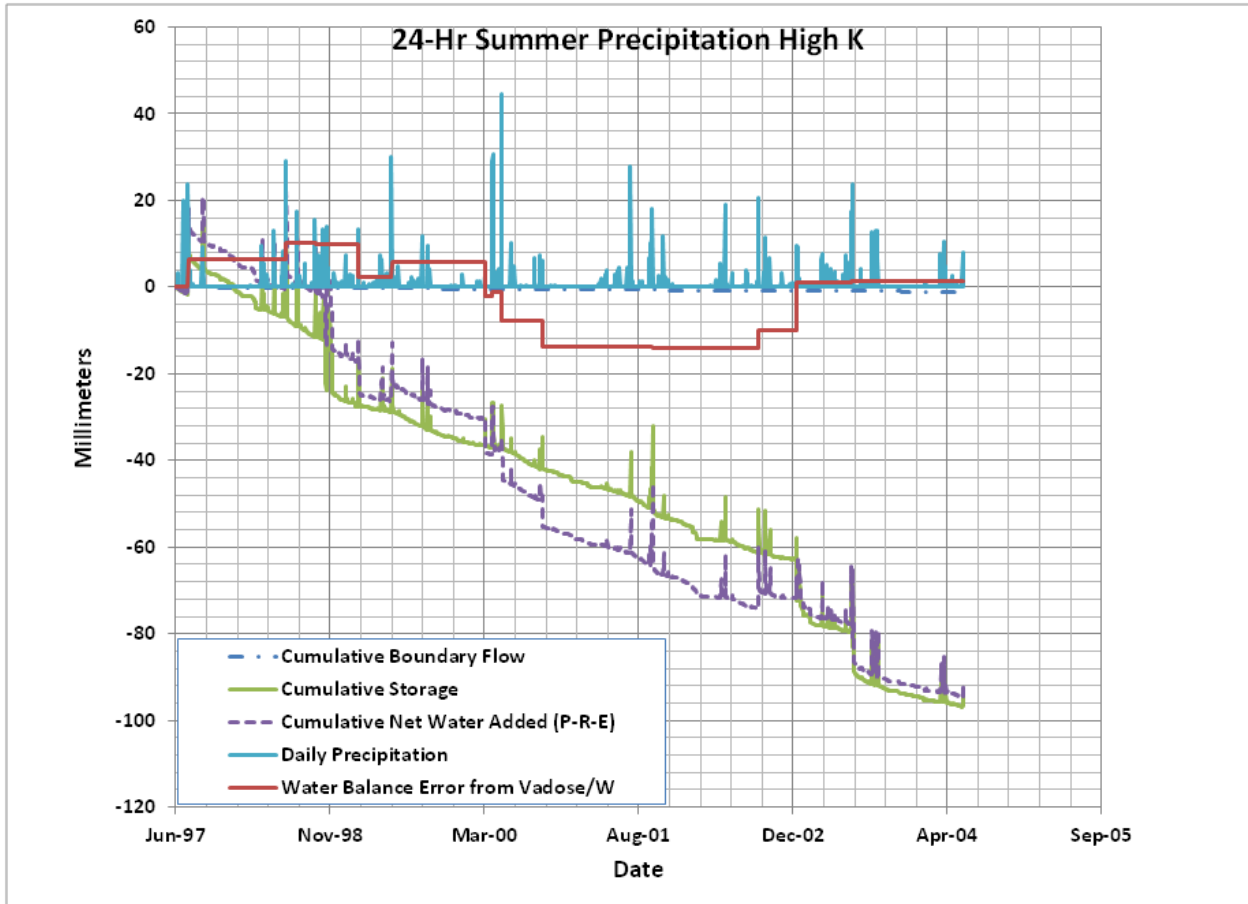


**Figure 4-28. Daily Precipitation, Cumulative Lower Boundary Flow, Water Balance Error, Cumulative Change in Storage, and Cumulative Water Added Based on the Semi-Refined Gas Hills West Pond 2 Model with Precipitation Distributed Uniformly Over 24 Hours and High Sandy Silty Clay Hydraulic Conductivity (1 mm = 0.039 in)**

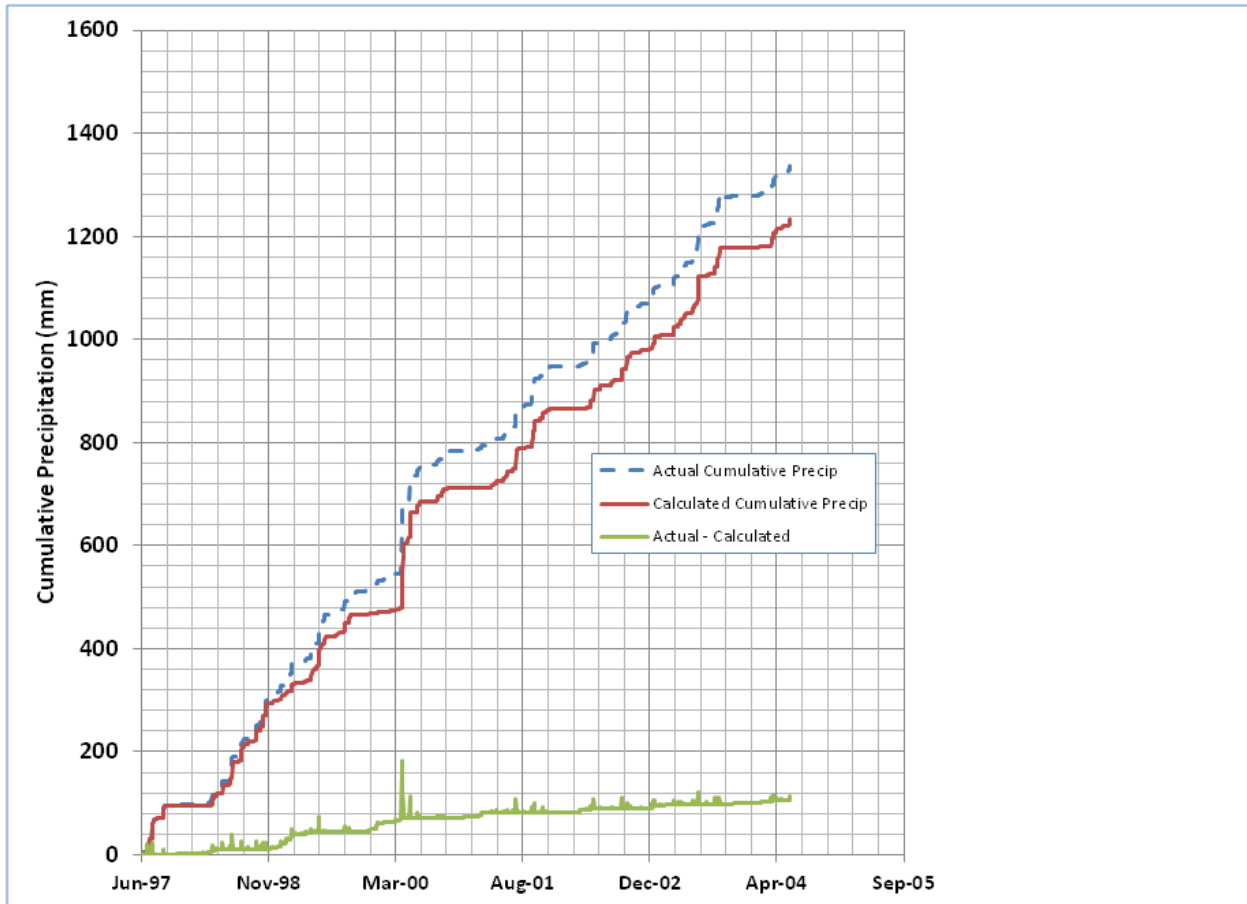


**Figure 4-29. Cumulative Precipitation Reported by Vadose/W Compared to Cumulative Precipitation Computed from the Fales Rock Input Data for Precipitation Distributed Over 24 Hours with High Sandy Silty Clay Hydraulic Conductivity (1 mm = 0.039 in)**

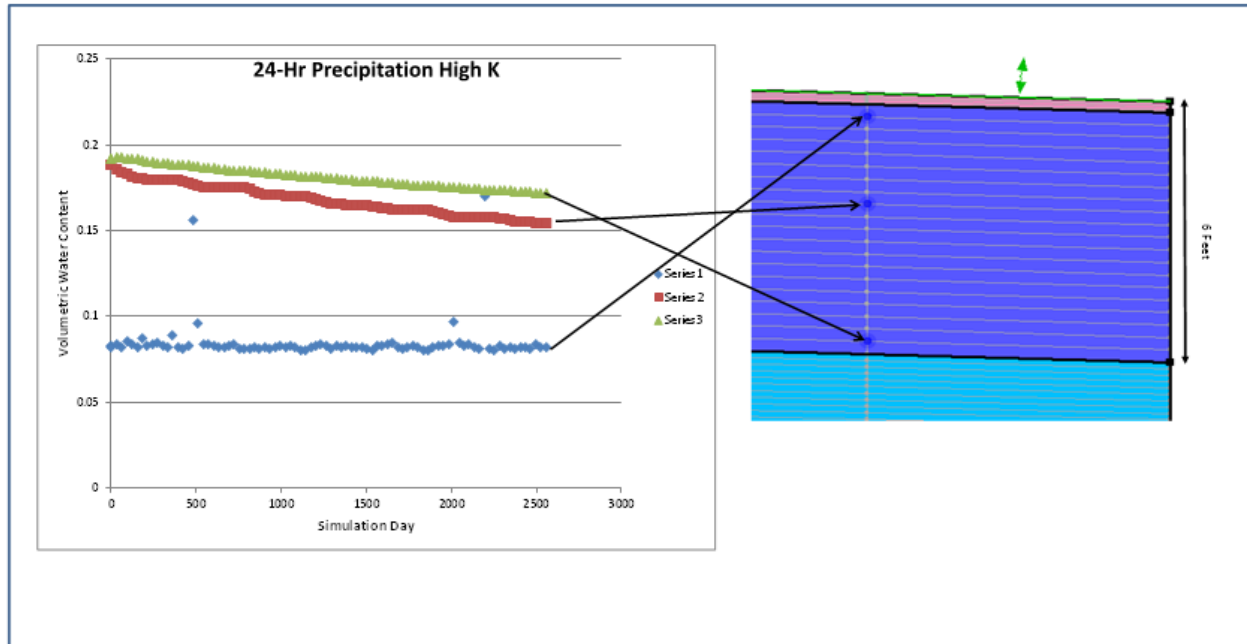


**Figure 4-30. Simulated Change in Volumetric Water Content at Selected Nodes in the Gas Hills West Semi-Refined Model Simulation with Precipitation Distributed Over 24 Hours with High Sandy Silty Clay Hydraulic Conductivity**

#### 4.4 Summary of Gas Hills West Pond 2 Simulations

The simulation results using the semi-refined model mesh, the three different precipitation distributions, and the elevated hydraulic conduction are summarized in Figure 4-31 in terms of average rate of change in storage, net water added, and water balance error. The inconsistency in the apparent water balances based on the data reported by Vadose/W for the various precipitation distributions is attributed to bookkeeping errors in the code discussed previously because the simulated changes in volumetric water content were generally consistent between the simulations, although not identical. The bookkeeping problems appear to be associated with the adaptive time stepping algorithm in Vadose/W that results in many very small time steps per day caused by sudden, large variations in pore water pressures. These sudden, large changes in pore water pressures result from higher precipitation intensities, with the highest intensities produced using the sinusoidal precipitation distribution and the lowest using the 24-hr distribution. The simulation using uniform 24-hr precipitation distribution and the elevated sandy silty clay hydraulic conductivity produced the best agreement between the change in storage and the net water added, and the lowest water balance error.

Despite the variations in the reported water balances, all of the simulations resulted in a net drying of the cover materials as indicated by the decrease in volumetric water content in the radon barrier over the course of the 7-yr simulations. Based on the simulated volumetric water contents, the soils comprising the radon barrier would be drying under current climate conditions and there would be no net infiltration through the cover into the tailings. This conclusion must be taken with caution, however, because the relative water balance error of the simulation was relatively large (on the order of 50 percent) for the more realistic simulations using the sinusoidal and 1-hr precipitation distribution even through the annualized water balance errors are small (0.1 to 0.2 in/yr [4 to 6 mm/yr]). Based on the difficulty of developing simulations with

a very small water balance error for the Gas Hills West site and that net infiltration through the cover, if any, is likely to be a very small fraction of annual precipitation and the overall site water balance, a firm conclusion about the performance of the cover with respect to net infiltration cannot be drawn from the simulations performed.

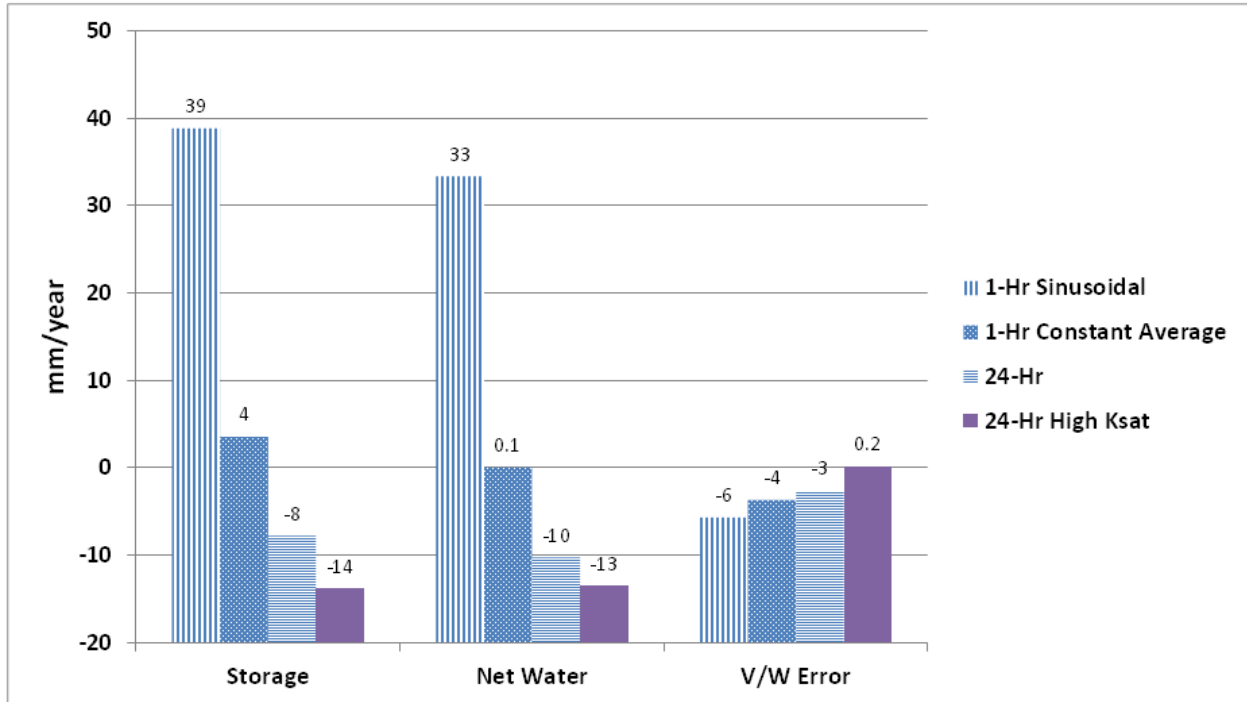


**Figure 4-31. Comparison of Results of Simulations Using Different Summer Precipitation Distributions and Elevated Saturated Hydraulic Conductivity of Sandy°Silty°Clay Materials**

## 5 HIGHLAND MODEL AND SIMULATION RESULTS

### 5.1 Description of the Highland (Exxon), Wyoming, Model

The Highland, Wyoming, final cover consists of random fill where needed to elevate the landscape to the final design level, plus 1.07 m (3.5 ft) of radon barrier, plus 0.15 m (0.5 ft) of topsoil. The clayey radon barrier likely is composed of material from the Fowler Formation, described as discontinuous sandstone and shale units (Water, Waste & Land, 1988; Figure 2):

- Sandstone: grain size varies from medium-grained sand to gravel, most commonly medium to very coarse-grained sand; beds vary from loose friable sand to well-cemented (carbonate) sandstones
- Siltstone and Claystone (shale): may contain thin, interbedded sandstones and lignite beds

Topsoil information for the Highland site was obtained from the U.S. Department of Agriculture's Natural Resources Conservation Service (NRCS). NRCS conducts soil surveys and publishes these data online (NRCS, 2014). The 1985 reclamation plan sent to State of Wyoming (Exxon Minerals Company, 1985) stated that: the Northern Brown "type and quality of topsoil used for reclamation at Highland are generally homogenous," which is why a hydraulic conductivity ratio ( $K\text{-ratio} = K_y/K_x$ ) of unity was selected for use (the explicitly defined hydraulic conductivity function in Vadose/W always defines  $K_x$ ).

A report on technical specifications for the reclamation of the Highland uranium tailings impoundment by Water, Waste and Land (1989a) provides the following unit descriptions:

**Topsoil:** The topsoil to be used is stockpiled at the site. "The topsoil shall be placed in one lift to obtain a final thickness of 6 inches. The material shall be spread evenly and disked." (Water, Waste and Land, 1989a)

"The final grade of the topsoil surface over the tailings area shall be within 0.1 foot of the specified grade as shown on the Drawings. The topsoil shall have an average thickness of six inches. There are no compaction specifications associated with the topsoil material." (Water, Waste and Land, 1989a)

**Radon Barrier:** "The soil used for the radon barrier shall consist of material from the diversion channel, from the Middle Dump, or from the areas adjacent to the tailings basin that must be sloped to form the necessary transition from natural ground to the reclaimed area." (Water, Waste and Land, 1989a)

**Random Fill:** "The material used for random fill shall consist of material excavated from the diversion channel, material from the Middle Dump, material from the embankment, off site soils contaminated with wind-blown tailings or material obtained from areas adjacent to the tailings basin. The Middle Dump, along with the material from the diversion channel will serve as the primary borrow areas." (Water, Waste and Land, 1989a)

"There are no requirements on the material properties or the degree of compaction of the random fill" (Water, Waste and Land, 1989a).

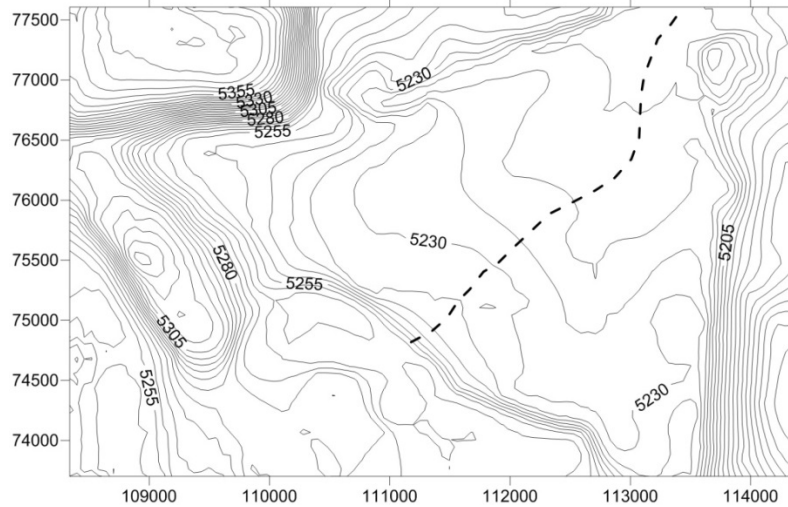
A report about construction quality assurance testing for reclamation of the Highland uranium mill tailings impoundment by Water, Waste and Land (1991) provided the following additional random fill description:

**Random Fill:** “Random fill soils consisted of materials previously stockpiled by ECMC on the middle dump or excavated from the diversion channel (Figure 1.1). Generally, these soils were similar to or sandier than radon barrier soils.” (Water, Waste and Land, 1991)

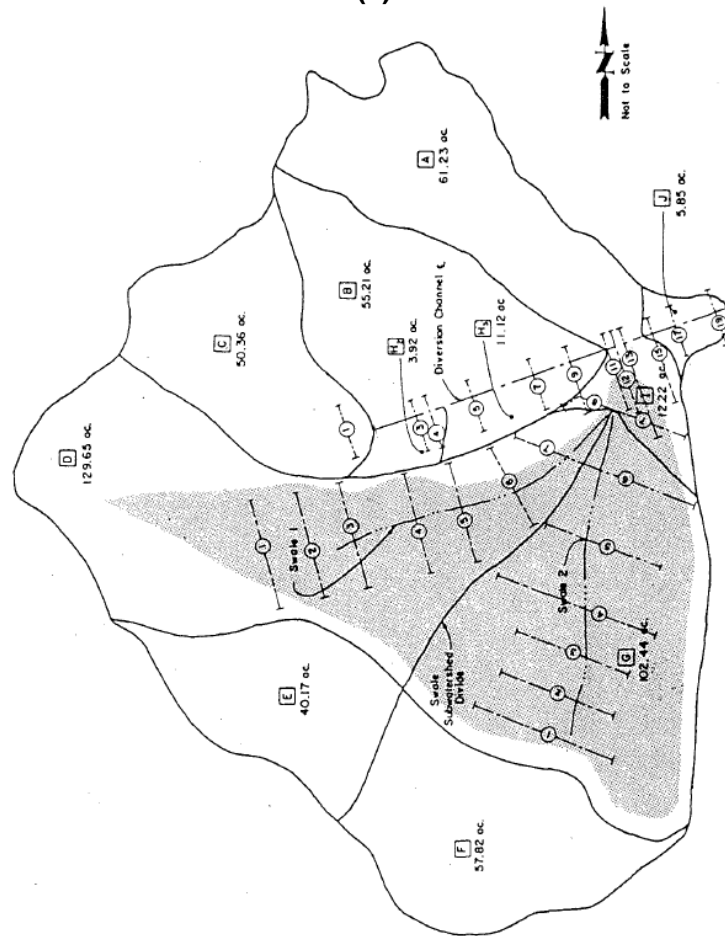
Due to the lack of compaction requirements and the potentially sandier composition, random fill cannot be modeled as if it were an extra thickness of radon barrier. Therefore, CNWRA staff assume that random fill is equivalent to sandy tailings for the purposes of this modeling activity.

Originally, “Condition 40 (A) of the Source Material License No. SUA-1139 requires all radon cover materials used in reclamation of the Highland tailings basin to be classified as CL (clay) materials with not more than 20 percent by weight being retained on the no. 200 sieve.” (Water, Waste and Land, 1989b). However, Exxon subsequently requested two license amendments to allow materials of both larger (i.e., sandier) and smaller (i.e., clayier) particle size characteristics to be used as radon barrier material (Water, Waste and Land, 1989b,c). In contrast to the statement by Water, Waste and Land (1989b) that the sandier 40 percent passing material was still CL (clay of low plasticity; lean clay), the Unified Soil Classification System indicates that CL only pertains to material with 50 percent or more passing the no. 200 sieve. Thus, the sandier radon barrier material approved for use is either SC (clayey sand) with greater than 50 percent retained on the no. 200 sieve, or else may have a borderline designation of CL/SC. By way of an additional license amendment, material with very high clay content (i.e., 95 percent passing the no. 200 sieve), which did not meet the original compacted bulk density specification, was also approved for use (Water, Waste and Land, 1989c) in construction of the Highland radon barrier. This approved material was CL (low plasticity, lean clay) to CH (high plasticity, fat clay), due to the requested liquid limit of up to 60 percent (CL has a liquid limit of  $\leq 50$  percent).

CNWRA staff digitized a map of the as-built topography of the final cover (Shepherd Miller, 2002, their Figure 7.4—Reclaimed Tailings Basin Contours at Completion of Work in 2001) in ArcGIS. Using Surfer, staff extracted the SW–NE swale divide cross-section (Figure 5-1) from the three-dimensional topography of the cover, crossing a total distance of 1,138 m (3,734 ft) in the direction toward the cover discharge point. Water, Waste & Land, Inc. (1984, Figure 2.11) provided a map view of the approximate lateral distribution of sandy tailings and two slime zones in the Highland tailings basin. The selected model cross-section along the swale divide crosses through the northern slimes zone. Staff also digitized the fill topography contours from a cut-and-fill map view of the tailings impoundment in Water, Waste, and Land, Inc. (1984; Figure 5.5—Tailings Grading Plan) and then extracted a cross-section of the fill topography along the swale divide transect. The random fill is assumed to consist of fine-grained sandy tailings removed from regions of the impoundment where the topography had to be cut to meet design elevation. Beneath the random fill, within slime zones, silty-slime tailings are assumed to fill the volume. Water, Waste & Land, Inc. (1984) explained that the cover thickness must be a minimum of 1.22 m (4 ft) above sandy tailings, but must be a minimum of 1.52 m (5 ft) above slimes.



(a)



(b)

**Figure 5-1. (a) Selected Transect for a Two-Dimensional Net Infiltration Model across the Highland Uranium Mill Tailings Impoundment Cover at the Swale Divide; (b) Swale Subwatershed Divide (Water, Waste & Land, 1984; Figure 5.6). Topsoil Along the Swale Divide is Vegetated.**

### 5.1.1 Model Domain and Mesh

Within Vadose/W, the base of the final cover was defined by subtracting 1.22 m (4 ft) from the topographic model; then 1.22 m (4 ft) of surface layers were built upon it (Figure 5-2). The surface layers are the portion of the model directly influenced by the climate variables and vegetation parameters. In this model, the surface layers consist of all materials within the top 2 m (6.6 ft) of the land surface, including in some cases the sandy tailings and some fraction of silty slimes. Surface layers are directly subject to climate-driven forcings. The uppermost surface layer at the land-atmosphere interface consists of a small fraction of the topsoil that was assigned a less variable hydraulic conductivity function to aid convergence, per GEO-SLOPE (2012) recommendations.

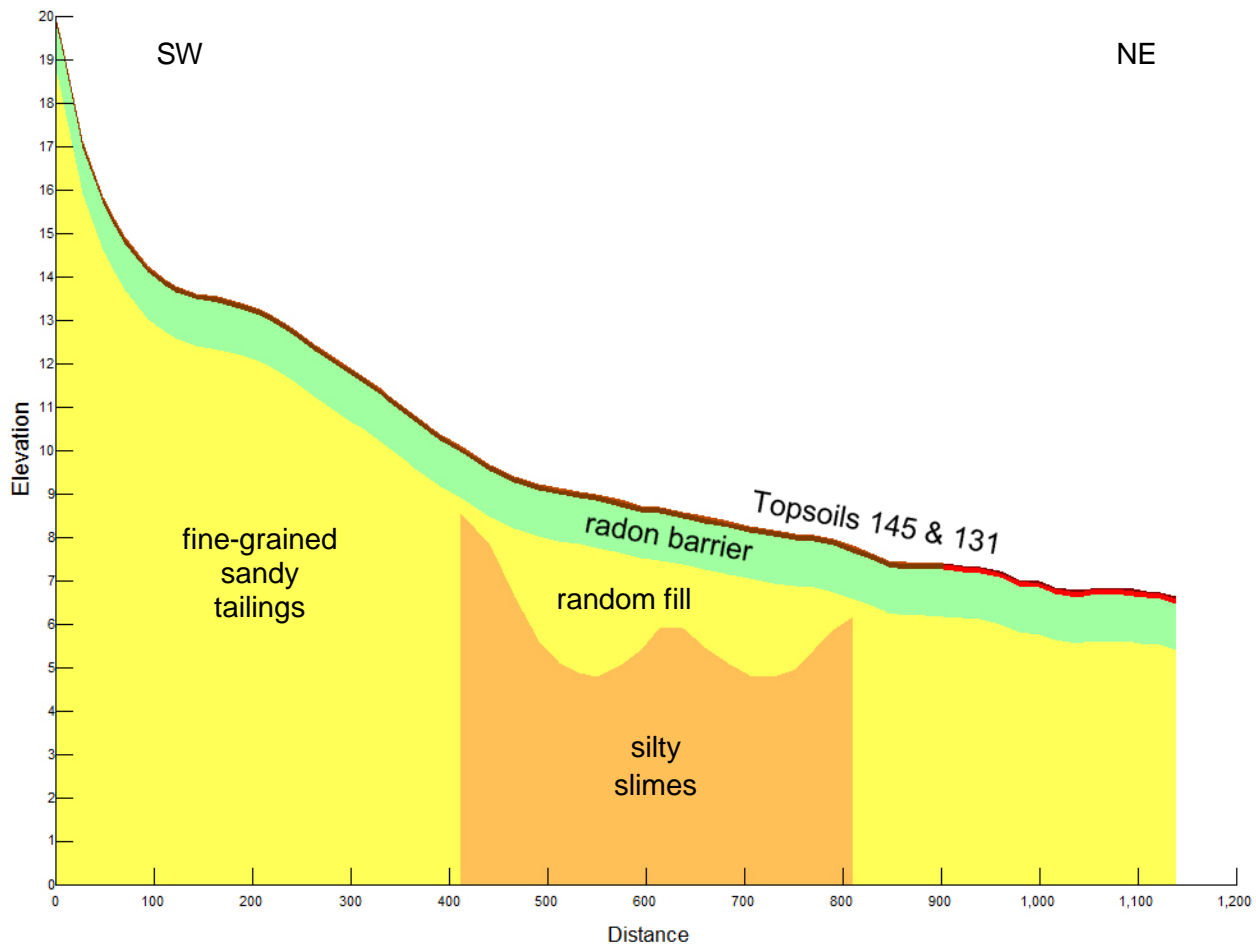


**Figure 5-2. Cross-Section through the Highland Uranium Mill Tailings Impoundment and Soil Cover along the Swale Divide**

CNWRA staff opted to construct a quasi-one-dimensional Vadose/W model of the Highland soil column (Figure 5-3) to simplify the system. A 1.0-m (3.3-ft)-wide, 3.8-m (12.5-ft) deep model domain was selected at a location approximately 790 m (2,592 ft) along the two-dimensional cross-section of Figure 5-2. The model domain represents silty slimes underlying random fill (or sandy tailings), underlying a 1.07-m (3.5-ft)-thick radon barrier layer. Above the radon barrier are two surface layers: the lowermost topsoil unit (brown) is 0.11 m (4.43 in) thick, and the land surface with its reduced hydraulic conductivity variation (red-brown) is 0.04 m (1.57 in) thick. Where permeability or capillary breaks may be expected at the top or bottom of a model layer,

adjacent elements surrounding that layer should be approximately the same size for numerical stability. Where large vertical gradients are expected, element sizes are on the order of 2-mm thick; the mesh consists of 312 elements (Table 5-1, Figure 5-4). Surface layers subject to the climate and vegetation boundary conditions comprise the upper 2 m (6.6 ft) of the domain.

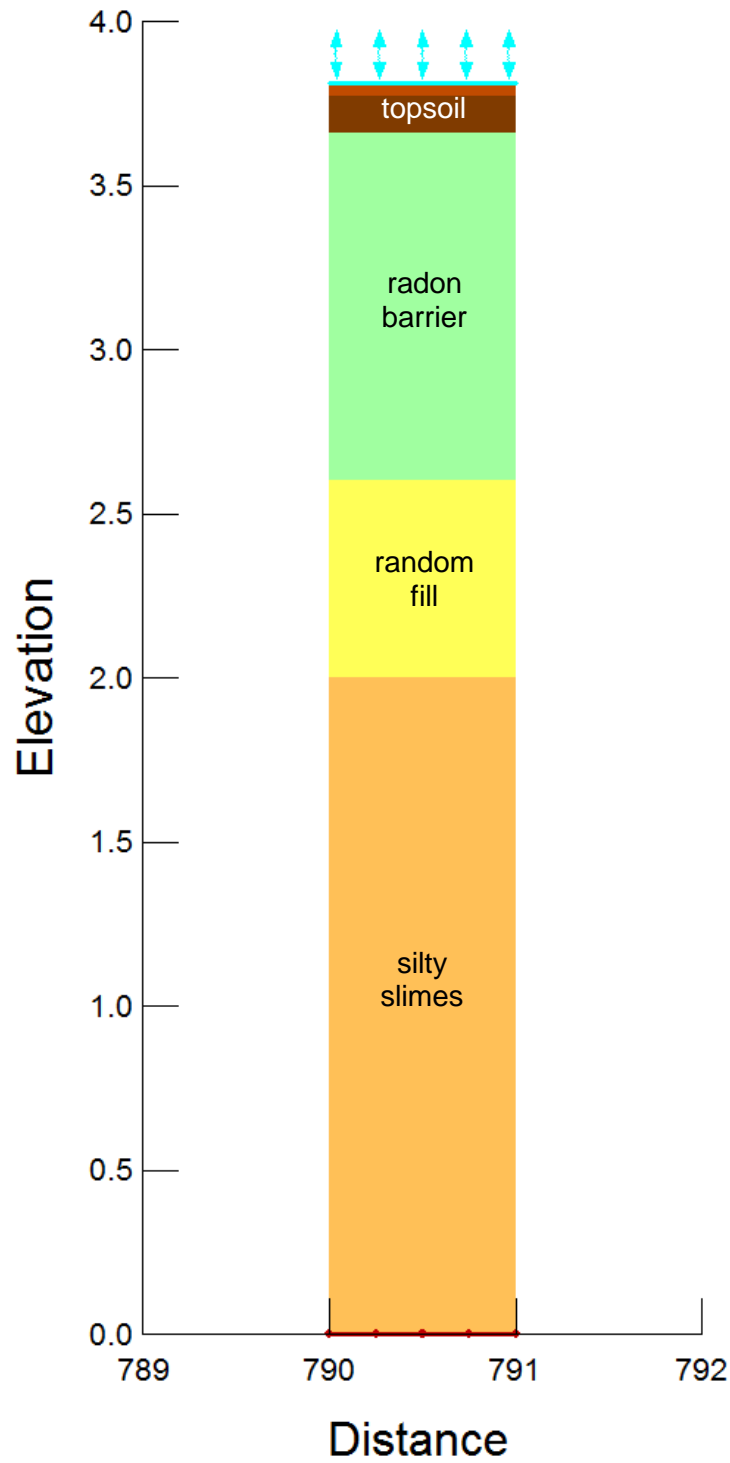


Figure 5-3. Highland Model Domain

| Table 5-1. Highland Model Discretization with 2-mm Element Size in Critical Zones |               |                     |                  |
|---|---------------|---------------------|------------------|
| Model Region  | # of Elements | ~Element Size (mm)* | Surface Layer ID |
| Topsoil 145 Interface   | 20            | 2                   | Layer 8          |
| Topsoil 145   | 56            | 2                   | Layer 7          |
| Top of Radon Barrier  | 5             | 2                   | Layer 6          |
| Middle of Radon Barrier   | 42            | 20                  | Layer 5          |
| Bottom of Radon Barrier   | 113           | 2                   | Layer 4          |
| Top of Fine Sandy Tailings  | 50            | 2                   | Layer 3          |
| Sandy Tailings  | 6             | 83                  | Layer 2          |
| Top of Silty Slimes (Root Depth Limit)  | 2             | 92                  | Layer 1          |
| Silty Slimes  | 18            | 101                 | Layer 0          |
| Total   | 312           |                     |                  |
| *1 mm = 0.039 in  |               |                     |                  |

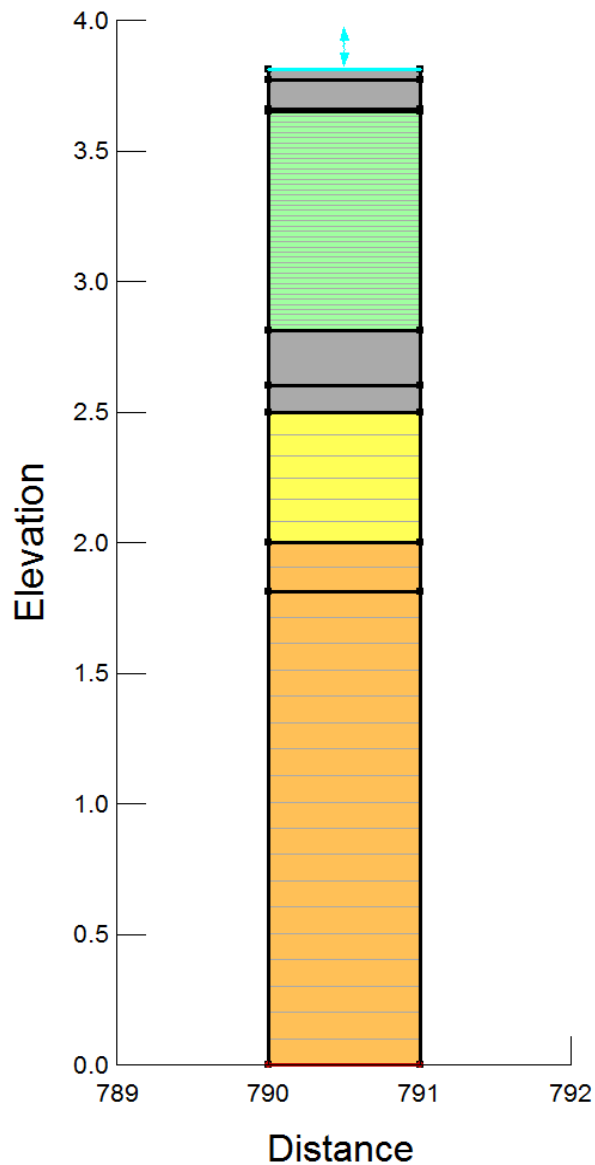


Figure 5-4. Highland Model Discretization. Gray Layers Illustrate Dense Discretization.

## 5.1.2 Material Properties

### *Hydraulic Properties*

Characteristic curves for Highland topsoil units were estimated based upon their general descriptions and information available from the NRCS (2014). This online resource was consulted for soil survey information that would be relevant to the cover topsoil (Table 5-2; Figure 5-5).

| <b>Soil Unit</b>                  | <b>Soil Unit Name</b>                                   | <b>Acres</b> | <b>%AOI</b> |
|-----------------------------------|---|--------------|-------------|
| 122                               | Hiland–Bowbac complex, 6 to 15 percent slopes           | 5.2          | 2.2         |
| 131                               | Shingle–Badland–Samday complex, 10 to 30 percent slopes | 11.1         | 4.8         |
| 145                               | Ustic Torriorthents, reclaimed, 3 to 30 percent slopes  | 194.1        | 84.0        |
| 212                               | Ustic Torriorthents, gullied                            | 1.0          | 0.4         |
| 215                               | Water   | 19.7         | 8.5         |
| Totals for Area of Interest (AOI) |   | 231.0        | 100.0       |

Soil Units 122 and 212 are not directly relevant to the net infiltration model because they principally occur on the eastern slope of the tailings dam.

Soil Unit 131, composed of clay loam and clay, occurs where the two drainage swales converge on the diversion channel at the northeastern corner of the soil cover; approximately the northeastern 230 m (755 ft) of the swale divide model may be composed of similar reworked soils.

Soil Unit 145, likely a sandy loam, comprises the majority of the soil cover.

Characteristics of soil units 131 and 145 are summarized in Table 5-3 (description of unit 131 is limited to Shingle and Samday soils, given Badland bedrock is not present at the ground surface of the cover). Soil units 131 and 145 all fall under the general Ustic Torriorthents soil classification. The ustic moisture regime is aridic and moisture-limited, yet moisture is available when conditions are suitable for plant growth. Orthents are well-drained and of medium-to-fine texture; they show little-to-no evidence of pedogenic horizon development where they occur on steep active slopes or where parent materials contain no permanent weatherable minerals. Typically, Orthents are shallow soils. Torriorthents are dry and possibly salty soils due to the dominant role of evaporation in concentrating soluble salts.

The swale divide transect length is 1,138 m (3,734 ft); staff estimate that toward the southwest, the first 908 m (2,979 ft) of topsoil along the transect consists of Soil Unit 145, whereas toward the northeast, the last 230 m (755 ft) of topsoil along the transect consists of Soil Unit 131 (Figure 5-2).

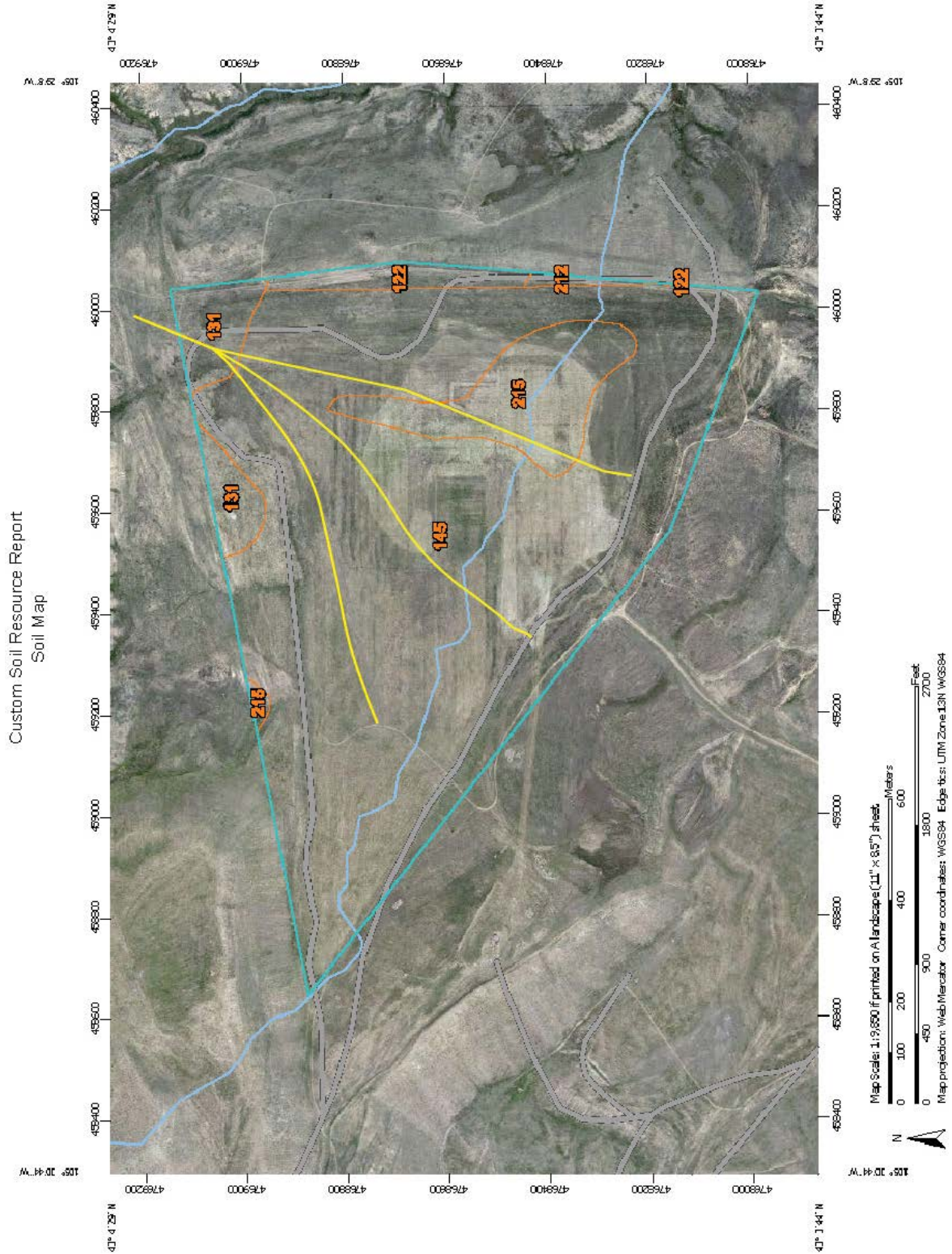


**Figure 5-5. Map View of Highland Mill Tailings Impoundment Soil Units (NRCS, 2014) Superimposed by Swales and Approximation of Swale Divide (Yellow). An Unnamed, Ephemeral Tributary of the North Fork of Box Creek, Dammed to Create the Highlands Tailings Impoundment, is Shown Superimposed on the Cover (Lt Blue). See also Table 5-2.**

| <b>Table 5-3. Characteristics of Soil Units 131 and 145 at the Highland Uranium Mill Tailings Impoundment (NRCS, 2014)</b>  |  |  |  |
|---|--|--|--|
| <b>Setting</b>  | <b>Shingle</b>   | <b>Samday</b>                                | <b>Ustic Torriorthents</b>   |
| MAP   | 254 to 356 mm (10 to 14 in)  |  |  |
| MAAT  | 7.2 to 10 °C (45 to 50 °F)   |  |  |
| Frost-free period   | 110 to 130 days  |  |  |
| Landform  | Hills  |  |  |
| Landform position (2D)  | summit, backslope  |  | —  |
| Landform position (3D)  | crest  |  | sideslope  |
| Down-slope shape  | Linear   |  |  |
| Across-slope shape  | Convex   |  |  |
| Parent material   | weathered residuum of sandstone and shale  | weathered residuum of calcareous shale       | weathered residuum or alluvium derived from sedimentary rock   |
| <b>Typical Profile</b>  |  |  |  |
|   | <b>Shingle</b>   | <b>Samday</b>                                | <b>Ustic Torriorthents</b>   |
| A   | 0–10 cm (0–4 in): moderately alkaline clay loam  | 0–5 cm (0–2 in): slightly alkaline clay loam | —  |
| C   | 10–33 cm (4–13 in): moderately alkaline clay   | 5–46 cm (2–18 in): moderately alkaline clay  | —  |
| Cr  | 33–152 cm (13–60 in): bedrock  | 46–152 cm (18–60 in): bedrock                | —  |
| H1  | —  | —  | 0–152 cm (0–60 in): variable   |
| <b>Properties/Qualities</b>   |  |  |  |
|   | <b>Shingle</b>   | <b>Samday</b>                                | <b>Ustic Torriorthents</b>   |
| Depth to restrictive feature  | 25–50 cm (10–20 in) to paralithic bedrock  |  | >2 m (>80 in)  |
| Natural drainage class  | well drained   |  |  |
| $K_{sat}$ of the least transmissive layer [m/day (ft/yr)]   | very to moderately low<br>0–0.366 (0–43.8)   |  | high*<br>0.866–3.46 (1040–4140)  |
| Available water storage in profile  | very low   |  | —  |
|   | ~6.35 cm (~2.5 in)   | ~7.37 cm (~2.9 in)                           | —  |
| Land capability classification 7e   | Very severe limitations restrict soil use mainly to grazing, forestland, or wildlife habitat; erosion risk is high unless close-growing plant cover is maintained      |  |  |
| Hydrologic soil group   | D: High runoff potential when thoroughly wet; water movement is restricted to very restricted; typically has >40 percent clay, <50 percent sand, with clayey textures. |  | B: Moderately low runoff potential when thoroughly wet; water movement is unimpeded; typically has 10–20 percent clay, 50–90 percent sand, with loamy sand or sandy loam textures. |
| *Natural Resources Conservation Service. "Part 630 Hydrology, Chapter 7: Hydrologic Soil Groups." In <i>National Engineering Handbook</i> . Natural Resources Conservation Service, U.S. Department of Agriculture. May 2007. |  |  |  |

| Unit | $K_{sat}$<br>[m/day (ft/yr)]       | VWC ( $m^3/m^3$ ) at: |        | Liquid Limit (%) | Plasticity Index (%) | %Clay | %Sand | %Silt |
|------|------------------------------------|-----------------------|--------|------------------|----------------------|-------|-------|-------|
|      |                                    | 1,500 kPa*            | 33 kPa |                  |                      |       |       |       |
| 122  | 1.67 (2000)                        | 0.142                 | 0.227  | 33.7             | 13.7                 | 25.3  | 63.0  | 11.7  |
| 131  | 0.792 (950)                        | 0.153                 | 0.295  | 36.7             | 16.7                 | 31.0  | 35.0  | 34.0  |
| 145  | 0.866 (1,040)<br>—<br>3.46 (4,140) | —                     | —      | —                | —                    | 1     | 98    | 1     |
| 212  | 0.792 (950)                        | 0.109                 | 0.263  | 30.0             | 10.0                 | 20.0  | 40.0  | 40.0  |

\*1 kPa = 0.33 ft H<sub>2</sub>O

The 1985 reclamation plan indicated that topsoil samples would be collected and analyzed for particle size distribution prior to seeding (Exxon Minerals Company, 1985); one such data set was found in a “Response to NRC Comments” document by Water, Waste and Land (1986). The particle size data from this sample (Table 5-5) suggests that the topsoil is a gravelly sand; not the loamy sand or sandy loam suggested by NRCS data in Table 5-2. This topsoil will tend to be dry, and when wet, dries quickly.

| Percent Finer | Grain Diameter (mm)* |
|---------------|----------------------|
| 67            | 4.757                |
| 52            | 2.000                |
| 42            | 0.841                |
| 26            | 0.420                |
| 7             | 0.149                |
| 2             | 0.074                |

\*1 mm = 0.039 in

Topsoil 145 moisture characteristic estimates were developed (Figure 5-6) by transforming the Table 5-4 particle size data using the physicoempirical methods outlined by Arya and Paris (1981) and Arya, et al. (1999a,b).

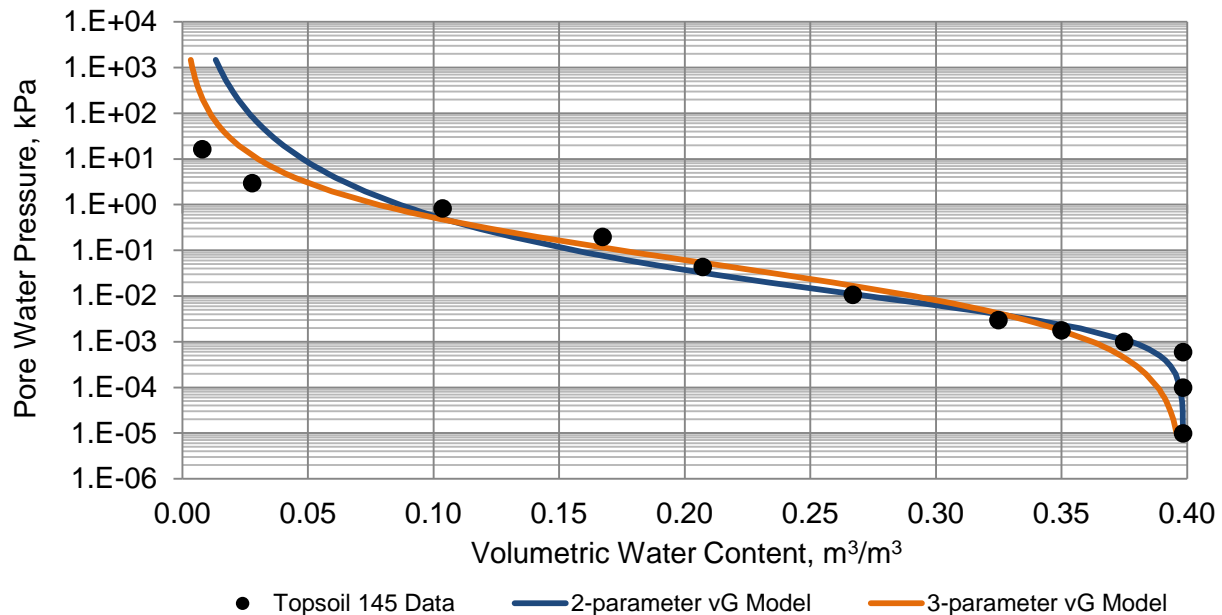


**Figure 5-6. Transformed Topsoil 145 Particle Size Data and van Genuchten Model Fits**

Topsoil 145 “data” for volumetric water contents greater than 27 percent are estimates based on expert judgement because the particle size analysis did not provide information for grain diameters >5 mm [>0.2 in] {67 percent of grains were finer than 4.757 mm [0.19 in], but binned data to cover the full range of 100 percent of the sample mass were not provided}. Several data points were added near the knee of the curve to force it to bend appropriately when approaching the porosity value.

Van Genuchten (1980) parameters for a 2-parameter ( $\alpha, n$  where  $m$  is a function of  $n$ ) model ( $R^2 = 0.981$ ) fitted to the transformed data (Figure 5-6) are:

- $\alpha = 0.0026 \text{ kPa}$  ( $8.7 \times 10^{-4} \text{ ft H}_2\text{O}$ )
- $n = 1.257$
- $m = 0.204$
- $VWC_{res} = 0 \text{ m}^3/\text{m}^3$

Likewise, van Genuchten parameters for a 3-parameter ( $\alpha, n, m$  where  $m$  is independent of  $n$ ) model ( $R^2 = 0.986$ ) fitted to the transformed data (Figure 5-6) are:

- $\alpha = 0.0310 \text{ kPa}$  ( $1.0 \times 10^{-2} \text{ ft H}_2\text{O}$ )
- $n = 0.586$
- $m = 0.756$
- $VWC_{res} = 0 \text{ m}^3/\text{m}^3$

Vadose/W only allows direct input of a 2-parameter van Genuchten model, yet the 3-parameter model exhibits a better fit to the data under dry conditions. Rather than using either of these models, a data point function was developed that combined aspects of both van Genuchten models into a hybrid model that fitted the transformed data better at both wet and dry ends of the function. A comparison of the original 2-parameter van Genuchten function and the final hybrid data point function is shown in Figure 5-7.

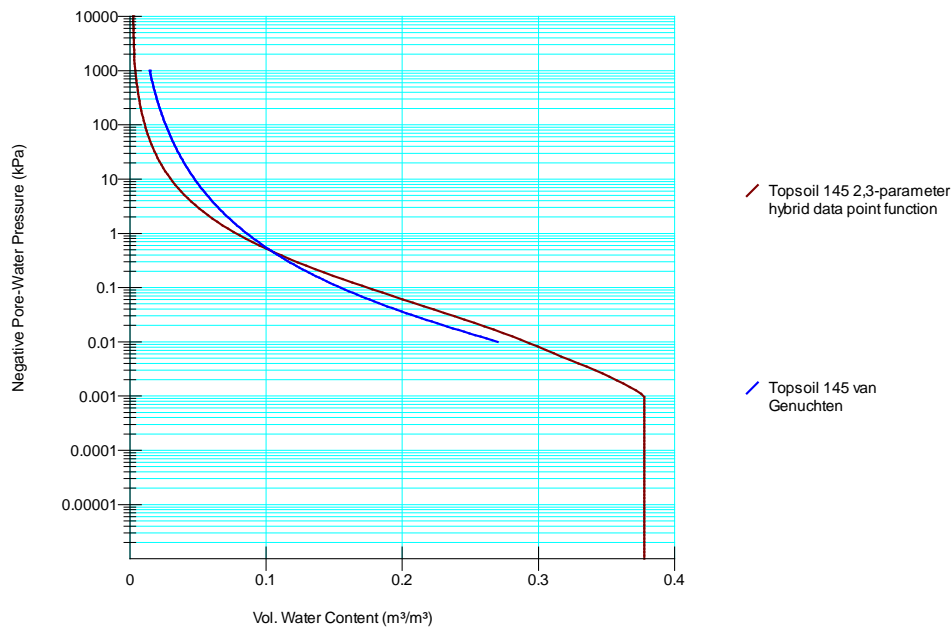


**Figure 5-7. Comparison of Topsoil 145 2-Parameter van Genuchten and Hybrid Data Point Functions**

Van Genuchten's (1980) method was used to estimate the hydraulic conductivity of Topsoil 145 as a function of volumetric water content (Figure 5-8); this method requires that  $n = 1/(1 - m)$ , as with the 2-parameter soil moisture characteristic function used in Vadose/W. This hydraulic conductivity function is only applied to the lowermost topsoil unit in the model domain. The hydraulic conductivity function for the ground surface–atmosphere interfacial topsoil layer (Figure 5-7) is defined as a simple linear function that only decays a couple orders of magnitude over the entire pore water pressure range, which aids convergence, per GEO-SLOPE International, Ltd. (2012).

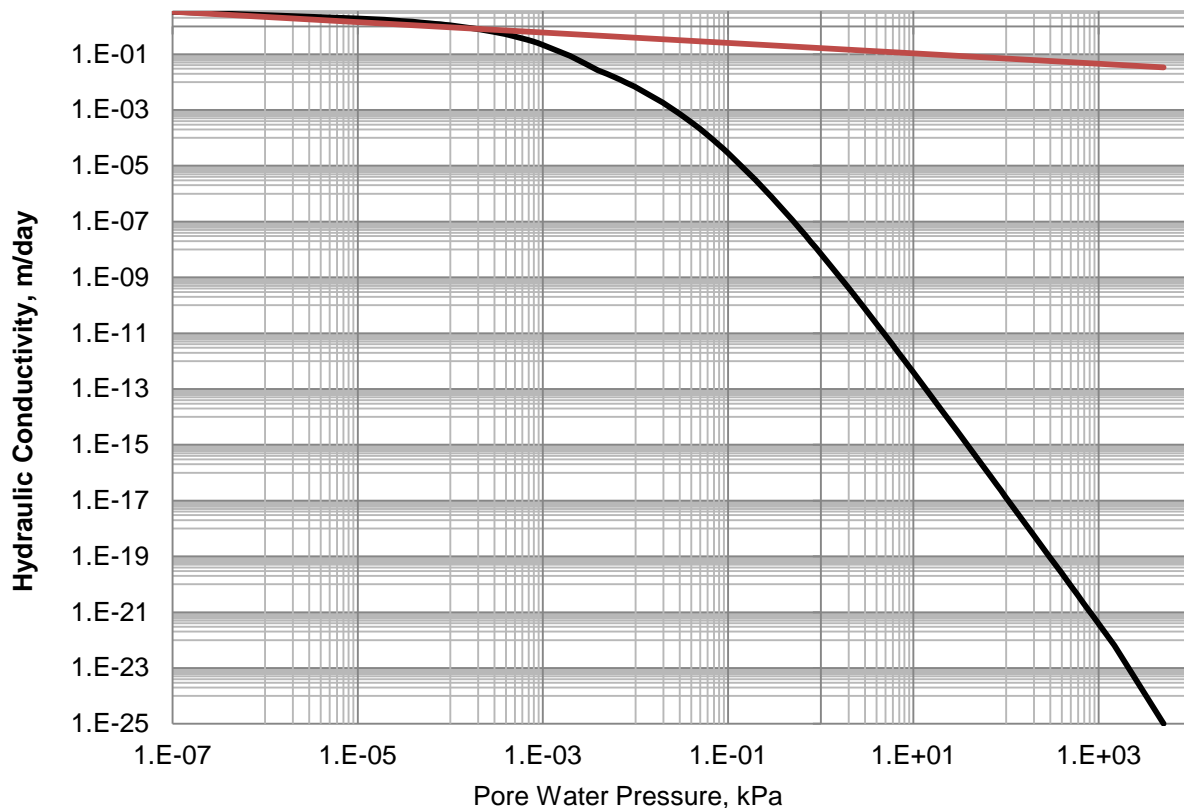


**Figure 5-8. Topsoil 145 Hydraulic Conductivity Functions of Pore Water Pressure for Deep (Black) and Shallow (Red) Topsoil Units**

Previous Highland-site modeling activities performed by other organizations and attendant criticisms of their selected parameters (Exxon Production Research Company, 1982; Williams, 1982; Water, Waste & Land, 1984, 1988) provided useful insight into appropriate hydraulic material properties for the radon barrier and mill tailings units. The best estimate (BE in Table 5-6) for saturated hydraulic conductivity ( $K_{sat}$ ) comes from the measured value of “sandier” radon barrier borrow material (which must be CL/SC, if not SC), given as  $1 \times 10^{-7}$  cm/s (0.1 ft/yr) (Water, Waste and Land, 1989b). This is the only measured value of radon barrier material that staff found for Highland, and it is considerably less permeable than Highland site backfill. This value is also less than what had been estimated for silty slimes. Early measured values of backfill permeability were reported as  $9.7 \times 10^{-6}$ ,  $4.1 \times 10^{-5}$ ,  $6.3 \times 10^{-4}$  cm/s (10, 42, and 650 ft/yr) (Exxon Production Research Company, 1982; Water, Waste and Land, 1989d). Given the radon barrier is composed of a carefully selected and compacted material that is classified as CL, CL/SC, SC, or CH, it is difficult to see how a hydraulic conductivity as great as  $6.3 \times 10^{-4}$  cm/s (650 ft/yr) could apply to the radon barrier when a

sandy sample of the material was measured to be as low as  $10^{-7}$  cm/s (0.1 ft/yr). Rather, it seems that the lowest hydraulic conductivity expected could be even lower than what was measured for the sandier radon barrier material. As far as where to draw the line on the upper end of the assumed range, it seems that in the absence of fractures or decayed root macropores, a clayey radon barrier would be less permeable than silty slimes. Extending the upper end of the range beyond  $9.7 \times 10^{-6}$  cm/s (10 ft/yr) appears to lack support.

Given the original specification for the radon barrier material (CL) and the subsequent two license amendments for use of sandier (CL/SC or SC) and clayier (CH) materials, Table 5-6 summarizes the expected range of variation in this soil cover unit. From Water, Waste and Land (1984), two samples of intermediate-type radon barrier material had 1,500 kPa water contents of 21 percent; drainable porosity was said to be 20 percent. There seems to be some uncertainty in regard to drainable porosity, and it could be that Water, Waste and Land (1984) rounded up a measured drainable porosity to 20 percent when reporting the value. For a sensitivity analysis, the range 20–22 for residual volumetric water content might be used. Five samples of sandy radon barrier material were tested for residual volumetric water content, so the mean value and the range for this material is known. For the clayier material, only porosity and 1,500 kPa water content were given; not a range. For sensitivity analyses, the residual volumetric water content range of 22–24 might be used.

|                     | %Passing No. 200 | Max Dry Density g/cm <sup>3*</sup> | Opt H <sub>2</sub> O Content, % | VWC <sub>res</sub> /1500 kPa |           | VWC <sub>sat</sub> |           |
|---------------------|------------------|------------------------------------|---------------------------------|------------------------------|-----------|--------------------|-----------|
|                     |                  |                                    |                                 | BE                           | Range     | BE                 | Range     |
| <b>Sandier</b>      | ≥40 to ≤79.9     | 1.79–1.87                          | 13–16                           | 13.1                         | 12.6–13.8 | 32.0               | 30.7–33.7 |
| <b>Intermediate</b> | ≥80 to ≤94.9     | 1.62–1.78                          | 16–22                           | 21.0                         | 20.0–22.0 | 38.0               | 35.3–40.0 |
| <b>Clayier</b>      | ≥95              | 1.55–1.61                          | 21–25                           | 23.0                         | 22.0–24.0 | 44.4               | 40.7–45.4 |

\*1 g/cm<sup>3</sup> = 62.4 lb/ft<sup>3</sup>

Geotechdata.info (2015), a geotechnical database website, documents saturated hydraulic conductivities for Unified Soil Classification System (USCS) soil categories; the values obtained for categories represented in the Highland radon barrier are reproduced in Table 5-7. The single saturated hydraulic conductivity value obtained from a sandy Highland radon barrier sample is the same as the CL–CH compacted clay value, and it falls within the overall CL range for low plasticity clay, silty clay, and sandy clay and within the overall CH range for high plasticity clay. Clayey sands (SC), however, are more permeable than the measured Highland sample.

| USCS  | Soil Description  | K <sub>sat</sub> (cm/day)* |                       |
|-------|---|----------------------------|-----------------------|
|       |   | Min                        | Max                   |
| CL    | Inorganic clays, silty clays, sandy clays of low plasticity | $4.32 \times 10^{-3}$      | $4.32 \times 10^{-1}$ |
| SC    | Clayey sands  | $4.75 \times 10^{-2}$      | $4.75 \times 10^{-1}$ |
| CH    | Inorganic clays of high plasticity                          | $8.64 \times 10^{-4}$      | $8.64 \times 10^{-1}$ |
| CL–CH | Compacted clay  | —                          | $8.64 \times 10^{-3}$ |

\*1 cm/day = 0.0328 ft/day

The U.S. Department of Agriculture’s U.S. Salinity Laboratory once supported development of the pedotransfer function code, Rosetta, for estimating soil moisture characteristics and

hydraulic conductivity functions from soil texture and bulk density data (Schaap, 1999). This code does not run on modern computers and is not currently being supported by the developer, yet its published table of class-average hydraulic properties may still be consulted for representative functions. Staff used the Rosetta parameters to examine possible shapes for clay-type soil moisture characteristic curves. Note that  $\alpha$  is in units of  $\text{cm}^{-1}$  in Rosetta, unlike units used in Vadose/W (Table 5-8). To obtain a sandy clay residual water content of ~13.1 percent at 15,000 kPa (Table 5-6), the model parameters  $\log(\alpha)$  and  $\log(n)$  should be  $-1.476 + 0.57$  and  $0.082 + 0.06$ , respectively (Table 5-8; i.e.,  $\alpha = 0.12417$  and  $n = 1.387$ ). To obtain a silty clay model representing the original specification for radon barrier material (residual water content of ~21.0 percent at 15,000 kPa; Table 5-6) while maintaining a shape more consistent with the silt component, the model parameters  $\log(\alpha)$  and  $\log(n)$  should be  $-1.790 + 0.64$  and  $0.121$ , respectively (Table 5-8; i.e.,  $\alpha = 0.0707946$  and  $n = 1.321$ ). Finally, to obtain a clayey residual water content of ~23.0 percent at 15,000 kPa (Table 5-6) while maintaining a shape more consistent with clay, the model parameters  $\log(\alpha)$  and  $\log(n)$  should be  $-1.825 + 0.68$  and  $0.98$ , respectively (Table 5-8; i.e.,  $\alpha = 0.0707946$  and  $n = 1.253$ ). These three potential radon barrier characteristic curves are illustrated in Figure 5-9. Were enough time and resources available, sensitivity analyses could be run to understand the impact of the various types of radon barrier materials present in the Highland cover on net infiltration, but for this particular modeling effort, a single type of material was tested—that for the silty clay material, initially specified in the reclamation plan prior to subsequent license amendments that later allowed a broader set of material properties to compose the cover.

| Texture | <i>N</i> | $\text{VWC}_{\text{res}}$<br>( $\text{m}^3/\text{m}^3$ ) |             | $\text{VWC}_{\text{sat}}$<br>( $\text{m}^3/\text{m}^3$ ) |             | $\log(\alpha)$ [ $\log(1/\text{cm})$ ] |            | $1/\alpha$ ( $\text{cm} \cdot \text{H}_2\text{O}$ ) | $\log(n)$ |            |
|---------|----------|--|-------------|--|-------------|--|------------|---|-----------|------------|
| Clay    | 84       | 0.098  | $\pm 0.107$ | 0.459  | $\pm 0.079$ | -1.825                                 | $\pm 0.68$ | 66.8  | 0.098     | $\pm 0.07$ |
| S Clay  | 11       | 0.117  | $\pm 0.114$ | 0.385  | $\pm 0.046$ | -1.476                                 | $\pm 0.57$ | 29.9  | 0.082     | $\pm 0.06$ |
| Si Clay | 28       | 0.111  | $\pm 0.119$ | 0.481  | $\pm 0.080$ | -1.790                                 | $\pm 0.64$ | 61.7  | 0.121     | $\pm 0.10$ |

\*1 cm = 0.39 in

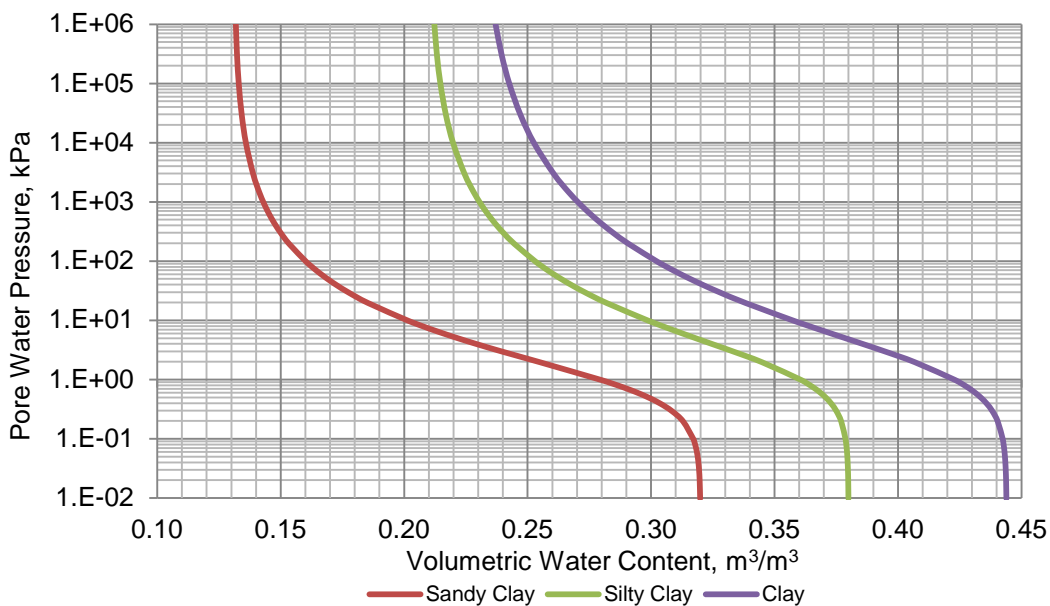


**Figure 5-9. Soil Moisture Characteristic Functions that Represent the Three Approved Radon Barrier Materials Used in the Highland Uranium Milling Tailings Impoundment Soil Cover. The Silty Clay Function was Used in Modeling. (1 kPa = 0.33 ft H<sub>2</sub>O)**

Using the van Genuchten (1980) method, the silty clay function of Figure 5-10 was produced to represent the radon barrier hydraulic conductivity function of pore water pressure.

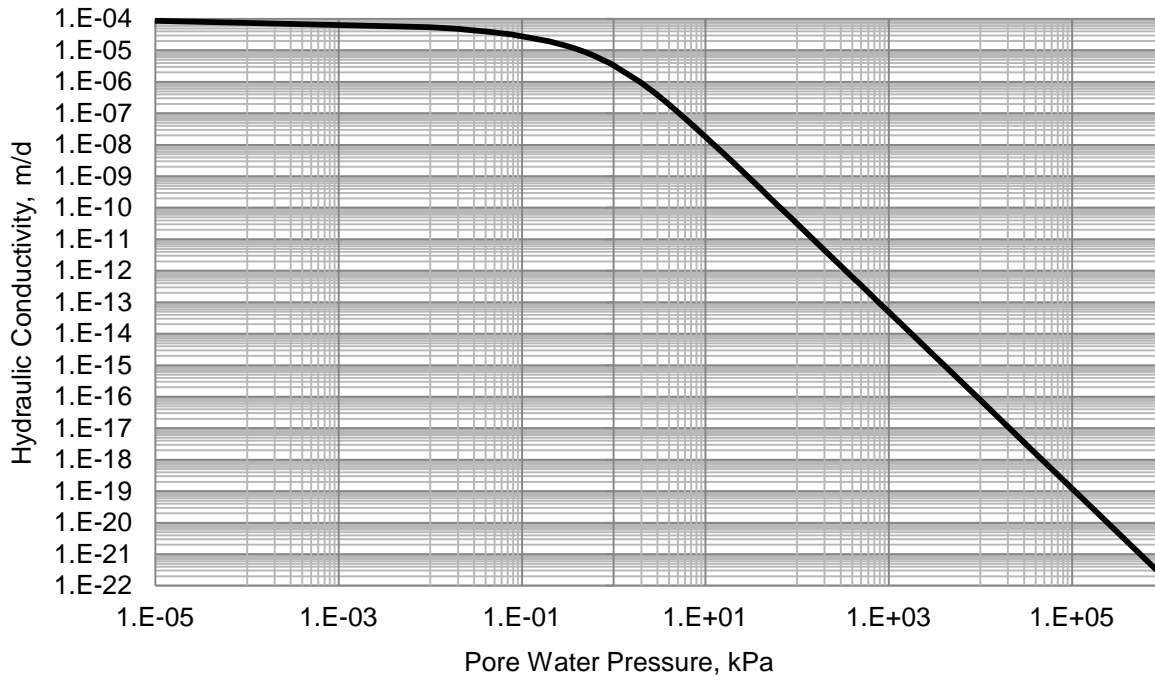


**Figure 5-10. Silty Clay Hydraulic Conductivity Model for the Highland Radon Barrier (1 kPa = 0.33 ft H<sub>2</sub>O; 1 m/day = 3.28 ft/day)**

Sandy tailings in the Highland impoundment are derived from local sandstone, and likely have similar hydraulic properties, but have been modified by lack of cement that would lithify sand particles. For this reason, sandy tailings likely are *more permeable* than the sandstone from which they are derived. For the sandy tailings, staff used porosity of 0.395, residual volumetric water content of 0.106, and bulk density of 1.61 g/cm<sup>3</sup>, which are similar to or the same as values used for the radon model of Water, Waste and Land (1984). The relative permeability to water and moisture characteristic functions measured from Highland sandstone Core XII, reproduced in Figures 5-11 and 5-12 (Exxon Production Research Company, 1982; their Figures 28 and 31) were digitized to represent sandy tailings in the Highland impoundment.

Based upon digitization of curves shown in Figures 5-10 and 5-11, the Highland sandstone data converted to metric units for the Vadose/W model are given in Tables 5-9 and 5-10.

| <b>Table 5-9. Relative Permeability (<math>k_{rw}</math>), Fluid Saturations, Pore Water Pressures, and Hydraulic Conductivity Data Points for Highland Tailings Sand, Estimated Based Upon Figures 5-10 and 5-11 and <math>K_{sat}</math> of 1.27 m/day</b> |                    |                      |                            |              |
|--|--------------------|----------------------|----------------------------|--------------|
| $k_{rw}$ (-)   | Gas Saturation (%) | Water Saturation (%) | Pore Water Pressure (kPa)* | $K$ (m/day)† |
| 0.0000   | 100.00             | 00.00                | 30220.83                   | 0.0000       |
| 0.0120   | 23.40              | 76.60                | 5.25                       | 0.0152       |
| 0.0296   | 17.09              | 82.91                | 3.46                       | 0.0376       |
| 0.1056   | 9.45               | 90.55                | 2.15                       | 0.1341       |
| 0.1611   | 7.10               | 92.90                | 1.87                       | 0.2046       |
| 0.5370   | 2.18               | 97.82                | 1.41                       | 0.6820       |
| 1.0000   | 0.00               | 100.00               | 1.24                       | 1.2700       |

\*1 kPa = 0.33 ft H<sub>2</sub>O  
†1 m/d = 3.28 ft/d

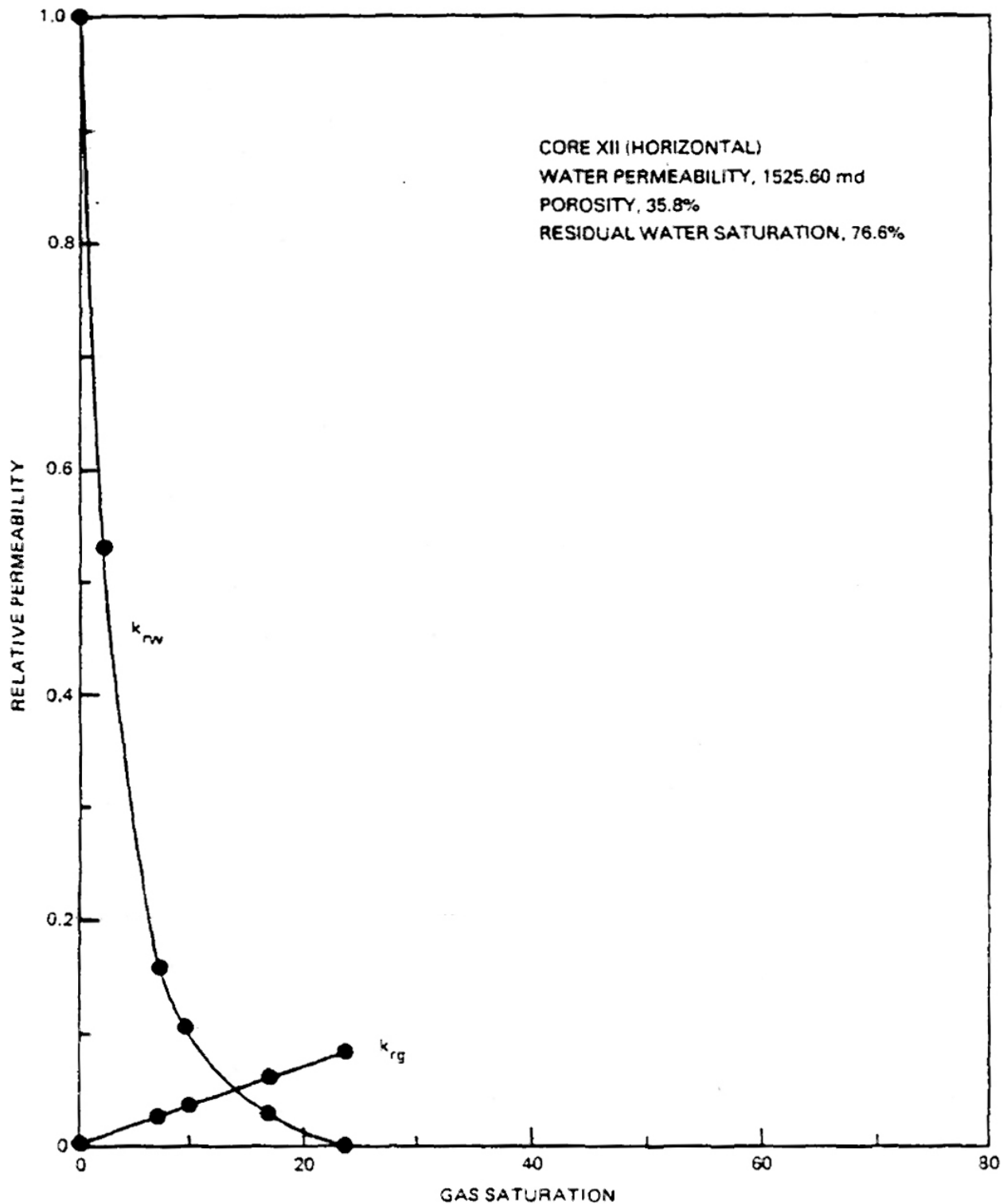


Figure 5-11. Horizontal Air ( $k_{rg}$ ) and Water ( $k_{rw}$ ) Relative Permeabilities and Intrinsic Permeabilities [in millidarcies (md)] of Tailings Dam Sand Core XII, Selected for use by Exxon Production Research Company (1982; Their Figure 28) in Their Modeling of Highland Sandstone Units; the  $k_{rw}$  Relationship Shown was used in this Modeling to Represent Sandy Tailings. Note 1 darcy =  $0.99 \times 10^{-12} \text{ m}^2$

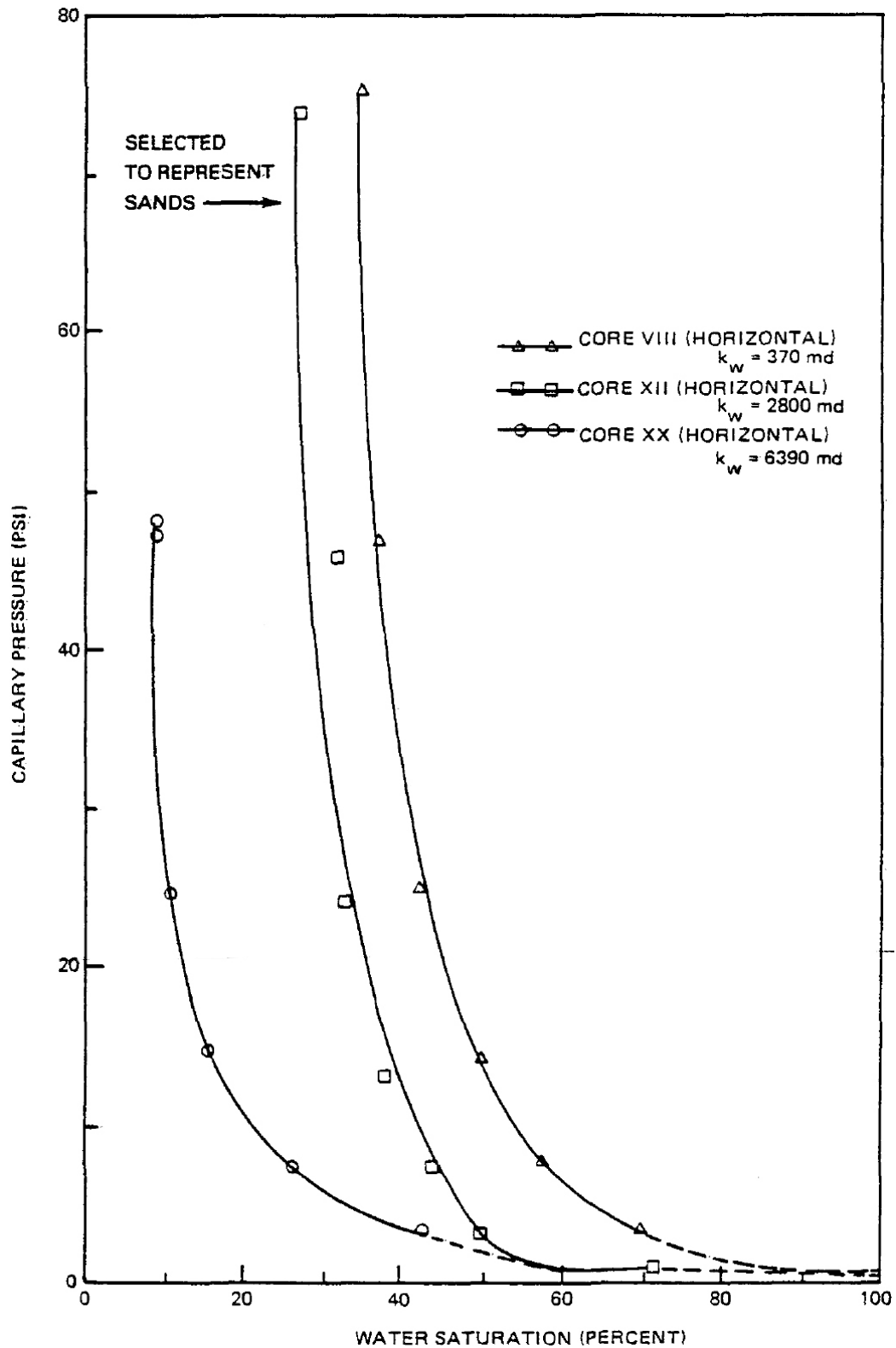
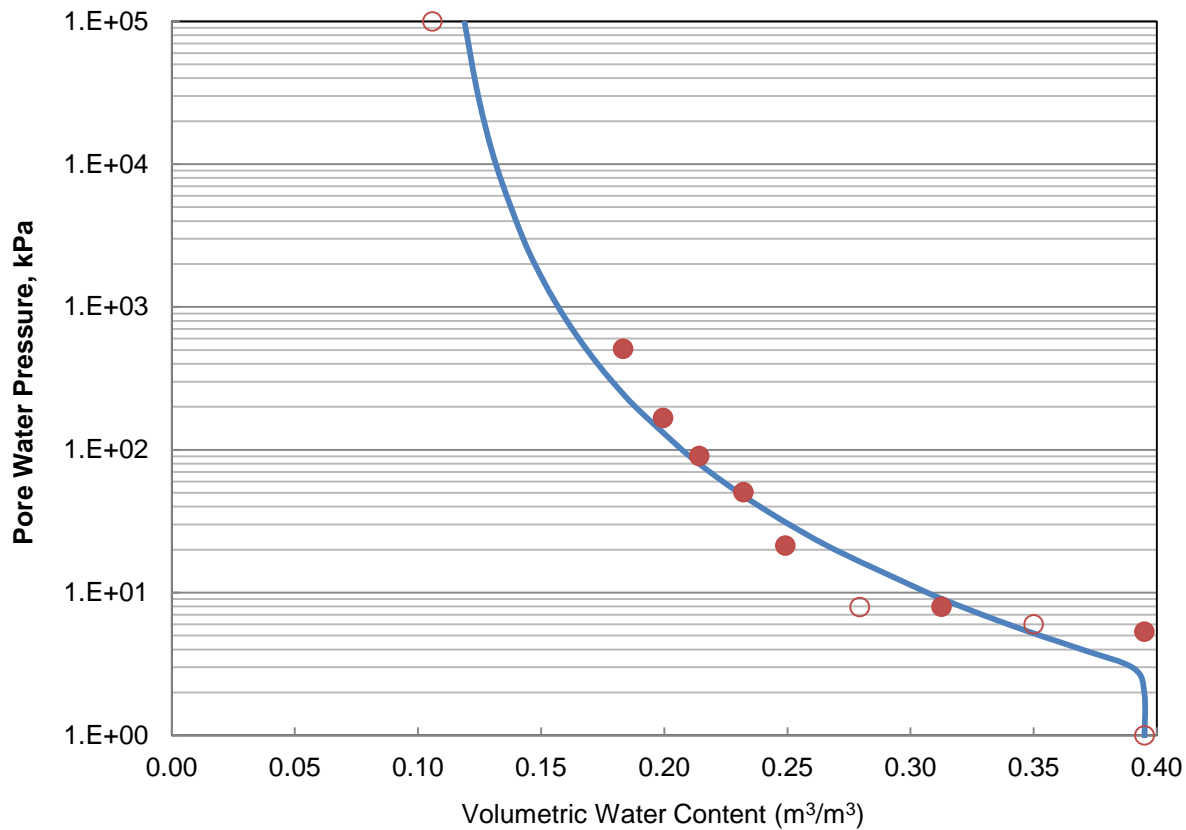


Figure 5-12. Horizontal Soil Water Characteristic Curves from Tailings Dam Sand Cores; That for Core XII was Selected by Exxon Production Research Company (1982; Their Figure 31) to Model Highland Sandstone Units and in this Modeling to Represent Sandy Tailings. (1 psi = 6.89 kPa)

| Table 5-10. Water Saturation, Pore Water Pressure, and Volumetric Water Content<br>[Including van Genuchten (vG) Model] Data Points Based Upon<br>Core XII in Figure 5-11 and Porosity Estimate |                            |          |                              |          |
|---|----------------------------|----------|------------------------------|----------|
| Water Saturation  | Pore Water Pressure (kPa)* |          | Volumetric Water Content (%) |          |
|   | Data                       |          | Data                         | vG Model |
| 0.000   |                            | 99994.66 | 0.106                        | 0.119    |
| 0.268   |                            | 509.18   | 0.183                        | 0.168    |
| 0.324   |                            | 167.06   | 0.200                        | 0.193    |
| 0.375   |                            | 90.18    | 0.214                        | 0.210    |
| 0.437   |                            | 50.40    | 0.232                        | 0.230    |
| 0.496   |                            | 21.24    | 0.249                        | 0.266    |
| 0.600   |                            | 7.93     | 0.279                        | 0.321    |
| 0.715   |                            | 7.93     | 0.313                        | 0.321    |
| 0.844   |                            | 6.00     | 0.350                        | 0.340    |
| 1.000   |                            | 5.31     | 0.395                        | 0.348    |
| 1.000   |                            | 1.00     | 0.395                        | 0.395    |

\*1 kPa = 0.33 ft H<sub>2</sub>O

The filled data points in the sandy tailings soil moisture curve (Figure 5-13) represent those digitized from Figure 5-12, whereas the open data points were added by staff to facilitate obtaining the desired residual volumetric water content and the bend at the knee of the curve (note the data point at 60 percent saturation/27.9 percent water content was easily read off what appears to be the licensee's hand-drawn curve in Figure 5-12).



**Figure 5-13. Sandy Tailings Moisture Characteristic Based Upon the Horizontal Soil Water Characteristic Curves of Tailings Dam Sand Core XII (Figure 5-11; 1 kPa = 0.33 ft H<sub>2</sub>O)**

The resulting 3-parameter van Genuchten model is:

- $VWC_{res} = 0.106$
- $VWC_{sat} = 0.395$
- $\alpha = 2.936$
- $n = 14.206$
- $m = 0.021$

The  $R^2$  of the 3-parameter van Genuchten model was 0.947, suggesting the model accounts for more than 94 percent of the variability in the modeled data. Because Vadose/W does not directly ingest a 3-parameter van Genuchten model, equivalent fine sandy tailings data pairs were entered into the Highland material model as a data point function, but only after down-shifting the curve by an order of magnitude (dividing pore water pressures by 10) to account for the lack of cement in the sandy tailings. Had the curve, as it was, been used directly, the sandy tailings air-entry pressure would have been greater than that of the radon barrier material, which was not sensible.

To prepare the van Genuchten (1980) hydraulic conductivity function for the sandy tailings, the  $m$ -value from a 2-parameter model, 0.248, was used (Figure 5-13). Data points shown in Figure 5-14 are equivalent to those plotted in Figure 5-11, with the exception that the equivalent pore water pressures were divided by 10, consistent with the soil moisture characteristic and the pressures used to estimate the hydraulic conductivity function.

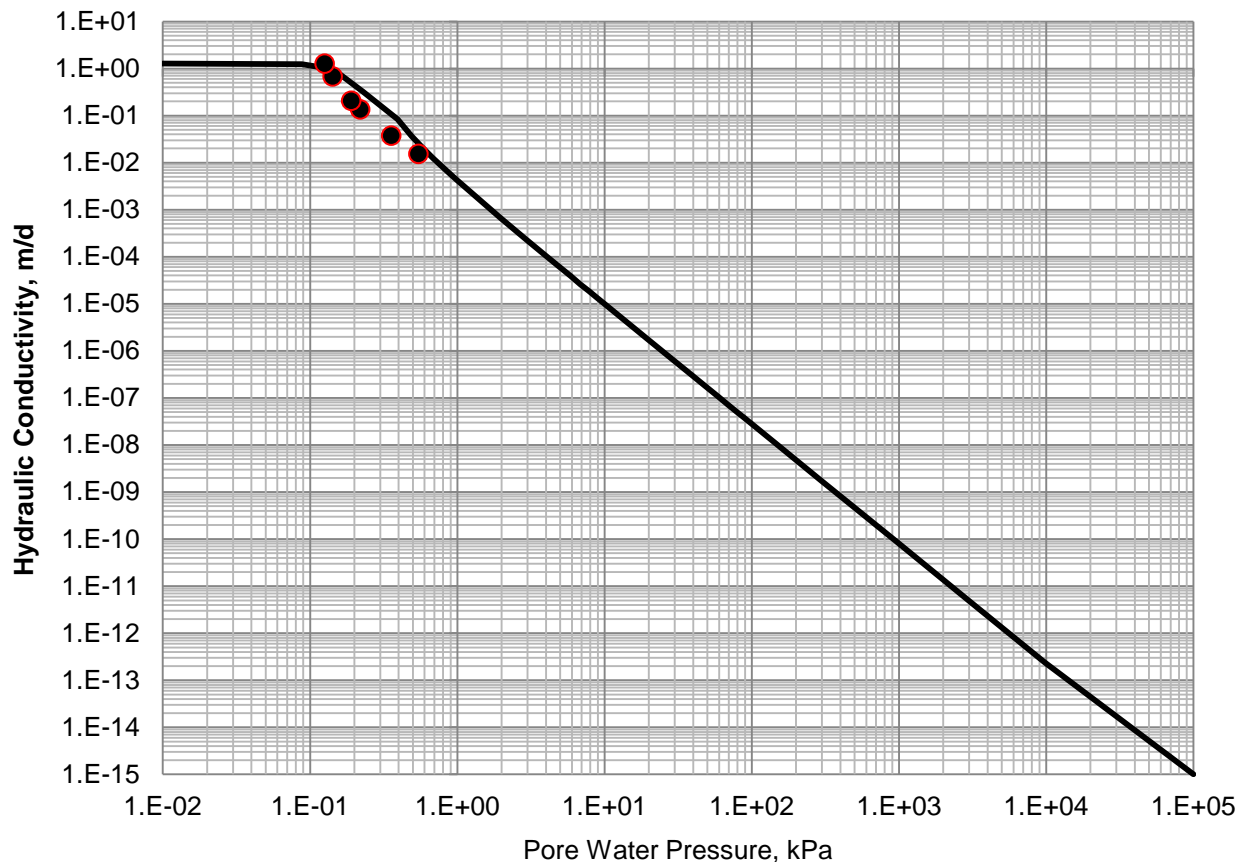


**Figure 5-14. Highland Sandy Tailings Hydraulic Conductivity Function**  
(1 kPa = 0.33 ft H<sub>2</sub>O; 1 m/day = 3.28 ft/day)

Based upon what is known about the residual moisture content of the slimes, they may be more like a silty clay than a silt, therefore, the slimes moisture characteristic was developed based upon Rosetta's silty clay texture class (Table 5-8). These model parameters had been used previously to develop the moisture characteristic function for the radon barrier; in this case, only the porosity differs.

- $\alpha = 0.071 \text{ cm}^{-1} = 0.722 \text{ kPa}^{-1}$
- $n = 1.32$
- $VWC_{res} = 0.21 \text{ m}^3/\text{m}^3$
- $VWC_{sat} = 0.49 \text{ m}^3/\text{m}^3$

Assuming  $m = 1 - 1/n$ , and using  $K_{sat} = 4.18 \times 10^{-3} \text{ m/day}$ , the van Genuchten model for the hydraulic conductivity of silty clay slimes was developed. The complete set of moisture characteristic and hydraulic conductivity functions imported into Vadose/W are presented in Figures 5-15 and 5-16.

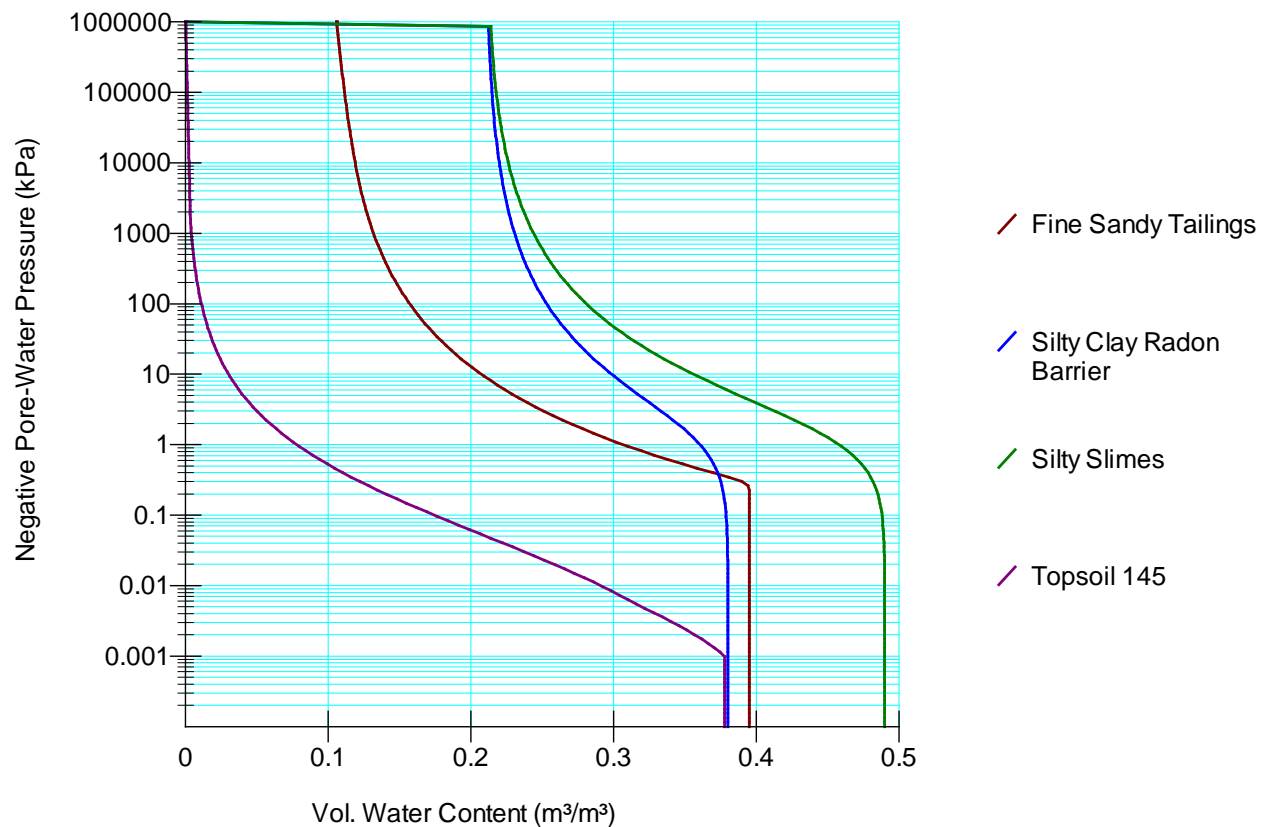


**Figure 5-15. Summary Comparison of Highland Soil Column Moisture Characteristic Functions**

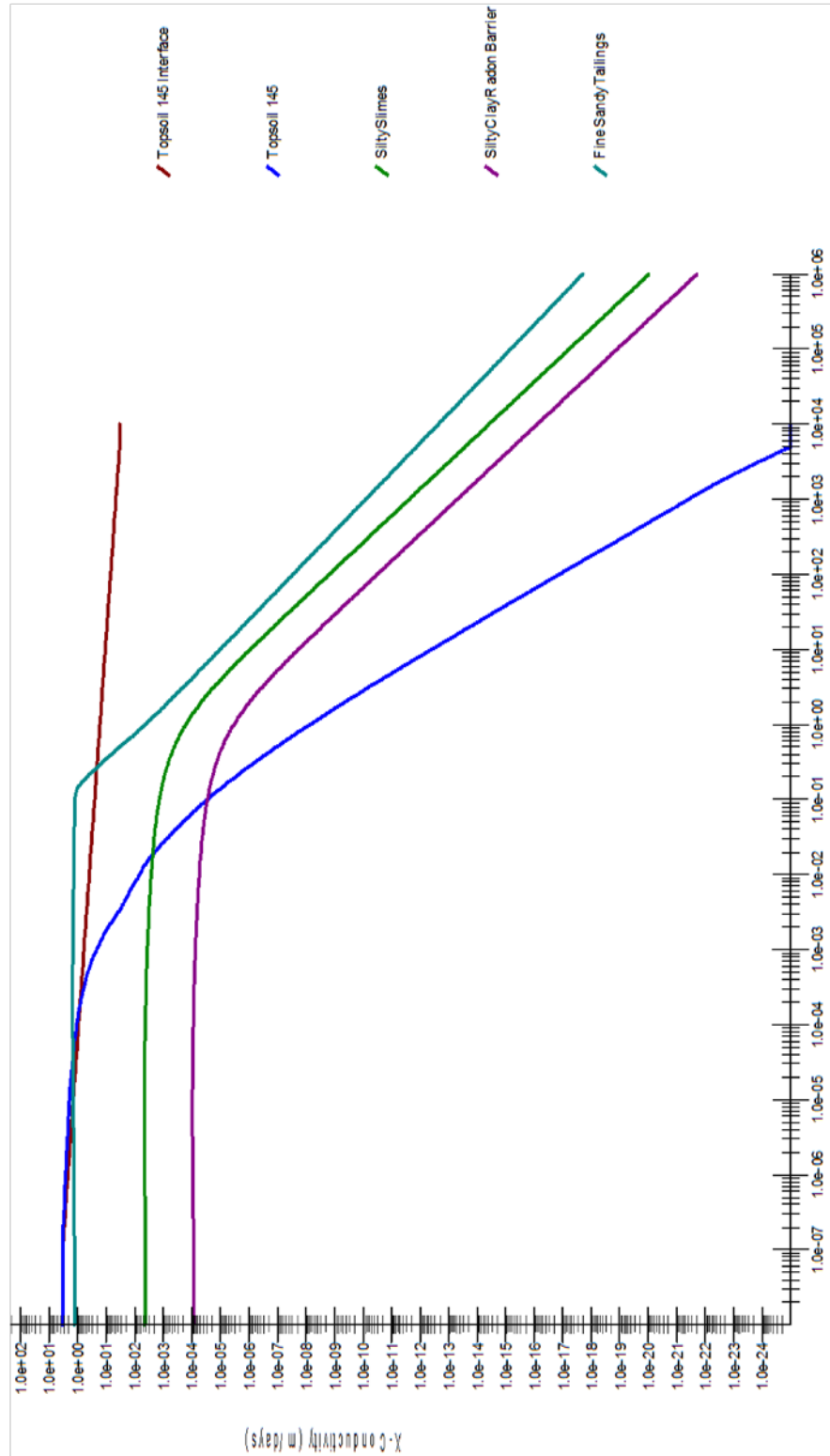


**Figure 5-16. Summary Comparison of Highland Soil Column Horizontal Hydraulic Conductivity Functions of Negative Pore Water Pressure (i.e., Matric Suction)**

Hydraulic property best estimates and sensitivity analysis ranges recommended for use in Highland soil cover net infiltration models are summarized in Table 5-11. The radon barrier is a permeability barrier relative to the overlying topsoil. There is a capillary barrier at the base of

the radon barrier. No permeability barrier exists at the interface of the fine sandy tailings and silty slimes.

| <b>Table 5-11. Best Estimates/Sensitivity-Analysis Ranges for Highland Site Hydraulic Properties (Exxon Production Research Company, 1982; NRCS, 2014; Water, Waste &amp; Land, 1984, 1988, 1989a,b,c, 1991)</b> |   |   |                |  |              |                               |
|--|---|---|----------------|--|--------------|-------------------------------|
| <b>Material</b>  | <b><math>K_{sat}</math> [m/day (ft/yr)]</b> |   | <b>K-Ratio</b> | <b><math>VWC_{sat}</math> (<math>m^3/m^3</math>)</b> |              | <b><math>VWC_{res}</math></b> |
|  | <b>Best Estimate</b>                        | <b>Range</b>                              |                | <b>Best Estimate*</b>                                | <b>Range</b> | <b>Best Estimate</b>          |
| Soil Unit 145  | 3.34<br>(4000)                              | 0.835 – 3.34<br>(1000 – 4000)             | 1              | 0.3985   | 0.36–0.43    | 0.00                          |
| Radon Barrier  | $8.64 \times 10^{-5}$<br>(0.1)              | $8.64 - 847 \times 10^{-5}$<br>(0.1 – 10) | 1              | 0.38   | 0.31–0.45    | 0.21                          |
| Sandy Tailings   | 1.27<br>(1520)                              | 0.0835 – 3.34<br>(100 – 4000)             | 0.1            | 0.395  | 0.34–0.40    | 0.106                         |
| Slime Tailings   | $4.18 \times 10^{-3}$<br>(5)                | $8.35 - 75.2 \times 10^{-4}$<br>(1 – 9)   | 0.1            | 0.49   | 0.35–0.49    | 0.21                          |

\*Table 5.1 of Water, Waste and Land (1984), which concerns the cover design, was the source of the porosity “best estimates.” These high-end values should be given greater weight than the low-end estimates from less-directly related modeling activities used to develop the “range.”

### *Thermal Properties*

Given that the Highland topsoil sample was composed of gravelly sand, staff selected the Becker, et al. (1992) mean gravel thermal conductivity function of saturation for use. Sand has a broad thermal conductivity range (Figure 3-2) that fully encompasses the mean gravel function, and the mean gravel function has a nearly identical curvature to that of the mean sand, although it is more thermally conductive at all saturations. Because the topsoil is a gravelly sand, not a gravel, CNWRA staff extended the mean gravel correlation beyond the 40 percent saturation limit of a typical gravel. After converting the mean gravel saturation to equivalent volumetric water content, the thermal conductivity data point function for the topsoil model layers is given in Table 5-12.

| <b>Table 5-12. Becker, et al. (1992) Mean Gravel Thermal Conductivity (<math>K_{th}</math>) Data Point Function for Highland's Gravelly Sand Topsoil</b> |   |
|--|---|
| <b>VWC (<math>m^3/m^3</math>)</b>  | <b><math>K_{th}</math> kJ/(day·m·°C)*</b> |
| 0.0000   | 50  |
| 0.0193   | 62  |
| 0.0336   | 75  |
| 0.0450   | 87  |
| 0.0550   | 100                                       |
| 0.0651   | 112                                       |
| 0.0770   | 125                                       |
| 0.0921   | 137                                       |
| 0.1129   | 149                                       |
| 0.1422   | 162                                       |
| 0.1594   | 168                                       |
| 0.1845   | 174                                       |
| 0.2458   | 187                                       |
| 0.3351   | 199                                       |
| 0.3985   | 206                                       |

\*1 kJ/day·m·°C = 0.161 Btu/day·ft·°F

For the Highland radon barrier, the three allowable types of radon barrier material were sandy clay, silty clay, and clay. Given the Becker, et al. (1992) functions for thermal conductivity (Figure 3-2), the mean curves for clay and silt are quite similar. If fundamentally the radon barrier is mostly clayey, modified by some contribution of sand or silt, using the mean clay thermal conductivity function (Table 5-13) ought to be acceptable for all three radon barrier types in the absence of site-specific information.

| <b>Table 5-13. Becker, et al. (1992) Mean Clay Thermal Conductivity (<math>K_{th}</math>) Data Point Function for Highland's Silty Clay Radon Barrier</b> |   |
|---|---|
| <b>VWC (<math>m^3/m^3</math>)</b>   | <b><math>K_{th}</math> kJ/(day·m·°C)*</b> |
| 0.2100  | 25  |
| 0.2267  | 37  |
| 0.2410  | 50  |
| 0.2538  | 62  |
| 0.2660  | 75  |
| 0.2785  | 87  |
| 0.2922  | 100                                       |
| 0.3080  | 112                                       |
| 0.3271  | 125                                       |
| 0.3507  | 137                                       |
| 0.3800  | 149                                       |

\*1 kJ/day·m·°C = 0.161 Btu/day·ft·°F

For the sandy tailings, CNWRA staff used porosity of 0.395 to calculate equivalent volumetric water content for the Becker, et al. (1992) mean sand thermal conductivity function (Table 5-14).

| <b>Table 5-14. Becker, et al. (1992) Mean Sandy Thermal Conductivity (<math>K_{th}</math>) Data Point Function for Highland's Sandy Tailings</b> |  |
|--|--|
| <b>VWC (<math>m^3/m^3</math>)</b>  | <b><math>K_{th}</math>, kJ/(day·m·°C)*</b> |
| 0.1059   | 44   |
| 0.1143   | 50   |
| 0.1215   | 56   |
| 0.1275   | 62   |
| 0.1328   | 69   |
| 0.1375   | 75   |
| 0.1417   | 81   |
| 0.1458   | 87   |
| 0.1497   | 93   |
| 0.1537   | 100  |
| 0.1580   | 106  |
| 0.1626   | 112  |
| 0.1679   | 118  |
| 0.1740   | 125  |
| 0.1811   | 131  |
| 0.1896   | 137  |
| 0.1997   | 143  |
| 0.2120   | 149  |
| 0.2268   | 156  |
| 0.2448   | 162  |
| 0.2667   | 168  |
| 0.2933   | 174  |
| 0.3259   | 181  |
| 0.3655   | 187  |
| 0.3950   | 191  |

\*1 kJ/day·m·°C = 0.161 Btu/day·ft·°F

For the silty clay slimes, staff used the Becker, et al. (1992) mean silt thermal conductivity relationship (Table 5-15) based on an understanding that the other material properties of this unit suggest it is more silty than the silty clay radon barrier ( $K_{sat}$ , for example). The mean silt and mean clay thermal conductivity relationship are very similar, per Becker, et al. (1992).

**Table 5-15. Becker, et al. (1992) Mean Silt Thermal Conductivity ( $K_{th}$ ) Data Point Function for Highland's Silty Clay Slimes**

| VWC ( $m^3/m^3$ ) | $K_{th}$ , kJ/(day·m·°C)* |
|-------------------|---------------------------|
| 0.2100            | 31                        |
| 0.2324            | 37                        |
| 0.2512            | 44                        |
| 0.2671            | 50                        |
| 0.2808            | 56                        |
| 0.2928            | 62                        |
| 0.3035            | 69                        |
| 0.3135            | 75                        |
| 0.3231            | 81                        |
| 0.3327            | 87                        |
| 0.3426            | 93                        |
| 0.3534            | 100                       |
| 0.3654            | 106                       |
| 0.3790            | 112                       |
| 0.3949            | 118                       |
| 0.4137            | 125                       |
| 0.4244            | 128                       |
| 0.4362            | 131                       |
| 0.4490            | 134                       |
| 0.4631            | 137                       |
| 0.4786            | 140                       |
| 0.4900            | 142                       |

\*1 kJ/day·m·°C = 0.161 Btu/day·ft·°F

The complete set of thermal conductivity functions imported into the Highland Vadose/W model is presented in Figure 5-17.

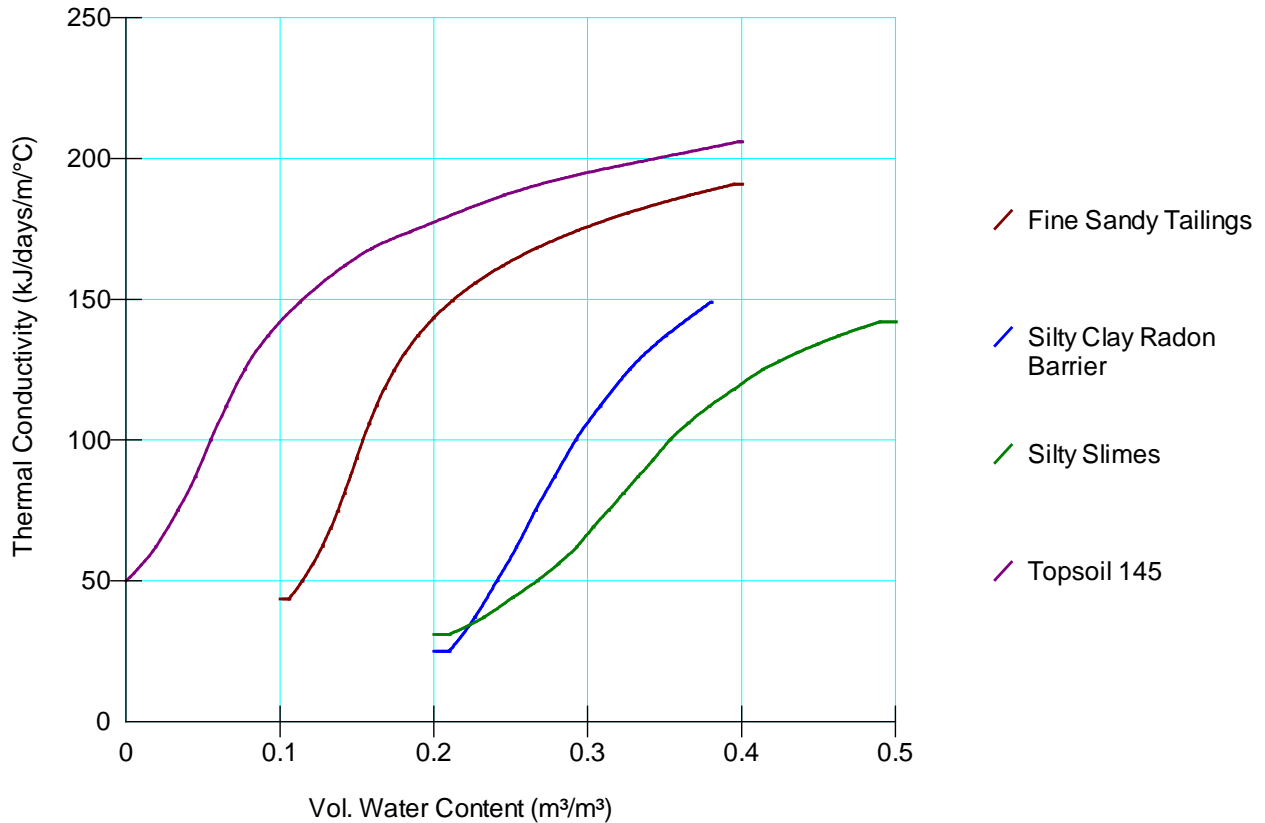


**Figure 5-17. Summary Comparison of Highland Thermal Conductivity Functions (1 kJ/day·m·°C = 0.16 Btu/day·ft·°F)**

For the volumetric specific heat capacity functions of volumetric water content, staff used the built-in de Vries (1963) estimation function to develop these relationships. The volumetric water content range for each material delineates the range over which the volumetric specific heat must be defined. The mass specific heat of 0.71 kJ/kg·°C (0.17 Btu/lb·°F) was used for all model layers. The y-intercept, which is the dry soil volumetric specific heat or the heat capacity with when the volumetric water content is zero, is the product of the dry bulk density and the mass specific heat capacity of the soil mineral solids.

All volumetric specific heat capacity functions defined for the Highland model layers are illustrated in Figure 5-18.

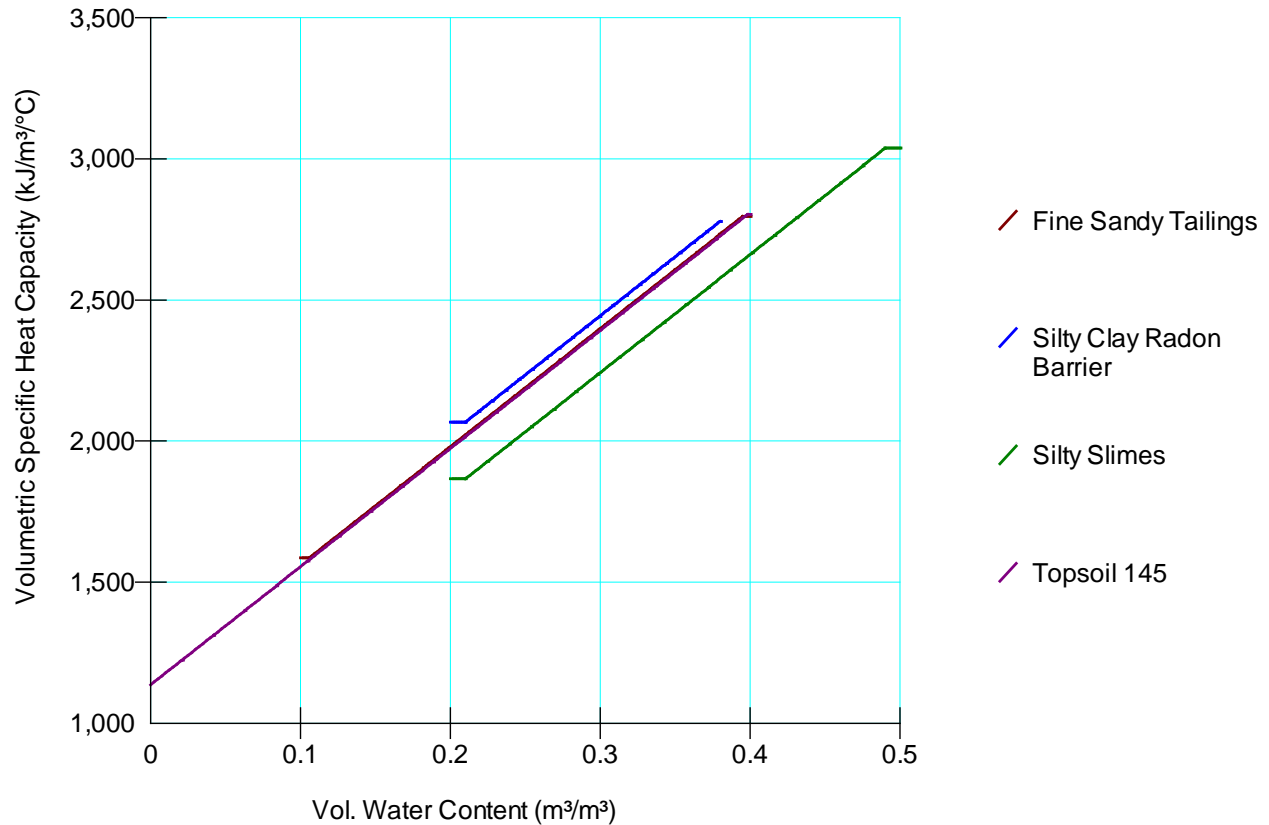


**Figure 5-18. Summary Comparison of Highland Volumetric Specific Heat Capacity Functions (1 kJ/m<sup>3</sup>·°C = 14.92 Btu/ft<sup>3</sup>·°F)**

### 5.1.3 Boundary Conditions (Including Vegetation)

#### *Climate Boundary Conditions*

The latitude of the Highland site, 43.066667°, was input to the Vadose/W model so that the software would estimate site-specific net radiation, sunrises, and sunsets. A sinusoidal distribution pattern for temperature, relative humidity, and precipitation was selected. In so doing, a 2-hr maximum time-step was implicitly defined.

Daily minimum and maximum temperatures, minimum and maximum relative humidity, mean wind speed, and liquid precipitation amount and timing were input using the Rochelle Hills Remote Automated Weather Station data (Western Regional Climate Center, 2015b; see Figure 2-1). The Rochelle Hills weather station was selected due its nearby location, similar elevation, and long record length (22+ yrs). Missing data, where present, were replaced with an average parameter value computed using the prior and next valid entries in the data record, with the exception of precipitation, which was entered as zero, when missing. Staff examined the Rochelle Hills data set for outliers. Outliers occurred during the second year in the Maximum Temperature record as unusually hot days during the cool season (e.g., up to 60 °C or 140 °F). Staff treated 44 such outliers as if they were missing data. Likewise, there were outliers during the second year in the Minimum Temperature record during the same timeframe as well as later

that occurred as unusually hot days during the cool season (e.g., up to 53.3 °C or 128 °F). Staff treated 18 outliers during the second year and another 9 outliers later in the record as missing data. Any potential problems with the other climate records (relative humidity, wind speed, and liquid precipitation) were less clear, and thus no other values were eliminated from the Rochelle Hills record. In the future, modeling should also account for solid precipitation by creating a representative hybrid precipitation record that appropriately weights relevant SNOTEL solid precipitation data for the Rochelle Hills region.

Liquid precipitation was applied at Highland using probable hours of precipitation on a seasonal basis to create daily precipitation start and stop times using information contained in Figure 5-19 (reproduced from the Wyoming Climate Atlas). Vadose/W currently has a limitation that rainfall must occur during a single interval on a given day (up to a full 24-hr window); separate morning and afternoon events are not allowed. Using the data in Figure 5-19 and subject to the stated limitation, staff assigned probable hours of precipitation on a monthly basis (Table 5-16); most precipitation falls in periods of four hours or less. Due to the spotty nature of precipitation during the months of December and January, staff applied a start/stop time of 0/24 hours for these two months, meaning a drizzly rain falls all day on days that precipitation occurs. All other months have shorter windows of precipitation that coincide with likely hours of rainfall.

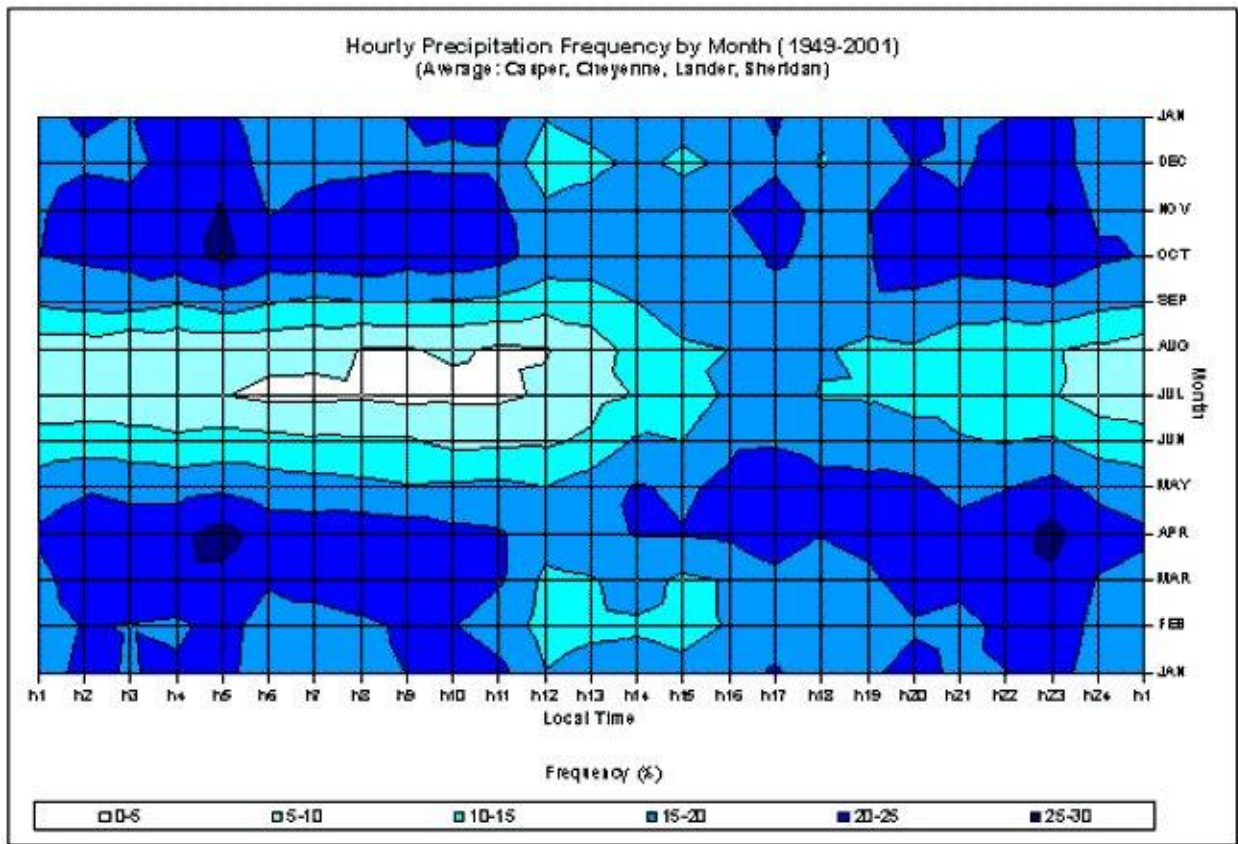


**Figure 5-19. Hourly Precipitation Frequency by Month (1949–2001) Based on Station Data in Casper, Cheyenne, Lander and Sheridan, Wyoming (Curtis and Grimes, 2004)**

| Months    | Precipitation Allocation Window |      |
|-----------|---------------------------------|------|
|           | Start                           | Stop |
| January   | 0.0                             | 24.0 |
| February  | 2.0                             | 6.0  |
| March     | 3.0                             | 7.0  |
| April     | 16.0                            | 20.0 |
| May       | 16.0                            | 20.0 |
| June      | 15.0                            | 19.0 |
| July      | 15.0                            | 19.0 |
| August    | 15.0                            | 19.0 |
| September | 19.0                            | 24.0 |
| October   | 3.0                             | 7.0  |
| November  | 2.0                             | 6.0  |
| December  | 0.0                             | 24.0 |

*Vegetation Boundary Conditions*

A report on technical specifications for the reclamation of the Highland uranium tailings impoundment by Water, Waste and Land (1989a) provides the permanent reclamation seed mixture given in Table 5-17.

| Species                       | Percent of Mix |
|-------------------------------|----------------|
| Rosana Western Wheatgrass     | 30             |
| Critana Thickspike Wheatgrass | 25             |
| Slender Wheatgrass            | 20             |
| Regar Meadow Brome            | 10             |
| Four-Wing Saltbush            | 5              |
| Winterfat                     | 10             |

Climate-driven vegetation boundary conditions were specified, including:

- Leaf Area Index Function of Growing Season
- Root Depth Function of Growing Season
- Plant Moisture Limiting Function of Pore Water Pressure

The average growing season at Highland lasts approximately 129 days, from the end of May until the end of September. The Rochelle Hills weather station also reports Growing Degree Days in base 4.4 °C (40 °F) and base 10 °C (50 °F), which are potentially useful in determining vegetation boundary condition functions. The Leaf Area Index is non-zero only after shoots emerge from the ground surface (Figure 5-20). The Rooting Depth Function begins to descend from winter stasis (Figure 5-21) approximately one week earlier than when Leaf Area Index transitions from zero to positive. Soil temperature controls the early-season rate of root growth in the region that is above 20-cm (8-in)-deep where freezing may occur. For cold regions like Wyoming, the thawing/warming process will cause the root depth vs. growing season curve to plateau in late-winter/early spring, from whence root growth will at first very slowly increase as the soil thaws/warms to near-optimal growing temperature and then the rate will become near-linear until senescence or first frost, at which time the rate begins to slow to an asymptote at a final seasonally achievable root depth. A triangular (▼-shaped) root system was applied in

Vadose/W to account for the dominant tap-rooted species amongst the seeded plants. Roots are allowed to descend no more than a depth of 2 m (6.6 ft), which is the depth of the base of the climate/vegetation-affected surface layers in the Highland model. Note that this allows roots to descend into the sandy tailings in this model. Evidence suggests that some vegetation planted on the Highland cover will penetrate tailings to a much greater depth than this.

The Plant Moisture Limiting (*PML*) function (Figure 5-22) for Highland was replicated from the example, considered typical, given in GEO-SLOPE (2012) (their Figure 12-3). The data input for the *PML* function are given in Table 5-18.

| Table 5-18. Plant Moisture Limiting Function |       |                     |
|--|-------|---------------------|
| Pore Water Pressure (kPa)                    |       | Limiting Factor (-) |
| (Limiting Point)                             | 100   | 1.00                |
|  | 500   | 0.80                |
|  | 750   | 0.50                |
|  | 1,000 | 0.25                |
|  | 1,250 | 0.07                |
| (Wilting Point)                              | 1,500 | 0.00                |

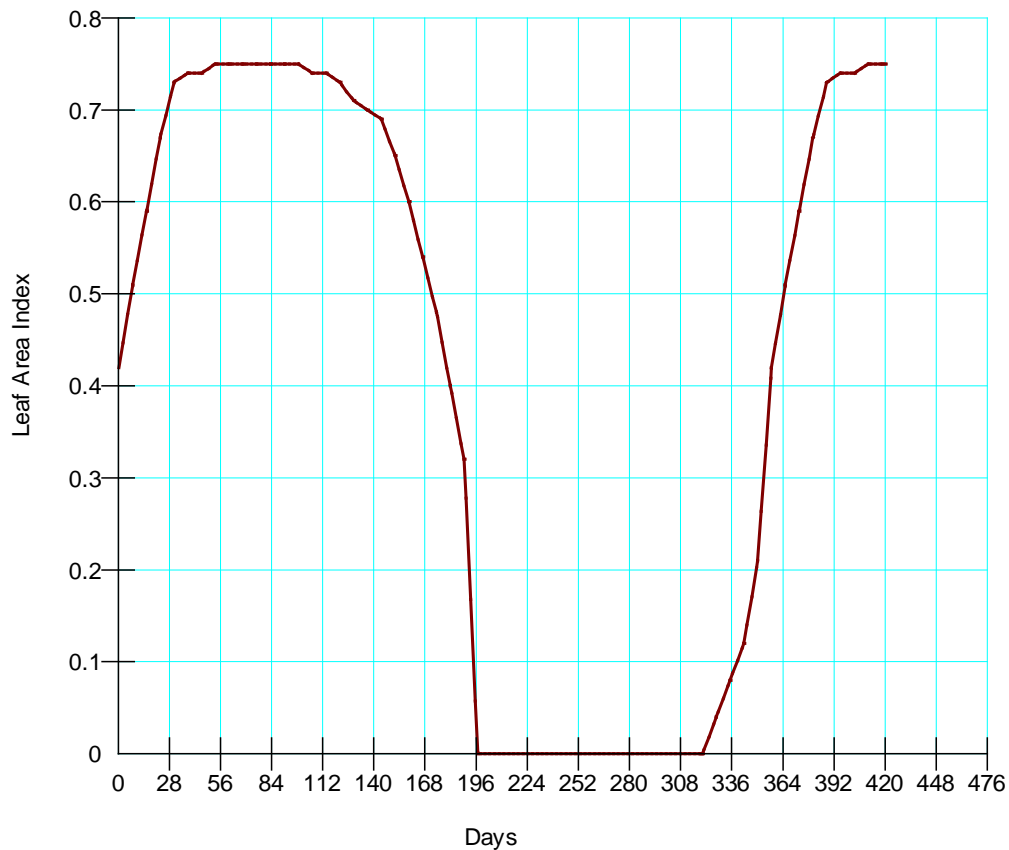
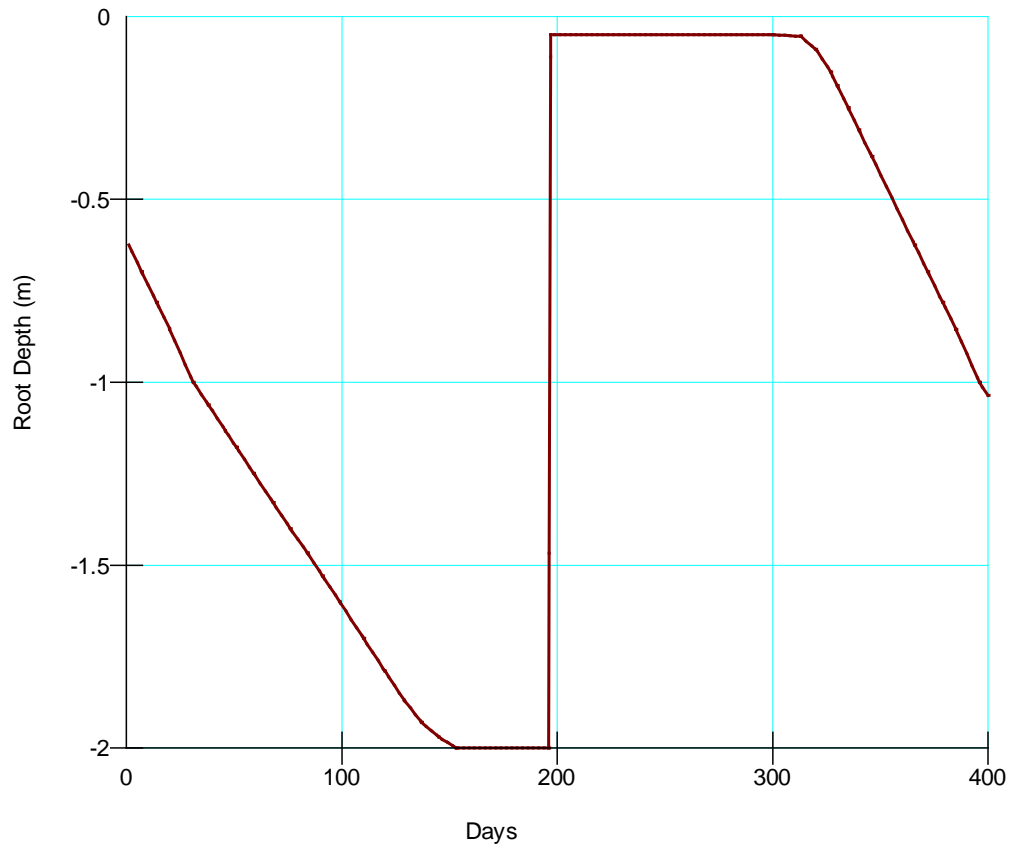
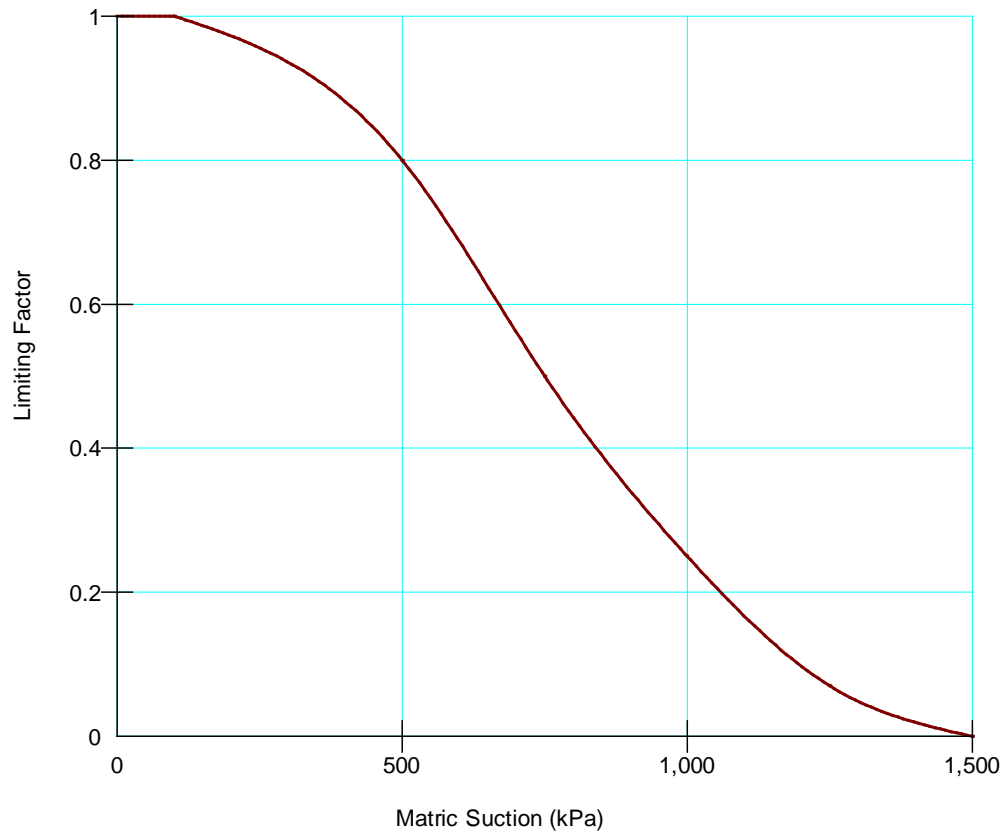


Figure 5-20. Estimated Leaf Area Index Function for the Highland Site



**Figure 5-21. Estimated Rooting Depth Function for the Highland Site  
(1 m = 3.28 ft)**



**Figure 5-22. Typical Plant Moisture Limiting Factor Function of Pore Water Pressure (i.e., Matric Suction) Used in the Highland Model (1 kPa = 0.33 ft H<sub>2</sub>O)**

*Hydraulic Boundary Conditions other than Climate*

For unknown reasons, the Highland model, as constructed, was incapable of supporting a unit gradient boundary condition at the base of the model domain. To overcome this limitation, an equivalent condition was applied using a prescribed head of  $-0.659$  m ( $-2.16$  ft) =  $-6.465$  kPa ( $0.938$  psi).

*Thermal Boundary Conditions other than Climate*

Based on Hu and Feng (2003) and the Rochelle Hills (RH) air temperature data, the ground temperature at the Highland site at 10-cm (4-in) depth likely has a seasonal distribution similar to that estimated by staff in Figure 5-23. Ground temperature behavior from October through December is not well-resolved in Figure 5-23 because of an absence of ground temperature contours near Highland in the Hu and Feng (2003) map of the United States. To obtain a more complete understanding of ground temperature behavior near Highland, Wyoming, multilevel ground temperature data (Figures 5-24 and 5-25) were examined from a site in Torrington, Wyoming.

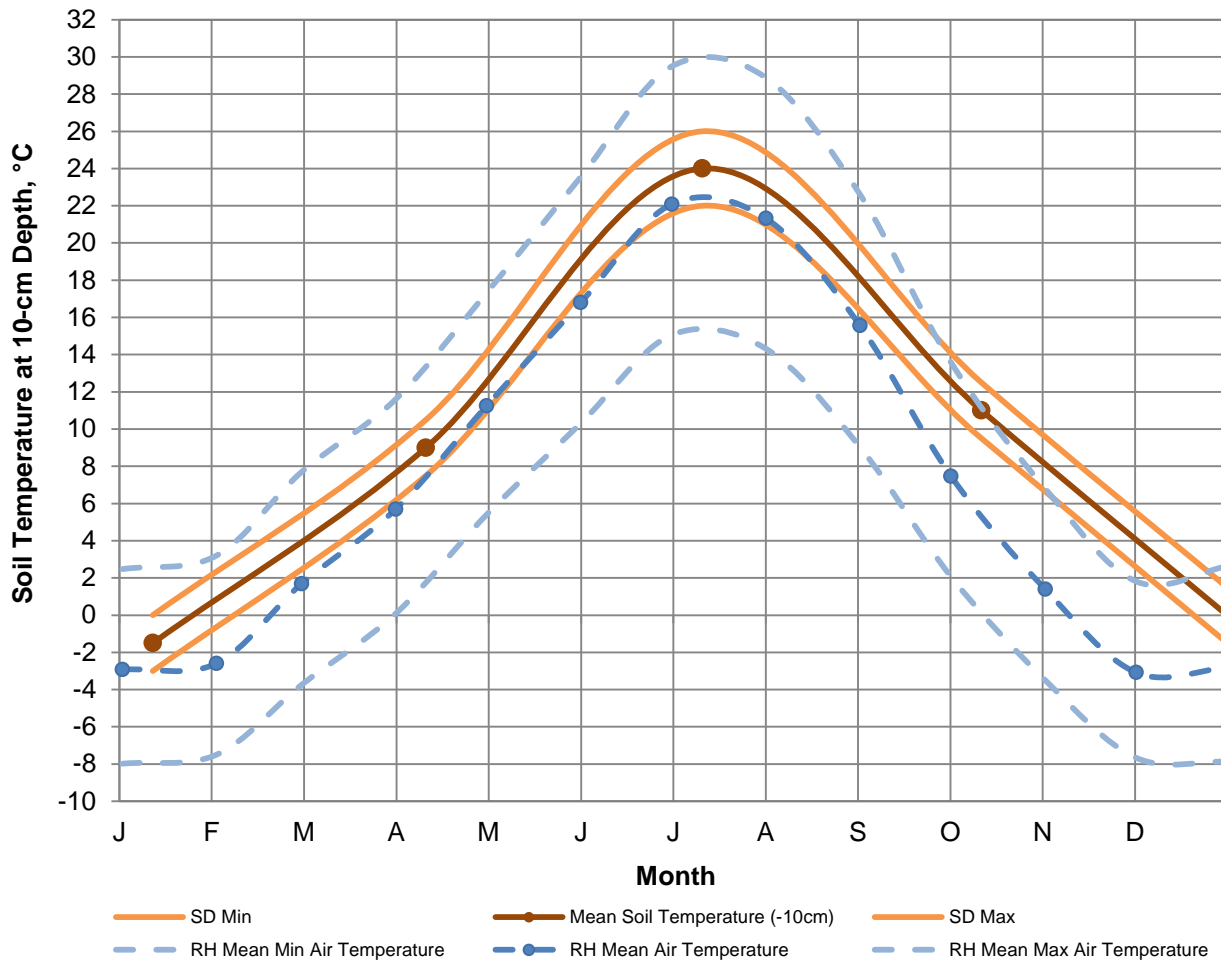


**Figure 5-23. Highland Seasonal Soil Temperature Estimate at 10-Centimeter Depth (Brown) Based Upon Hu and Feng (2003; their Figure 8) and Rochelle Hills (RH) Air Temperatures (Blue); Hu and Feng (2003) Standard Deviations (SD) also Shown (Orange).**

The Torrington Experimental Farm, Wyoming, is near the Nebraska border and ~164 km (~102 mi) southeast of Highland. The mean annual ground temperature throughout the upper 1.8 m (72 in) of the soil column at Torrington was 10.5 °C (51 °F), consistent with Hu and Feng (2003), which indicates the average annual soil temperature in this region of Wyoming is ~11 °C (52 °F) within the first meter.

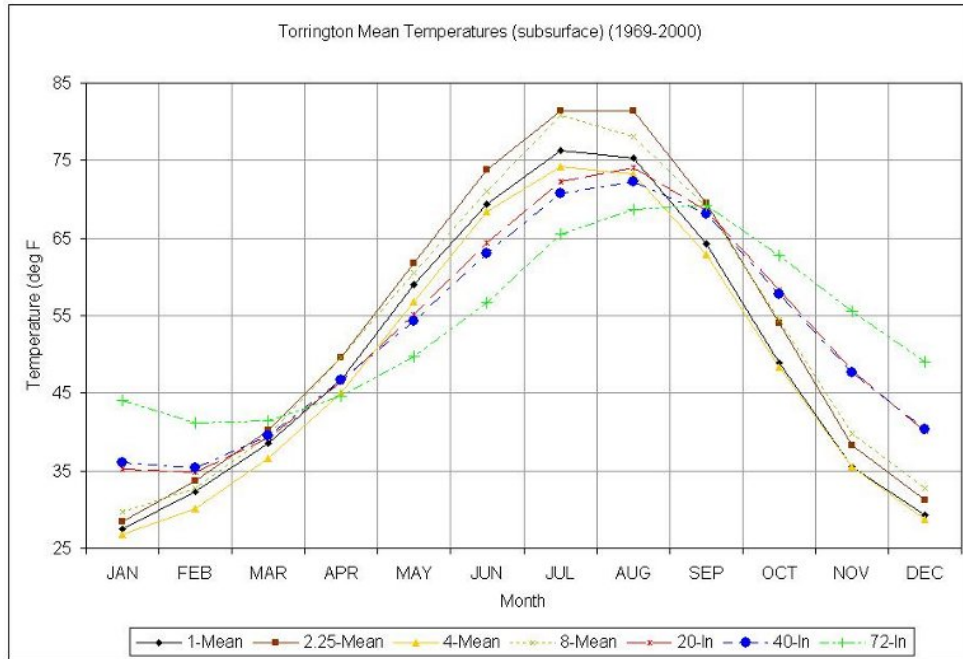


**Figure 5-24. Mean Multilevel Subsurface Ground Temperatures Measured at Torrington, Wyoming (Curtis and Grimes, 2004; Figure 3.36)**

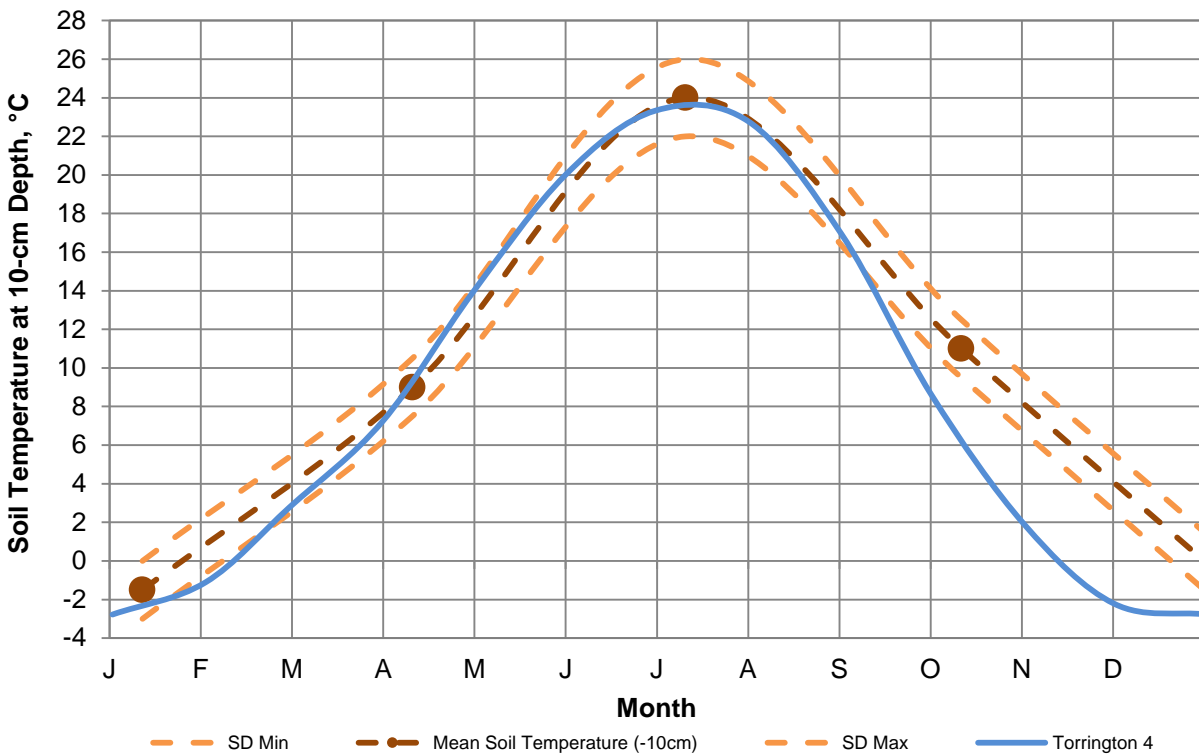


**Figure 5-25. 10-Centimeter [4-in] Ground Temperatures Measured at Torrington, Wyoming (Figure 5-24), Compared to Staff's Equivalent Ground Temperature Estimate from Figure 5-23. Seasonal Ground Temperatures at this Depth are in Substantial Agreement; Torrington Multilevel Data Were Thus Used as a Proxy for Highland Ground Temperatures.**

Staff computed the mean annual temperature profile for Torrington using the data available in Figure 5-24 to estimate the annual temperature gradient deep in the soil column. Using the trendline from the two deepest temperature sensors at Torrington (Figure 5-26), a mean annual soil temperature equal to 14.5 °C (58 °F) was extrapolated for a depth of 3.8-m (12.5-ft), which is the zero-datum of this model. For the thermal boundary condition, this constant temperature was applied at the base of the model.

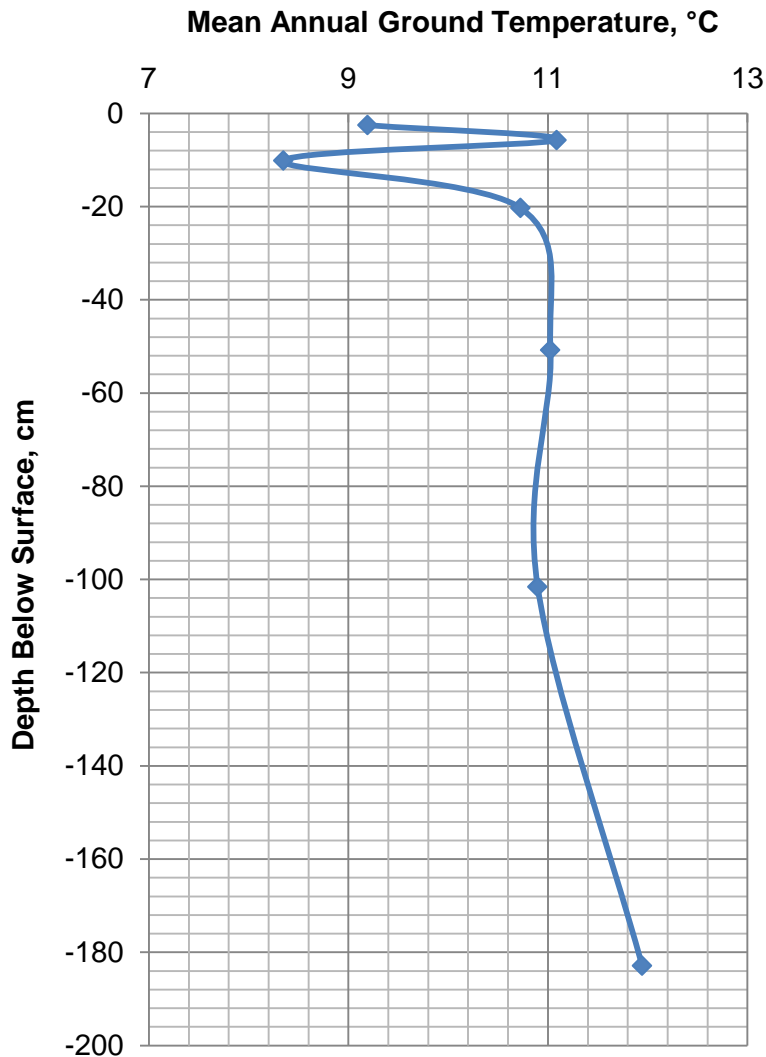


**Figure 5-26. Mean Annual Ground Temperatures Computed from Multilevel Data (Figure 5-24) Measured at Torrington, Wyoming (1 cm = 0.39 in)**

### 5.1.4 Initial Conditions

#### Hydraulic Initial Conditions

A constant flux model (specified flux = 0.1 mm/yr =  $2.74 \times 10^{-7}$  m/day applied at the upper boundary) was run with exponential time-stepping until a stable pore water pressure distribution was attained that could be used to initialize climate-driven models. The Parallel Direct Equation Solver and default setting for “Maximum Percent Change in Head Per Time Step” (i.e., 2.5 percent) were used. For the allowable timestep range, the minimum was set to the default value of 0.01 days (14.4 mins). The maximum number of iterations allowed prior to moving on to the next timestep was 50. The model was run to simulate  $1.654 \times 10^8$  days (452,753 yrs). The initial (0 days) and final ( $1.654 \times 10^8$  days) hydraulic conditions (pore water pressures) are presented in Figure 5-27, where the final conditions were used to start the Rochelle Hills year-long climate spin-up model.

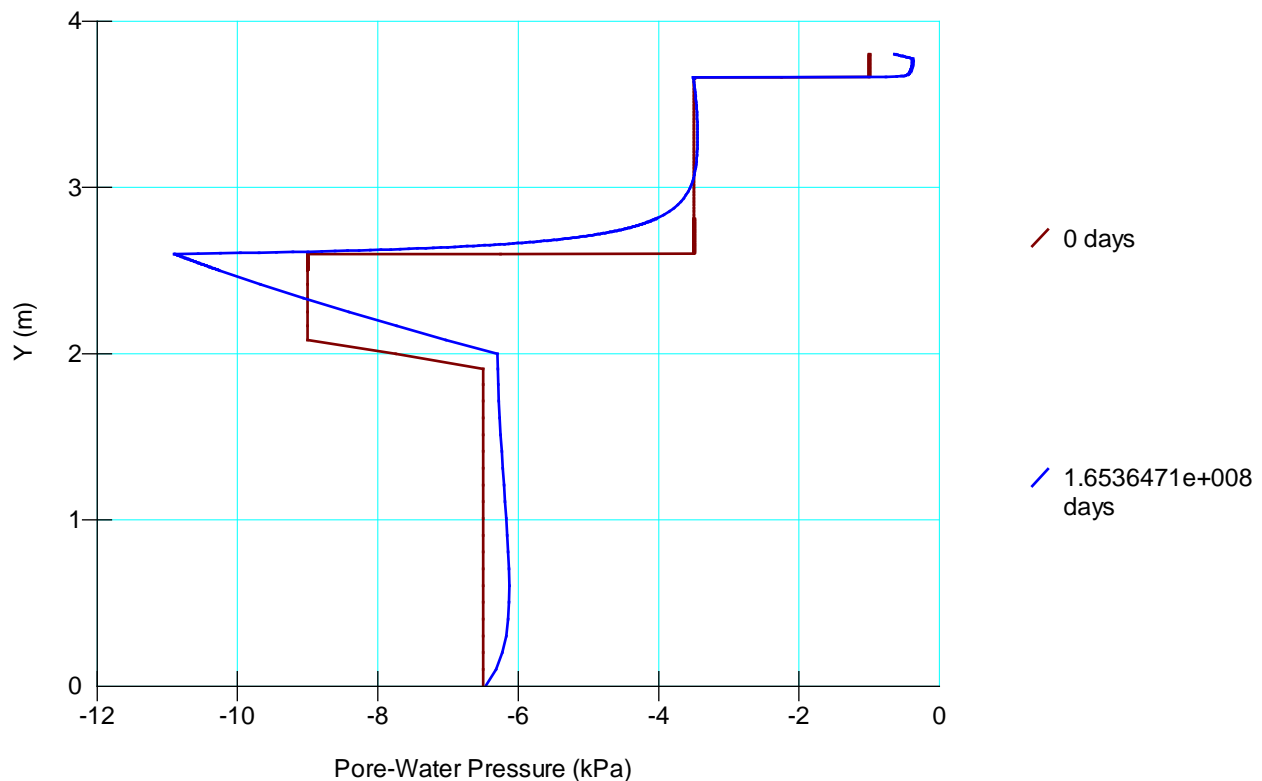


**Figure 5-27. Approximation of Hydrostatic Initial Condition Estimated for Use in Starting a Year-Long Rochelle Hills Climate Spinup Simulation of the Highland Soil Cover (1 kPa = 0.33 ft H<sub>2</sub>O; 1 m = 3.28 ft)**

The final hydraulic conditions from Figure 5-27 were applied to a year-long climate-spinup model on the date May 1, 1993. The maximum percent change in head between two timesteps was decreased to 1 percent. The minimum allowable timestep was decreased to 0.001 days (1.44 mins). The radon barrier and tailings proceeded to dry-out during the year-long climate spinup simulation (Figure 5-28).

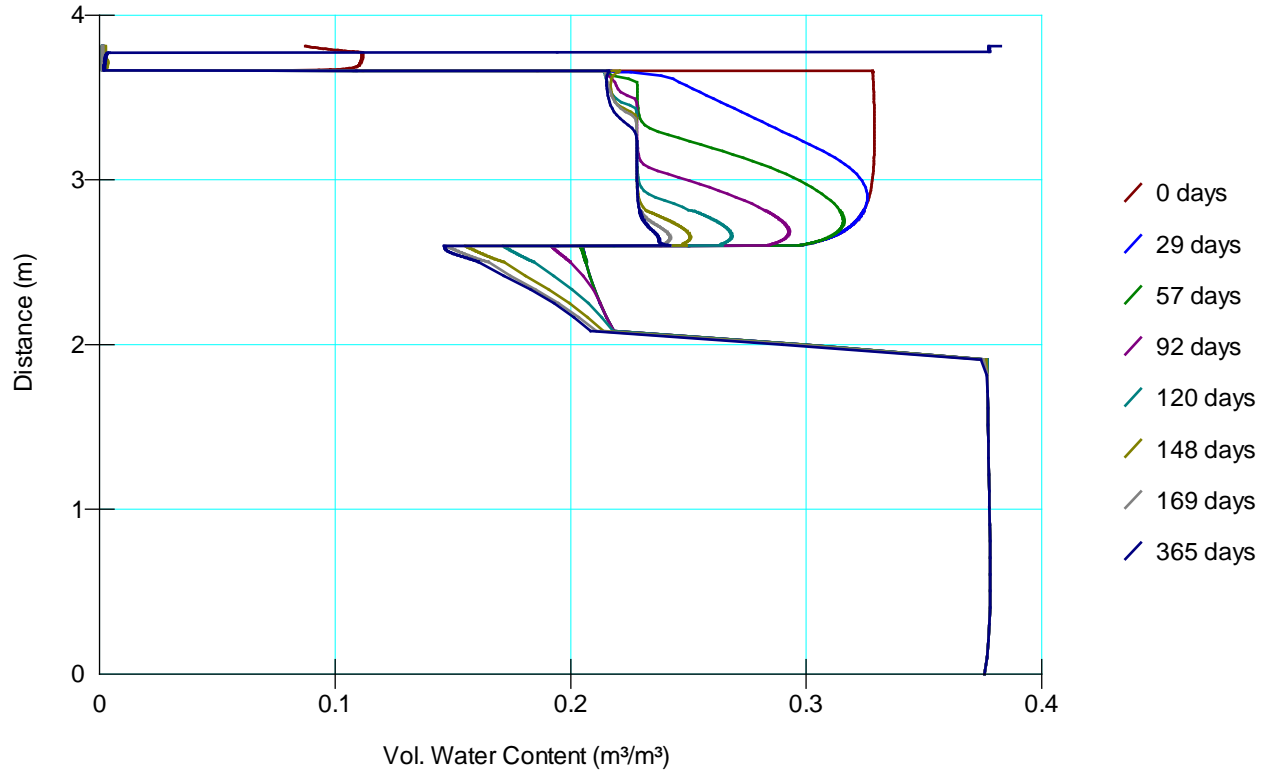


**Figure 5-28. Volumetric Water Content Markedly Decreased in Deep Layers during Year-Long Rochelle Hills Climate Spinup Simulation of the Highland Soil Cover (1 m = 3.28 ft)**

The initial (0 days) and final (365 days) hydraulic conditions (pore water pressures) are presented in Figure 5-29, where the final conditions were used to start the first Rochelle Hills long-term climate model.

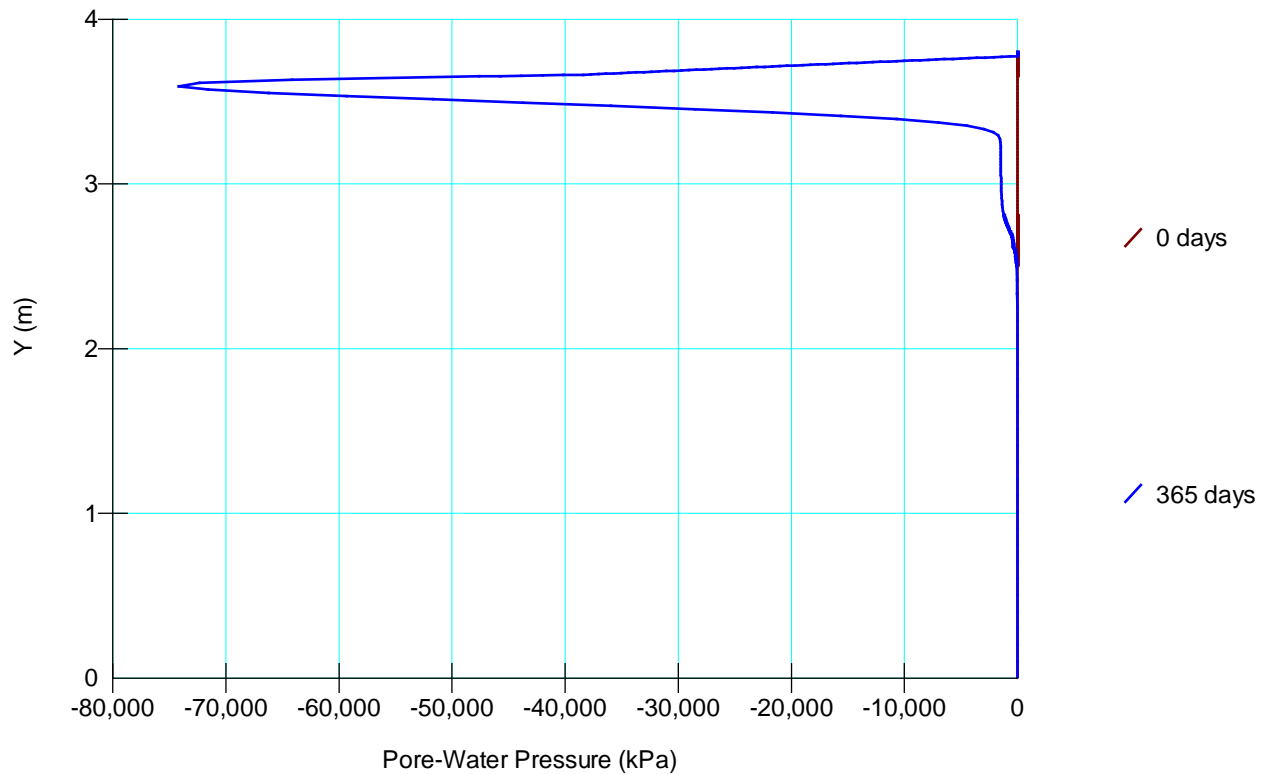


**Figure 5-29. Initial Conditions (i.e., Pore Water Pressure Profile) for Starting the Long-Term Rochelle Hills Climate-Driven Model of the Highland Soil Cover (1 kPa = 0.33 ft H<sub>2</sub>O; 1 m = 3.28 ft)**

A 7,830-day (21.44-yr) Rochelle Hills climate-driven simulation was started on the date May 1, 1993, based upon imported pore water pressure distribution obtained on Day 365 of the year-long climate-spinup model (Figure 5-29). This model ran with daily climate input from May 1, 1993 through October 7, 2014. The maximum number of iterations allowed prior to moving on to the next timestep was increased to 70. For the allowable timestep range, the minimum was explicitly set to 0.001 day, whereas the maximum was implicitly set to 2 hrs by an explicit sinusoidal climate distribution selection. The maximum percent change in head between two timesteps was set to 1 percent. Water balance outputs were saved at every adaptive timestep and other results (e.g., fluxes) were saved every 30 days for quantitative and graphical analyses. This simulation required 27 hours to run to completion. A fault occurred on Day 3,697 that affected the storage calculation, and thus the water balance error (Figure 5-30). There were no reported convergence problems at that timestep; the last major nonconvergence occurred approximately 150 to 200 simulated days earlier. The day and timestep on which the error occurred was June 14, 2003, during which no rain fell. This may have been a bookkeeping error (as previously discussed in Section 3.1.1).

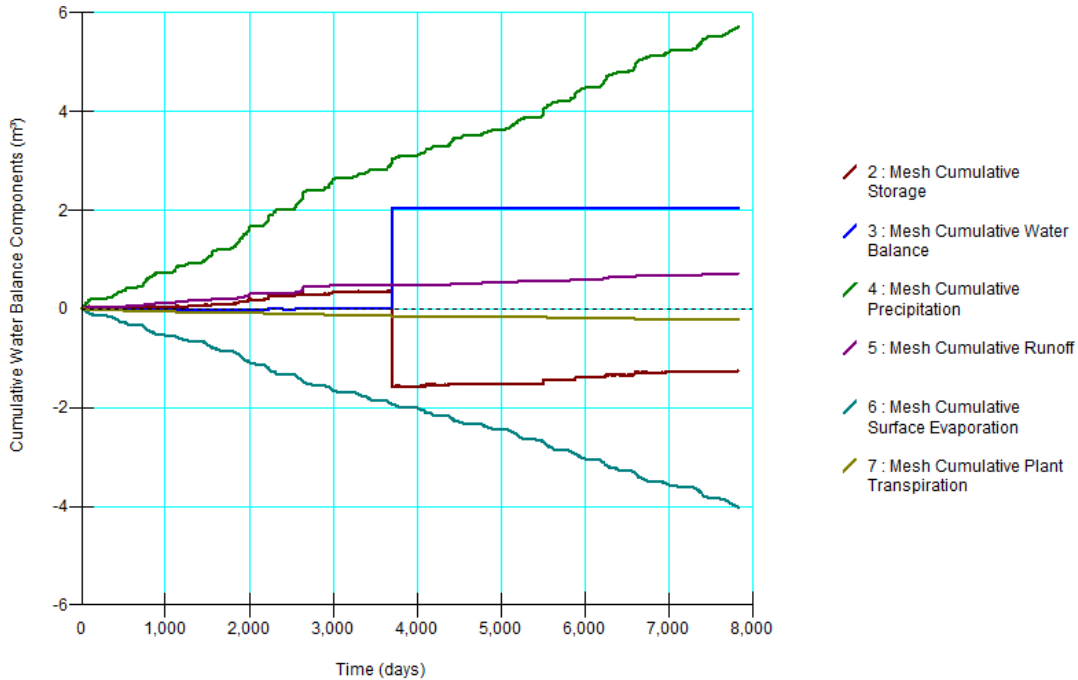


**Figure 5-30. Unexplained Water Balance Error Occurred During Day 3,697 of Preliminary Long-Term Rochelle Hills Climate Simulation (1 m<sup>3</sup> = 35.3 ft<sup>3</sup>)**

Because of the fault affecting the water balance error, a new long-term Rochelle Hills climate-driven simulation was run after importing the most recent pore water pressure (and temperature) results from May 10, 2014/Day 7680 as initial conditions (Figure 5-31, 0<sup>th</sup> day of final simulation), because this written output is seasonally nearest to the selected Rochelle Hills climate record start date of May 1.

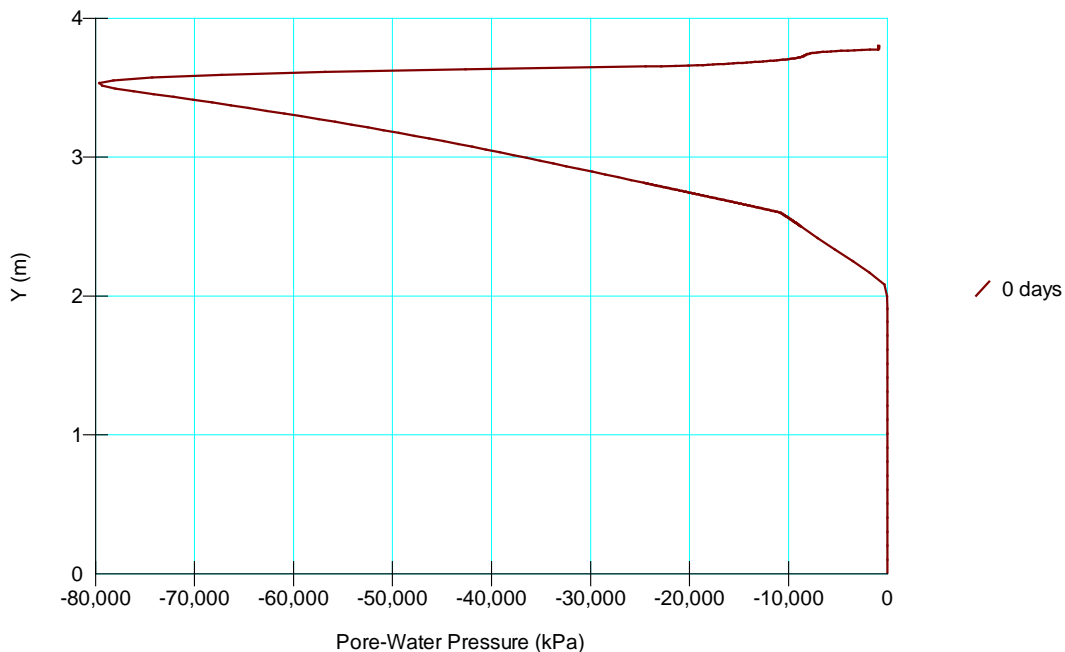


**Figure 5-31. Initial Conditions (i.e., Pore Water Pressure Profile) for the Final Long-Term, Climate-Driven Simulation of the Highland Soil Cover (1 kPa = 0.33 ft H<sub>2</sub>O; 1 m = 3.28 ft)**

*Thermal Initial Conditions*

The annual average soil temperature profile at Torrington, Wyoming (see Section 5.1.3 and Figure 5-26 for additional background information about this data source), was used to set activation temperatures (i.e., thermal initial conditions) on a material-property/depth-level basis (Table 5-19, Figure 5-32 Day 0) on the date May 1, 1993, for the year-long Rochelle Hills climate-spinup simulation.

| <b>Table 5-19. Preliminary Highland Thermal Initial Conditions (Day 0 in Figure 5-31)</b> |                                    |
|---|------------------------------------|
| <b>Highland Material</b>  | <b>Activation Temperature (°C)</b> |
| Topsoil Interface 145   | 9.0                                |
| Topsoil 145   | 10.0                               |
| Sandy-to-Gravelly Silty Clay Radon Barrier & Root Zone                                    | 11.0                               |
| Fine-Grained Sandy Tailings   | 11.5                               |
| Silty Slimes  | 13.0                               |

The thermal initial conditions used to start the long-term Rochelle Hills climate-driven simulation on May 1, 1993, are presented in Figure 5-32, Day 365.

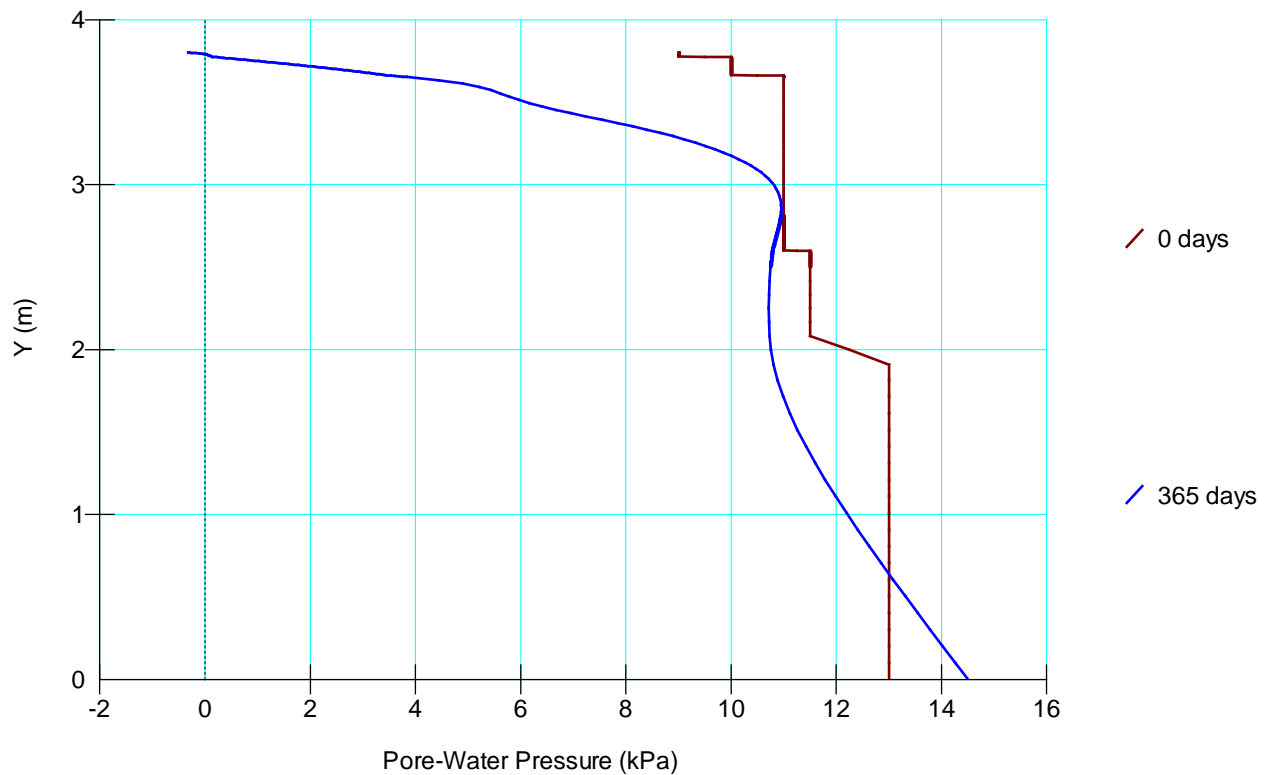


**Figure 5-32. Initial Conditions (i.e., Temperature Profile; Day 365) for Starting the Long-Term Rochelle Hills Climate-Driven Simulation of the Highland Soil Cover (1 kPa = 0.33 ft H<sub>2</sub>O; 1 m = 3.28 ft)**

## 5.2 Simulation Results

The final mesh cumulative mass balance components and error are illustrated in Figure 5-33. The water balance error (WBE) rate over the length of the simulation was approximately 5.25 mm/yr (0.2 in/yr). Cumulative storage is positive; evaporation, transpiration and runoff losses altogether are cumulatively less than cumulative precipitation.

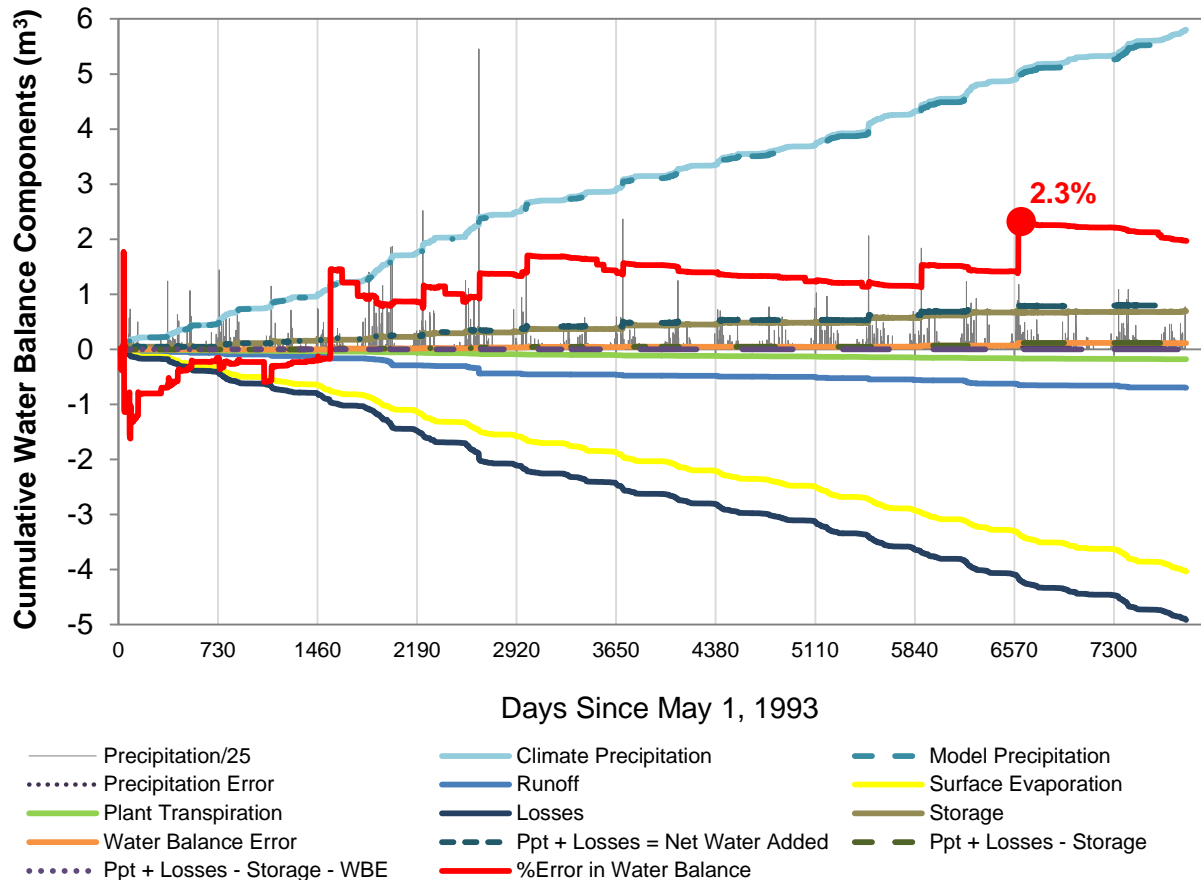


**Figure 5-33. Cumulative Water Balance Components (1 m<sup>3</sup> = 35.3 ft<sup>3</sup>)**

The volumetric water content of the radon barrier and the tailings units seems to decrease monotonically, as shown in Figure 5-34. However, close inspection of the temporal evolution of the vertical hydraulic conductivity of the upper sandy tailings at a height of 2.2 to 2.6 m (7.2 to 8.5 ft) above the zero-datum suggests there may be deep percolation below the radon barrier between Days 0 and 3,287 (Figure 5-35) because the uppermost extent of the sandy tailings are becoming more permeable with time as a function of increased water content. Continuous drying appears to occur between Days 3287 and 5113 (Figure 5-36), but deep percolation must again occur between Day 5113 and the end of the simulation (Figure 5-37). There is a single year between Days 6940 and 7305, as shown in Figure 5-36, when deep percolation may temporarily switch off.

In summary, depending on the representativeness of the selected model parameters used in this model, the Highland soil cover may not be impervious to net infiltration or prohibit deep percolation from entering the uranium mill tailings.

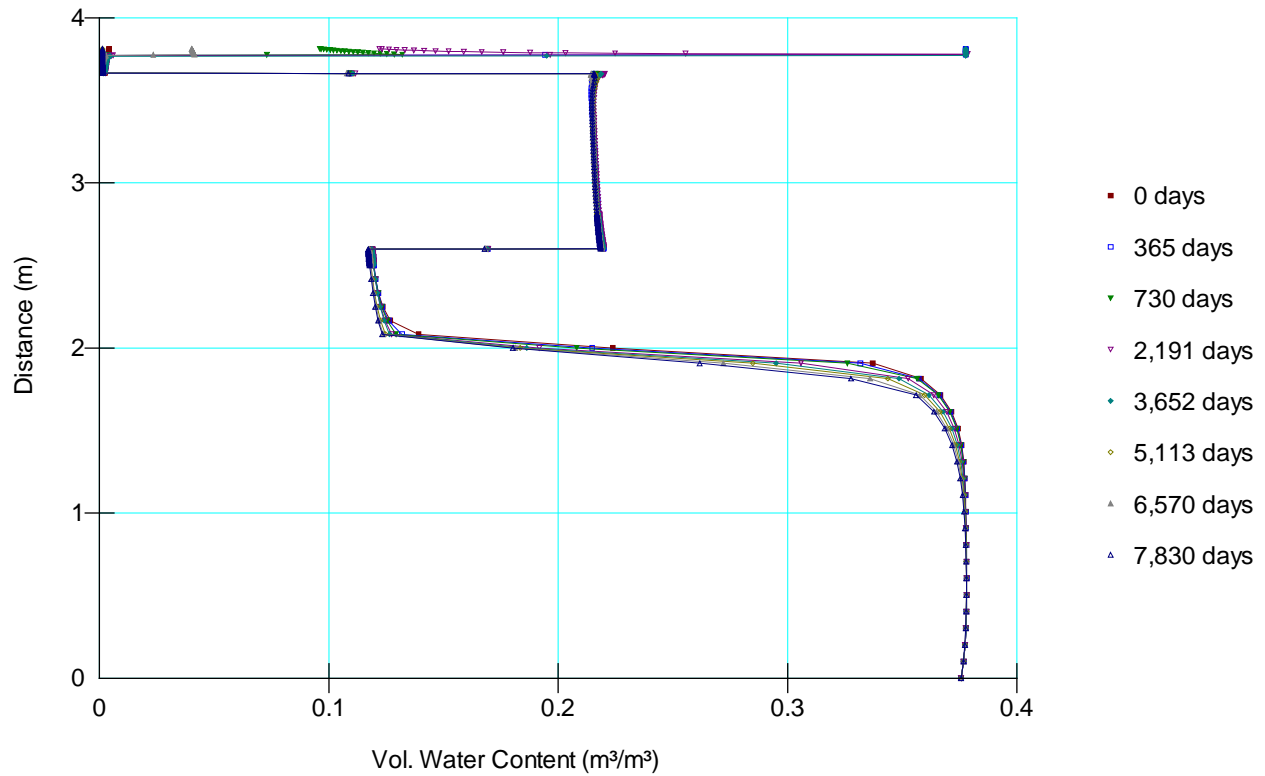


**Figure 5-34. Apparent Monotonic Decrease in Magnitude of Volumetric Water Content within and below the Radon Barrier (1 m = 3.28 ft)**

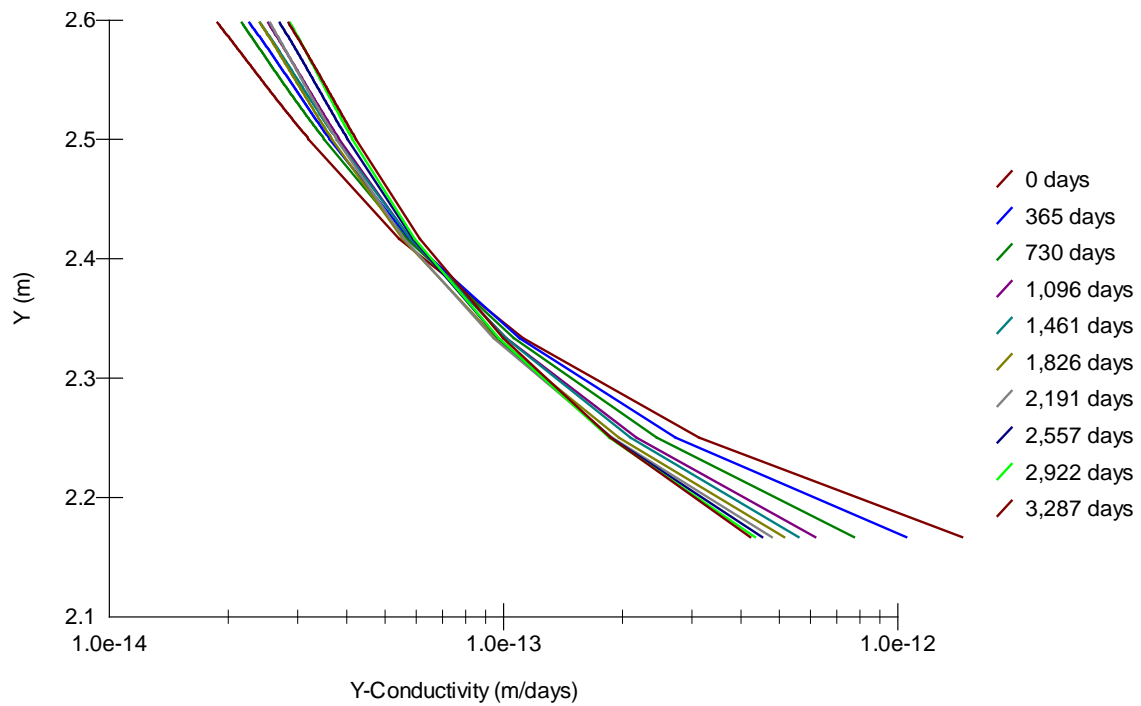


**Figure 5-35. Temporal Evolution of Vertical Hydraulic Conductivity in the Highland Sandy Tailings Suggests Pulses of Deep Percolation May Extend below Radon Barrier (Curves are Crisscrossing) from Day 0 through 3,287 (1 m/day = 3.28 ft/day)**

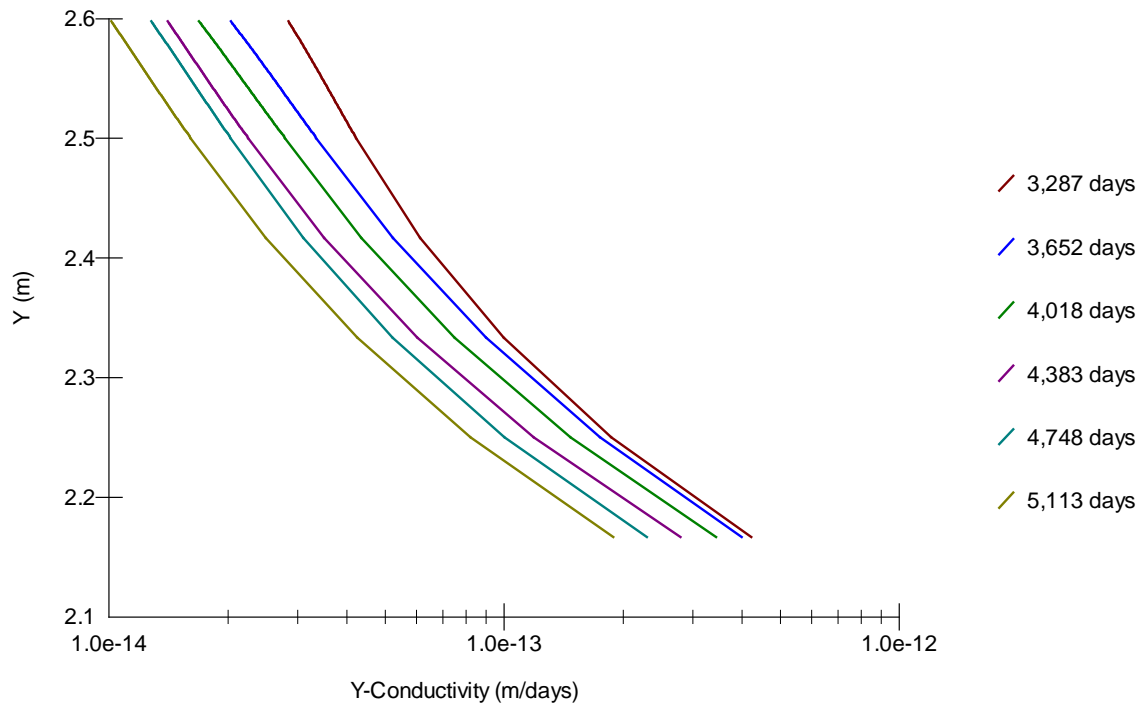


**Figure 5-36. Temporal Evolution of Vertical Hydraulic Conductivity in the Highland Sandy Tailings Suggests Continuous Drying below Radon Barrier during This Interval (Curves Progress to the Left in an Orderly Manner with Increasing Time; (1 m/day = 3.28 ft/day)**

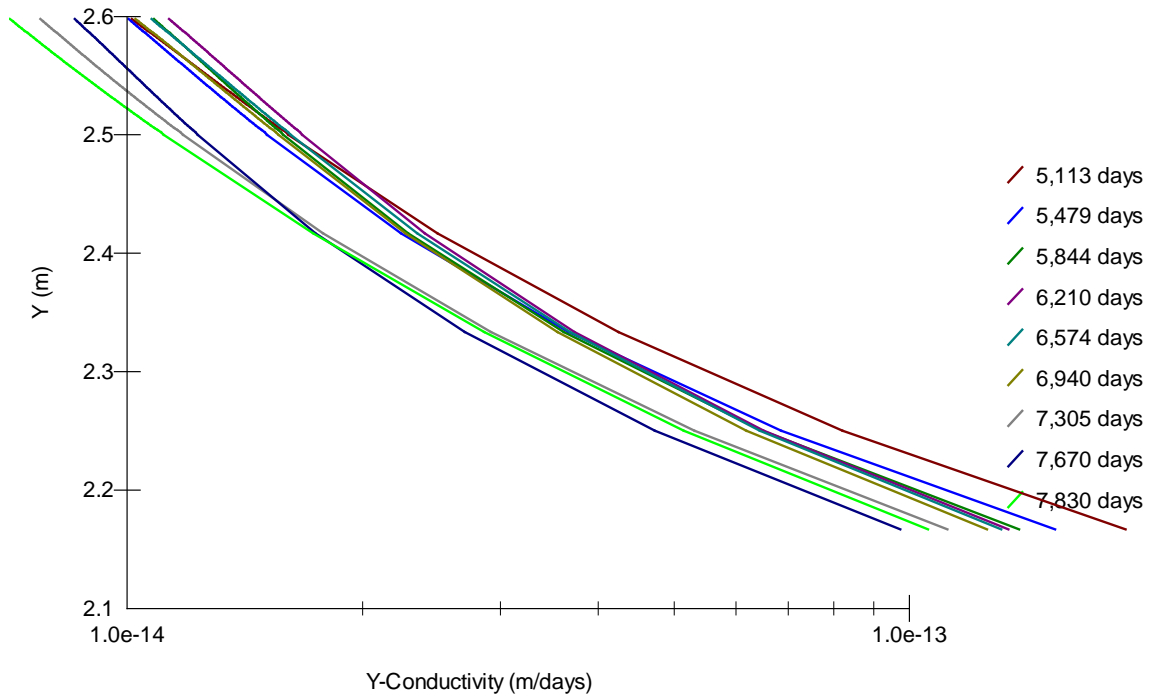


**Figure 5-37. Temporal Evolution of Vertical Hydraulic Conductivity in the Highland Sandy Tailings Suggests Pulses of Deep Percolation May Extend Below Radon Barrier (Curves are Crisscrossing) from Day 5,113 to 6,940 and from Day 7,305 to 7,830 (1 m/day = 3.28 ft/day)**

## 6 CHURCH ROCK NORTH CELL MODEL AND SIMULATION RESULTS

### 6.1 Description of the Church Rock (UNC), New Mexico, Model

The Church Rock, New Mexico, central cell interim soil cover is 0.69 m (2.25 ft) thick and composed, at a minimum, of a 0.53-m (1.75-ft)-thick clayey sand to sandy clay radon barrier plus overlying layers of  $D_{50} = 3.8$  cm (1.5 in) basaltic rock mulch and clayey sand to sandy clay topsoil totaling 0.15 m (0.5 ft) thick (Canonie Environmental, 1995). While portions of the cover may be thicker than these minimum values to meet planned grades, CNWRA staff reached an agreement with NRC staff that the model should represent potential infiltration through the thinnest-allowable soil cover layers to produce conservative results.

The radon barrier was protected from wind and water erosion by a 7.62-cm (3-in)-thick layer of overlying rock mulch and interstitial clayey sand to sandy clay topsoil beneath a 7.62-cm (3-in)-thick layer of clayey sand to sandy clay topsoil (Canonie Environmental, 1991).

The Church Rock central cell interim cover was not intentionally vegetated because the rock mulch layer was designed to produce a higher and more stable long-term moisture content in the underlying radon barrier by decreasing the effective evaporative zone and reducing overland runoff compared to what could be attained using a vegetated cover (Canonie Environmental, 1991). Soil cover engineers anticipated that precipitation would provide a long-term moisture content at Church Rock that approximates field-capacity rather than wilting-point moisture content (Canonie Environmental, 1991). The rock mulch consists of basaltic rock with pores impregnated by the same sandy clay that was used as topsoil. Note that during the period when the radon barrier was partially constructed, yet before the rock mulch layer had been added, that temporary cover was purposefully temporarily vegetated (Canonie Environmental, 1991); that stage of the soil cover was not modeled for this report.

Tailings re-grading was performed prior to installation of the soil cover to shield slimes with a minimum of 2.13 m (7 ft) of coarse tailings or other fill. The final coarse tailings surface was compacted to a minimum of 90 percent of the maximum dry density as determined by the Standard Proctor method of compaction (ASTM D698) prior to placing the radon barrier (Canonie Environmental, 1991). The Church Rock model described herein was developed with coarse, sandy loam tailings at its base because modeling the underlying slimes is unnecessary to the development of an understanding of the potential for deep percolation to enter into the thick section of coarse tailings. Regarding the coarse tailings, Canonie Environmental (1991) states, "coarse tailings located below the cover classify as poorly graded sands and are considered relatively free draining. These characteristics are indicative of relatively large pore diameters, indicating these materials have a low potential for capillary action. Since this material below the cover material will not support capillary action, the ability to transport water to the frost line by capillary action does not exist."

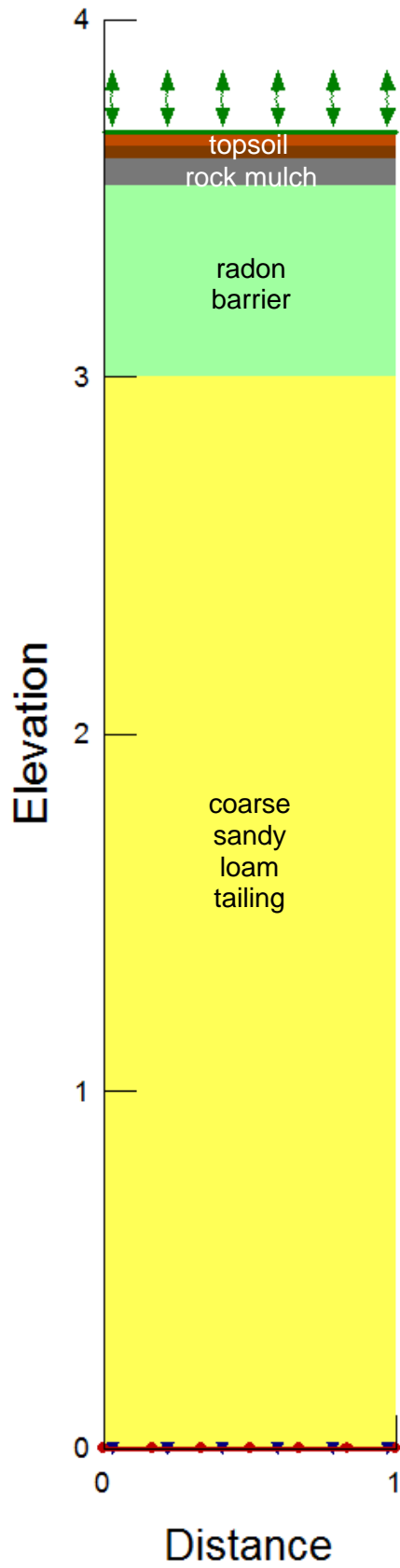
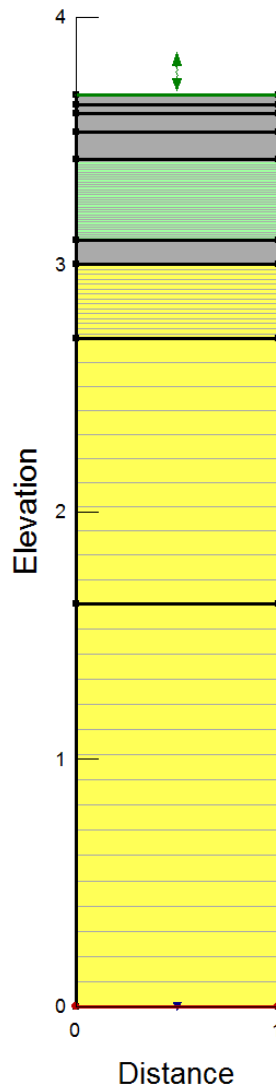


Figure 6-1. Church Rock Model Domain

### 6.1.1 Model Domain and Mesh

Surface layers of the model are directly influenced by climate variables. In the Church Rock central cell model, the surface layers consist of upper sections of the coarse, sandy loam tailings, the sandy clay radon barrier, the basaltic rock mulch, and the sandy clay topsoil, to a depth of approximately 2.06 m (6.74 ft) below the land surface. Staff constructed a 1.0-m (3.3-ft)-wide, 3.7-m (12.1-ft)-thick quasi-one-dimensional Vadose/W model of the Church Rock central cell soil column (Figure 6-1). The model domain represents sandy tailings (yellow), underlying a 0.53-m (1.75-ft)-thick radon barrier layer (green), underlying a layer of 0.08-m (3-in)-thick rock mulch (gray) and two sandy clay topsoil layers: the lowermost topsoil unit (brown) is 0.0362 m (1.43 in) thick, and the land surface (reddish brown) with its less variable hydraulic conductivity function (GEO-SLOPE, 2012) is 0.04 m (1.57 in) thick. Where permeability or capillary breaks may be expected at the top or bottom of a model layer, adjacent elements surrounding that layer should be approximately the same size for numerical stability (GEO-SLOPE, 2012). Where large vertical gradients are expected, element sizes are on the order of 2-mm thick; the mesh consists of 255 elements (Figure 6-2, Table 6-1).



**Figure 6-2. Church Rock Central Cell Model Discretization. Gray Layers Illustrate Dense Discretization.**

| <b>Model Region</b>               | <b># of Elements</b> | <b>~Element Size (mm)</b> | <b>Region Thickness (m)</b> | <b>Surface Layer ID</b> |
|-----------------------------------|----------------------|---------------------------|-----------------------------|-------------------------|
| Topsoil Interface with Atmosphere | 20                   | 2                         | 0.04                        | Layer 8                 |
| Underlying Topsoil                | 18                   | 2                         | 0.0362                      | Layer 7                 |
| Rock Mulch                        | 38                   | 2                         | 0.0762                      | Layer 6                 |
| Top of Radon Barrier              | 55                   | 2                         | 0.11                        | Layer 5                 |
| Middle of Radon Barrier           | 32                   | 10                        | 0.3234                      | Layer 4                 |
| Bottom of Radon Barrier           | 50                   | 2                         | 0.10                        | Layer 3                 |
| Top of Sandy Tailings             | 15                   | 20                        | 0.30                        | Layer 2                 |
| Middle of Sandy Tailings          | 11                   | 97                        | 1.07                        | Layer 1                 |
| Sandy Tailings                    | 16                   | 102                       | 1.63                        | Layer 0                 |
| <b>Total</b>                      | <b>255</b>           |                           |                             |                         |

### **6.1.2 Material Properties**

#### *Hydraulic Properties*

The Church Rock, New Mexico, central cell interim cover consists of a topsoil identical in its material properties to underlying rock mulch fill material, as well as to the underlying radon barrier. The soil particle sizes for source materials used to construct the radon barrier were consistent with the following classifications: silty clay (CL), clayey sand (SC), silt (ML), or silty sand (SM). These source materials were blended to produce a homogenized radon barrier medium (Canonie Environmental, 1991). The source material most commonly used was silt or clay, and typically a clay with an average percent passing the No. 200 sieve of 56 percent (Canonie Environmental, 1991). The homogenized radon barrier material is modeled as sandy clay.

Gradation analyses of the radon barrier (Canonie Environmental, 1995; Appendix C) indicates its composition ranges from silty clay to sandy lean clay with an average of 1 to 2 percent greater than 1.3 cm (0.5 in) diameter. This soil is finer than the clayey sand to sandy clay called for in the specifications (Canonie Environmental, 1991). Use of finer material was an improvement on the design specification because it enabled greater penetration of fines into basaltic rock interstices and increased the cohesion of the soil/rock matrix.

Granulometric data for radon barrier samples documented in Canonie Environmental (1995) and in MWH Americas, Inc. (2014) were transformed to estimate the shape of the moisture characteristic function (Figure 6-3). The few available direct measurements of moisture characteristic data for this material were used to shift the transformed function on the pore water pressure axis to partly match the measured data (Figure 6-3). Radon barrier moisture characteristic data were available from samples identified as 88-RP-P-5 (Canonie Environmental, 1991), TI-CS01-04A, and TI-CS01-04A-R (MWH Americas, Inc., 2014). Measured moisture data were primarily from the region of the curve having intermediate moisture content, and no data were available to support material behavior in the dry region, which makes the granulometric data very useful (Figure 6-3). The resulting moisture content function was entered into Vadose/W as a data point function.

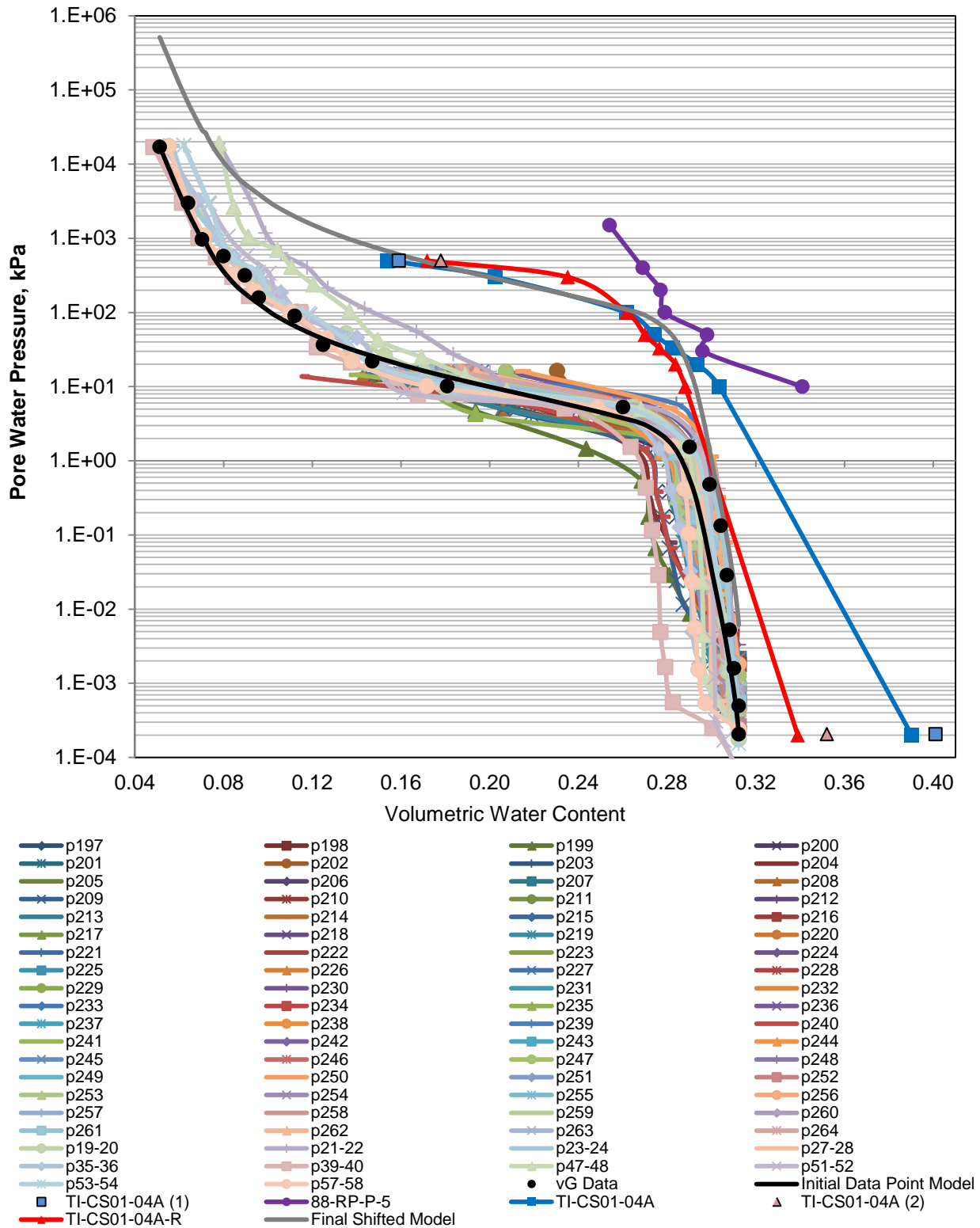


**Figure 6-3. Development of Moisture Characteristic Function for the Church Rock Radon Barrier and Topsoil (i.e., Final Shifted Model). Plentiful Granulometric Data (Canonie Environmental, 1995; MWH Americas, Inc., 2014) were Transformed to Determine Curve Shape and Shifted to Partially Match One of a Few Directly Measured Soil Moisture Samples (i.e., 88-RP-P-5, TI-CS01-04A, and TI-CS01-04A-R).**

Church Rock central cell constant hydraulic parameters for each material in the model domain were based on information given in Canonie Environmental (1995) and MWH Americas, Inc. (2014), and are documented in Table 6-2.

| Table 6-2. Church Rock Central Cell Constant Hydraulic Parameters Based Upon Canonie Environmental (1995) and MWH Americas, Inc. (2014) |                                   |                    |        |                   |        |                       |
|---|-----------------------------------|--------------------|--------|-------------------|--------|-----------------------|
| Material  | Classification                    | $\alpha$<br>(kPa)* | $n$    | VWC ( $m^3/m^3$ ) |        | $K_{sat}$<br>(m/day)† |
|   |                                   |                    |        | sat               | res    |                       |
| Topsoil   | Silty to sandy lean clay          |                    |        | 0.31              | 0.0484 | 0.0032                |
| Rock Mulch  | Basalt & silty to sandy lean clay | 7.75               | 1.223  | 0.10              | 0.0156 | 2.96E-5               |
| Radon Barrier   | Silty to sandy lean clay          |                    |        | 0.31              | 0.0484 | 0.0032                |
| Sandy Tailings  | Coarse, sandy loam                | 2.6214             | 1.4048 | 0.37              | 0.015  | 2.12                  |

\*1 kPa = 0.33 ft H<sub>2</sub>O  
 †1 m/day = 3.28 ft/day

The complete set of moisture characteristic curves used in the Church Rock central cell soil cover model are illustrated in Figure 6-4; likewise, the complete set of hydraulic conductivity functions are illustrated in Figure 6-5, including the linear, reduced variability conductivity function for the topsoil layer at the land surface/atmospheric interface.

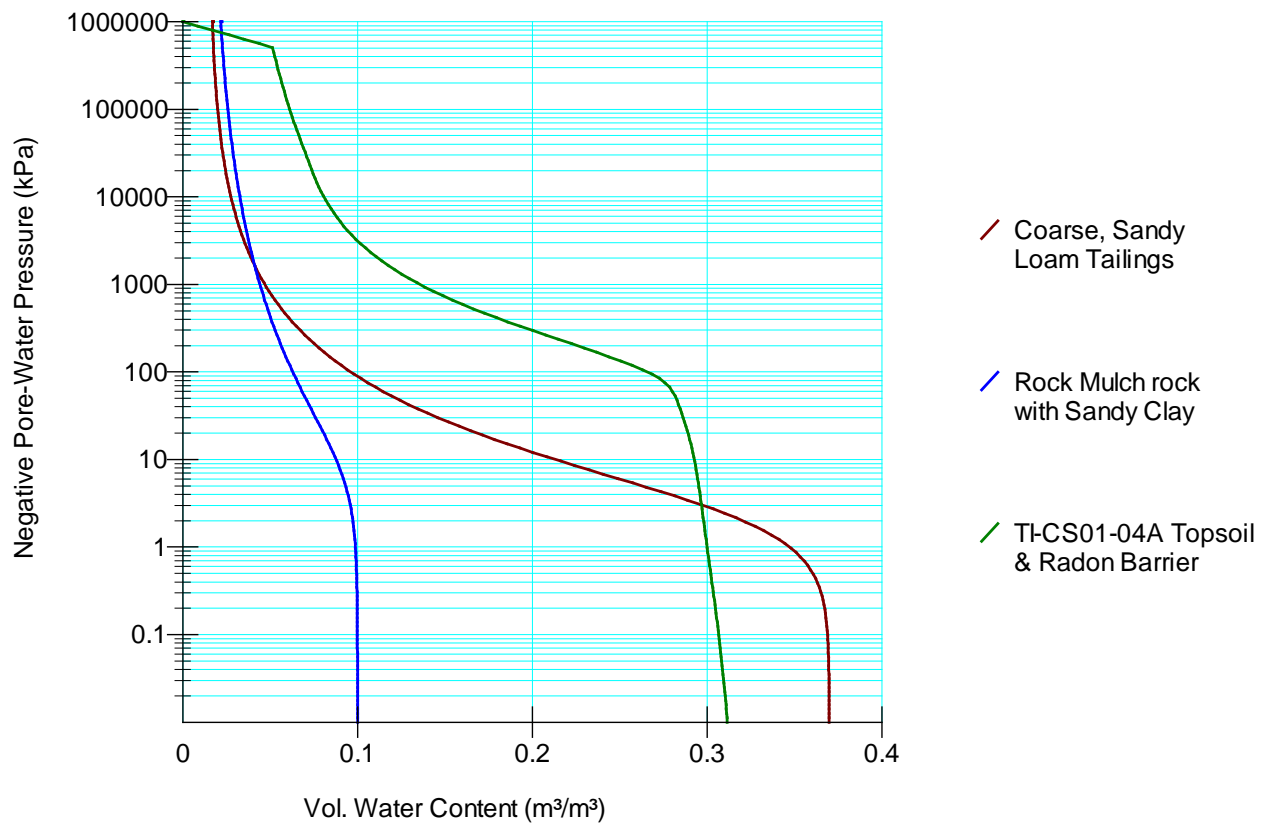


**Figure 6-4. Summary Comparison of Church Rock Soil Column Moisture Characteristic Functions (1 kPa = 0.33 ft H<sub>2</sub>O)**

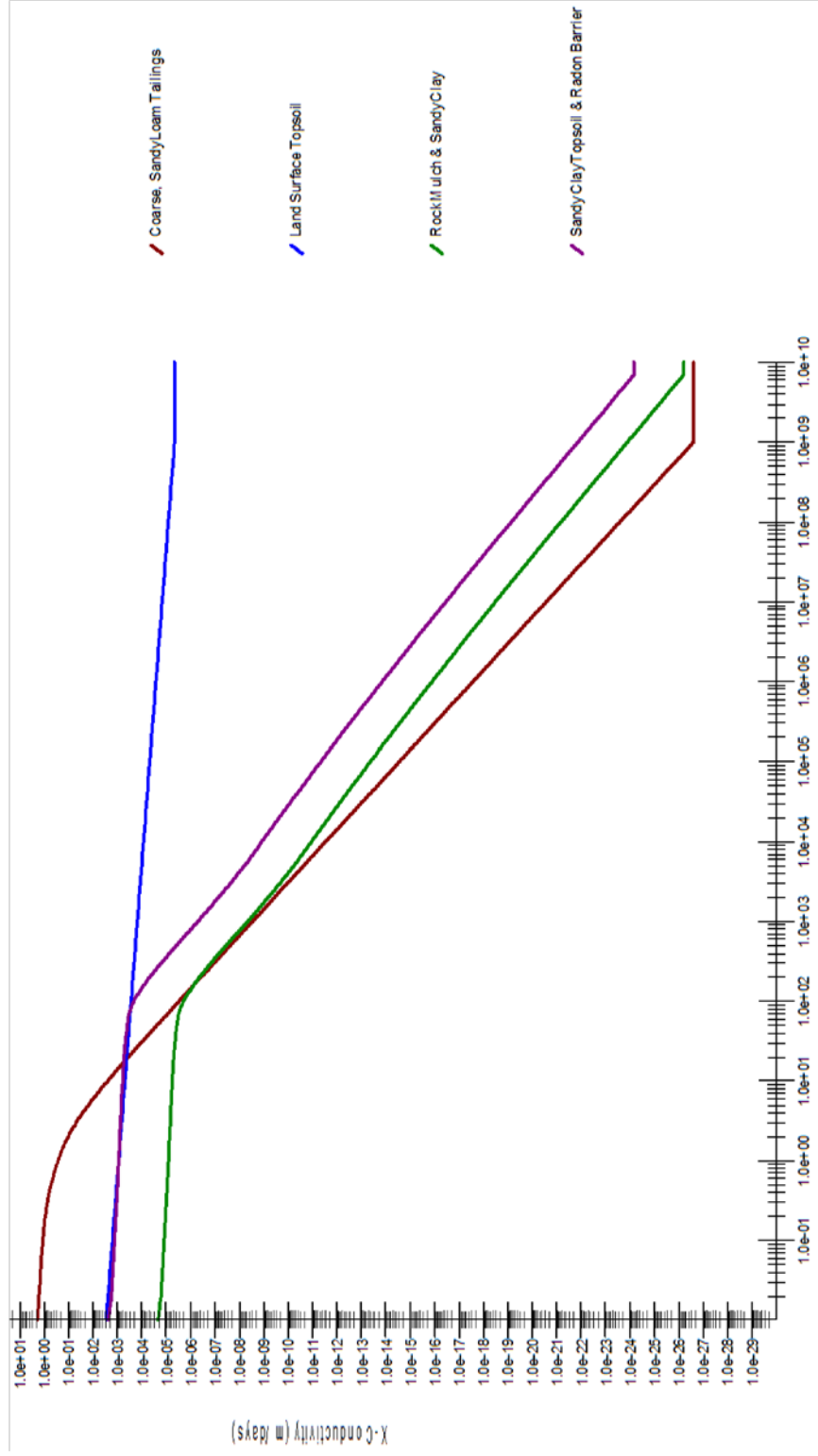


**Figure 6-5. Summary Comparison of Church Rock Hydraulic Conductivity Functions of Pore Water Pressure (i.e., Matric Suction)**

### Thermal Properties

The thermal conductivity of the sandy clay of the topsoil and radon barrier is probably well represented by the Becker, et al. (1992) mean clay curve, given it is generally enveloped by the low-to-mean sand curves (Figure 3-2).

The basaltic rock of the rock mulch is likely similar to gravel in its thermal conductivity; the Becker, et al. (1992) low gravel thermal conductivity curve extended beyond 40 percent to full saturation was used to represent the rock mulch and sandy clay unit, because it is enveloped by the mean and high clay thermal conductivity curves (Figure 3-2).

For the coarse, sandy loam (loam being equal parts sand, silt and clay) tailings, the Becker, et al. (1992) mean sand thermal conductivity curve was used; note that this curve is similar to the high silt and high clay thermal conductivity curves (Figure 3-2).

Altogether, the complete set of thermal conductivity data point functions imported into the Church Rock Vadose/W model are as illustrated in Figure 6-6.

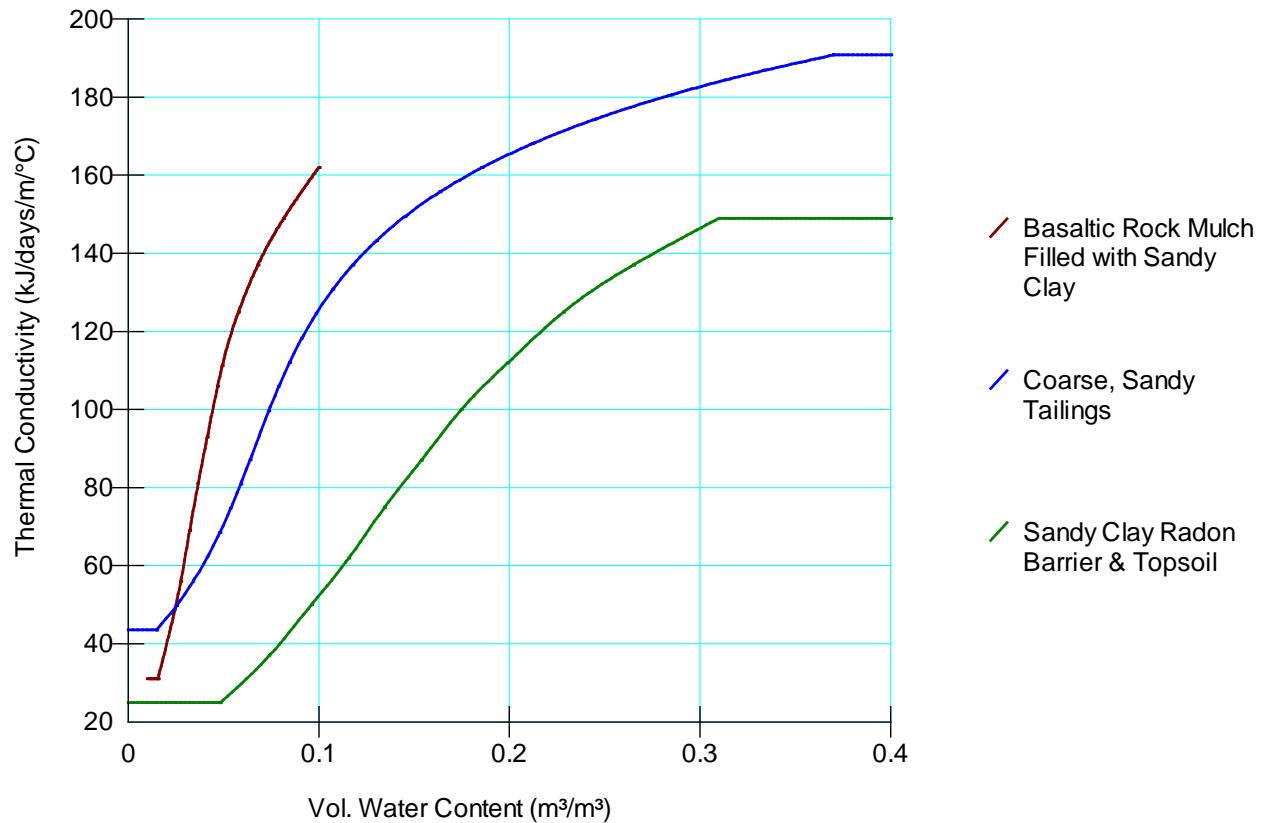


**Figure 6-6. Summary Comparison of Church Rock Central Cell Thermal Conductivity Functions (1 kJ/day·m·°C = 0.16 Btu/day·ft·°F)**

For the volumetric specific heat capacity functions of volumetric water content, staff used mass specific heat capacity of 0.71 kJ/kg·°C (0.17 Btu/lb·°F) for radon barrier/topsoil minerals and 0.84 kJ/kg·°C (0.20 Btu/lb·°F) for the basaltic rock mulch in the de Vries estimation routine, yielding the volumetric specific heat capacity functions illustrated in Figure 6-7.

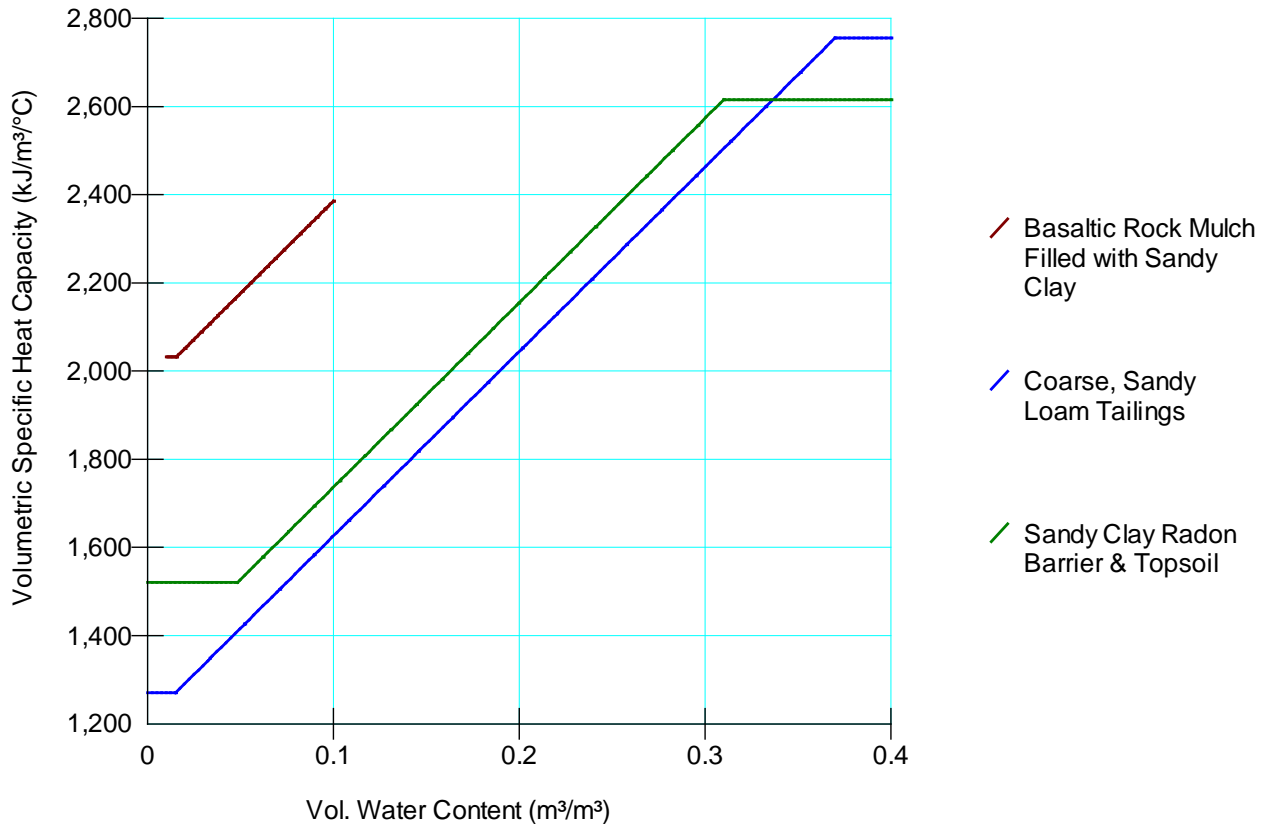


**Figure 6-7. Summary Comparison of Church Rock Central Cell Volumetric Specific Heat Capacity Functions (1 kJ/m<sup>3</sup>·°C = 14.92 Btu/ft<sup>3</sup>·°F)**

### 6.1.3 Boundary Conditions (Vegetation was not Modeled)

#### *Climate Boundary Conditions*

The latitude of the Church Rock site, 35.647331°, was input to the Vadose/W model so that the software would estimate site-specific net radiation, sunrises, and sunsets. A sinusoidal distribution pattern for temperature, relative humidity, and precipitation was selected. In so doing, a 2-hr maximum time-step was implicitly defined.

According to Canonic Environmental (1991), the Church Rock uranium mill tailings impoundment is subject to an arid to semi-arid continental climate, receiving direct sun on more than 50 percent of days. Winds are generally moderate out of the west and southwest. Wind frequency and velocity are typically highest during the spring season. Temperatures average approximately 10 °C (50 °F), with a July maximum daily average of 20 °C (68 °F) and a January minimum daily average of -0.6 °C (31 °F). Mean annual average precipitation is approximately 35.6 cm (14 in) and the majority falls during summer monsoon season. Net pan evaporation averages approximately 137.2 cm (54 in), exceeding net precipitation.

Daily minimum and maximum temperatures, minimum and maximum relative humidity, mean wind speed, and liquid precipitation amount and timing were input using the Zuni Buttes remote automated weather station data (Western Regional Climate Center, 2015c; see Figure 2-2); this weather record began on April 5, 2006, and continues to present day. The Zuni Buttes weather station was selected due to its location being only 70 km (43 mi) distant and its similar elevation relative to the Church Rock soil cover; the current record length is 8.8 yrs. The mean annual average liquid precipitation at this weather station is less than that reported by Canonic Environmental (1991) for Church Rock, but a portion of this difference may be attributable to snowfall, which is not measured at the weather station. If time and resources had allowed, these data might have been adjusted to better represent precipitation at Church Rock. In the future, modeling should also account for solid precipitation by creating a representative hybrid precipitation record that appropriately weights relevant SNOTEL solid precipitation data for the Zuni Buttes region. The Zuni Buttes station was offline during a significant portion of December 2010 and January 2011; missing data were replaced with an average parameter value computed using the prior and next valid entries in the data record, excepting liquid precipitation, which was entered as zero, when missing. There were no clear outliers to be eliminated from the data records.

Precipitation was applied at Church Rock (Table 6-3) using probable hours of monsoonal precipitation (Ropelewski, et al., 2005) to create daily precipitation start and stop times; during non-monsoon months, precipitation was applied sinusoidally over the length of a day. As the long-term Vadose/W climate-driven simulation ran, a few monsoon season days were found to cause substantial water balance errors due to non-convergence problems; thus, precipitation on these few dates was applied over the length of the day as an exception to the rules of Table 6-3.

| <b>Months</b>       | <b>Precipitation Allocation Window</b> |             |
|---------------------|--|-------------|
|                     | <b>Start</b>                           | <b>Stop</b> |
| January – June 15   | 0.0                                    | 24.0        |
| June 15 – September | 17.0                                   | 20.0        |
| October – December  | 0.0                                    | 24.0        |

*Hydraulic Boundary Conditions other than Climate*

The Church Rock model had a unit gradient hydraulic boundary condition applied at the base of the model domain.

*Thermal Boundary Conditions other than Climate*

Three ground temperature stations in New Mexico are located in the northwest uranium mining region (Hu and Feng, 2003); these appear to measure temperature only at a depth of 10 cm, with annual average temperatures of 16 to 17 °C (61 to 63 °F). Staff found no ground temperature data for depths greater than 1 m (3.3 ft). In the absence of suitable information, staff applied a constant temperature boundary condition of 14.5 °C (58 °F). Post-modeling review of results suggested that a slightly warmer boundary condition, possibly 15 °C (59 °F), may have been more appropriate.

## 6.1.4 Initial Conditions

### *Hydraulic Initial Conditions*

A constant flux model (specified flux = 0.1 mm/yr =  $2.74 \times 10^{-7}$  m/day applied at the upper boundary) was run with exponential adaptive time-stepping until a stable pore water pressure distribution was attained that could be used to initialize climate-driven models. The Parallel Direct Equation Solver and a maximum of 1 percent change in pressure head between two time steps were used. For the allowable time step range, the minimum was set to the default value of 0.01 days (14.4 mins). The maximum number of iterations allowed prior to moving on to the next timestep was 50. This simulation, which proceeded very slowly, was run through several iterations in an effort to more quickly identify the long-term stable pore water pressure distribution for a constant base flux boundary condition applied at the ground surface. In the final iteration (Figure 6-8), the simulation ran for 21 yrs to converge upon a final solution.

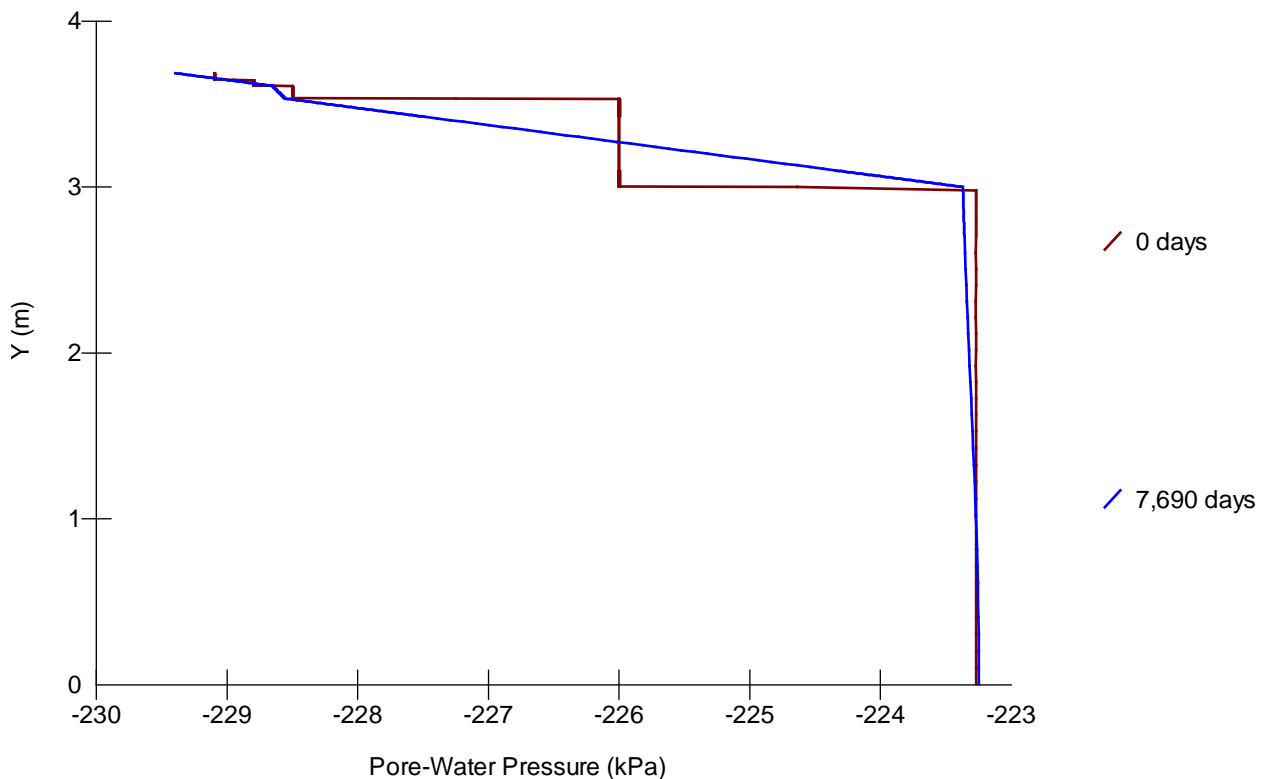


**Figure 6-8. Approximation of Hydrostatic Initial Condition Estimated for Use in Starting a Year-Long Zuni Buttes Climate Spinup Simulation of the Church Rock Central Cell Soil Cover (1 kPa = 0.33 ft H<sub>2</sub>O; 1 m = 3.28 ft)**

The pore water pressure distribution on Day 7,690, illustrated in Figure 6-8, was used to start the Zuni Buttes year-long climate spin-up simulation with a start date of April 5, 2006. The minimum allowable timestep was decreased to 0.001 days (1.44 mins). The maximum number of iterations allowed prior to moving on to the next timestep was increased to 70. The radon barrier and tailings generally proceeded to dry-out during the year-long climate spinup simulation (Figure 6-9). The end-of-year pore water pressure distribution obtained from this model is shown in Figure 6-10.

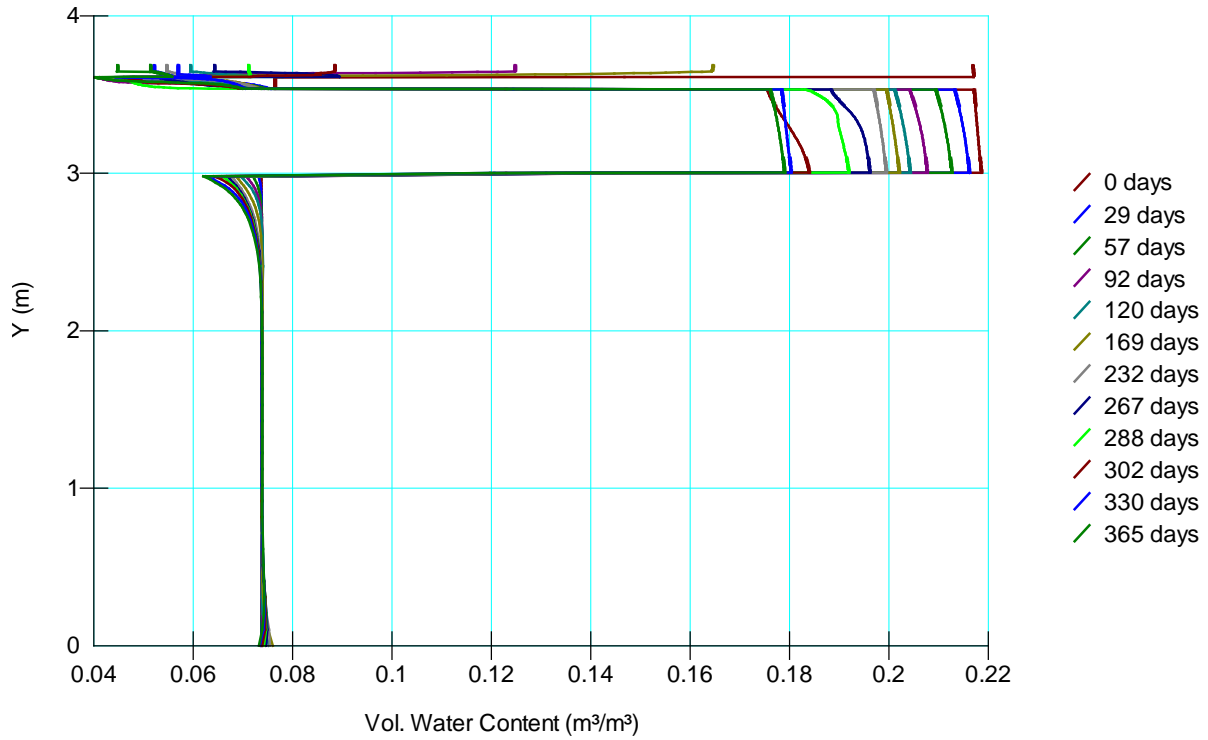


**Figure 6-9. Volumetric Water Content Markedly Decreased in Deep Layers during Year-Long Zuni Buttes Climate Spinup Simulation of the Church Rock Soil Cover (1 m = 3.28 ft)**

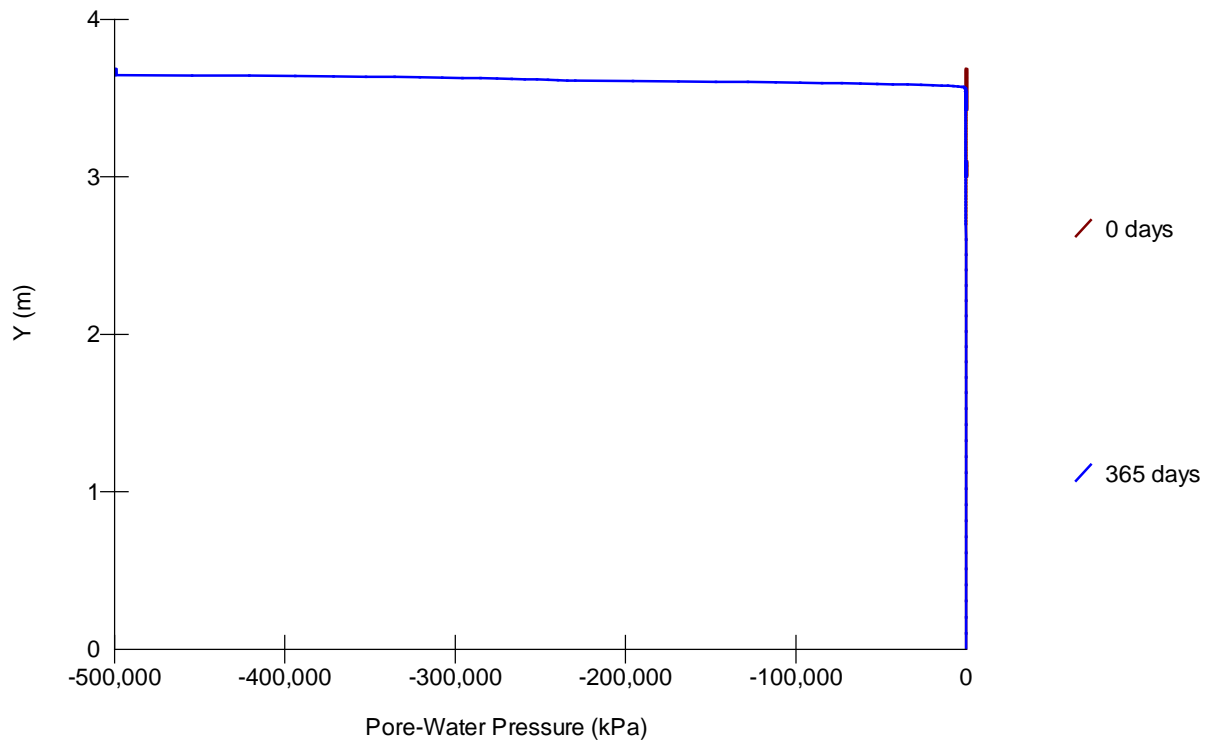


**Figure 6-10. Initial Conditions for Starting the Long-term Zuni Buttes Climate-Driven Simulation of the Church Rock Soil Cover (1 kPa = 0.33 ft H<sub>2</sub>O; 1 m = 3.28 ft)**

An expanded, 7,830-day (21.5-yr) Zuni Buttes climate-driven simulation was started on the date April 5, 2006, based upon imported pore water pressure distribution obtained on Day 365 of the year-long climate spinup simulation (Figure 6-10). This model ran with daily climate input starting on April 5, 2006, repeating portions of the record multiple times as necessary to attain a total simulation run spanning 7,830 days (equal to the length of the climate record used in the long-term Highland climate simulation). Because the soil column was observed to be significantly drying-out during the year-long climate spinup simulation, this approach was deemed appropriate for achieving a soil column moisture distribution that was well-equilibrated to local climate forcings. Water balance outputs were saved at every adaptive timestep and other results (e.g., fluxes) were saved every 30 days for quantitative and graphical analyses.

The initial and two resulting pore water pressure distributions are illustrated in Figure 6-11: a distribution from Day 7,680 (April 14) was used to initialize a final 3,210-day (8.8-yr) Zuni Buttes climate-driven model, starting on April 14, 2006 and ending on January 26, 2015. For completeness, the distribution from Day 7,830 shows pore water pressures at the end of this 21.5-yr simulation. Figure 6-11 shows that considerable drying of the upper section of the soil column occurred during this simulation.

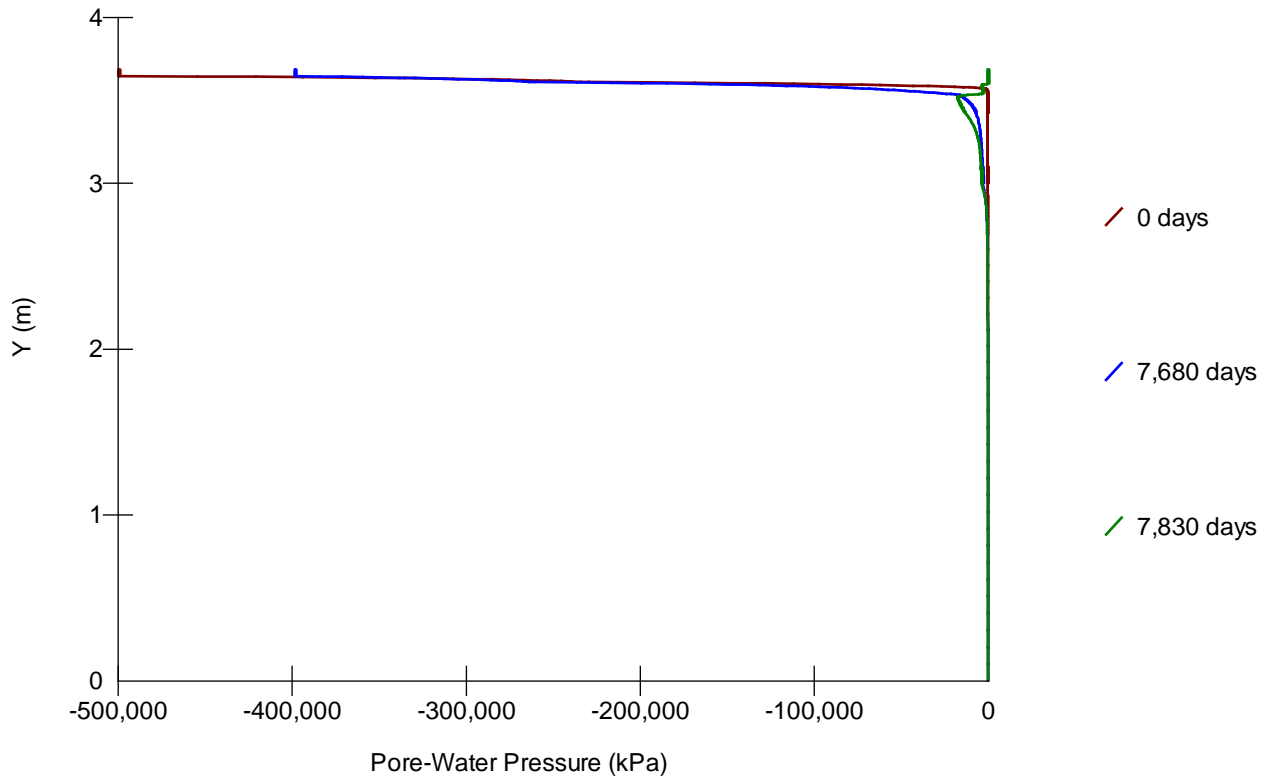


**Figure 6-11. Hydraulic Initial Conditions (Day 7,680) for Starting the Final 3,210-Day-Long Zuni Buttes Climate-Driven Simulation of the Church Rock Soil Cover (1 kPa = 0.33 ft H<sub>2</sub>O; 1 m = 3.28 ft)**

To understand more fully the drying that occurred, it was observed that the volumetric water content decreased annually during the first through eighth years of this Church Rock simulation (Figure 6-12).

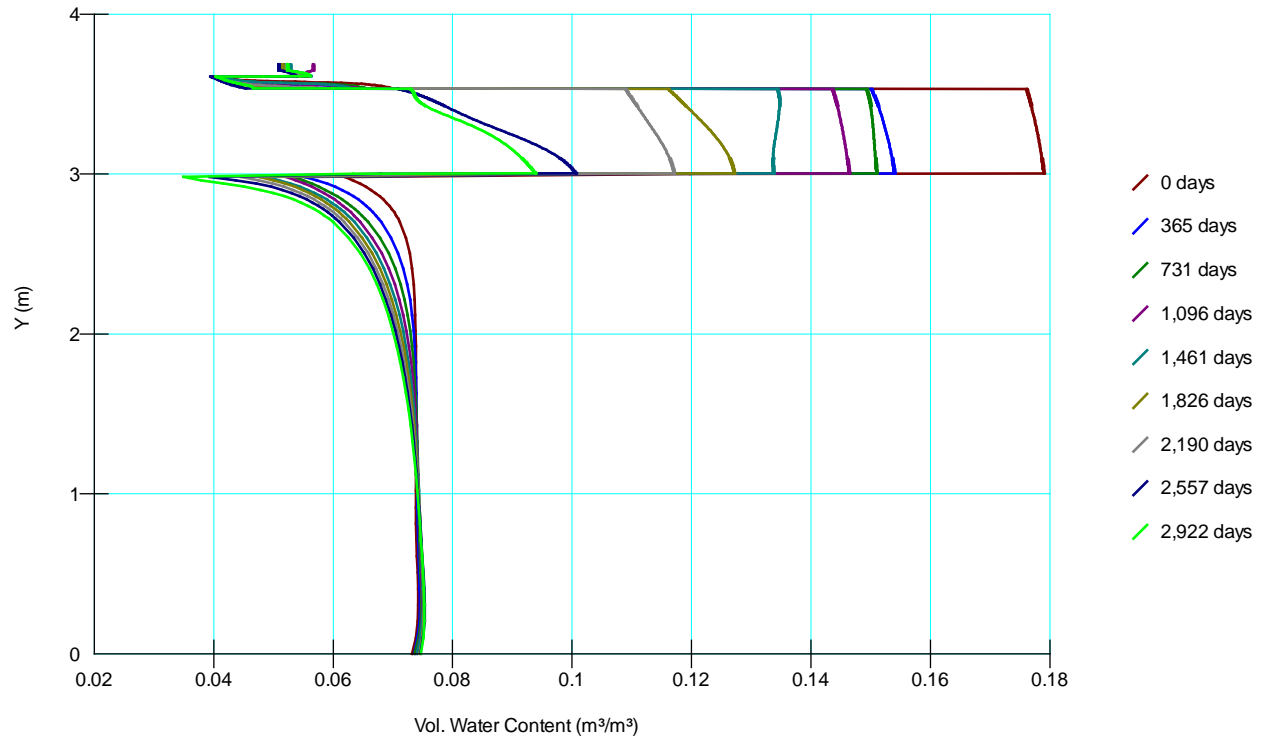


**Figure 6-12. Annually Decreasing Volumetric Water Contents Observed as Moisture in the Soil Column Equilibrates with Local Climate Forcing During Years 1–8 (1 m = 3.28 ft)**

After the eighth year, volumetric water content in the radon barrier became considerably more variable, sometimes increasing relative to the prior year (Figure 6-13).

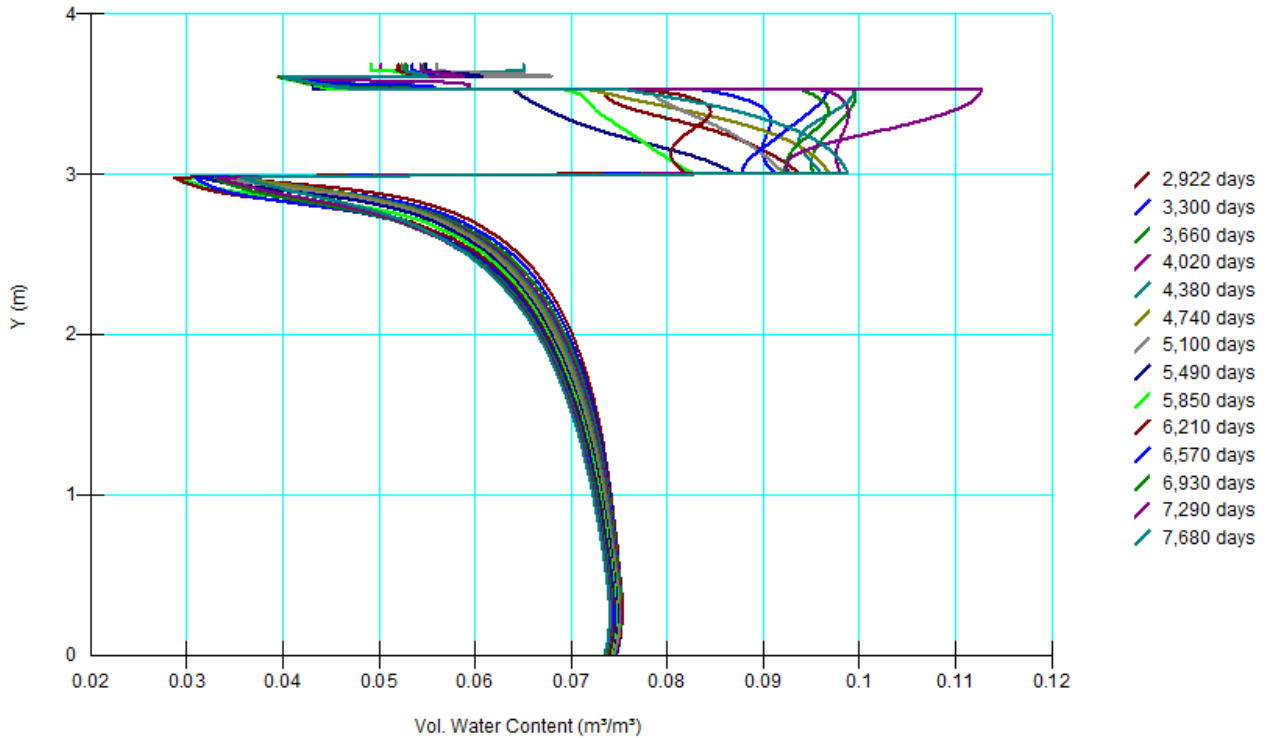


**Figure 6-13. Soil Column Responds to Local Climate Forcing after Equilibration has Occurred During Years 8–21 (1 m = 3.28 ft)**

Staff decided that a final, 3,210-day-long Church Rock central cell simulation was needed, using the pore water pressure (and temperature) output from the final day of the 7,830-day-long simulation nearest April 5 (output was written every 30 days, so outputs from April 5 were not available). The date for which outputs were available nearest April 5 was April 14 (e.g., Day 7,680 of Figure 6-11); therefore, the final Church Rock simulation was initialized on April 14, 2006 and ran 3,210 days until January 26, 2015. The maximum number of iterations allowed prior to moving on to the next timestep was increased to 90. Water balance outputs were saved at every adaptive timestep and other results (e.g., fluxes, pore water pressures, temperatures) were generally saved every 30 days for quantitative and graphical analyses. This simulation was run multiple times as staff became aware of certain periods of time that were particularly interesting. In some cases, output was written on a daily basis for enhanced analysis. Consult Section 6.2 for more information about these final results.

*Thermal Initial Conditions*

In the absence of suitable ground temperature information, the Zuni Buttes year-long climate spinup model was initialized (Figure 6-14, Day 0) with a ground temperature of 14.5 °C (58 °F).

The final temperature distribution on Day 365 of the year-long climate spinup model (Figure 6-14) was used to initialize the subsequent Zuni Buttes expanded climate-driven model of 22.5-yr length.

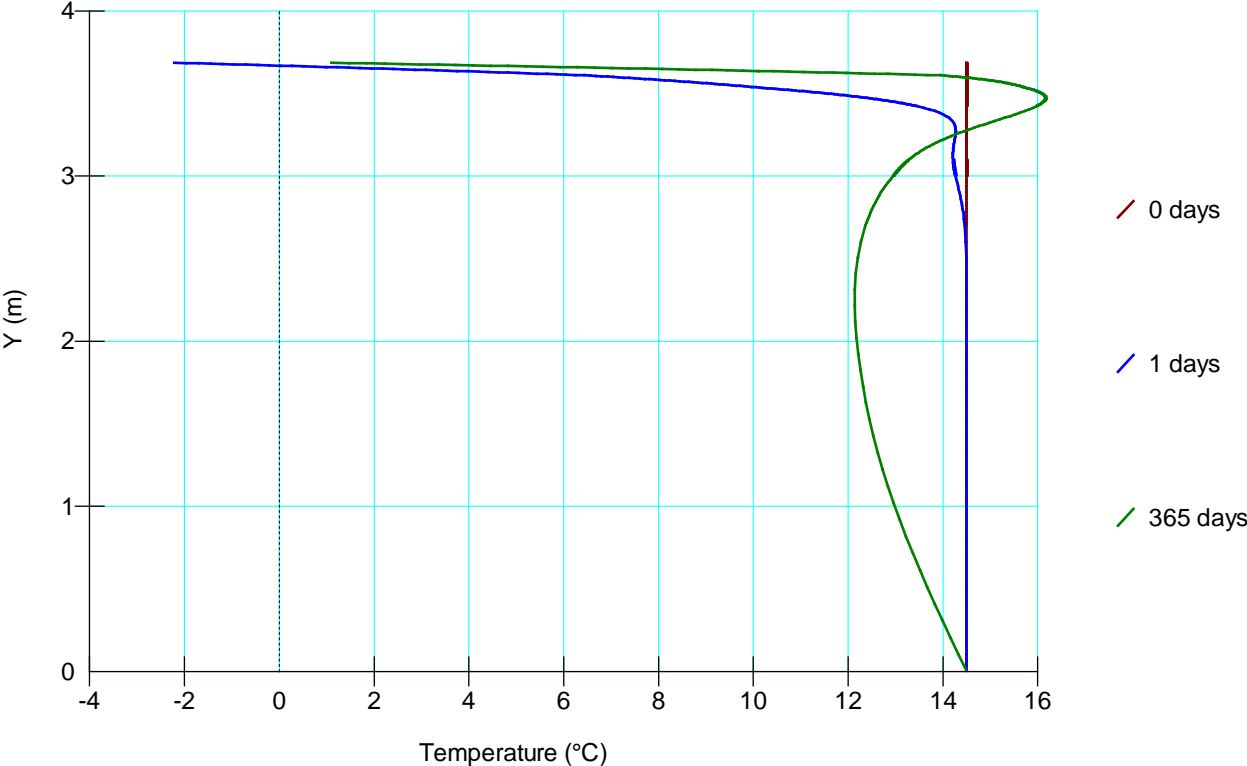


**Figure 6-14. Thermal Initial Conditions (Day 365/April 4) for Starting the Zuni Buttes Expanded-Length Climate-Driven Simulation of the Church Rock Soil Cover (1 m = 3.28 ft)**

The Day 7,680 (April 14) ground temperature distribution (Figure 6-15) from the Zuni Buttes expanded climate model was used to initialize the final 3,210-day Zuni Buttes climate simulation, which ran from April 14, 2006 until January 26, 2015. Note that the Day 0 ground temperature distribution corresponds to solar forcing on April 5, 2006.

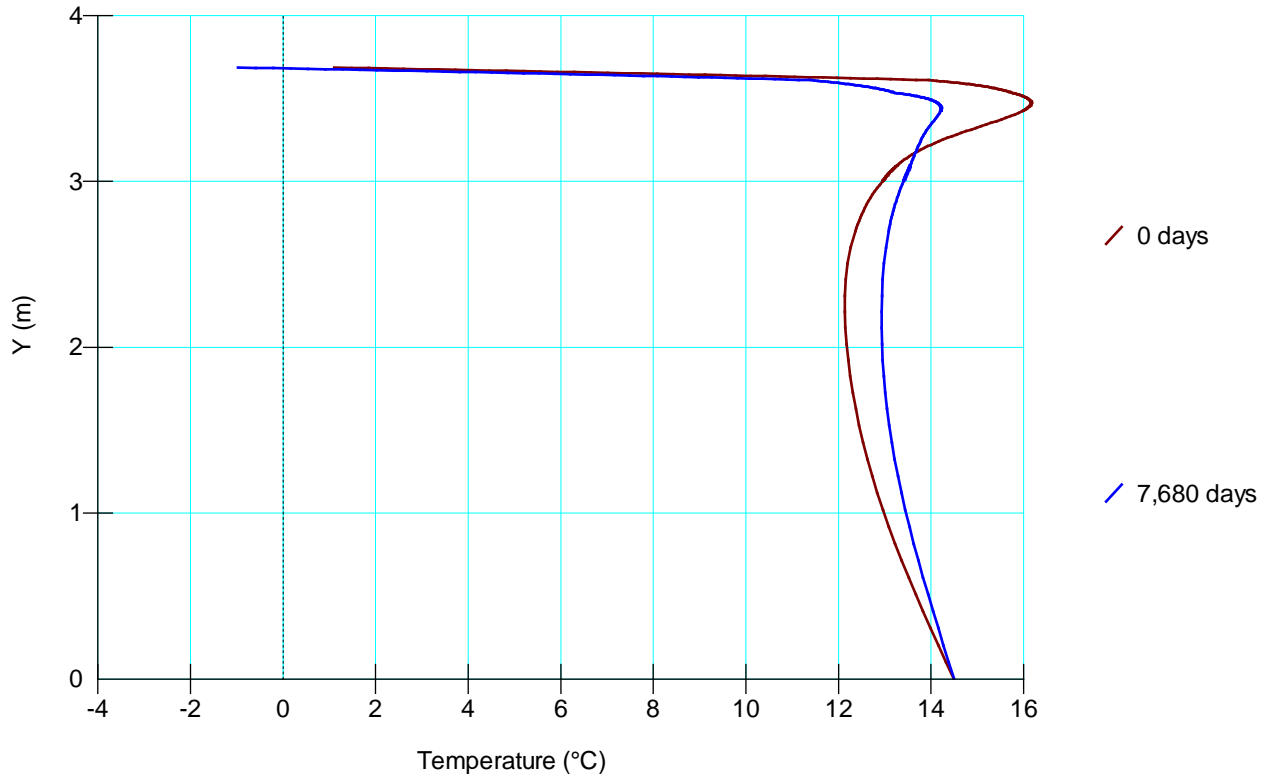


**Figure 6-15. Thermal Initial Conditions (Day 7,680/April 14) for Starting the Final Zuni Buttes Climate-Driven Simulation of the Church Rock Soil Cover (1 m = 3.28 ft)**

## 6.2 Simulation Results

The final simulation was climate-driven using the available Zuni Buttes climate record only, with no recycling of climate input. The simulation spans a 3,210-day period between April 14, 2006, and January 26, 2015. Output was written every 30 days, annually, and daily during two periods that preceded or were contemporaneous with deep percolation into the sandy tailings. In summary, outputs (e.g., fluxes, pore water pressures, temperatures) were written on Days 0, 1, 366, daily from Day 604 to 674, 732, daily from Day 974 to 995, 1,097, 1,462, 1,827, 2,193, 2,558, 2,923, and at the end of each 30-day “month.”

During preliminary simulation runs for this relatively dry soil column, mass balance errors were more prolific than they had been during prior runs involving wetter soil conditions. Mass balance error events were checked against the precipitation start/stop times to observe which events occurred during monsoon season when performance was worsened by the intensity of the rainfall. Significant mass balance errors occurring on Days 128, 160, 1952, 1953, 1622, 1623, 2706, and 3088 were attributed to monsoon storm intensity and were minimized in the final simulation by spreading rainfall amounts over the full day. Other significant mass balance errors occurred on days during which no rain fell or on days during the non-monsoon season when rainfall was gentle over a day-long period. Such errors could not be minimized. The final

mesh cumulative mass balance components and error are illustrated in Figure 6-16. The mass balance error rate over the length of the simulation was approximately 2.5 mm/yr. Cumulative storage is negative; evaporation and runoff losses combined are cumulatively greater than cumulative precipitation.

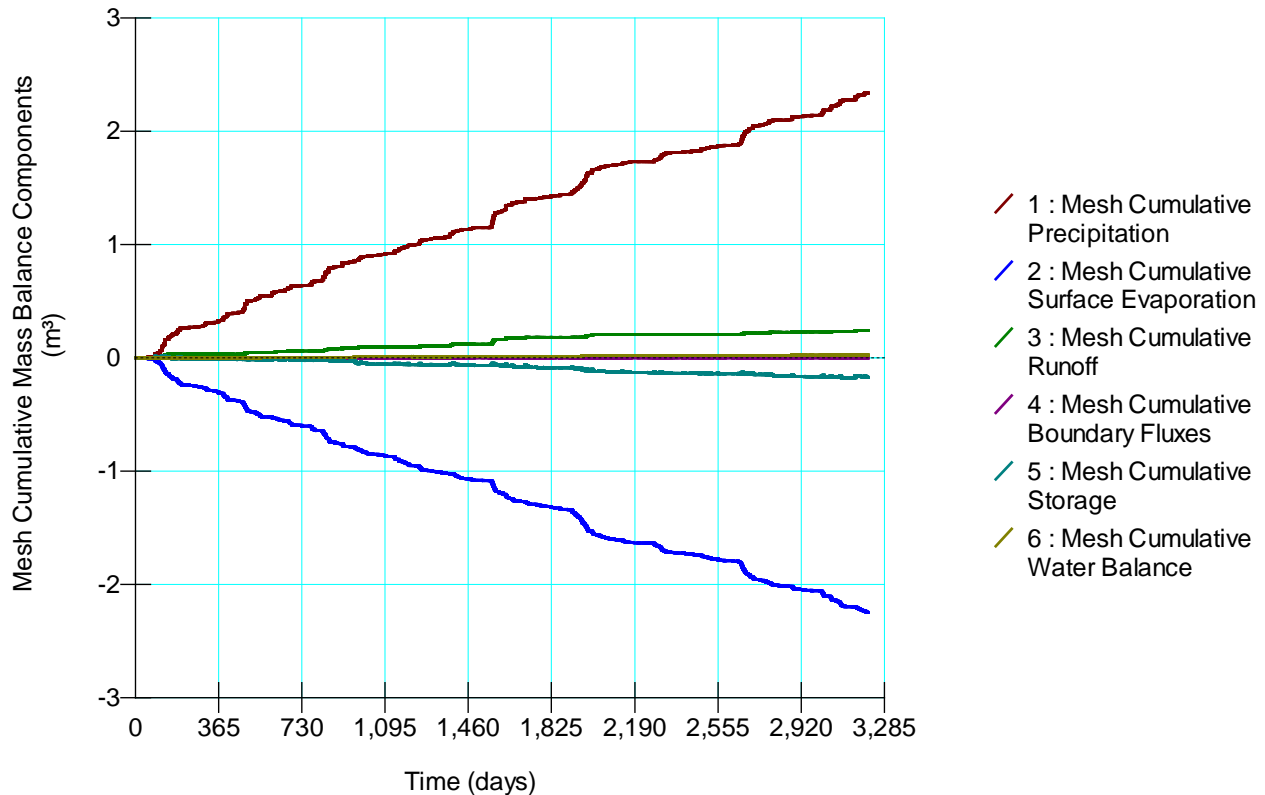


**Figure 6-16. Mesh Cumulative Mass Balance Components and Resulting Error (0.022 m<sup>3</sup> over 8.8 yrs = 2.5 mm/yr) in the Zuni Buttes Climate-Driven Church Rock Central Cell Soil Cover Simulation (1 m<sup>3</sup> = 35.3 ft<sup>3</sup>)**

April 14 anniversary volumetric water contents plus the simulation end-state are illustrated in Figure 6-17. Figure 6-18 focuses only on the distribution within the coarse, sandy loam tailings. The uppermost portion of the tailings is much drier than the deeper sections, and also experiences larger changes in drying than the deeper sections. The tailings become drier toward the end of the simulation, but not until after they wet-up during the end of the second and throughout the third years due to rain events and deep percolation.

During the simulation, from Day 0 to Day 632, the coarse, sandy loam tailings are in a drying mode (Figure 6-19). After Day 632, the upper tailings begin to wet-up to higher moisture content than they had at the start of the simulation, until Day 1860, after which they are in a drying mode, ending at the condition shown on Day 3,210 in Figure 6-19. This suggests water was infiltrating beyond the radon barrier from Day 633 until Day 1860. Note that Days 604–674 span the period from December 8, 2007 through February 16, 2008; Days 974–995 span the period from December 12, 2008 through January 2, 2009. Deep percolation caused the volumetric water content to markedly increase within the sandy tailings, and once drying finally began it took 900 days for the volumetric water content near the top of the sandy tailings to recover (Figure 6-20).

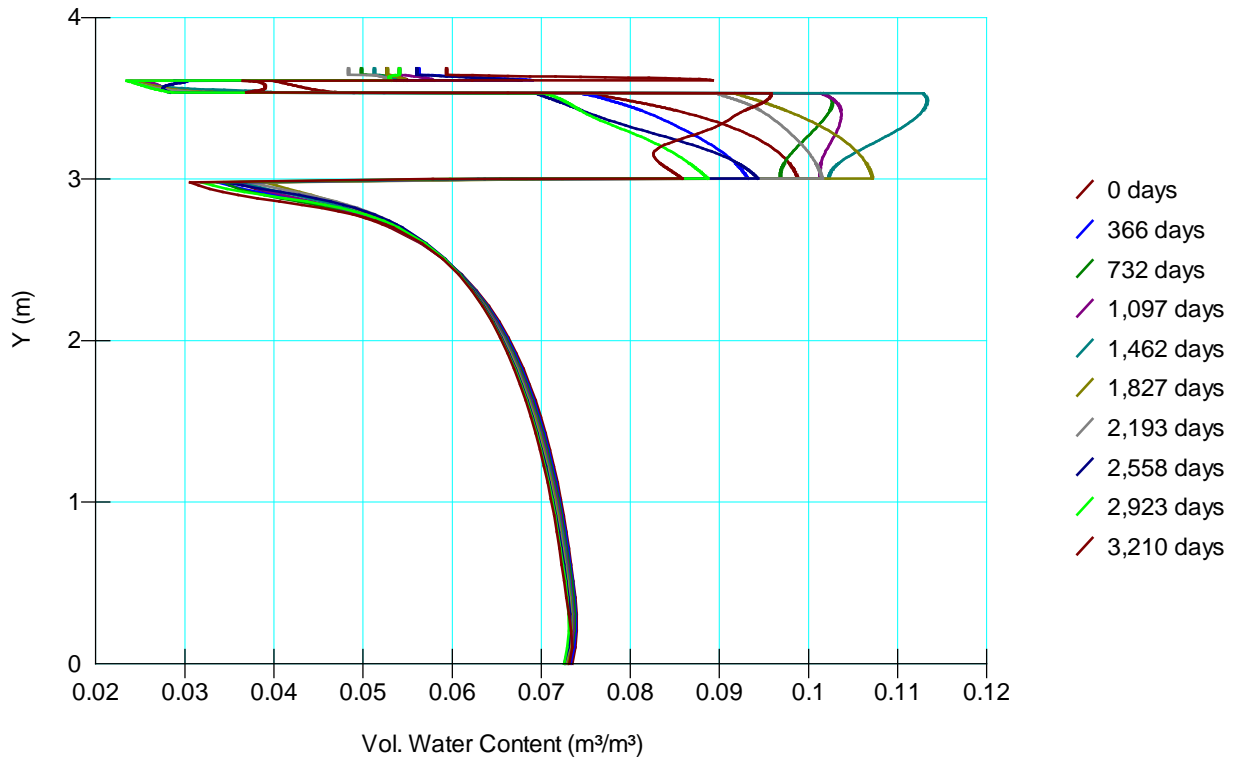


**Figure 6-17. April 14 Anniversary Volumetric Water Contents in the Church Rock Central Cell Soil Column (1 m = 3.28 ft)**

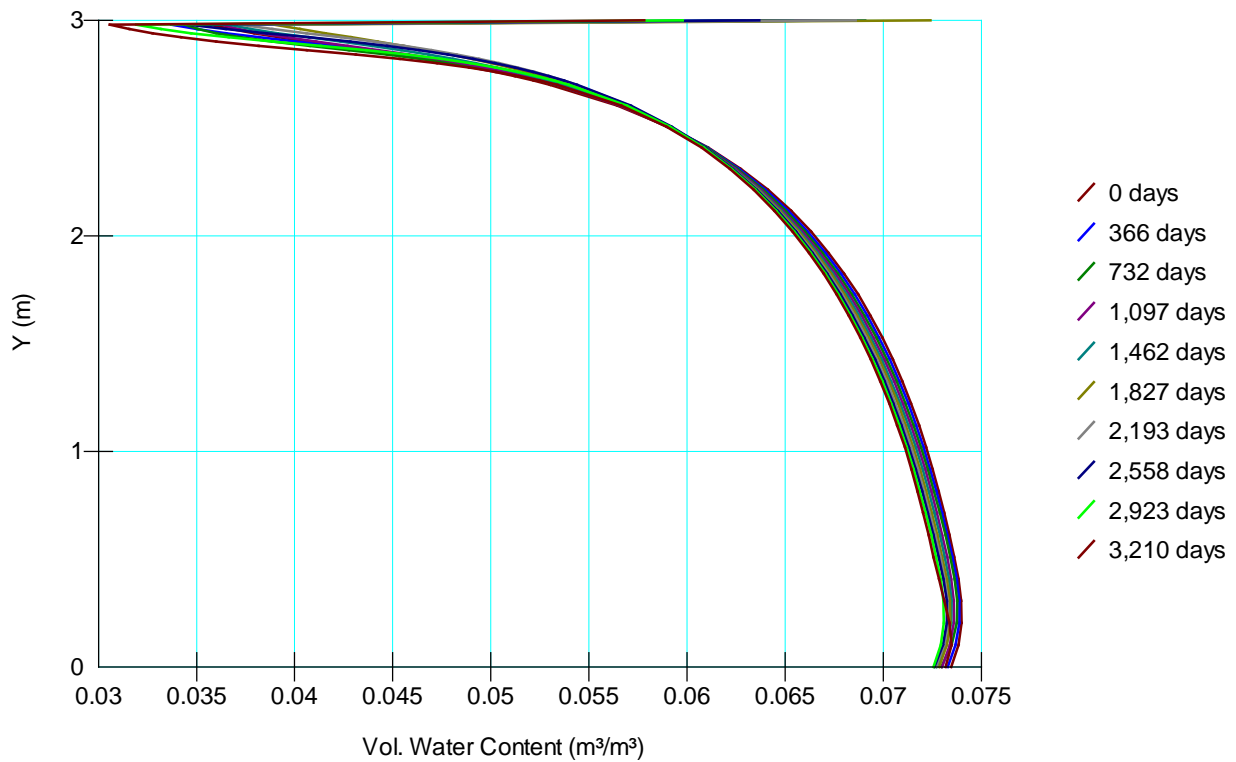


**Figure 6-18. April 14 Anniversary Volumetric Water Contents in the Church Rock Coarse, Sandy Loam Tailings (1 m = 3.28 ft)**

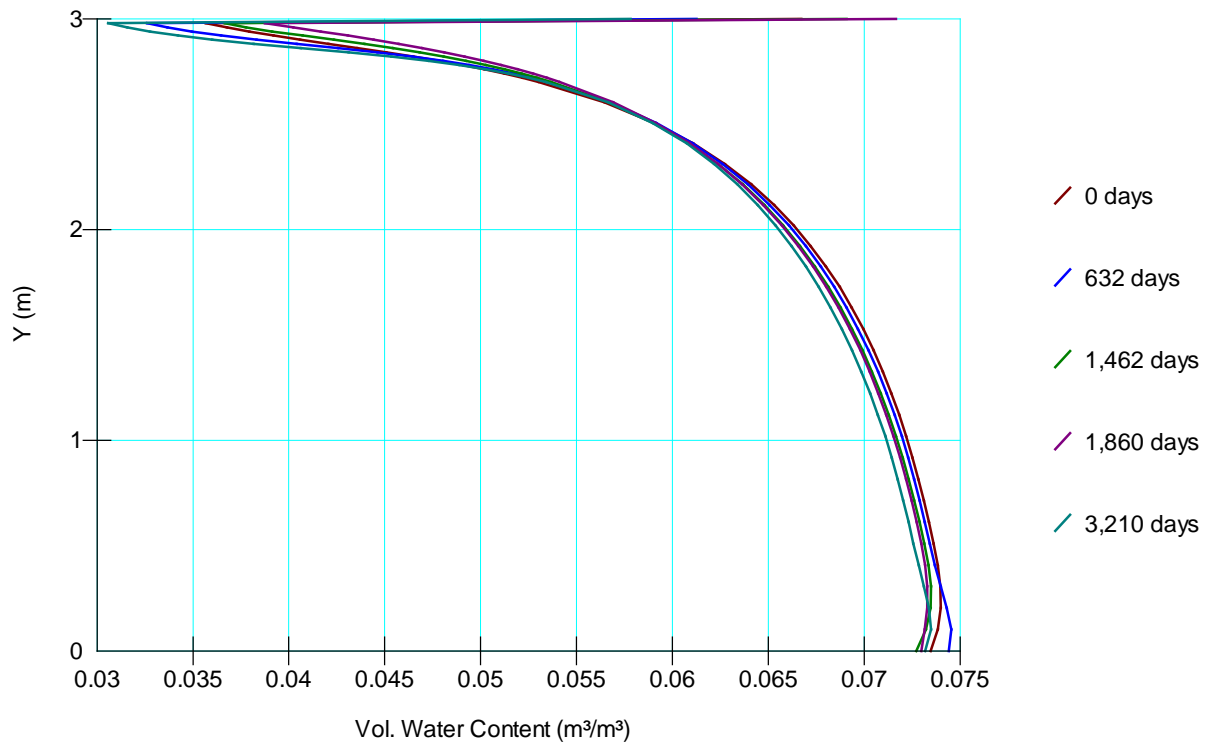


**Figure 6-19. Illustration of Drying (Days 0 to 632)/Wetting (Days 632 to 1860)/Drying (Days 1860 to 3210) Periods in the Church Rock Tailings (1 m = 3.28 ft)**

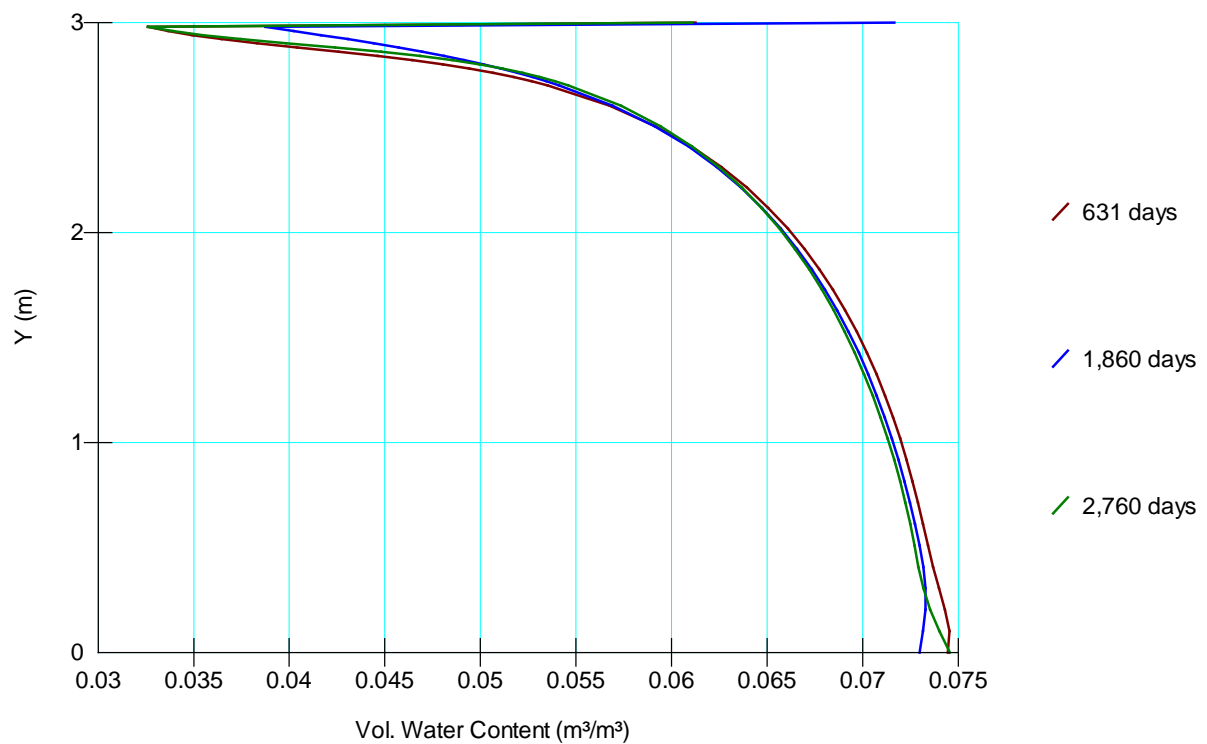


**Figure 6-20. Volumetric Water Content within the Upper Sandy Tailings Recovered to Approximate Day 631 Conditions (on Day 2760) 900 Days After Attaining their Maximum Volumetric Water Content (on Day 1860) (1 m = 3.28 ft)**

Pulses of water that occasionally increase the hydraulic conductivity of the radon barrier are easily observed because they are dramatic. More subtle are hydraulic conductivity increases near the top of the tailings. Significant pulses of water entered the radon barrier during periods spanning Days 604 to 669 (December 8, 2007 through February 11, 2008) and Days 974 to 992 (December 12 through 30, 2008). The period spanning December 8, 2007 through February 16, 2008, was split into three sub-periods to illustrate the changing dynamics within the radon barrier: Days 604–632 (Figure 6-21); Days 633–653 (Figure 6-22), and Days 654–669 (Figure 6-23). These figures illustrate how actively the radon barrier responded to water input prior to and following the point in time at which the volumetric water content in the underlying tailings began to increase. Staff interpret that these pulses of water began to enter the sandy tailings after Day 632, increasing their volumetric water content and hydraulic conductivity. Dynamics within the radon barrier that indicate the progression of infiltration pulses during the period from December 12 through 30, 2008, are illustrated in Figure 6-24.

While hydraulic conductivity increases, representing infiltration pulses, are seen to move deeply into the radon barrier (Figures 6-21 through 6-24), they are not observed to travel all the way to the base of the radon barrier prior to re-equilibrating, probably because the specific timing of the output write-out is not contemporaneous with the specific moment of each day that a pulse arrives at the deepest part of the radon barrier and enters the tailings.

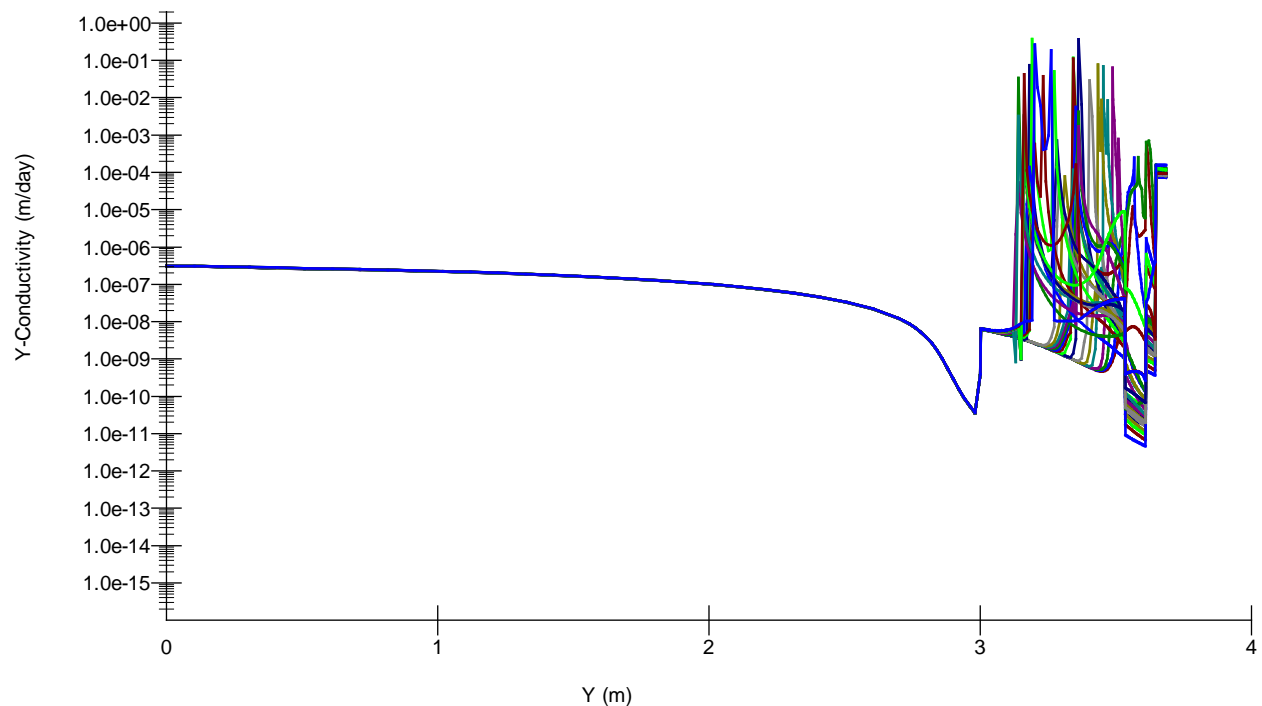


**Figure 6-21. Infiltration Pulses Enter the Radon Barrier during the Period Spanning December 8, 2007 through January 3, 2008 (Days 604–632)**  
**(1 m/day = 3.28 ft/day; 1 m = 3.28 ft)**

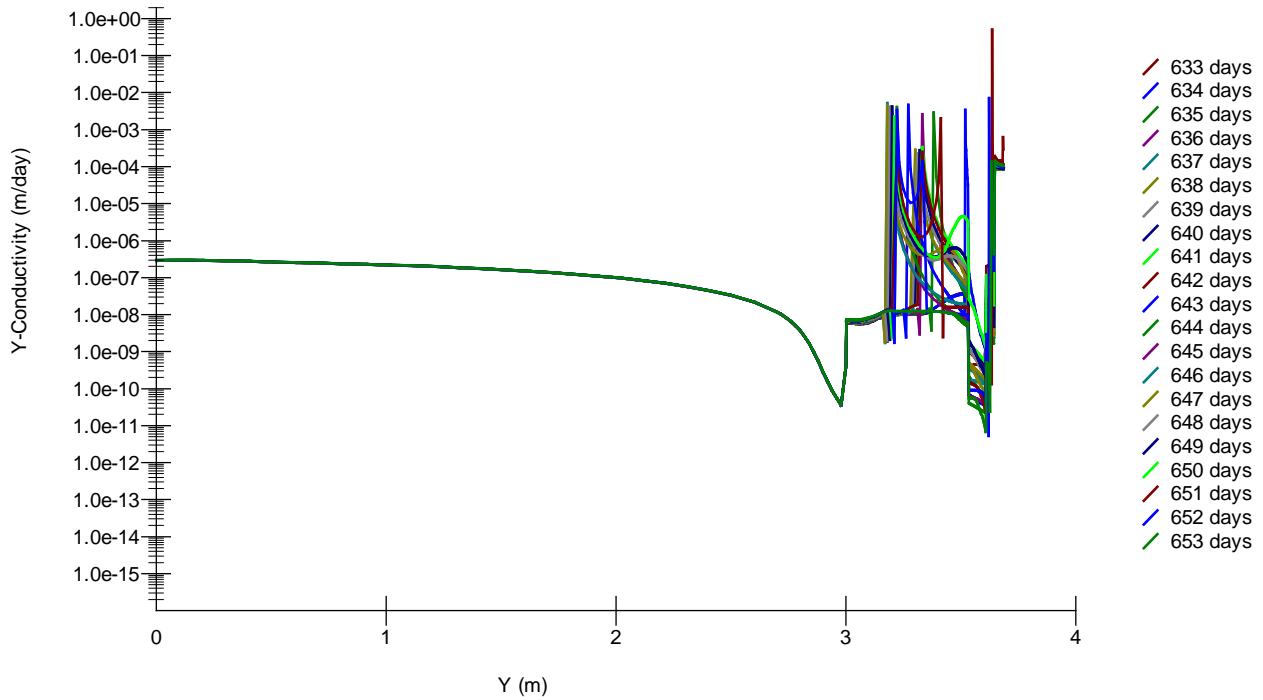


**Figure 6-22. Infiltration Pulses Enter the Radon Barrier during the Period Spanning January 3–26, 2008 (Days 633–653) (1 m/day = 3.28 ft/day; 1 m = 3.28 ft)**

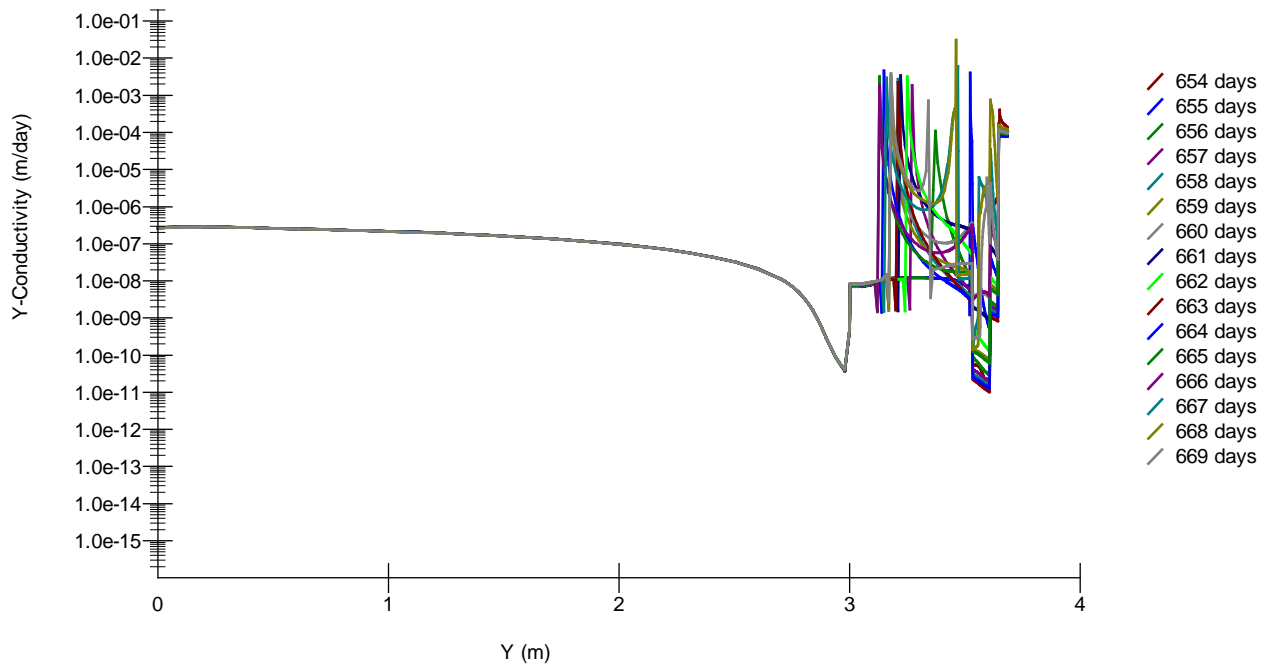


**Figure 6-23. Infiltration Pulses Enter the Radon Barrier during the Period Spanning January 27 through February 11, 2008 (Days 654–669) (1 m/day = 3.28 ft/day; 1 m = 3.28 ft)**

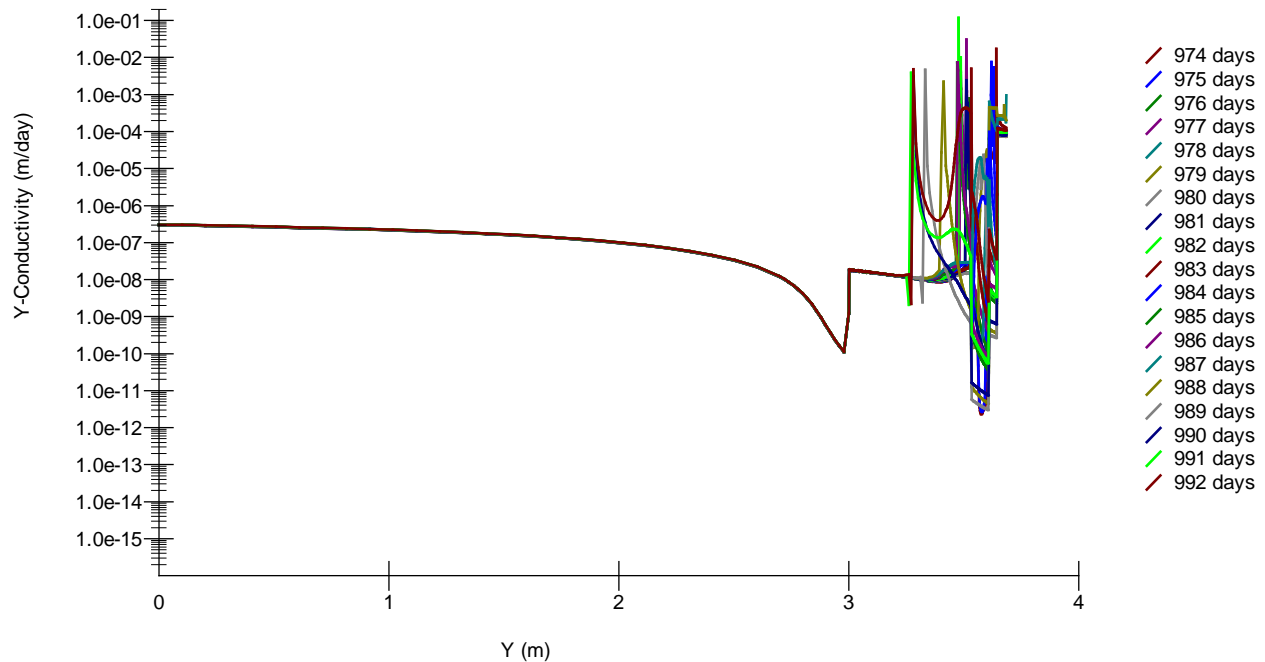


**Figure 6-24. Infiltration Pulses Enter the Radon Barrier during the Period Spanning December 12–30, 2008 (Days 974–992) (1 m/day = 3.28 ft/day; 1 m = 3.28 ft)**

Water infiltration into the radon barrier from Day 604 through Day 632 yielded deep percolation into the underlying coarse, sandy loam tailings starting on Day 632 and a commensurate 1,228-day-long increase in their hydraulic conductivity. The hydraulic conductivity of the upper section of the tailings continued to increase until Day 1,860 (Figure 6-25), at which point they began to decrease due to net water loss (evaporation plus drainage). Starting on Day 1,860, the hydraulic conductivity decreased for 900 days prior to attaining a condition similar to that on the day that deep percolation began (Figure 6-26). After this, the upper tailings hydraulic conductivity decreased at every step over the remaining portion of the climate record (Figure 6-27) due to loss of water, despite additional pulses of infiltration into the radon barrier.

In summary, depending on the representativeness of the selected model parameters used in this model, the Church Rock central cell soil cover may not be impervious to net infiltration or prohibit deep percolation from entering the uranium mill tailings.

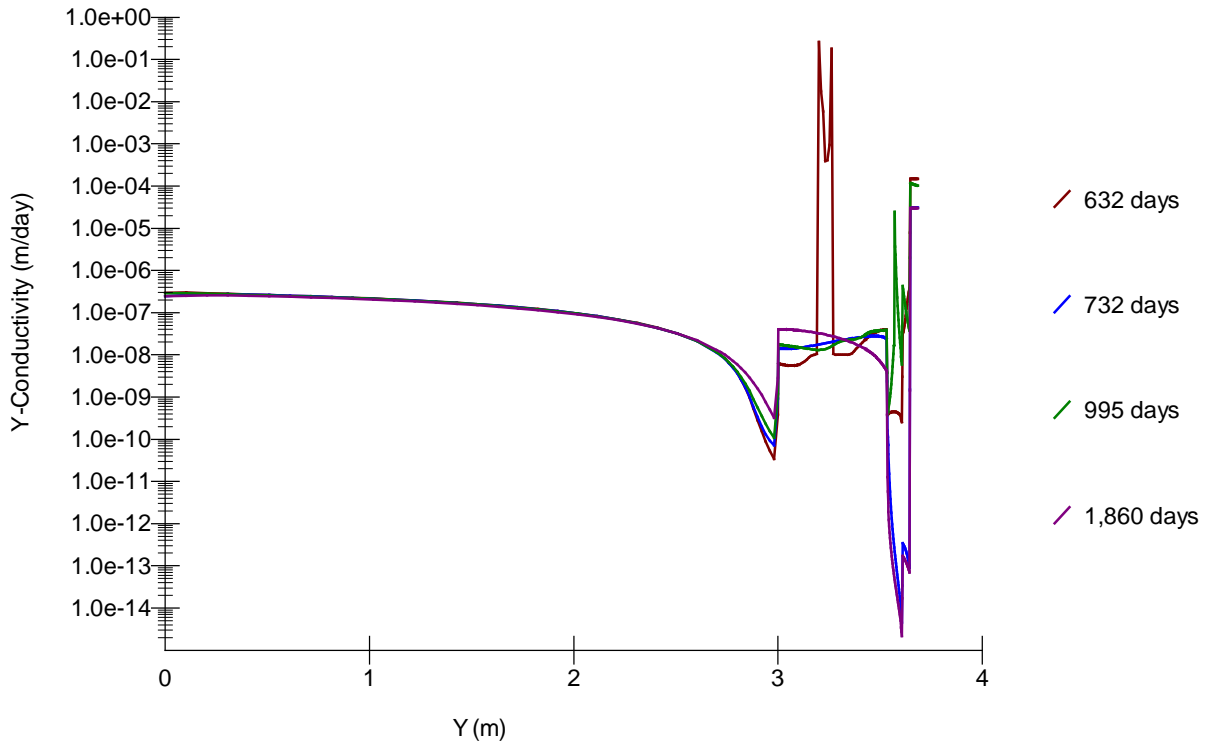


**Figure 6-25. Hydraulic Conductivity Monotonically Increased in the Upper Section of the Church Rock Coarse, Sandy Loam Tailings Over a Period of 1,228 Days (1 m/day = 3.28 ft/day; 1 m = 3.28 ft)**

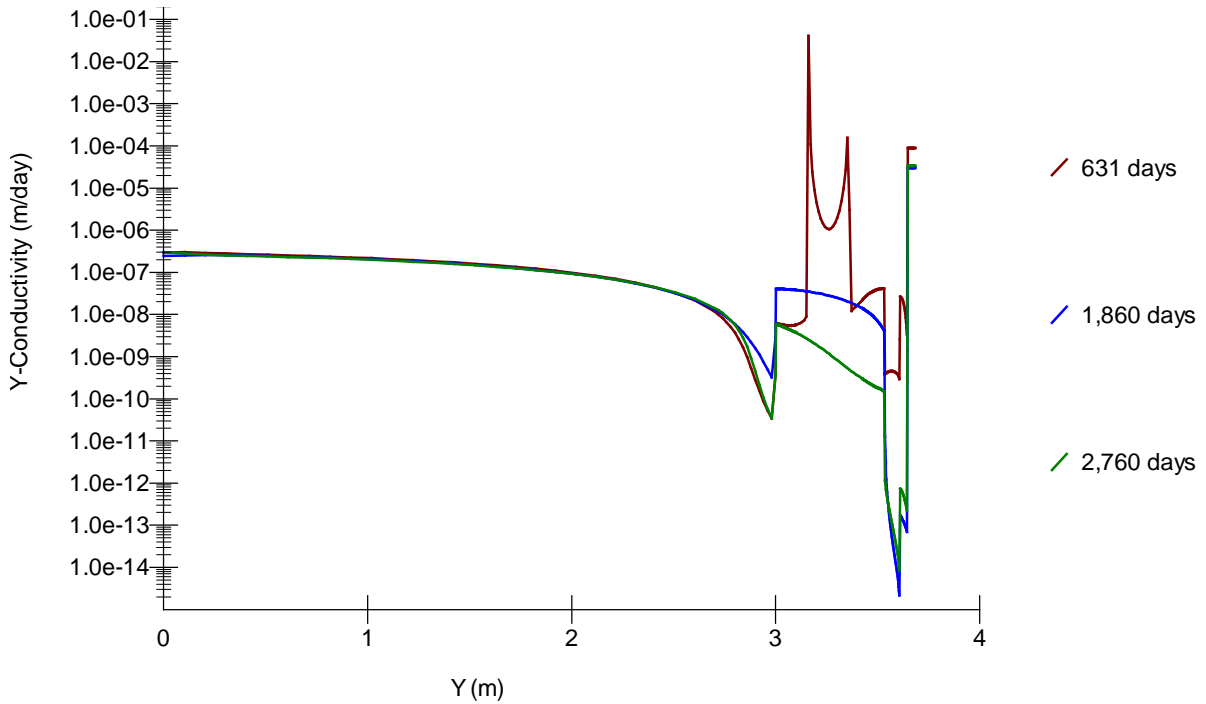


**Figure 6-26. After Deep Percolation Into the Church Rock Coarse, Sandy Loam Tailings Ceased, 900 Days of Drying Occurred Before the Permeability Profile Recovered to Conditions Approximately the Same As When Deep Percolation Began (1 m/day = 3.28 ft/day; 1 m = 3.28 ft)**

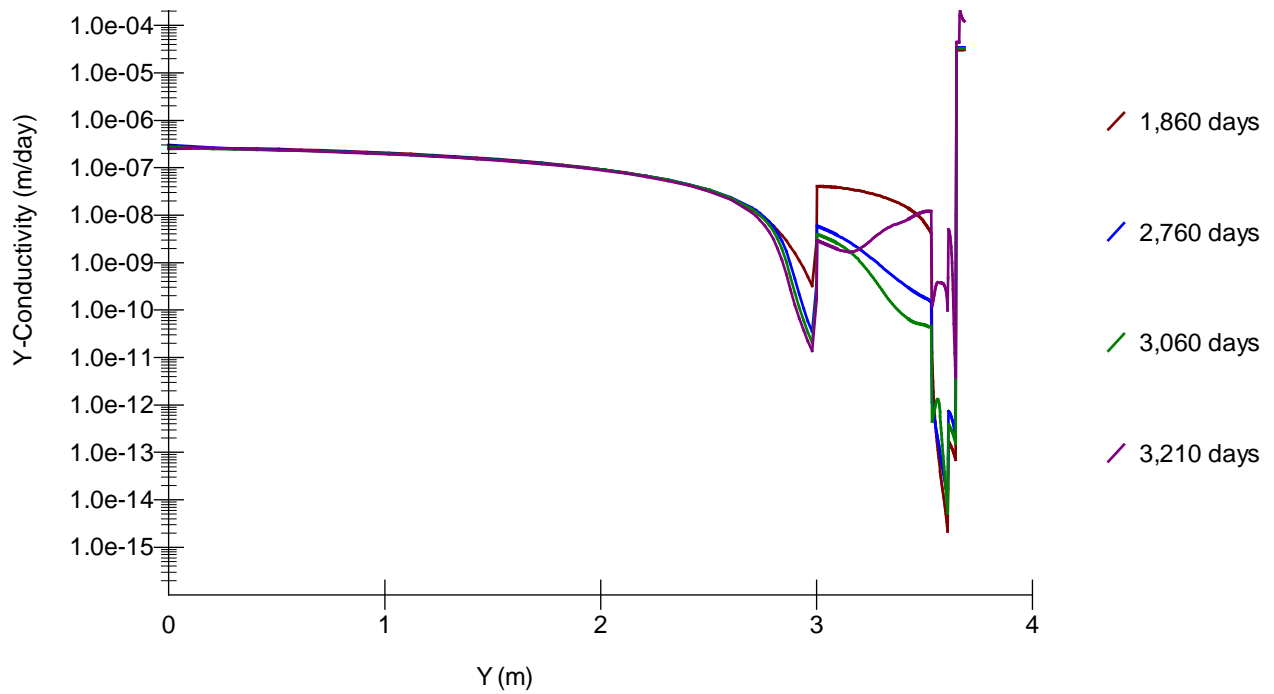


**Figure 6-27. Upper Section of the Coarse, Sandy Loam Tailings Exhibit Further Reduction in Permeability until the End of the Climate Record  
(1 m/day = 3.28 ft/day; 1 m = 3.28 ft)**

## 7 EVALUATION OF MODEL RESULTS AND RECOMMENDATIONS

The simulations documented in this report were performed to lay groundwork for estimating whether or not earthen soil covers installed over Title-II-In-Closure uranium mill tailings impoundments prevent net infiltration of meteoric water from entering the tailings. The simulations are not intended to determine if original pore water within the tailings is continuing to drain into underlying soil. Due to numerical issues associated with the simulations, in-depth analysis of the parameters and their uncertainty affecting the simulation of net infiltration was not possible within the funding and timeframe of the contract.

### 7.1 Site Selection

The Gas Hills West (American Nuclear), Wyoming, Pond 2 tailings impoundment cell; the Highland (Exxon), Wyoming, tailings impoundment cell; and the Church Rock (UNC), New Mexico, central cell were selected from amongst the Title-II-In-Closure soil covers for modeling because for these three represent the full range of

- Climate conditions
- Erosion barriers types [vegetated topsoil; sparsely vegetated rock mulch (volunteers only), and riprap] and
- Surface drainage feature types.

Sufficient information was available on the soil types used to construct the earthen covers to develop plausible parameter sets for their material properties.

The Gas Hills West site is centrally located in Wyoming. Based on information summarized in Walter and Dinwiddie (2014), the Gas Hills West cover has a rock mulch erosion barrier similar to that of the Gas Hills North site, which is located only 3 km [2 mi] to the northeast. While the Gas Hills East site is located only approximately 12 km [7.5 mi] east-northeast of the Gas Hills West site, its disposal cells have a much thicker and coarser riprap erosion barrier. The Highland site is located in east-central Wyoming, 177 km [110 mi] east-northeast of Gas Hills West, but at a lower elevation (Figure 2-1). It is similar to the Bear Creek, Shirley Basin, and Split Rock sites in terms of climate and vegetated soil cover. The Church Rock site is located in north central New Mexico with a climate similar to that of the other Title-II-In-Closure sites in New Mexico [i.e., Ambrosia Lake West and Bluewater]. Church Rock has a rock mulch erosion barrier with sparse vegetation, whereas Bluewater has a riprap erosion barrier.

### 7.2 Numerical Model and Limitations

The Vadose/W 2012 code was selected for performing the simulations because it includes algorithms for computing evaporative and transpirative water loss under variable meteorological conditions, and diversion of precipitation as surface runoff and ponding. Vadose/W also includes algorithms for simulating soil freezing and thawing, and the effects of these processes on infiltration. Of particular importance in selecting this code was its relatively sophisticated methods for simulating evapotranspiration and runoff, which are needed to establish the climate-driven boundary condition for the upper surface of the model mesh.

Vadose/W simulates flow through unsaturated porous media by computing the change in pore water pressure as a result of imposed boundary conditions which, in the case of the sites

investigated here, are entirely due to the climate record specified by the user. In evaluating the performance of Vadose/W for the purposes of estimating net infiltration through uranium mill tailings impoundment earthen covers, accurate water balance estimates from the simulations are more important than accurate estimates of the pore water pressures within the cover and underlying tailings. This is because net annual infiltration, if any, is likely to be a small percentage of the annual precipitation and annual water balance at these semi-arid and arid site locations. Thus, small errors in computing the precipitation and runoff, possibly due to bookkeeping errors of the code, can result in large relative errors when comparing the net infiltration computed from boundary fluxes or the change in storage to the net infiltration based on the surface water balance.

With respect to the errors in computing the change in storage, extreme temporal or spatial changes in pore water pressures can cause errors in the computed change in storage due to either small numerical errors in computing the pore water pressures or non-convergence of the pore water pressure solution at particular nodes. In the case of the models for the Title-II-In-Closure sites, these extreme conditions most commonly occur in the surface of the cover that becomes extremely dry [large negative pore water pressures] between precipitation events or at boundaries between coarse- and fine-grained material layers. Based on the experience of others [Benson, et al. 2004, 2005; Bohnhoff, 2005; Khire and Mijares, 2008; Bohnhoff, et al., 2009; Mijares, et al., 2010], very fine discretization, i.e., element sizes on the order of millimeters, can be required to obtain water balance errors of less than 1 mm/yr (0.04 in/yr). Experience with the Title-II-In-Closure site models investigated here indicated that even the use of very fine node spacing do not always result in acceptable water balance errors. Water balance errors and uncertainties associated with the components of the water balance reported by Vadose/W led to some uncertainty in interpreting the results of the simulations with respect to whether or not net infiltration through the covers was likely to occur based on the hydraulic properties of the soil covers at the sites and the local climate.

### **7.3 Results of Gas Hills West Simulations**

The model for the Gas Hills West site was developed for Pond 2. Relatively little information was available with which to confidently describe the hydraulic and thermal properties of the materials used to construct the soil cover. Based on this paucity of information, the simulations were performed using representative values of soil water characteristics and thermal properties. The simulations were performed using the simple thermal model in Vadose/W. Although simulations using a highly discretized mesh were attempted, the associated run time was impractically long, taking up to 24 hrs to simulate only a few hundred days of the Fales Rock climate record. Thus, final simulations were performed using only a semi-refined mesh.

Simulation results using the semi-refined model mesh, three different precipitation distributions, and elevated hydraulic conductivity are summarized in Figure 7-1 in terms of average rate of change in storage, net water added, and water balance error. The simulations were performed using different temporal distributions of summer precipitation intensity to evaluate its effect on the water balance and with the saturated hydraulic conductivity of the sandy silty clay cover materials increased by a factor of 10 from the nominal value. The inconsistency in the apparent water balances based on the data reported by Vadose/W for the various precipitation distributions is attributed to bookkeeping errors in the code because the simulated changes in volumetric water content were generally consistent between the simulations, although not identical. The bookkeeping problems appear to be associated with the adaptive time-stepping algorithm in Vadose/W that results in many very small time steps per day caused by sudden, large variations in pore water pressures. These sudden, large changes in pore water pressures

result from higher precipitation intensities, with the highest intensities produced using the sinusoidal precipitation distribution and the lowest using the 24-hr distribution. The simulation using uniform 24-hr precipitation distribution and the elevated sandy silty clay hydraulic conductivity produced the best agreement between the change in storage and the net water added, and the lowest water balance error.

Despite the variations in the reported water balances, all of the simulations resulted in a net drying of the cover materials as indicated by the decrease in volumetric water content in the radon barrier over the course of the 7-yr simulations. Based on the simulated volumetric water contents, the soils comprising the radon barrier would be drying under current climate conditions and there would be no net infiltration through the cover into the tailings. This conclusion must be taken with caution, however, because the relative water balance error of the simulation was relatively large (on the order of 50 percent) for the more realistic simulations using the sinusoidal and 1-hr precipitation distribution, even though the annualized water balance errors are small (4 to 6 mm/yr [0.1 to 0.2 in/yr]). Based on the difficulty in developing simulations with a very small water balance error for the Gas Hills West site and that net infiltration through the cover, if any, is likely to be a very small fraction of annual precipitation and the overall site water balance, a firm conclusion about the performance of the cover with respect to net infiltration cannot be drawn from the simulations performed.

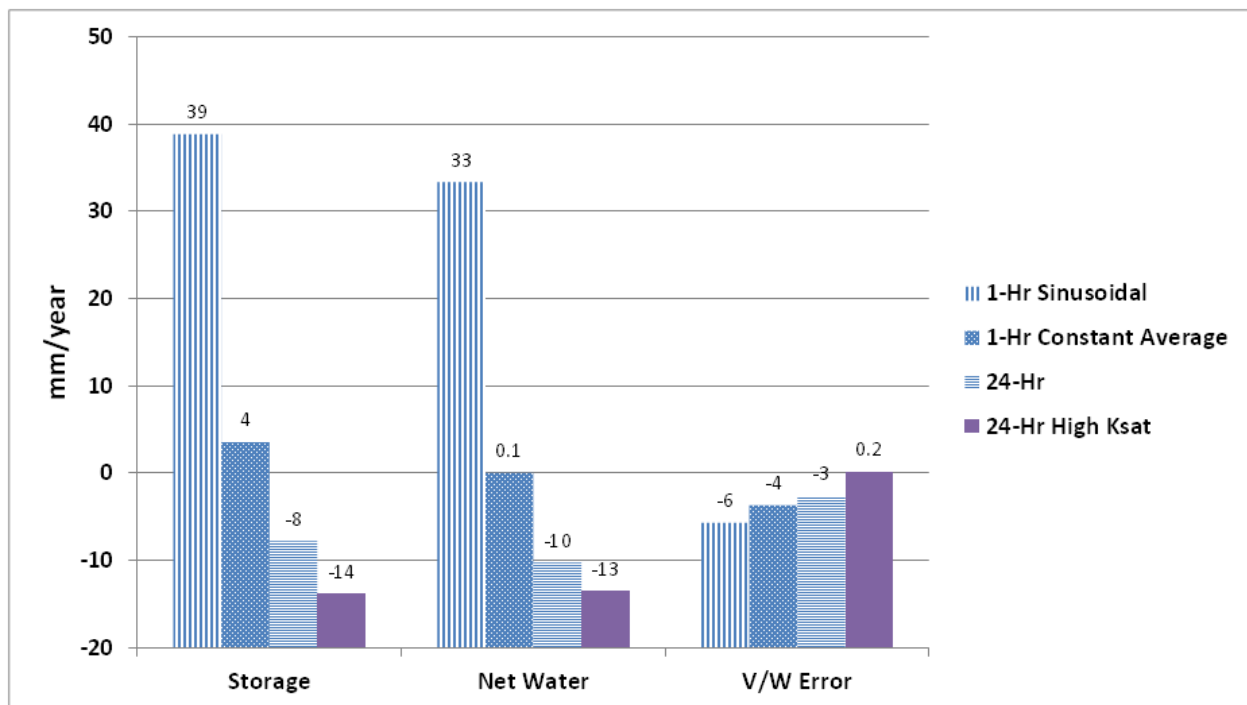


**Figure 7-1. Comparison of Results of Gas Hills West, Wyoming, Simulations Using Different Summer Precipitation Distributions and Elevated Saturated Hydraulic Conductivity of Sandy Silty Clay Materials**

#### 7.4 Results of Highland Site Simulations

The simulation of the Highland site model was performed with a one-dimensional, highly discretized finite-element mesh; the smallest elements were on the order of 2 mm [0.08 in]. Multiple simulations were performed to refine the performance of the Highland site model and investigate anomalies in the reported components of the water balance and the water balance

error. Using the best estimates of soil properties, the water balance components and error based on the simulation are illustrated in Figure 7-2. The water balance error rate over the length of the simulation was approximately 5.25 mm/yr (0.2 in/yr). The results of the simulation seem somewhat contradictory. The cumulative change in storage is positive, indicating a net increase in the water content of the model domain, as is the calculated net water added (precipitation less net evaporation, transpiration and runoff). The average rate of storage increase for the 22-yr simulation period is 32 mm/yr [1.3 in/yr] or 12 percent of mean annual precipitation. The calculated net water added was comparable. However, the simulated change in volumetric water content in the radon barrier and tailings decreased monotonically during the simulation except for short episodes of deep percolation into the tailings. The discrepancy between the apparent increase in water indicated by the water balance and the overall decrease in volumetric water content in the model domain precludes any firm conclusion about the performance of the tailings cover based on the simulation results.

Depending on the representativeness of the selected model parameters used in this model, the Highland soil cover may not prevent infiltration from entering the uranium mill tailings or deep percolation through the tailings.

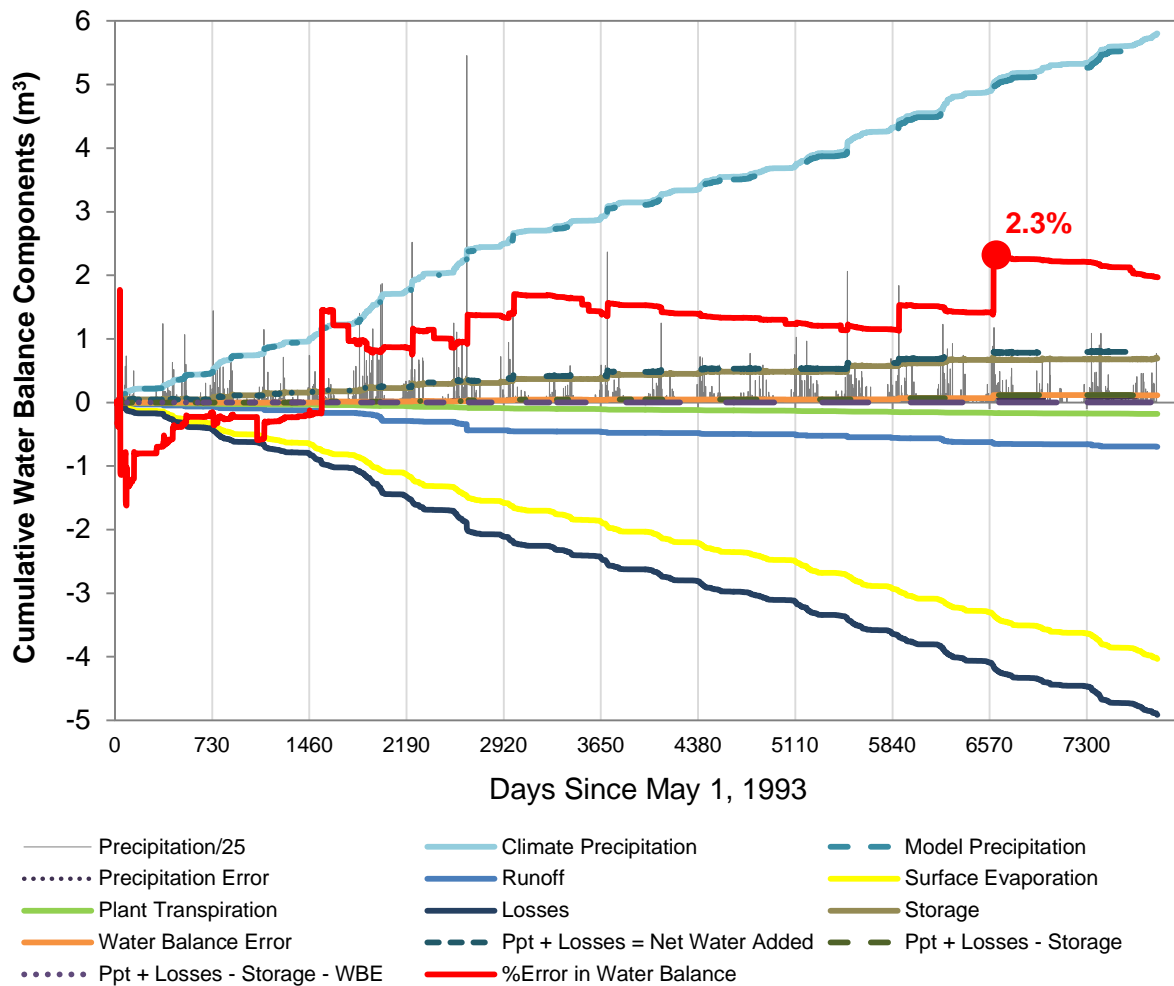


**Figure 7-2. Mesh Cumulative Water Balance Components for the Highland, Wyoming, Simulation (1 m<sup>3</sup> = 35.3 ft<sup>3</sup>)**

## **7.5 Results for Church Rock Simulations**

The simulation of the Church Rock site model also was performed with a one-dimensional, highly discretized finite-element mesh; the smallest elements were on the order of 2 mm [0.08 in] in thickness. The applied meteorological record spanned 3,210 days. The simulation was performed using the best estimates of soil hydraulic and thermal properties with no vegetation.

Despite the highly-refined nature of the model mesh, the simulation was affected by multiple events that contributed to the water balance error. Water balance error events were checked against the precipitation start/stop times to observe which events occurred during monsoon season when performance was worsened by the intensity of the rainfall. Significant water balance errors on specific days were attributed to monsoon storm intensity and were minimized in the simulation by spreading rainfall amounts over the full day. Other significant water balance errors occurred on days during which no rain fell or on days during the non-monsoon season when rainfall was gentle over a day-long period. Such errors could not be minimized.

The mesh cumulative water balance components and error are illustrated in Figure 7-3. The water balance error rate over the length of the simulation was approximately 2.5 mm/yr (0.1 in/yr). Cumulative storage is negative, averaging -19.8 mm/yr [-0.78 in/yr] as was the calculated net water added, thus the water balance indicates no net infiltration into the model domain.

Detailed analysis of the temporal variations in volumetric water content (or effective hydraulic conductivity as a sensitive surrogate for the water content) indicate large seasonal and annual variations in the water content in the radon barrier with occasional episodes of net infiltration into the tailings. Depending on the representativeness of the selected model parameters used in this model, the Church Rock central cell soil cover may not be impervious to net infiltration or prohibit deep percolation from entering the uranium mill tailings. Overall, however, there was no net increase in the volumetric water content in the tailings that would indicate a net accumulation of water in the model domain and ultimately deep percolation through the tailings.

## **7.6 Summary and Recommendations**

Firm conclusions regarding the performance of the tailings covers at the Gas Hills West, Highland, and Church Rock sites cannot be drawn from the simulation reports due to the water balance errors, uncertainty in the water balance components reported by Vadose/W and the discrepancies between the apparent water balances and changes in volumetric water contents in the model domains.

### **7.6.1 Summary of Numerical Simulations and Water Balance Issues**

Gas Hills West: The inconsistency in the apparent water balances based on the data reported by Vadose/W for the various precipitation distributions is attributed to bookkeeping errors in the code because the simulated changes in volumetric water content were generally consistent between the simulations, although not identical. The bookkeeping problems appear to be associated with the adaptive time stepping algorithm in Vadose/W that results in many very small time steps per day caused by sudden, large variations in pore water pressures. These sudden, large changes in pore water pressures result from higher precipitation intensities, with the highest intensities produced using the sinusoidal precipitation distribution and the lowest using the 24-hr distribution. The simulation using uniform 24-hr precipitation

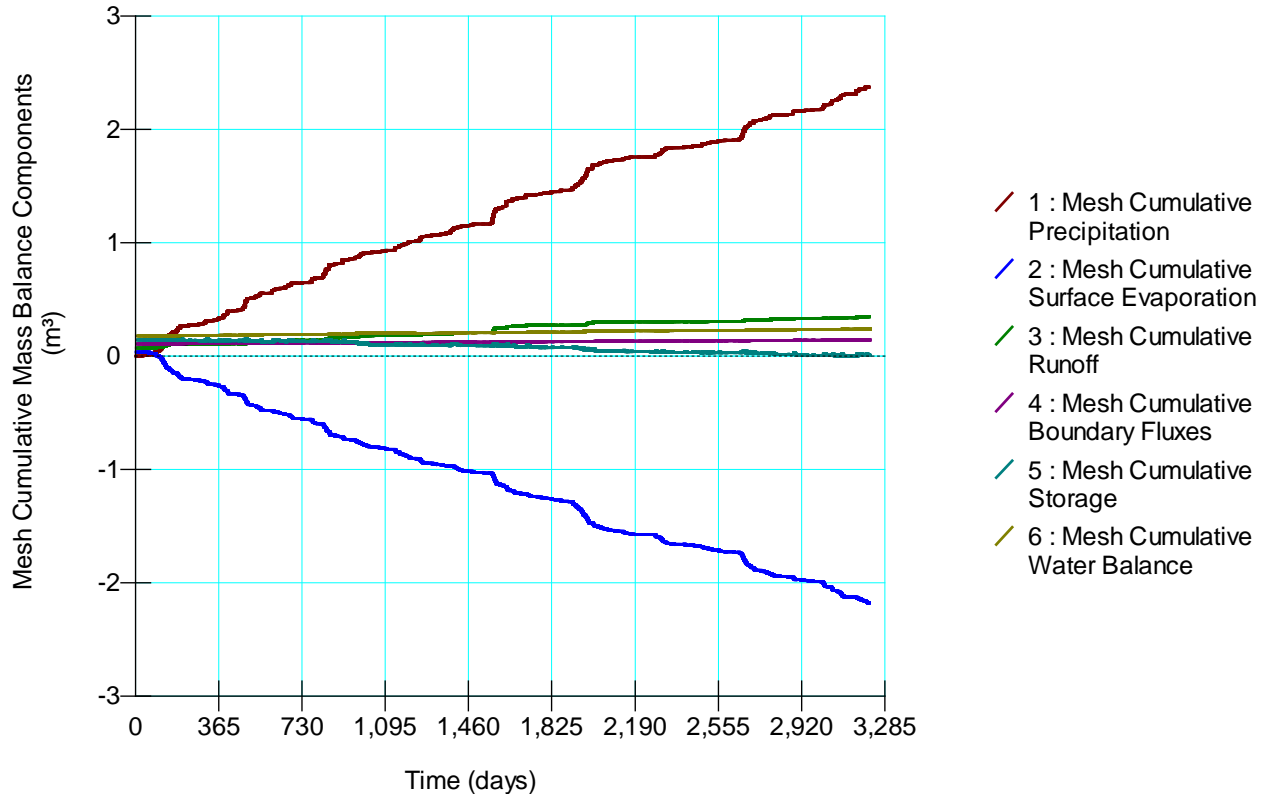


**Figure 7-3. Mesh Cumulative Water Balance Components and Resulting Error (0.022 m<sup>3</sup> over 8.8 yrs = 2.5 mm/yr) in the Zuni Buttes Climate-Driven Church Rock Central Cell Soil Cover Simulation (1 m<sup>3</sup> = 35.3 ft<sup>3</sup>)**

distribution and the elevated sandy silty clay hydraulic conductivity produced the best agreement between the change in storage and the net water added, and the lowest water balance error.

Highland: For an indeterminate reason, the Highland model was incapable of supporting a unit gradient boundary condition at the base of the model domain. A discrepancy between the apparent increase in water indicated by the water balance and the overall decrease in volumetric water content in the model domain precludes any firm conclusion about the performance of the tailings cover based on the simulation results.

Church Rock: Significant water balance errors on specific days were attributed to monsoon storm intensity and were minimized in the simulation by spreading rainfall amounts over the full day. Other significant water balance errors occurred on days during which no rain fell or on days during the non-monsoon season when rainfall was gentle over a day-long period. Such errors could not be minimized.

## 7.6.2 Recommendations for Future Simulations

Although the simulations that CNWRA staff conducted generally suggest that the radon barriers at the three sites are acting as “store and release” covers that prevent net infiltration from accumulating in the tailings deposits and ultimately percolating through the tailings, the simulations were largely limited to specific values of cover material hydraulic properties. Given the inherent uncertainty and variability in these properties, additional simulations would

be required to characterize their effect on the hydraulic performance of the covers. Such parametric simulations could not be performed within the scope of the current work due to the effort required to investigate the computational performance and idiosyncrasies of the Vadose/W code and the lengthy runtimes of the refined mesh models. Finally, future modeling should account for anticipated solid precipitation rates, whereas the modeling reported herein only accounted for liquid precipitation recorded at nearby RAWS weather stations. Precipitation records for use in modeling may need to be hybridized by combining RAWS liquid precipitation data with appropriately weighted values of solid precipitation measured at the nearest SNOTEL station.

Now that the limitations and numerical performance of the Vadose/W code are better understood, more extensive parametric analyses would be possible. These parametric analyses should include:

- Evaluating the sensitivity of the simulation results to the soil cover hydraulic properties
- Simulating the effect of ponding in engineered swales and local depressions in the soil covers
- Further investigation of the importance of soil freeze/thaw and soil thermal properties on the simulation results

Although these parametric simulations would still be affected by the ambiguities associated with the water balance information reported by Vadose/W and water balance errors associated with rapid wetting of the soils, the parametric analysis would provide insights into whether or not the as-built soil covers at the Title-II-In-Closure sites are likely to prevent net infiltration into and through the tailings.

## 8 REFERENCES

- Arya, L.M. and J.F. Paris. "A Physico-Empirical Model to Predict the Soil Moisture Characteristic from Particle Size Distribution and Bulk Density Data." *Soil Science Society of America Journal*. Vol. 45. pp. 1023–1030. 1981.
- Arya, L.M., F.J. Leij, M.Th. van Genuchten, and P.J. Shouse. "Scaling Parameter to Predict the Soil Water Characteristic from Particle-Size Distribution Data." *Soil Science Society of America Journal*. Vol. 63. pp. 510–519. 1999a.
- Arya L.M., F.J. Leij, M.Th. van Genuchten. "Relationship Between Particle-Size Distribution and Soil Water Retention." Proceedings of the International Workshop on Characterization and Measurement of the Hydraulic Properties of Unsaturated Porous Media, Riverside, California, October 22–24, 1997. F.J. Leij, M.Th. van Genuchten, and L. Wu (eds). Riverside, California: University of California, Department of Environmental Sciences. pp. 931–946. 1999b.
- Becker, B.R., A. Misra, and B. Fricke. "Development of Correlations for Soil Thermal Conductivity." *International Communications in Heat and Mass Transfer*. Vol. 19. pp. 59–68. 1992.
- Benson, C.H., G.L. Bohnhoff, P. Apinwantragoon, A.S. Ogorzalek, C.D. Shackelford, and W.H. Albright. "Comparison of Model Predictions and Field Data for an ET Cover." Tailings and Mine Waste '04: Proceedings of the Eleventh Tailings and Mine Waste Conference, 10–13 October 2004, Vail, Colorado. L. Hinshaw, (ed). London, England: Taylor and Francis Group. 2004.
- Benson, C.H., G.L. Bohnhoff, A.S. Ogorzalek, C.D. Shackelford, P. Apinwantragoon, and W.H. Albright. "Field Data and Model Predictions for a Monolithic Alternative Cover." In Waste Containment and Remediation: Proceedings of the Geo-Frontiers Conference 2005, 24–26 January 2005, Austin, Texas. Reston, Virginia: American Society of Civil Engineers. pp. 1–16. 2005. <<http://ascelibrary.org/doi/book/10.1061/9780784407899>>
- Bohnhoff, G.L. "Water Balance Predictions and Field Data for Water Balance Covers in Semi-Arid Regions." M.S. Thesis. Madison, Wisconsin: University of Wisconsin. 2005.
- Bohnhoff, G.L., A.S. Ogorzalek, C.H. Benson, C.D. Shackelford and P. Apiwantragoon. "Field Data and Water-Balance Predictions for a Monolithic Cover in a Semiarid Climate." *Journal of Geotechnical and Geoenvironmental Engineering*. Vol. 135, No. 3. pp. 333–348. 2009.
- Canonie Environmental. "Tailings Reclamation Plan as approved by NRC March 1, 1991, License No. SUA-1475 (Church Rock Facility)." Volume I – Text. ML103230316. Gallup, New Mexico. 1991.
- Canonie Environmental. "As-Built Report: Central Cell Final Reclamation (Church Rock Facility)." Gallup, New Mexico, June 1995.
- Curtis, J. and K. Grimes. *Wyoming Climate Atlas*. Laramie, Wyoming: University of Wyoming. 2004. <[www.wrds.uwyo.edu/sco/climateatlas/title\\_page.html](http://www.wrds.uwyo.edu/sco/climateatlas/title_page.html)> (27 January 2015).
- de Vries, D.A. "The Thermal Properties of Soil." *Physics of Plant Environment*. Amsterdam, Netherlands: North-Holland Publishing Co. pp. 210–235. 1963.

Exxon Production Research Company. *Highland Uranium Tailings Impoundment Seepage Study*. Houston, Texas: Exxon Production Research Company, Mining and Synthetic Fuels Division. 1982.

GEO-SLOPE International, Ltd. *Vadose Zone Modeling with VADOSE/W: An Engineering Methodology*. Calgary, Alberta, Canada: GEO-SLOPE International, Ltd. 2012.

Geotechdata.info. "Soil Permeability Coefficient." 2013.  
<[www.geotechdata.info/parameter/permeability.html](http://www.geotechdata.info/parameter/permeability.html)> (January 21, 2015).

Hu, Q. and S. Feng. "A Daily Soil Temperature Dataset and Soil Temperature Climatology of the Contiguous United States." *Journal of Applied Meteorology*. Vol. 42, No. 8. pp. 1139–1156. 2003.

Huang, S.L. and N.B. Aughenbaugh. "Sublimation of Pore Ice in Frozen Silt." *Journal of Cold Regions Engineering*. Vol. 1, No. 4. pp. 171–181. 1987.

Johansen, O. "Thermal Conductivity of Soils." Ph.D. thesis. Trondheim, Norway (CRREL Draft Translation 637, 1977) ADA 044002. 1975.

Kelln, C. "Water Balance Reported by Vadose/W." Email communication (August 28) to G. Walter, Center for Nuclear Waste Regulatory Analyses. Calgary, Alberta, Canada: GEO-SLOPE International, Ltd. 2014.

Khire, M.V. and R.G. Mijares. "Influence of the Waste Layer on Percolation Estimates for Earthen Caps Located in a Sub-humid Climate." *GeoCongress 2008: Geosustainability and Geohazard Mitigation—Proceedings of the 2008 GeoCongress, 9–12 March, 2008*, New Orleans, Louisiana. Reston, Virginia: American Society of Civil Engineers. 2008.

Mijares, R.G., M.V. Khire, and T. Johnson. "Lysimeters Versus Actual Earthen Caps: Numerical Assessment of Soil Water Storage." *GeoFlorida 2010: Advances in Analysis, Modeling & Design—Proceedings of GeoFlorida 2010, 20–24 February 2010*, West Palm Beach, Florida. Reston, Virginia: American Society of Civil Engineers. 2010.

MWH Americas, Inc. "Pre-Design Studies Northeast Church Rock Mine Site Removal Action (Church Rock Mill Site)." Fort Collins, Colorado. 2014.

NRCS. "Web Soil Survey v. 3.1." Natural Resources Conservation Service; U.S. Department of Agriculture. <<http://websoilsurvey.nrcs.usda.gov/>> (May 29, 2014).

Rawls, W.J., L.R. Ahuja, D.L. Brakensiek. "Estimating Soil Hydraulic Properties from Soils Data." *Indirect Methods for Estimating the Hydraulic Properties of Unsaturated Soils*. M.Th. van Genuchten and F.J. Lund, eds. *Proceedings of the International Workshop on Indirect Methods for Estimating the Hydraulic Properties of Unsaturated Soils*, Riverside, California, October 11–13, 1989. Riverside, California: U.S. Salinity Laboratory, Agricultural Research Service, U.S. Department of Agriculture. 1992.

Ropelewski, C.F., D.S. Gutzler, R.W. Higgins, and C.R. Mechoso. "The North American Monsoon System." Review Topic A4: American Monsoon. Chapter 14 in *The Global Monsoon System: Research and Forecast* [Report of the International Committee of the Third

International Workshop on Monsoons (IWM-III)] (C.-P. Chang, B. Wang, and N.-C.G. Lau, eds) 2005. <[http://iri.columbia.edu/~chet/04NAMS-NOV\\_pdf\\_ver.pdf](http://iri.columbia.edu/~chet/04NAMS-NOV_pdf_ver.pdf)> <[www.wmo.int/pages/prog/arep/tmrp/documents/global\\_monsoon\\_system\\_IMW3.pdf](http://www.wmo.int/pages/prog/arep/tmrp/documents/global_monsoon_system_IMW3.pdf)> (January 30, 2015).

Schaap, M.G. *Rosetta Version 1.0 User Manual*. Riverside, California: ARS–USDA. 1999.

Shepherd Miller. *As-Built and Construction Quality Assurance Report for the Uranium Tailings Basin at the Highland Reclamation Project*. Fort Collins, Colorado: Shepherd Miller. 2002.

Shepherd Miller. “American Nuclear Corporation Site Source Materials License SUA–667 Final Reclamation Plan for Tailings Pond #2.” ML110750100. Fort Collins, Colorado: Shepherd Miller. 1996.

Tratch, D. “Moisture Uptake within the Root Zone.” M.Sc. Thesis. Saskatoon, Saskatchewan, Canada: Department of Civil Engineering, University of Saskatchewan. 1996.

van Genuchten, M.Th. “Closed-Form Equation for Predicting the Hydraulic Conductivity of Unsaturated Soils.” *Soil Science Society of America Journal*. Vol. 44, No. 5. pp. 892–898. 1980.

Walter, G.R. and C.L. Dinwiddie. “Proposed Plan of Action to Characterize Final Soil Cover Properties and Obtain Input Parameter Values for Near-Field Modeling with the Vadose/W 2012 Code. Center for Nuclear Waste Regulatory Analyses, Task 28, Subtask 3, Activity 2 Report.” San Antonio, Texas: Center for Nuclear Waste Regulatory Analyses. 2014.

Water, Waste & Land, Inc. *Construction Quality Assurance Testing for Reclamation of the Uranium Tailings Basin at the Highland Reclamation Project*. Fort Collins, Colorado: Water, Waste & Land, Inc. 1991.

Water, Waste & Land, Inc. *Technical Specifications for the Reclamation of the Uranium Tailings Impoundment at Exxon's Highland Project*. Fort Collins, Colorado: Water, Waste & Land, Inc. 1989a.

Water, Waste & Land, Inc. “Letter to Exxon Coal and Minerals Company (David Range) from Louis Miller presenting evaluation of sandier borrow material for radon barrier material.” Fort Collins, Colorado: Water, Waste & Land, Inc. 1989b.

Water, Waste & Land, Inc. “Letter to Exxon Coal and Minerals Company (David Range) from Louis Miller recommending use of higher clay content borrow material for radon barrier material.” Fort Collins, Colorado: Water, Waste & Land, Inc. 1989c.

Water, Waste & Land, Inc. *Supporting Information to License Amendment Response Highland Reclamation Project, Glenrock, Wyoming*. Fort Collins, Colorado: Water, Waste & Land, Inc. 1989d.

Water, Waste & Land, Inc. *Phase 2 Final Report: Exxon Highland Tailings Basin Seepage Analyses*. Fort Collins, Colorado: Water, Waste & Land, Inc. 1988.

Water, Waste & Land, Inc. “Response to NRC Comments.” May 30, 1986.

Water, Waste & Land, Inc. *Final Reclamation Plan for the Highland Uranium Operations Tailings Basin*. Fort Collins, Colorado: Water, Waste & Land, Inc. 1984.

Western Regional Climate Center. "Fales Rock Wyoming." Remote Automated Weather Station archive, Western Regional Climate Center. 2015a. <[www.raws.dri.edu/cgi-bin/rawMAIN.pl?wyWFAL](http://www.raws.dri.edu/cgi-bin/rawMAIN.pl?wyWFAL)> (January 27, 2015).

Western Regional Climate Center. "Rochelle Hills Wyoming." Remote Automated Weather Station archive, Western Regional Climate Center. 2015b. <[www.raws.dri.edu/cgi-bin/rawMAIN.pl?wyWRCH](http://www.raws.dri.edu/cgi-bin/rawMAIN.pl?wyWRCH)> (January 27, 2015).

Western Regional Climate Center. "Zuni Buttes New Mexico." Remote Automated Weather Station archive, Western Regional Climate Center. 2015c. <[www.raws.dri.edu/cgi-bin/rawMAIN.pl?nmXZUB](http://www.raws.dri.edu/cgi-bin/rawMAIN.pl?nmXZUB)> (January 27, 2015).

Williams, R.E. "Comments on a Report Entitled 'Highland Uranium Tailings Impoundment Seepage Study,' by Exxon Production Research Company, Mining and Synthetic Fuels Division." ML102800233. Letter Report to Harry Pettengill of NRC's Uranium Resource Recovery Licensing Branch. Viola, Idaho: Williams-Robinette & Associates, Inc. 1982.